

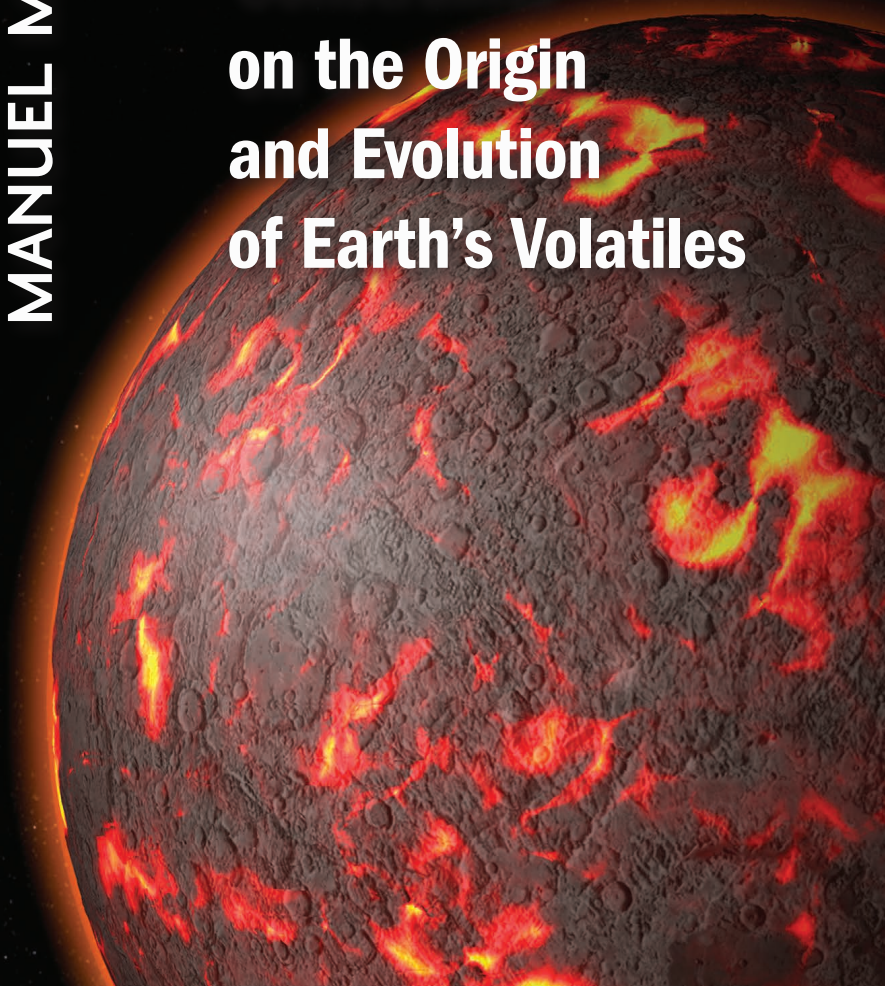
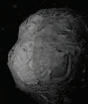
# Geochemical Perspectives



VOLUME 2, NUMBER 2 | JULY 2013

MANUEL MOREIRA

## Noble Gas Constraints on the Origin and Evolution of Earth's Volatiles



Each issue of *Geochemical Perspectives* presents a single article with an in-depth view on the past, present and future of a field of geochemistry, seen through the eyes of highly respected members of our community. The articles combine research and history of the field's development and the scientist's opinions about future directions. We welcome personal glimpses into the author's scientific life, how ideas were generated and pitfalls along the way. *Perspectives* articles are intended to appeal to the entire geochemical community, not only to experts. They are not reviews or monographs; they go beyond the current state of the art, providing opinions about future directions and impact in the field.

Copyright 2013 European Association of Geochemistry, EAG. All rights reserved. This journal and the individual contributions contained in it are protected under copyright by the EAG. The following terms and conditions apply to their use: no part of this publication may be reproduced, translated to another language, stored in a retrieval system or transmitted in any form or by any means, electronic, graphic, mechanical, photocopying, recording or otherwise, without prior written permission of the publisher. For information on how to seek permission for reproduction, visit:

[www.geochemicalperspectives.org](http://www.geochemicalperspectives.org)  
or contact [office@geochemicalperspectives.org](mailto:office@geochemicalperspectives.org).

The publisher assumes no responsibility for any statement of fact or opinion expressed in the published material.

ISSN 2223-7755 (print)

ISSN 2224-2759 (online)

DOI 10.7185/geochempersp.2.2

**Principal Editor for this issue**

**Tim Elliott**

**Reviewers**

**Chris Ballentine**, University of Manchester, UK

**Pete Burnard**, CRPG-CNRS Nancy, France

**Cover Layout** Pouliot Guay Graphistes

**Typesetter** Info 1000 Mots

**Printer** J.B. Deschamps



## Editorial Board



**LIANE G. BENNING**  
University of Leeds,  
United Kingdom



**JANNE BLICHERT-TOFT**  
ENS Lyon  
France



**TIM ELLIOTT**  
University of Bristol,  
United Kingdom



**ERIC H. OELKERS**  
CNRS Toulouse,  
France



**SUSAN L.S. STIPP**  
University of Copenhagen,  
Denmark

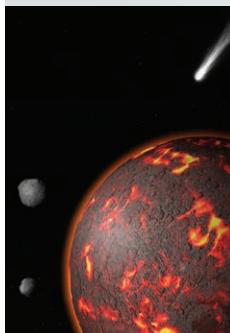
## Editorial Manager

**MARIE-AUDE HULSHOFF**

## Graphical Advisor

**JUAN DIEGO RODRIGUEZ BLANCO**

University of Copenhagen, Denmark



## ABOUT THE COVER

How and when were the atmospheres of the terrestrial planets formed is a major scientific issue. Large fractions of the atmospheres were produced during the first million years of the planetary accretion. This period is however difficult to depict geochemically due to reduced sampling and to the complexity of all the physical processes occurring during planetary accretion (impacts, photo-evaporation, convection of a magma ocean...).

Image credit: Antoine Pitrou (IPGP)

# CONTENTS

<b>Acknowledgements</b> .....	IV
-------------------------------	----

<b>Noble Gas Constraints on the Origin and Evolution of Earth's Volatiles</b> .....	229
---	-----

<b>Abstract</b> .....	229
-----------------------	-----

1 . Introduction. ....	230
1.1 The Noble Gases as a Geochemical Tool <i>par Excellence</i> .....	230
1.2 Chemical Geodynamics or the Use of Geochemistry to Constrain the Earth's Evolution .....	235
1.2.1 Pioneers of chemical geodynamics .....	235
1.2.2 Fundamentals of isotope geochemistry .....	238
1.3 A Brief History of Earth Formation and its Evolution .....	239
1.4 Article Outline .....	242
2. Noble Gases in Planetary Building Blocks. ....	244
2.1 Introduction .....	244
2.2 Elemental and Isotopic Ratios in the Sun: the Bulk Solar System Composition. ....	246
2.3 The Origin of the Ubiquitous "Phase Q" in Meteorites. ....	247

2.4	The Neon Alphabet.....	254
2.4.1	Neon A: pre-solar diamonds.....	255
2.4.2	The component B in meteorites: the result of solar wind implantation .....	257
2.5	Martian Mantle has a Solar Xenon (or Q) and Earth-like Atmospheric Xenon .....	263
2.6	Conclusions .....	265
3.	Helium Isotopes and the Two-Reservoir Mantle Story .....	267
3.1	The Discovery of $^3\text{He}$ on Earth.....	267
3.2	Helium Isotope Systematics in Oceanic Basalts.....	270
3.2.1	Mid ocean ridge basalts (MORB) .....	273
3.2.2	Oceanic island basalts (OIB) .....	275
3.3	Conclusions .....	282
4.	Radiogenic Argon and Xenon in the Mantle and the 'Age' of Mantle Degassing .....	283
4.1	Radiogenic Argon in MORB and OIB .....	284
4.2	The Terrestrial Argon Budget.....	289
4.3	Radiogenic and Fissiogenic Xenon on the Earth.....	291
4.3.1	Brief outlook on xenology .....	291
4.3.2	Radiogenic xenon from $^{129}\text{I}$ extinct radioactivity in the MORB source .....	295
4.4	Determination of the Composition of the Non-radiogenic Atmosphere .....	299
4.4.1	Xenon from extinct $^{244}\text{Pu}$ radioactivity on Earth.....	301
4.4.2	Brief history of the discovery of $^{244}\text{Pu}$ on Earth .....	301
4.4.3	Fissiogenic xenon in the Earth's mantle .....	302
4.4.4	Fissiogenic xenon isotopes in OIB: a pure $^{244}\text{Pu}$ signature and the evidence for an isolation of the OIB source since 4.4Ga .....	305
4.5	Conclusions .....	307
5.	Solar Neon and Argon in the Mantle and the Constraints on the Origin of Noble Gases On Earth.....	308
5.1	The Discovery of Solar-like Neon in the Mantle.....	308
5.2	Atmospheric Contamination in Oceanic Samples.....	314
5.3	Atmospheric Contamination Correction for Determination of All Noble Gas Isotopic Ratios.....	317
5.4	The He-Ne Correlation in the Mantle and the Unique Primitive Source.....	319
5.5	Solar Argon in the Mantle? .....	321
5.6	Conclusions about the Neon and Argon Isotopic Composition in the Mantle .....	323





6.	The Existence of the Primitive Noble Gas Reservoir . . . . .	324
6.1	Noble Gases Suggest a Deep “Primitive” Reservoir for the OIB Source . . . . .	324
6.2	The Canonical Model: the Two-layer Mantle . . . . .	325
6.3	The Basal Magma Ocean (BMO) Model . . . . .	326
6.4	The Core . . . . .	327
6.5	Anderson’s Revolt . . . . .	331
6.6	Is the Low $^4\text{He}/^3\text{He}$ Reservoir a Residue of Melting? . . . . .	334
6.7	Relationship with Lithophile Elements and the Question of a Non-chondritic Earth . . . . .	336
6.8	Conclusions . . . . .	338
7.	Subduction of Atmospheric Noble Gases into the Mantle and the Paradigm of the Subduction Barrier . . . . .	339
7.1	Subducting Material . . . . .	340
7.2	Chondritic Noble Gases in the Primitive Mantle? . . . . .	342
7.3	Subduction-Degassing Model and the “Xenon Replenishment” of the Mantle . . . . .	346
7.4	Conclusions . . . . .	351
8.	Discussion of the Origin of Noble Gases on Earth and the Evolution of the Mantle/Atmosphere System . . . . .	352
8.1	Summary of the Previous Sections and General Remarks . . . . .	352
8.2	Neon B or Solar Neon in the Mantle? . . . . .	357
8.3	Mantle Degassing . . . . .	359
8.4	Atmosphere: a Closed System (Loss or Addition)? . . . . .	364
8.4.1	Late veneer of chondritic material in order to explain (or not) the atmospheric neon . . . . .	364
8.4.2	A different atmospheric xenon composition in the Archean . . . . .	366
8.5	The Krypton-Xenon Systematics and the Dual Origin of the Atmosphere . . . . .	369
8.6	Conclusions . . . . .	371
9.	Concluding Comments and Questions . . . . .	374
	<b>References . . . . .</b>	<b>377</b>
	<b>Glossary . . . . .</b>	<b>396</b>
	<b>Index . . . . .</b>	<b>400</b>





# ACKNOWLEDGEMENTS

I would like first to acknowledge all the colleagues from both the “old” generation and the “new” with whom I have worked for 20 years; in particular, I have special thoughts for my mentor *Claude Allègre* without whom nothing could have been possible. The noble gas “Paris” group would not have existed without *Thomas, Philippe, Dédé, Petit Chef* and *Fabien*. I am grateful for what they did and this work is dedicated to them. I have also special thoughts for my PhD students (*Cécile, Lorraine, Claire, Claire, Stéphane, Aude, Marine*) who through their work contributed hugely to the knowledge of the noble gas geochemistry.

*Tim Elliott, Eric Oelkers, Peter Burnard, Chris Ballentine* and *Mark Kurz* helped tremendously to improve the quality of the manuscript. *Antoine, Emmelyne* and *Joel* are thanked for their help during the preparation of this manuscript.

I would like to dedicate this work to my parents who died too early.

# NOBLE GAS CONSTRAINTS ON THE ORIGIN AND EVOLUTION OF EARTH'S VOLATILES

## ABSTRACT

This issue of *Geochemical Perspectives* examines the noble gas geochemistry of meteorites and the Earth to provide essential constraints on the origin of volatiles on our own and other terrestrial planets. Noble gases (He, Ne, Ar, Kr, Xe and Rn) belong to the last column of the Mendeleev's table, implying they are chemically inert in contrast to the other highly volatile elements. This important feature allows their primordial elemental and isotopic compositions on Earth to be determined without having to consider the additional complexities of chemical or biological influences. Any variations of elemental or isotopic ratios of the noble gases reflects either physical processes such as diffusion, adsorption, degassing, or solubilisation or the effects of natural radioactivity. Moreover, among the highly volatile elements, the noble gases are the only ones that are able to provide constraints on the timing of geochemical fractionations that have occurred since Earth's accretion, thanks to the natural radioactivity of several parent nuclides with a range of different half-lives,  $^{235,238}\text{U}$ ,  $^{232}\text{Th}$ ,  $^{40}\text{K}$ ,  $^{244}\text{Pu}$ ,  $^{129}\text{I}$ .

In this issue, I describe the distribution and isotopic compositions of noble gases in meteorites, mantle-derived rocks and the atmosphere, from both a historical point of view and using some major, new discoveries in that field that



have recently changed opinions on mantle/atmosphere evolution and on the origin of volatiles on terrestrial planets. In particular, I discuss the nature of the parent bodies and of the noble gas carriers, the existence and location of a reservoir rich in primordial noble gases sampled by mantle plumes, the subduction of atmospheric noble gas into the mantle and the evolution of the atmosphere evolution since the Earth's accretion. Of course, this contribution does not have the ambition of addressing all the issues of noble gas geochemistry, but it raises some key questions and contemplates the potential future direction of research into the origin of noble gases and other volatiles in terrestrial planets in the coming years.

## 1.

## INTRODUCTION

Volatiles have a complex and still discussed origin on terrestrial planets. In contrast to the giant planets that accreted their atmosphere by gravity, the atmospheres of Mars, Earth and Venus have different sources. Although a residual atmosphere from a primitive dense solar atmosphere cannot be fully discarded, since Brown (1949) it is generally accepted that the atmospheres of the terrestrial planets have a secondary origin. Degassing of the interiors of the planets, either very early, or during their geological history, can have formed these atmospheres where the volatiles were accreted together with other refractory elements. Or, if the terrestrial planets were accreted “dry”, volatiles could have been carried later, after planet formation by impacts of volatile-rich materials such as carbonaceous chondrites or cometary material coming from the outer part of the Solar System. The three terrestrial planets have atmospheres that share chemical and isotopic characteristics suggesting a common origin but different histories linked to their different geological histories. Concerning the major volatiles, such as CO<sub>2</sub> or water, obviously biology, temperature conditions allowing liquid water or the presence or not of a magnetic field for example, have permitted chemical and isotopic transformations of the primitive atmospheres, which have led to their current chemical compositions (*i.e.* N<sub>2</sub>-rich atmosphere on Earth, no water on Venus). Among the volatile elements, only noble gases can trace the origin and the evolution of the atmospheres without the filter of geochemistry. In the next sections I will present this geochemical tool with the main goal of providing constraints on the origin of the atmospheres of the terrestrial planets.

### 1.1 The Noble Gases as a Geochemical Tool *par Excellence*

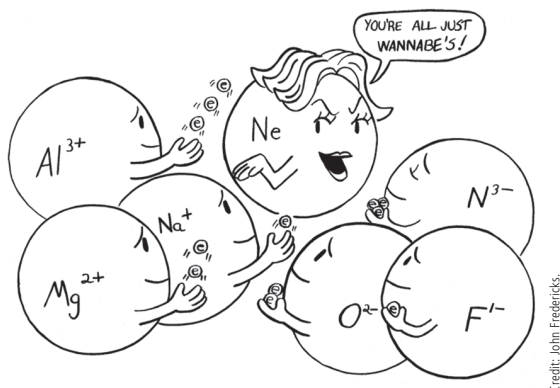
The noble gas family<sup>1</sup> provides fantastic tools to investigate the origin of volatiles on the terrestrial planets. They show the unique characteristics among the elements of being chemically inert because their outer shells of electrons are

---

1. The term « rare gases » is often used. This is a historical nomenclature. Argon is not rare in the atmosphere (1%)!



full<sup>2</sup> (Fig. 1.1). This feature means their composition is not modified by biological and chemical reactions during the Earth's history, in stark contrast to other very volatile elements such as C, N, H. Moreover, noble gases number 5 (+1, if one includes the radioactive noble gas radon, which will not be considered in this article), spanning very different atomic masses, from 3 amu to 136 amu, resulting in large elemental fractionations during physical processes such as diffusion, ion implantation, or adsorption. The noble gases also possess many isotopes, both non-radiogenic and radiogenic, and among the radiogenic isotopes used in mantle geochemistry, the half-lives of the different parents (<sup>40</sup>K, <sup>235,238</sup>U, <sup>129</sup>I, <sup>244</sup>Pu) present a large spectrum of values from very short (17 Ma for <sup>129</sup>I) up to  $8.2 \times 10^{15}$  years for the spontaneous fission of <sup>238</sup>U. These radioactive chronometers put a timescale on the geological processes that affected the very volatile elements, and additionally constrain the CO<sub>2</sub>, water, and nitrogen geological cycles. As a consequence of their high volatility, the noble gases are very depleted in meteorites and in terrestrial planets compared to their relative abundance in the Sun or giant planets<sup>3</sup>. For example, the abundance of xenon in the Earth's upper mantle is estimated to be  $10^{-14} \text{ g g}^{-1}$  (0.01 ppt), whereas most of the other chemical elements are present in concentrations not lower than  $10^{-9} \text{ g g}^{-1}$  (ppb)<sup>4</sup>.



Credit: John Fredericks.

**Figure 1.1**

Cartoon showing that noble gases have their outer shell of valence electrons full.

2. Although complexes can be formed in some special conditions (*e.g.*, ArF, XeF, ...and as aficionados of plasma mass-spectrometry know, ArAr<sup>+</sup>), these are not stable and dissociate very quickly. Noble gases can be considered as chemically inert in Nature.
3. Helium is the second most abundant element!
4. These low abundances in geological samples require different analytical techniques for measurement than for other chemical elements (except maybe N). Noble gas mass spectrometers should have low volumes, peculiar ionisation sources, be run in static mode, use electron multipliers for detection of most isotopes except for <sup>4</sup>He and <sup>40</sup>Ar, need extraction to be executed directly on a line under vacuum connected to the mass spectrometer. Vacuum needs to be excellent ( $10^{-10}$  torr) to minimise blanks.





The first noble gas that was discovered was argon. *William Ramsay* (1852-1916) (Fig. 1.2) suggested its existence in the atmosphere in 1894 after the observation of Lord Rayleigh (1842-1919) that pure nitrogen was lighter than nitrogen purified from air by ~0.5% (Rayleigh, 1894). The detailed experiments conducted by the two scientists that led to that discovery are well described in Rayleigh and Ramsay (1895), with a superb style of writing.

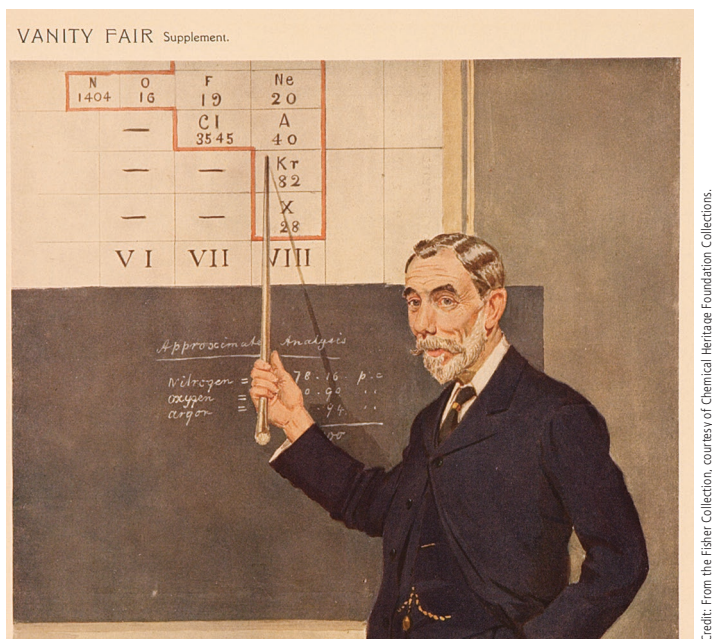


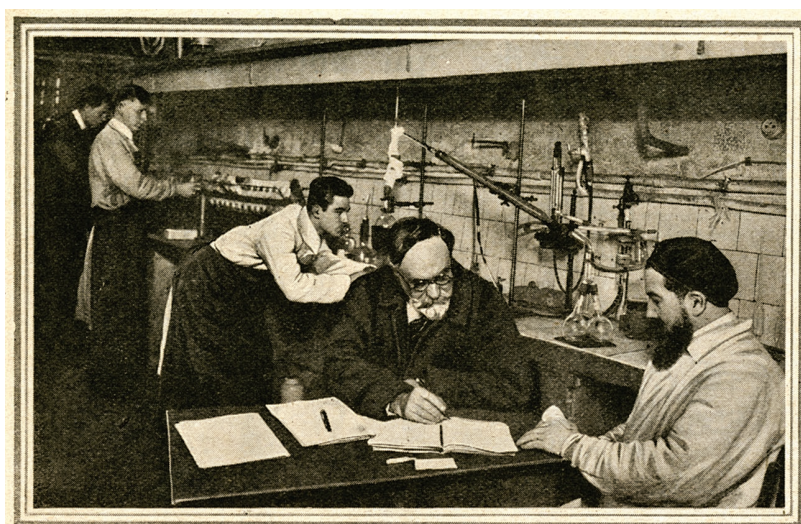
**Figure 1.2** “Chemistry”, a 1908 chromolithograph of William Ramsay. Ramsay discovered the noble gases (with Rayleigh and Travers).

With *Morris Travers* (1872-1961), they also discovered neon, krypton, and xenon in 1898. Helium, first discovered in the spectrum of Sun in 1868, was observed on Earth in 1881 by *Luigi Palmieri*<sup>5</sup> by measuring the spectrum of lava from Vesuvius (Palmieri, 1881). *Ramsay* observed helium in pitchblende minerals in 1895. This helium is mainly the radiogenic helium ( $^4\text{He}$ ), which is the alpha particle produced during the radioactive decay of the naturally occurring actinides.  $^3\text{He}$ , the primordial helium isotope was detected on Earth only in 1939 (Alvarez and Cornog, 1939a; b). A complete story of the discovery of noble gases is given by *Ramsay* itself in his Nobel Prize Lecture in 1906 (Ramsay, 1904).

5. Luigi Palmieri (1807-1896) was an Italian volcanologist and meteorologist.



In my opinion, *Charles Moureu* (1863-1929) (Fig. 1.3) was the first noble gas geochemist. In particular, he measured the abundances of the noble gases in springs from various places in France and published eminent articles on the interpretations of their relative abundances in the light of what was known about geology and astronomy in the early 1900's. In Box 1.1, I present a translation of one of his discussions about the abundances of noble gases in springs in order to illustrate my statement. For example, he used the elemental ratios (*e.g.*, Ar/Kr) as tracers of the Earth's formation by assuming that this ratio cannot have been significantly modified during geological processes because noble gases are chemically inert. Of course, there were limitations to his interpretation since he was not using primordial isotopes that had not yet been discovered. He also assumed that all the helium has a radiogenic origin, a hypothesis that stood until the discovery of  $^3\text{He}$  in the well gases in 1946 (Aldrich and Nier, 1946) and in the mantle in 1969 (Clarke *et al.*, 1969; Mamyrin *et al.*, 1969a). Nevertheless, the work of *Charles Moureu* well merits reading from a historical point of view because he used geochemical reasoning a long time before others.



*L'étude de nouveaux corps organiques, de nouvelles méthodes de préparation est également l'objet de recherches très assidues de M. Moureu et de ses collaborateurs. Voici une salle spécialement affectée à ces études. Nous voyons derrière M. Moureu et son chef de laboratoire, M. Dufraine, deux élèves à gauche qui dosent le carbone et l'hydrogène, un autre à droite qui fait une distillation fractionnée dans le vide.*

Image source: «Sciences et Voyages» published July 17th 1927 (N°255).

**Figure 1.3**

Charles Moureu in his laboratory (in the centre) in 1923. Charles Moureu is a French chemist, unfortunately less known than the other scientists from his time (*e.g.*, P. and M. Curie, H. Becquerel). He is known for his work on the autoxidation but has published at the beginning of the 20th century on noble gases in natural samples (*e.g.*, Moureu, 1913; Moureu, 1927; Moureu and Lepape, 1927). In my opinion, he is also clearly the first noble gas geochemist considering his methodology, approach and interpretations on the noble gases measured in springs.



The translation of the French caption says: "The study of new organic bodies, of new methods of preparation is also the subject of the very assiduous researches of M. Moureu and his colleagues. Here is a room specially devoted to these studies. We see behind Mr. Moureu and his laboratory manager, Mr. Dufraissne, two students on the left who proportion carbon and hydrogen, another on the right who is doing a fractional distillation under vacuum".

Charles Moureu, In Discours et Conférences sur la science  
et ses applications (1927):

### ***Astrophysical theory***

*A fundamental feature dominates all the properties of argon and its congeners (rare gases): these elements are chemically inert in the sense that they never could be combined with each other or with any other body. A physical property of the same elements, which operates as in our theory, is that they have the ability to maintain a gaseous state between very wide limits of temperature and pressure and, consequently, tend always to be evenly distributed throughout the space available for expansion. Let us, in thought, look back thorough the history of the genesis of the Solar System, to the nebula generator. All bodies, free elements or combinations, are in a gaseous state, and the Earth, with the inevitable vortices and mixing, must be a relatively homogeneous mixture in all its parts. The constituent fragment of the Earth detachs, and it includes almost three concentric regions: an incandescent mass merger, an essentially heterogeneous solid shell and the gas atmosphere. Geological phenomena, slow and continuous or abrupt and violent, continued uninterrupted. During this incessant evolution of the planet, all bodies endowed with chemical affinities have contracted mutual combinations. Only rare gases, due to their chemical inertness, remained entirely free, and in some points or by some mechanisms they are concentrated or diluted, they could only be indifferent witnesses in respect of all geological upheavals and of all the metamorphoses of the matter.*

*Lets us consider specifically krypton and argon. It is clear, from above that the relationship between the proportions of these two gases should be roughly the same at the beginning, at all points of the nebula. If, in the course of time, it happened that it has altered locally, physical actions are only able to be the cause: obstruction, diffusion, dissolution, etc.., And this ratio has therefore been subjected, at various points of the planet, to only small changes. In other words, the mixture of the two gases from this point of view, behave substantially as a definite compound.*

*This theory, as we have seen, borrows from astronomy and geology only classic ideas on the evolution of the Worlds. With its starting point in the Astro-nomical phase of the Earth, it is independent of any hypothesis on the genesis of thermal waters.*

#### **Box 1.1**

Translation of the discussion in a note published in 1927 about the origin of the volatiles on Earth, based on analyses of noble gas concentrations in springs (Moureu, 1913).



Today, noble gases are used in many fields of the Earth sciences such rock dating (K-Ar, Ar-Ar, I-Xe), thermochronology (U-He), geomorphology, volcanology, paleothermometry, and, what concerns us in this article, cosmochemistry and chemical geodynamics. This unique chemical family is clearly a fundamental tool in Earth sciences and the objective of this article is to present one aspect of the noble gas geochemistry, which concerns the origin of volatiles on Earth, using the study of their concentrations and isotopic ratios in terrestrial materials and by comparing them to compositions of meteorites and the Sun.

## 1.2 Chemical Geodynamics or the Use of Geochemistry to Constrain the Earth's Evolution

---

### 1.2.1 *Pioneers of chemical geodynamics*

Here I present a quick overview of “chemical geodynamics”, which consists of the use of the behaviour of chemical elements during geological processes to constrain the age, origin and evolution of major geological reservoirs. The evocative term “chemical geodynamics” was coined by Allègre (1982) and was subsequently trumpeted by Zindler and Hart (1986a), building on several decades of models that attempted to look at the global cycling of elements (*e.g.*, Armstrong, 1968; Zartman and Doe, 1981; O’Nions *et al.*, 1979; Chase, 1981; White *et al.*, 1976; White and Hofmann, 1982; Allègre, 1980, 1983a, 1987; Cohen and O’Nions, 1982; De Paolo and Wasserburg, 1979; Dupré and Allègre, 1980; Hart *et al.*, 1973; Hawkesworth *et al.*, 1979; Richard *et al.*, 1976; Schilling, 1975; White and Hofmann, 1982).

This field of Earth science started in earnest during the early 1970’s but some works using isotope geochemistry started earlier, in the 1960’s, particularly in the noble gas community (Butler *et al.*, 1963; Clarke *et al.*, 1969).

I want here to focus peculiar attention to one of these pioneers of “chemical geodynamics.” *Claude Allègre* is certainly one of the most eminent scientists in Earth sciences (Fig. 1.4). I am just not saying this because *Claude* was my PhD advisor! This is what most of the scientists who know him also say<sup>6</sup>. We met in 1993, when I was a masters student, and we have worked together since, with the exception of the two years of my post-doc at the Woods Hole Oceanographic Institution with *Mark Kurz*. Admittedly, I learned noble gas geochemistry with *Thomas Staudacher* and *Mark Kurz*, but I was taught the big picture of isotope geochemistry by *Claude*, and certainly also a method of working that some may not like.

---

6. He received in 1986 the Crawford Prize (“Nobel” prize for Earth Sciences), with G. Wasserburg, for the major input of their research on isotopic geochemistry and cosmochemistry.







Photo credit: Joël Dyon (IPGP)

**Figure 1.4** Claude Allègre, one of the fathers of the “chemical geodynamics” and my PhD advisor. On this photo, he is posing in front of the noble gas mass spectrometer ARESIBO which he designed (see Section 4).

*Claude Allègre* was the founder of the Laboratory of Geochemistry and Cosmochemistry in 1967<sup>7</sup> and he joined the Institut de Physique du Globe de Paris in 1968. The laboratory was located in the ugly Jussieu Campus that everybody loves to hate and looks like a giant castle from the dark ages with moats, dungeons and even ghosts. Yet the purpose of this castle was not to protect the scientific denizens within but to allow the rioting students of the sixties to be corralled inside. It is important to note that this laboratory participated in many of the key developments in isotope geochemistry, including mantle noble gas geochemistry. The geochemistry laboratory was founded in the late 1960’s, but the noble gas group as it exists today was created at the end of the 1970’s. In the rest of the article I will refer to the “Paris Group”, which consisted of “Master” *Thomas*

*Staudacher*, *Philippe Sarda*, *André Lecomte*, *André Girard* and, of course, *Claude Allègre* (a description of the fantastic mass spectrometers they have designed and constructed is given in Section 4). These people built the noble gas laboratory at IPGP of which I am now in charge.

*Claude Allègre* (Fig. 1.4) and other geochemists used the chemical properties of the (trace) elements to “follow” them during geological processes including melting, crystallisation, degassing or alteration in order to constrain the origin, fate, and chronology of different large scale reservoirs such as the core, mantle, continental crust, oceanic crust, and atmosphere... An understanding of these processes can be obtained by the study of major and trace element systematics, whereas the time constraints on these geological events can be gleaned from the natural radioactivity such as the decay of  $^{87}\text{Rb}$  to  $^{87}\text{Sr}$ , or  $^{238}\text{U}$  to  $^{206}\text{Pb}$ .

7. With Marc Javoy and Gilles Michard, both professors at University Paris Diderot and at the Institut de Physique du Globe de Paris.





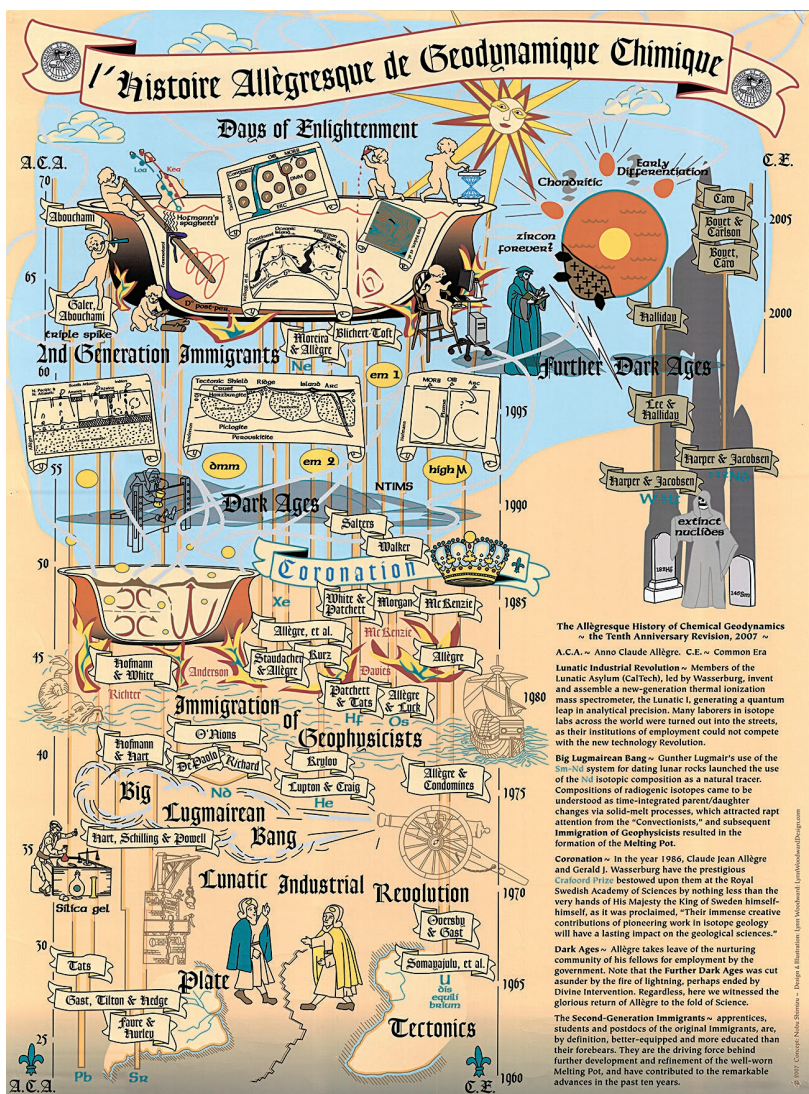


**Figure 1.5**

"Allegresque" history of the chemical geodynamics viewed by Nobu Shimizu and Stan Hart, two eminent geochemists and very good friends of Claude Allègre.



The Allegresque History of Chemical Geodynamics ~  
the Tenth Anniversary Revision, 2007

**A.C.A. ~ Anno Claude Allegre. C.E. N Common Era**

Lunatic Industrial Revolution ~ Members of the Lunatic Asylum (CalTech), led by Wasserburg, invent and assemble a new-generation thermal ionisation mass spectrometer, the Lunatic I, generating a quantum leap in analytical precision. Many laborers in isotope labs across the world were turned out into the streets, as their institutions of employment could not compete with the new technology Revolution.

Big Lugmairean Bang ~ Gunther Lugmair's use of the Sm-Nd system for dating lunar rocks launched the use of the Nd isotopic composition as a natural tracer. Compositions of radiogenic isotopes came to be understood as time-integrated parent/ daughter changes via solid-melt processes, which attracted rapt attention from the "Convectionists," and subsequent Immigration of Geophysicists resulted in the formation of the Melting Pot.

Coronation ~ In the year 1986, Claude Jean Allègre and Gerald J. Wasserburg have the prestigious Crafoord Prize bestowed upon them at the Royal Swedish Academy of Sciences by nothing less than the very hands of His Majesty the King of Sweden himself, as it was proclaimed, "Their immense creative contributions of pioneering work in isotope geology will have a lasting impact on the geological sciences."

Dark Ages ~ Allègre takes leave of the nurturing community of his fellows for employment by the government. Note that the Further Dark Ages was cut asunder by the fire of lightning, perhaps ended by Divine Intervention. Regardless, here we witnessed the glorious return of Allègre to the fold of Science.

The Second-Generation Immigrants ~ apprentices, students and postdocs of the original Immigrants, are, by definition, better-equipped and more educated than their forebears. They are the driving force behind further development and refinement of the well-worn Melting Pot, and have contributed to the remarkable advances in the past ten years.

**Box 1.2** Text from Figure 1.5.

### 1.2.2 Fundamentals of isotope geochemistry

During any geological process, the chemical elements are partitioned into reservoirs (isolated physical entities with distinct chemical compositions) or components, depending on their geochemical affinity. For example, during core formation, siderophile elements are preferentially concentrated into the core



whereas lithophile elements enter the overlying silicate reservoir. Similarly, incompatible elements are concentrated in melts (which go to form the crustal sub-division of the silicate reservoir) whereas compatible elements stay in the peridotitic mantle during mantle melting. Noble gases are incompatible during melting and so enter the melt phase but become insoluble in the host magma as the result of decompression en route to the surface. The noble gases thus follow CO<sub>2</sub> and water, and are degassed from magmatic systems, and therefore become concentrated into the atmosphere. Therefore, the mantle becomes increasingly more degassed of its primordial gases gradually over geological time. Any geological phenomenon that produces a chemical fractionation between chemical elements has different geochemical characteristics during this process. Time constraints on an event are provided using a system of two chemical elements in which one of the elements has an isotope that is radioactive and produces an isotope of another chemical element. Here, it is assumed that the isotopic fractionation between isotopes of the same element, such as can be observed for “stable isotopes” such as C, O, or N is negligible in these radiogenic systems. This assumption is reasonable as the processes we are looking at here are high temperature processes for which the isotopic fractionation is small<sup>8</sup>.

### 1.3 A Brief History of Earth Formation and its Evolution

Here I present a brief overview of how and when Earth was formed and has evolved. Obviously, it cannot be very complete and detailed since an entire book would be necessary. Here I give the big picture of Solar System formation and Earth accretion and differentiation.

The Solar System started as a large gas solar nebula containing ~1% in mass of dust. This cloud started to collapse and rotate. Most of the mass of the disk fell toward the centre of the accretion disk and formed the proto-sun. When the pressure and temperature were high enough, nuclear fusion started (*e.g.*, deuterium burning) and the Sun, as a star, was born (T Tauri stage of a star). Dust from the accretion disk was concentrated into the plane of the disk and started to aggregate to form solid objects that became larger and larger, forming planetesimals. Asteroids (and meteorites derived from them) are “trapped” samples of this early stage of accretion. With further impacts, these planetesimals grew to form planetary embryos (~size of Mars), and then planets the size of Earth.

---

8. This is not entirely correct. We will see in the next Sections that a mass fractionation of noble gas isotopes occurs during ion implantation, or during xenon ionisation under UV. However, these processes occur at low temperature. At mantle temperatures, noble gases are not supposed to significantly fractionate during melting or degassing, although diffusion can fractionate isotopes even at high temperatures. This is significant when the system is not at equilibrium. However, on first order, we have to stress the fact that mass isotope fractionation is negligible during high temperatures geological events.



Before this last sequence of the planetary accretion was finished, the gas from the accretion disk was photo-evaporated due to the intense UV radiation of the early sun, leaving a gas-disk of debris.

The starting point for the Solar System evolution comes from the CAI (Calcium Aluminium Inclusions) that are present in some of the most primitive meteorites, the chondrites. CAI are refractory condensates formed during a condensation sequence from a hot gas, rich in Ca, Al, Ti, the most (major) refractory elements. These are dated at 4.567 Ga (Amelin *et al.*, 2002).

Chondrites were formed a few million years later by aggregation of chondrules and CAI in a fine-grain matrix. Chondrules are mm-scale spheres made mainly of silicates, and represent melt that had rapidly crystallised under vacuum. They were formed slightly after CAI (a few Ma after) (Villeneuve *et al.*, 2009). Although it can be debated, chondrites are considered to be similar to the parent bodies of the Earth. Mars-size objects are formed in a relatively short time (a few Ma) according to Dauphas and Pourmand (2011) based on the Hf/W systematics in agreement with models of planetary formation. Earth-like planets took longer to be accreted because the mechanism of their accretion involves impacts between planetary embryos (Fig. 1.6), which requires a relatively long time (*e.g.*, Kleine *et al.*, 2009). An accretion time of a few tens of Ma is often proposed for the Earth based on the Hf-W systematics on Earth and Moon (*e.g.*, Kleine *et al.*, 2009). During accretion, it is possible that Earth was partially (or totally) molten because impacts and core segregation generate heat. This process favours degassing and core formation. The age of the core formation is estimated to be between 30 and 125 Ma after CAI based on the Hf/W system, but the model-age strongly depends on the accretion and core formation mechanisms (see review in Kleine *et al.*, 2009). The age of the atmosphere will be discussed in the next sections, but it seems clear that a large fraction of the atmosphere was degassed early from the Earth's mantle (less than 100 Ma after CAI), although degassing is still on-going as suggested by the present-day  $^3\text{He}$  flux observed at ridges (Clarke *et al.*, 1969) and the presence of radiogenic argon in the atmosphere, which was produced only late in Earth history due to the long half-life of the  $^{40}\text{K}$  (Hart *et al.*, 1978). The convective regime (*e.g.*, magma ocean) induced by accretion, crystallisation and core segregation then changed to a different convective regime, such as the plate tectonics on the Earth. During this second stage of the Earth's evolution, continental crust was formed, producing a mantle depleted in incompatible elements and the major cycles of elements took place.

The present-day trace element and isotopic compositions<sup>9</sup> in the mantle have been reviewed in detailed publications (*e.g.*, see the Treatise on Geochemistry, Volume 2, Holland and Turekian, 2003). I want to give here only the big picture of the mantle geochemistry. Details can be found in the abundant literature on isotope systematics in oceanic basalts. Isotope systematics on Earth

9. The « classic ones »: He, Nd, Sr, Pb. There are many other tracers of mantle processes (Hf, the new non-traditional stable isotopes, siderophiles...).





indicates that the mantle contains different primordial or non-primordial components, namely, the primordial mantle (undegassed, undepleted) with primitive noble gas signatures (Kurz *et al.*, 2009)<sup>10</sup>, recycled sediments (terrigenous, pelagic) (Farley *et al.*, 1992; Woodhead and Devey, 1993), recycled oceanic crust (Chauvel *et al.*, 1992; Hofmann and White, 1982; Kogisco *et al.*, 1997)<sup>11</sup>. The depleted mantle, sampled by Mid Oceanic Ridge Basalts (MORB), is clearly the residue of the continental crust extraction. It is depleted in highly incompatible elements such as Th or U, now present in the continental crust. The depletion depth of the mantle is controversial; at least the upper of the mantle (25% of the mantle), but some propose the entire mantle is depleted. As we will discuss in Section 6, a primordial reservoir for noble gases exists; either the bulk lower mantle (*e.g.*, Allègre and Moreira, 2004) or a deep part of it (core-mantle boundary for example; Tolstikhin and Hofmann, 2005). This reservoir is not degassed and may not be depleted by continental crust extraction, although this is debated (see Section 6). The other components observed in oceanic basalts are produced by plate tectonics and subduction into the mantle of oceanic slabs containing oceanic crust and sediments (dehydrated, melted or not).



**Figure 1.6**

Planetary accretion by impacts (from Brandon, 2011, with permission from Nature).

10. It has different acronyms: PM, sometimes FOZO, PREMA or more recently, SCHEM.

11. The so-called HIMU end-member.



## 1.4 Article Outline

Earth and Mars are depleted in moderately volatile elements such as Pb, K, and Rb, compared to chondrites (e.g., Fig. 1.7). This implies that highly volatile elements (e.g., noble gases, water, C, N) are extremely depleted in these planets (e.g., Albarède, 2009), and therefore the question of their origin on terrestrial planets is a major issue in the Earth sciences. Volatiles could have been carried to Earth late, after the accretion and differentiation by volatile-rich material such as carbonaceous chondrites or cometary material. This is the so-called Late Veneer theory. Alternatively volatiles could have been already present in the parent bodies despite their depletion in moderately volatile elements. In this article, I will provide an overview of the noble gas systematics in the mantle and in meteorites in order to provide constraints on the possible origins of volatiles on terrestrial planets and on the evolution of the mantle/atmosphere system. This is naturally my personal view of noble gas geochemistry, in 2013, acquired after (only) 20 years of research on the noble gases in the mantle. Obviously, it cannot be fully objective and I require the indulgence of my colleagues if they feel I did not refer sufficiently to their work or ideas. Particularly, I try in some sections to integrate recent observations that are not entirely accepted by the community and are still debated because they raise some very important issues about the noble gas origin and their evolution in the Earth's reservoirs (e.g., Holland and Ballentine, 2006; Holland *et al.*, 2009; Pujol *et al.*, 2011).

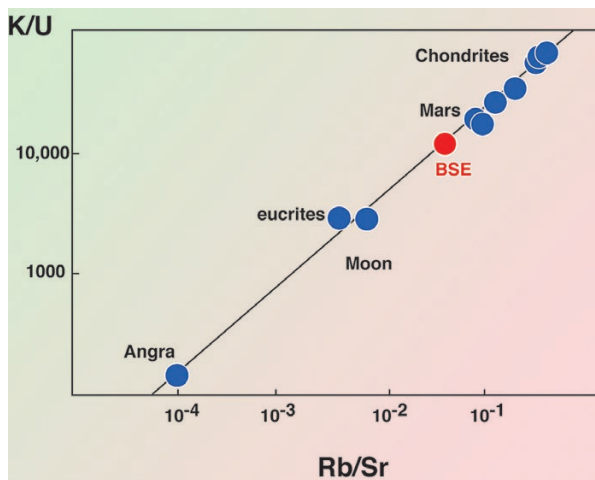


**Figure 1.7**

The K/U ratio plotted against the Rb/Sr ratio in different objects of the Solar System. This figure shows that Earth (BSE for Bulk Silicate Earth) is strongly depleted in moderately volatile elements such as K and Rb (U and Sr being refractory elements). Earth is therefore expected to be depleted in very volatile elements, including noble gases.



The second section summarises the knowledge we have on the noble gases in the primordial material, sampled by chondrites or by the Sun. Helium systematics will be described in Section 3, but without a detailed discussion on the origin of the measured helium isotopic ratios in oceanic basalts. I consider that the discussion on the mantle structure and origin of the atmosphere cannot be derived only from the helium systematics. For me, this makes no sense and I hope the reader will understand that my approach considers *all* the noble gases, and not only helium, in order to constrain the origin of volatiles on Earth and the mantle structure. This is why in Sections 4 and 5, I will describe the mantle geochemistry of Ne, Ar and Xe. Sections 6 and 7 focus on the discussion on the existence of a deep and primordial reservoir for noble gases, and on the possible recycling of atmospheric noble gases into the deep mantle. Section 8 gives the general idea of how and when the Earth and other terrestrial planets acquired their volatiles. I emphasise the relative contribution of the internal and external sources of volatiles and the issue of the closure of the Earth's atmosphere.



## 2.1 Introduction

This section presents a quick overview of the noble gas geochemistry in meteorites, as building blocks of the Earth. The Paris Group never analysed meteorites for two main reasons. The first is that the noble gas concentrations in meteorites are orders of magnitude higher than those of terrestrial samples, which were the main interest of the Paris group at that time (1980-2000). Therefore, contamination and memory effects were a major concern. The second, in my opinion, is that *Claude Allègre*, who likes simple ideas, was not really enthusiastic about the complexity of the noble gas systematics in meteorites.

In this section, I will provide my own view of noble gas cosmochemistry, with the idea of using it to help understand the origin of volatiles on Earth.

The relationship between chondrites and the Earth, so important for refractory elements, is not evident for highly volatile elements such as the noble gases. The Earth is depleted in moderately volatile elements such as K, Rb and Pb (e.g., Albarède, 2009 and Fig. 1.7), and therefore the Earth is expected to be highly depleted in noble gases compared to chondrites. Chondrites are themselves extremely (by a few orders of magnitudes) depleted in noble gases compared

to their solar abundances. To illustrate this depletion, Figure 2.1 shows the elemental abundances in C1 chondrites normalised to their solar abundances (Grevesse *et al.*, 2005). Noticeably He, Ne, Ar (and Kr-Xe, not shown) are depleted by orders of magnitude in C1 chondrites relative to the sun. Figure 2.2 represents the normalised noble gas element ratios in carbonaceous chondrites and the Earth's atmosphere relative to the solar elemental ratio and to  $^{36}\text{Ar}^{12}$ . Data from the carbonaceous chondrites presented in this figure are derived from the legendary

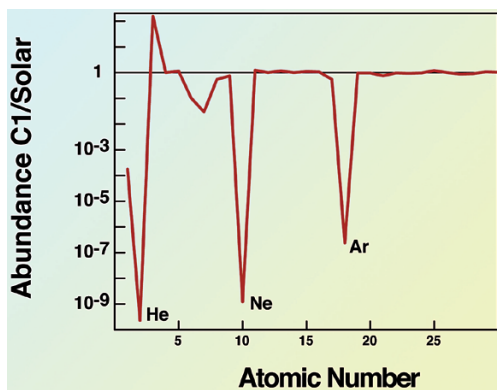


**Figure 2.1** Elemental abundances in C1 chondrites normalised to solar abundances. Data from Grevesse *et al.* (2005). This figure shows the extreme depletion in noble gases in C1 due to their high volatility.

12. Such a diagram is double normalised. It provides a readable scale and avoids bias from concentration variations between samples.



Mazor publication which analysed a large quantity of chondrites for all noble gases (Mazor *et al.*, 1970). The samples used in this figure were melted without chemical treatment, providing bulk measurements. (In many studies performed since Lewis *et al.* (1975), prior chemical treatment has been used to isolate specific carriers of noble gases, such as phase Q, discussed below, but this approach does not provide a representative average of the whole meteorite). Heavy noble gases are enriched in chondrites relative to their solar composition (Fig. 2.2). Perhaps somewhat confusingly, this pattern is often referred as “planetary”. For comparison, the elemental compositions of phase Q, which is the main heavy noble gas carrier (<sup>13</sup> and see later in this section), is represented on Figure 2.2 (values from Busemann *et al.*, 2000).

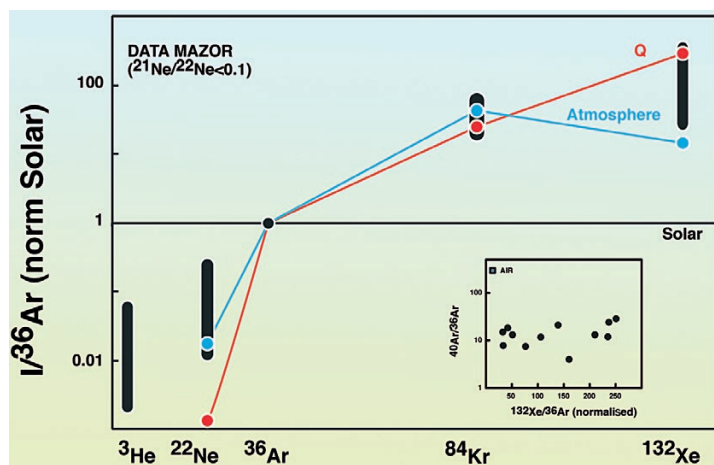


**Figure 2.2**

Noble gas element ratios measured in bulk carbonaceous chondrites normalised to their solar elemental ratios (e.g.,  $(^{22}\text{Ne}/^{36}\text{Ar})_{\text{sample}}/(^{22}\text{Ne}/^{36}\text{Ar})_{\text{solar}}$ ). Data from Mazor *et al.* (1970) for chondrites (but only chondrites with  $^{21}\text{Ne}/^{22}\text{Ne}$  lower than 0.1 are plotted to minimise the influence of cosmogenic He and Ne contributions, produced by interactions of the meteorite with cosmic rays on their journey to Earth) and Busemann *et al.* (2000) for the composition of phase Q, the main carrier of heavy noble gases in chondrites. The inset shows the  $^{132}\text{Xe}/^{36}\text{Ar}$  versus  $^{40}\text{Ar}/^{36}\text{Ar}$  ratios of the selected samples. No atmospheric contamination of the samples can be observed, which could explain the large spread of  $^{132}\text{Xe}/^{36}\text{Ar}$ . The Earth’s atmosphere shows a depletion in xenon, which is known as the “missing xenon”.

Please note the deficit in xenon in the Earth’s atmosphere compared to the chondrites and relative to other rare gases. This xenon depletion on Earth, dubbed the “missing xenon”, is particularly obvious compared to the elemental ratios in

13. Phase Q is the name of the main carrier of heavy noble gases in chondrites. It is a carbonaceous phase with an origin that is still debated. This component can be isolated from the chondrites by HF/HCl digestion.



phase Q. This “missing xenon” will be discussed in Section 8 because it provides essential constraints on the physical processes that affected the Earth’s atmosphere after its formation. Such depletion is also observed in the atmospheres of Mars and Venus, and therefore this “missing xenon” seems to be a characteristic of terrestrial planets.

Having established the overall features of elemental abundances I will now investigate the isotopic compositions of key components in the Solar System. Since the mass of the Solar System is overwhelmingly concentrated in the Sun, the logical approach is to look first at solar compositions and to compare the noble gas compositions of chondrites and terrestrial planets to these as a reference.

## 2.2 Elemental and Isotopic Ratios in the Sun: the Bulk Solar System Composition

The composition of the Sun has been derived mainly from four categories of samples. The first category is lunar soil recovered by Apollo astronauts, which was exposed to the solar wind for long time periods (e.g., Eberhardt *et al.*, 1972; Benkert *et al.*, 1993; Wieler and Baur, 1994; Rider *et al.*, 1995). Secondly, gas rich meteorites, presumed to be regoliths, are useful samples for the determination of the solar wind composition (e.g., Wieler *et al.*, 1989). Thirdly, the Genesis mission probe targets were exposed for more than 2 years, starting in 2001, to the solar wind and analyses were performed on these targets in several laboratories after their recovery in 2004 (e.g., Grimberg *et al.*, 2006; Grimberg *et al.*, 2008; Heber *et al.*, 2009; Pepin *et al.*, 2012; Meskik *et al.*, 2007; Heber *et al.*, 2012). Finally the atmosphere of Jupiter is assumed to have captured a representative portion of the solar nebula on formation and so provides a useful datum for Solar System gas composition.

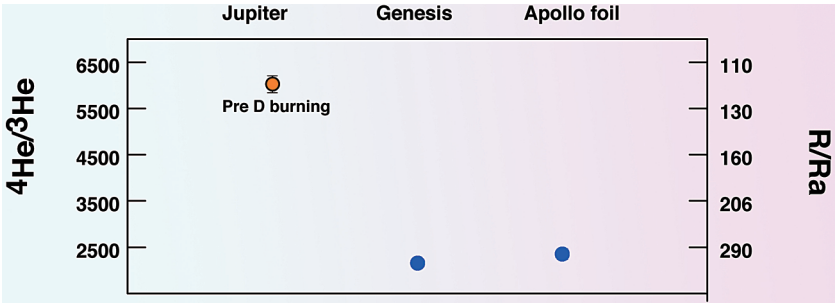


**Figure 2.3** The helium isotopic composition of Jupiter and solar wind (genesis and Apollo foil). Data from Geiss *et al.* (1972), Mahaffy *et al.* (1998) and Heber *et al.* (2009). The Jupiter helium isotopic ratio represents the initial composition of the Solar System. The solar ratio reflects the D burning via nuclear fusion, producing  $^3\text{He}$ .  $R/R_a$  is the  $^3\text{He}/^4\text{He}$  normalised to the atmospheric ratio.



Figure 2.3 shows the helium isotopic ratios of the solar wind as measured on Genesis targets, on Al foil targets exposed during the Apollo missions (*e.g.*, Geiss *et al.*, 1972), and in Jupiter as measured by a quadrupole mass spectrometer installed on the Galileo probe (Mahaffy *et al.*, 1998). The difference between the solar wind and the Jovian helium isotopic ratios is explained by deuterium (D) burning in the Sun, which has enriched the Sun in  $^3\text{He}$  by nuclear fusion of H and D post the accretion of nebula gas to form Jupiter. Therefore, the  $^4\text{He}/^3\text{He}$  ratio measured in Jupiter should better reflect the primordial composition of the Solar System, although it might not be the initial composition of the Earth if terrestrial helium reflects solar wind implantation in building blocks rather than the dissolution of dense primordial atmosphere into a magma ocean (see Section 8). For comparison, the lowest  $^4\text{He}/^3\text{He}$  ratio measured in mantle-derived rocks is 15,000 (Stuart *et al.*, 2003) and reflects the production and accumulation of  $^4\text{He}$  by radioactive decay of U and Th over the lifetime of the Earth.

Studies on neon and argon implanted in the Genesis targets were performed and have provided incredible results, although these are not always consistent with each other (*e.g.*, Grimberg *et al.*, 2006; Meshik *et al.*, 2007; Grimberg *et al.*, 2008; Heber *et al.*, 2009; Pepin *et al.*, 2012). Elemental and isotopic ratios of He, Ne, and Ar have been precisely determined on the Genesis targets (Fig. 2.4). One of the difficulties in determining solar wind isotopic ratios is that implantation fractionates isotopes, and when it is coupled with sputtering and backscattering, the resulting isotopic ratios are very different from the implanting solar wind (Grimberg *et al.*, 2006; Raquin and Moreira, 2009). Since it depends on knowledge of the solar wind implantation mechanism, determination of the solar wind composition can be tricky. The isotopic compositions determined on Genesis targets are considered to correspond to the present-day solar wind isotopic ratios for He, Ne and Ar. The Xe isotopic ratios were also measured on Genesis targets and confirmed results on the lunar soil analyses (Crowther and Gilmour, 2012; Eberhardt *et al.*, 1972; Wieler and Baur, 1994; Pepin *et al.*, 1995; Rider *et al.*, 1995). A detailed review of the elemental and isotopic compositions in the Sun, albeit written before the return of the Genesis samples, can be found in Wieler (2002).

Finally, it should be noted that the solar wind composition can be elementally and isotopically fractionated compared to the solar composition, which complicates the determination of the bulk solar system composition (*e.g.*, Heber *et al.*, 2012).

## 2.3 The Origin of the Ubiquitous “Phase Q” in Meteorites

Meteorites, with the exception of few cases, such as regolith breccia<sup>14</sup>, don’t show solar elemental and isotopic compositions for the heavy noble gases. Figure 2.2 shows that chondrites have elemental ratios that are fractionated compared to the

14. Regoliths are rich in solar noble gases because they were exposed to the solar wind for a long time.



solar ratios. For instance, the  $^{132}\text{Xe}/^{36}\text{Ar}$  is higher by a factor up to 200 compared to the solar ratio. The bulk Xe/Ar and Kr/Xe ratios are variable in carbonaceous chondrites as shown on Figure 2.5, but they are clearly distinct from solar ratios, as the heavy noble gases are enriched. On this figure, I added end-members that will be discussed later, P3, HL, Q, which are the principal noble gas carriers in chondrites (see Ott, 2003, for a review). Analyses of bulk chondrites, however, seem to be a proper approach to obtain the noble gas composition of the Earth's starting blocks. Such analyses provide the mean composition of all the constituents in the meteorite (such as P3, HL, Q), but this technique does not allow the determination of the compositions and the nature of the different noble

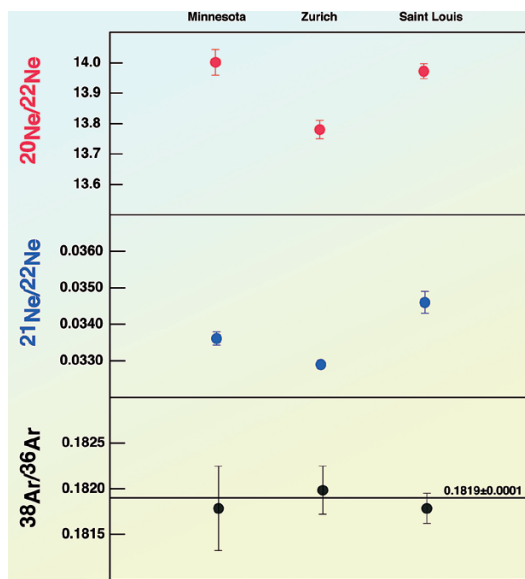


**Figure 2.4**

Noble gas isotopic ratios determined on Genesis targets provide the isotopic ratios of the solar wind. For comparison, the Earth's atmospheric ratios are 9.8 (~12.5 for the mantle), 0.029 and 0.188, for  $^{20}\text{Ne}/^{22}\text{Ne}$ ,  $^{21}\text{Ne}/^{22}\text{Ne}$  and  $^{38}\text{Ar}/^{36}\text{Ar}$ , respectively. The  $^{38}\text{Ar}/^{36}\text{Ar}$  determined by the Zürich (ETH) group was recalculated using the atmospheric ratio of 0.188 to be consistent with other analyses. Data from Meshik *et al.* (2007), Heber *et al.* (2009) and Pepin *et al.* (2012).

gas carriers, and how they behave during thermal or aqueous metamorphism. Interpreting the variations in Figure 2.5 is therefore difficult with bulk analyses alone.

In their ground-breaking article, Lewis and co-authors successfully isolated the host phase of the "strange xenon" they measured in the Allende meteorite (Lewis *et al.*, 1975). This work is the precursor of a long series of publications on the study of the noble gas carrier in meteorites, which I will summarise here.

Lewis *et al.* (1975) showed that heavy noble gases are carried in chondrites by a phase that remains after an HCl/HF attack (Fig. 2.6)<sup>15</sup>. The residue of this acid attack represents a small mass fraction (~1%) of the bulk meteorite, but

15. These successive acid attacks allow the extraction of different noble gas carriers from the meteorites. HCl/HF dissolves the silicate minerals that constitute the bulk of the chondrite, leaving behind only phases that are resistant to this strong acid digestion.



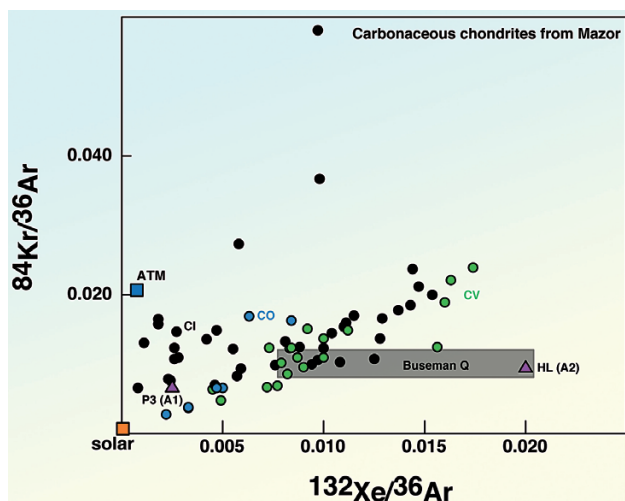


**Figure 2.5**

Noble gas elemental ratios in carbonaceous chondrites (grouped by petrographic CI, CM and CV sub-divisions) analysed by bulk fusion. Data from Mazor *et al.* (1970). The grey area represents the composition of the phase Q, the main carrier of heavy noble gases (Busemann *et al.*, 2000). The solar composition is from Heber *et al.* (2009) and the other components are from Ott (2002).

carries most of the heavy noble gases. This component was named “phase Q” by Lewis *et al.* (1975), where the letter Q stands for Quintessence. It has been shown that this phase Q has a carbonaceous nature (~kerogen), although its origin is debated (Lewis *et al.*, 1975; Ott *et al.*, 1981; Vis and Heymann, 1999; Busemann *et al.*, 2000; Gardinier *et al.*, 2000; Marrocchi *et al.*, 2005). Figure 2.7 shows the xenon isotopic ratios measured by Huss *et al.* (2003) during successive acid attacks on carbonaceous chondrites. The HCl/HF attack residue shows a mixture between two components, one being the phase Q, and the second being pre-solar grains (named here HL because of their peculiar Xe isotopic ratios), and is better observed on the residue after a further  $\text{HNO}_3$



Photo credit: Yves Marrocchi (CRPG, Nancy, France).

**Figure 2.6**

Residue after HF-HCl attack of a piece of a carbonaceous chondrite. The residue is the main carrier of heavy noble gases in chondrites and represents only a small fraction of the bulk meteorite. This residue also contains pre-solar grains.



attack (see the compositions of ‘etched residues’ in Fig. 2.7). This figure clearly illustrates that the xenon in carbonaceous chondrites is mainly carried in two solids: the phase Q and pre-solar grains, although phase Q is volumetrically by far the dominant component. Phase Q is observed in all chondrites (ordinary, carbonaceous and enstatite) (e.g., Schelhass *et al.*, 1990; Patzer and Schultz, 2002; Okazaki *et al.*, 2010).

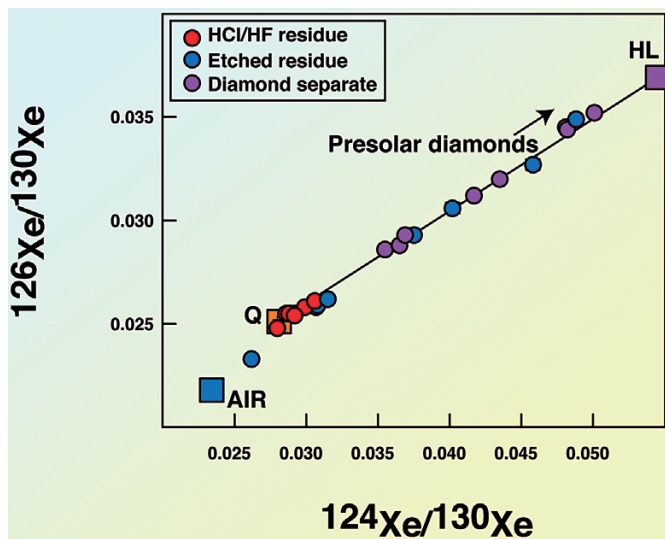


**Figure 2.7**

Three xenon isotope diagram. The three isotopes shown on the figure are stable and non-radiogenic. Chemical attacks on bulk chondrite allow the isolation of the two components carrying the xenon. The HCl/HF residue contains the phase Q and pre-solar grains and shows a mixture between these two components. Etching of this residue using  $\text{HNO}_3$  yields a further residue that comprises pre-solar grains with a distinctive isotopic composition that has been named “HL” (data from Huss *et al.*, 2003).

Figure 2.8 shows the elemental ratios of heavy noble gases in ordinary chondrites for the bulk meteorite together with their HCl-HF and  $\text{HNO}_3$  residues (from Schelhass *et al.*, 1990). This illustrates that argon in bulk chondrites is not entirely in phase Q (the residue of HCl-HF) or in pre-solar grains (the residue of  $\text{HNO}_3$  on phase Q). A third component, which is removed during HF-HCl attack, contains a large proportion of argon. For example, Schelhass *et al.* (1990) showed that in ordinary chondrites, the residue of HF/HCl attack is only ~1% of the bulk chondrite mass, but contains between 8 and 24% of the trapped  $^{36}\text{Ar}$  present in the meteorites, between 21 and 34% of the  $^{84}\text{Kr}$ , and between 30 and 72% of  $^{132}\text{Xe}$ . Therefore, although phase Q is one of the main carriers of heavy noble gases in chondrites, it is not the only one.



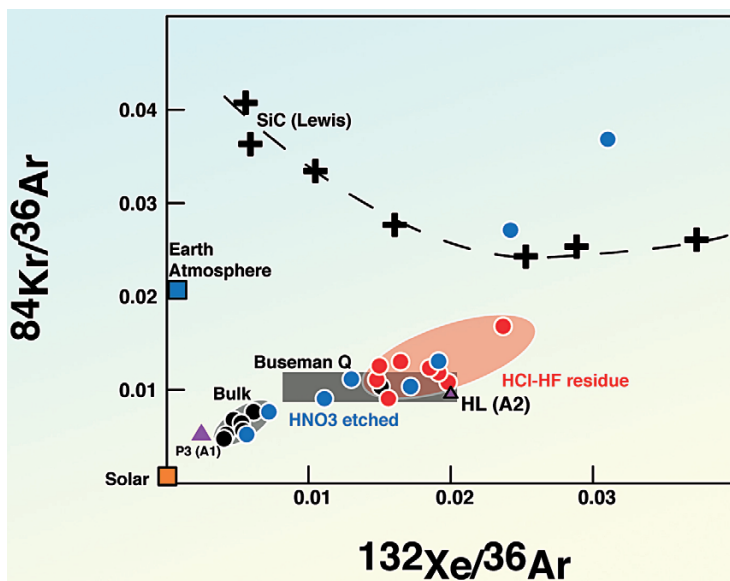


**Figure 2.8**

Noble gas elemental ratios in ordinary chondrites. Data from Schelhass *et al.* (1990); SiC (crosses) data from Lewis *et al.* (1993). The phase Q composition is derived from Busemann *et al.* (2000). A<sub>1</sub> and A<sub>2</sub> compositions from Ott (2002). This figure shows that the bulk samples contain a component rich in argon in addition to the phase Q, represented by the grey area.

The observed elemental and isotopic compositions of phase Q show that noble gases in phase Q are not solar (Figs. 2.5, 2.8 and 2.9). Phase Q has high xenon concentration, almost no He and Ne, and relatively high Ar and Kr abundances.

The Xe isotopic composition of Q is also mass-dependently fractionated compared to the solar composition (Fig. 2.9). The fractionation of the  $^{124}\text{Xe}/^{130}\text{Xe}$  ratio relative to the solar ratio is  $\sim 5\%$ <sup>16</sup>. Xenon is a heavy element, and therefore cannot be strongly isotopically fractionated except under special physical conditions. Two main physical processes were proposed to explain the elemental composition and the peculiar, fractionated isotopic ratios of Q. The first is ion implantation (*e.g.*, Bernatowicz and Hagee, 1987; Fig. 2.10). Alternatively, adsorption of xenon ions can also produce xenon isotopic fractionation (*e.g.*, Marrocchi *et al.*, 2011, and Fig. 2.11). Both processes are able to produce a similar isotopic fractionation to the one observed in the Phase Q, although not perfectly.

16. Xenon is fractionated isotopically by  $\sim 1.3\%$  amu<sup>-1</sup> in phase Q compared to the solar composition.

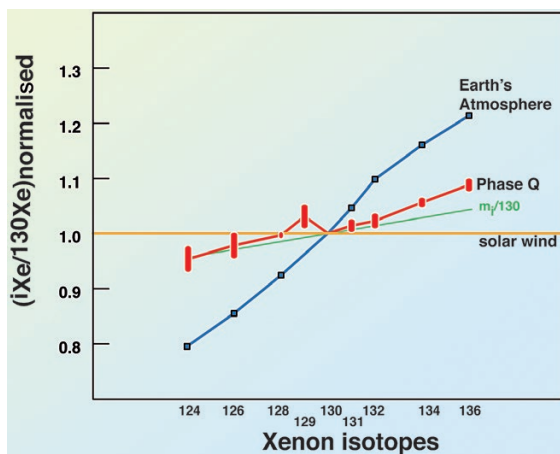


**Figure 2.9**

The xenon isotopic composition of phase Q normalised to the solar wind composition. Earth's atmosphere is given for comparison. Data for phase Q from Busemann *et al.* (2000). The fractionation that produced the xenon isotopic composition of phase Q is clearly mass-dependent. The  $^{129}\text{Xe}$  peak reflects the radioactivity of now extinct  $^{129}\text{I}$ , which has a half-life of 17 Ma. The green line represents the  $m_i/130$  line where  $m_i$  is the isotope mass. This suggests that phase Q-Xe derives from simple mass fractionation from the solar composition, to which is added radiogenic and fissionogenic xenon.

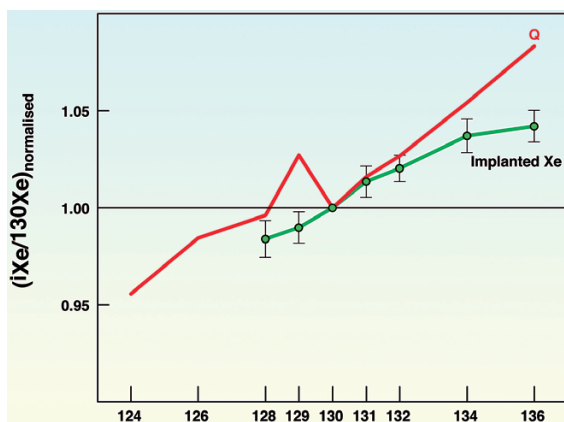


**Figure 2.10**

Isotopic fractionation of the xenon (iXe) during implantation in activated charcoal of low energy ions produced during cathodeless glow discharges. It shows that ion implantation from the solar wind can be a possible origin of the peculiar xenon isotopic composition of the phase Q (modified from Bernatowicz and Fahey, 1986).





An important constraint on the origin of phase Q is its noble gas elemental compositions. Figure 2.8 suggests that the high Xe/Kr and Xe/Ar ratios compared to the solar ratios reflect adsorption at relatively high temperature from the temperature-dependence of the relative absorption of different gases. To illustrate how adsorption on activated charcoal at low temperatures can fractionate noble gases. Figure 2.12 shows desorption curves of noble gases obtained in Paris on activated charcoal using a cryogenic cold head able to produce temperatures as low as 10 °K. At temperatures of 200-250 °K, the high Xe/Kr and Xe/Ar ratios observed in Q can be obtained on activated charcoal. Trapping temperatures cannot be too low; otherwise these two ratios would not be fractionated compared to the starting gas composition, as all gases are adsorbed. Such a process can explain the relative noble gas concentrations in phase Q if one considers that solar gas was adsorbed on carbonaceous phases at relatively high temperatures compared to that expected far from the Sun (~50 °K). Such a simple process can, however, not explain the isotopic fractionation observed since adsorption of neutral gases cannot fractionate isotopes. However, if xenon is ionised, it appears that a mass fractionation occurs during adsorption and can produce the xenon isotopic pattern of phase Q Marrocchi *et al.* (2011) (Fig. 2.11).

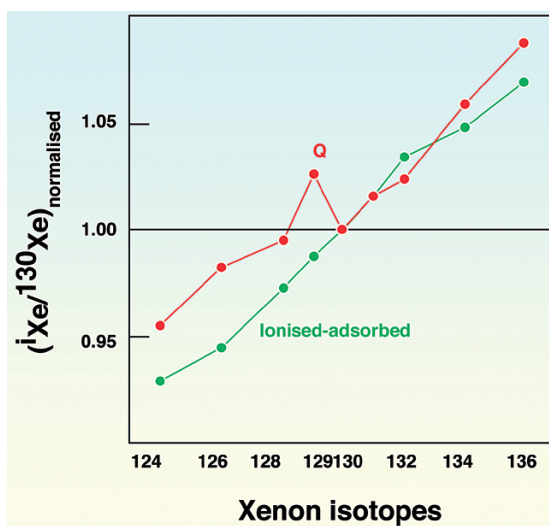


**Figure 2.11**

Marrocchi *et al.* (2011) proposed that adsorption of xenon ions produced in a radio-frequency plasma is a mechanism able to explain the peculiar xenon isotopic composition of phase Q. Similar experiments with neutral atoms were not capable of producing such isotopic fractionations. Adsorption is also a process that reproduces the elemental composition of noble gases in phase Q. Marrocchi *et al.* (2011) propose that UV radiation, produced by either nearby stars or by the young sun are able to ionise xenon, resulting in a fractionated isotopic composition after trapping on the surface of growing organic grains.  $^{129}\text{Xe}$  refers to the isotope i (124, 126 ...).



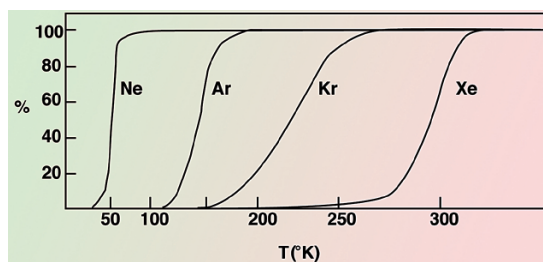


**Figure 2.12** Desorption curve of noble gases on activated charcoal obtained in Paris using a cryogenic trap represented as the percentage of gas that is desorbed. In order to adsorb only xenon, temperatures above 280 °K are necessary. This is true for neutral atoms (from Sarda, 1991).

As matters stand, I cannot choose between the two proposed processes (implantation vs adsorption of ions). From the point of view of elemental ratios, adsorption is more appealing, but from the isotopic point of view, solar wind implantation is also credible.

An essential feature of the xenon composition in chondrites is the resistance of phase Q to thermal metamorphism (Fig. 2.13), suggesting that this composition should have been present on Earth's parent bodies, unless they were melted and degassed, in which case the gas would be lost from small planetary bodies. As shown on Figure 2.13, whatever the type of chondrite, the Q composition is observed for xenon, although the Xe concentration decreases with the increasing thermal metamorphism (Schelhass *et al.*, 1990; Huss *et al.*, 1996). Busemann and Eugster (2002) have also proposed that Xe-Q is observed in achondrites (which have undergone melting), suggesting it is a very resistant component in meteorites.

In Section 7, evidence for the presence of a component having a composition similar to the one of Q in Earth's mantle will be discussed.

## 2.4 The Neon Alphabet

I give special attention to neon systematics for sentimental reasons; I did my PhD on the neon in oceanic basalts. Neon provides important constraints on the origin of volatile elements on Earth because it has a solar-like composition in the Earth's mantle, different from the mean chondritic composition. In this section, I briefly discuss what we call the neon alphabet because historically, in the three-neon-isotope diagram ( $^{20}\text{Ne}$ ,  $^{21}\text{Ne}$ ,  $^{22}\text{Ne}$ ), letters designate the end-members. These end-members correspond to real carriers, which may either be pre-solar grains or the carbonaceous phase Q, or they correspond to physical processes such as spallation or as we will see for the so-called "neon B", implantation of solar wind.



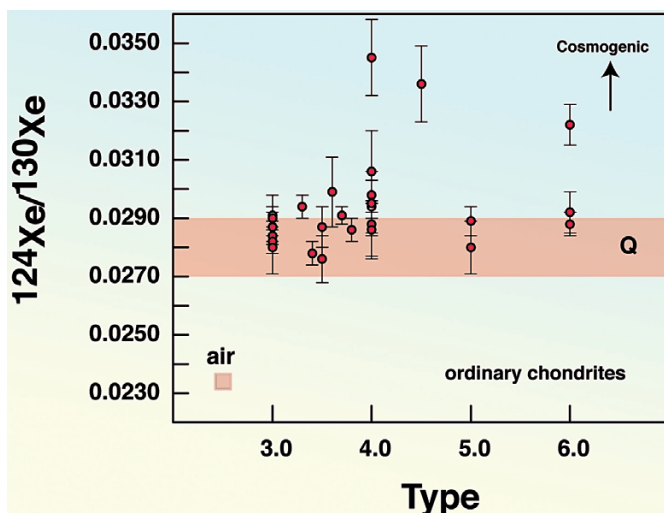


**Figure 2.13**  $^{124}\text{Xe}/^{130}\text{Xe}$  ratio in ordinary chondrites as a function of thermal metamorphism, which increases with grade from 3 to 6. Phase Q-Xenon is present in all ordinary chondrites suggesting it is resistant to thermal metamorphism. Xenon having the Q composition has also been observed in achondrites (Busemann and Eugster, 2002). Variations in the  $^{124}\text{Xe}/^{130}\text{Xe}$  ratio reflect a mixture between the phase Q and cosmogenic compositions. Moreover, please note that the bulk xenon concentration decreases with the thermal metamorphism.

### 2.4.1 Neon A: pre-solar diamonds

As we have seen above, pre-solar grains are found in the matrix of carbonaceous, ordinary, and enstatite chondrites. These grains show very specific isotopic anomalies of Kr and Xe relatively to the Sun. This is also true for neon, especially for the two end-members historically termed neon A and E (Black, 1972). A recent nomenclature of all the end-members and components observed in meteorites can be found in Ott (2002). Figure 2.14 shows the neon isotopic compositions obtained by fusion of representative samples of different classes of chondrites. These compositions indicate a ternary mixing whose end-members are neon A ( $^{20}\text{Ne}/^{22}\text{Ne} \sim 8.5$ ), cosmogenic neon ( $^{20}\text{Ne}/^{22}\text{Ne} \sim 1$ ), and an end-member named neon B ( $^{20}\text{Ne}/^{22}\text{Ne} \sim 12.5$ ), which we will discuss below which is certainly derived from solar wind irradiation. It is very difficult to see in this diagram if the neon Q (from phase Q) contributes to the bulk neon. Figure 2.2 shows that phase Q does not contain light noble gases and therefore, this carrier is not a significant contributor to the bulk neon. Only pre-solar-grains and the implanted solar wind are substantial sources of neon. Even if it is probably a non-exhaustive sampling of chondrites, we can extricate several important pieces of information



from Figure 2.14. The first observation is that ordinary, rumuruti, and enstatite chondrites are less influenced by the neon A. This suggests they contain fewer pre-solar grains than carbonaceous chondrites or they were made of material that was more influenced by the solar wind irradiation because they accreted closer to the sun; the solar wind being the source of neon B.

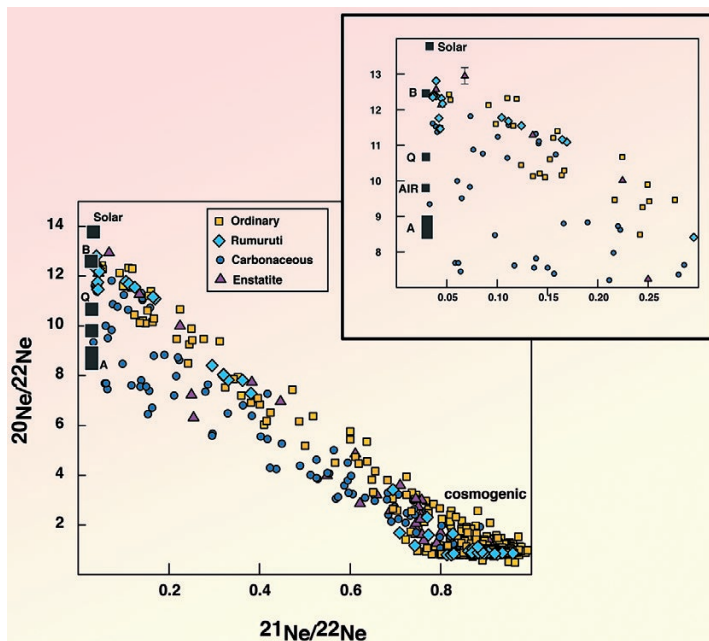


**Figure 2.14**

Three neon isotope diagram showing the neon composition of chondrites. The insert shows the names of the different end-members represented by black squares (A, B, Q, atmosphere). The cosmogenic end-member is the isotopic composition of the neon produced by spallation of the major elements of the meteorites. This component is secondary and does not reflect a primordial component. Data from Patzer and Schultz (2001), Schultz *et al.* (2005), Mazor *et al.* (1970), Schultz and Franke (2004) and Schelhass *et al.* (1990).

Figure 2.15 focuses on carbonaceous chondrites and shows the neon isotopic composition of the different sub-classes of carbonaceous chondrites. We observe that CV chondrites are influenced more by neon B than the CI chondrites, which are closer in composition to neon A. Other carbonaceous chondrites show a mixture between these two end-members, to which cosmogenic neon is added. It seems that it would be inaccurate to say that the carbonaceous chondrites have a neon composition of type A only. We see instead a great variability between the two components A and B within the carbonaceous chondrites. It is however correct to say that the other chondrites contain a higher proportion of neon B.



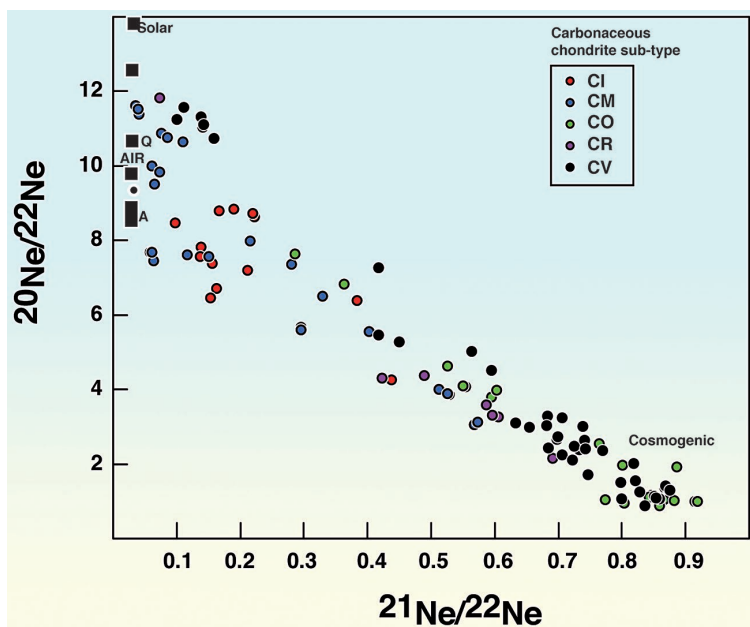


**Figure 2.15** Three neon isotope diagram in which only carbonaceous chondrites are represented (CI, CM, CO, CR, CV are different sub-types of carbonaceous chondrites). They are distinguished following their sub-classes. Data from Schultz and Franke (2004); only bulk analyses are used. A ternary mixing is clearly visible on this figure.

#### 2.4.2 The component B in meteorites: the result of solar wind implantation

The compositions most of what are called “gas-rich” meteorites (*e.g.*, with  $^4\text{He}$  concentrations higher than  $10^{-3} \text{ cm}^3 \text{STP g}^{-1}$ ) also suggest a mixing between three components; one a cosmogenic end-member (with  $^{20}\text{Ne}/^{22}\text{Ne}$  and  $^{21}\text{Ne}/^{22}\text{Ne} \sim 1$ ), and the two others having high  $^{20}\text{Ne}/^{22}\text{Ne}$  ( $\sim 12.5$  and  $8.5$ , for neon B and A, respectively) and low  $^{21}\text{Ne}/^{22}\text{Ne}$  (see Fig. 2.16). As discussed earlier these gas-rich meteorites are thought to be planetesimal regoliths that contain a large solar wind component. Before the Genesis probe returned and the analyses of neon isotopic ratios in its targets exposed to solar wind, it was believed that neon B was the mixture of two solar wind components: “normal” solar wind with a ratio of  $\sim 13.8$  and the solar energetic particles (SEP, *e.g.*, flares) with a ratio of  $\sim 11.5$ . This mechanism involving SEP is now challenged because it was not observed on Genesis targets (Grimberg *et al.*, 2006; Wieler *et al.*, 2007) and now it is proposed that neon B is a component by itself, which reflects the solar wind implantation coupled to sputtering (“erosion”) effects (Raquin and Moreira, 2006).



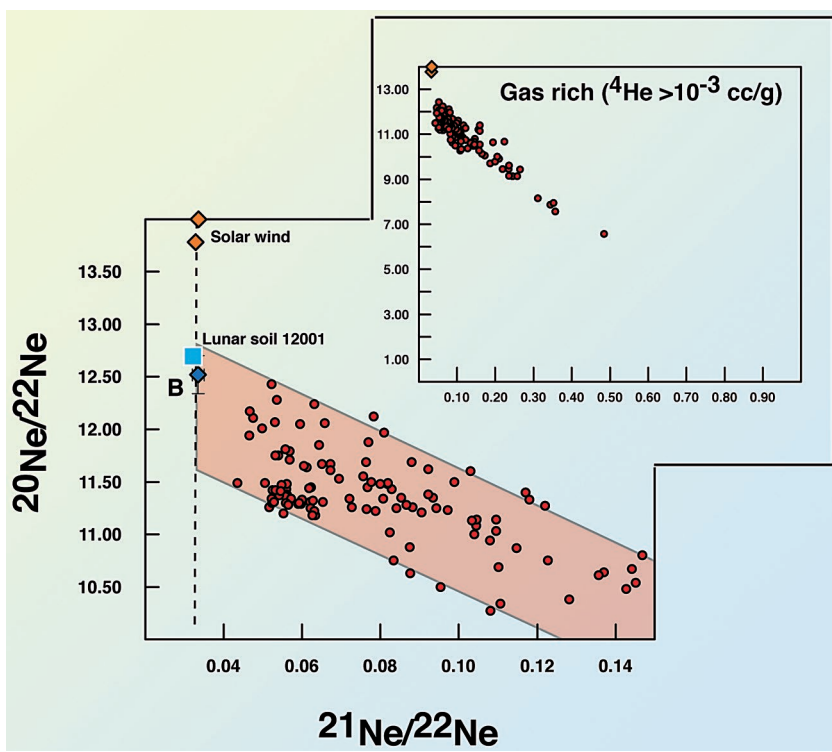


**Figure 2.16** Three neon isotope diagram of gas rich meteorites showing the neon B end-member interpreted as solar wind implantation. Data from Schultz and Franke (2004). Lunar soil estimates are taken from Eberhardt *et al.* (1972) and are discussed in the text.

Neon B has an estimated  $^{20}\text{Ne}/^{22}\text{Ne}$  ratio of  $12.52 \pm 0.18$  (Black, 1972) obtained from the deconvolution of meteorite neon measurements. It is not, strictly speaking, a primordial component, since it was certainly added by solar wind during the accretion of these bodies, or after their accretion, during regolith formation, as observed on lunar samples. Figure 2.1 has shown that chondrites are very depleted in noble gases compared to the solar wind. Therefore, any irradiation by the solar wind will provide a large quantity of solar-like noble gases in any refractory dust. Because this implantation process affects only the surface of the exposed objects, the incorporation of large quantities of solar gases occurs only on large surface/volume objects, *i.e.* dust (up to a few  $\mu\text{m}$ ). Then irradiated dust will contain sufficiently solar-like noble gases so any object that accreted such dust will have solar-like He, Ne, and may be Ar isotopic compositions.





My PhD student *Aude Raquin* and I proposed a model to explain the neon B value (Raquin and Moreira, 2009). This model suggests that neon B is the steady state value of the solar wind implantation coupled to sputtering. Ions from solar wind have the same speed, which is the escape velocity from the Sun. Therefore, ions with different masses have different kinetic energies, and the heaviest isotopes are implanted deeper than the lighter ones (see Fig. 2.17). This produces an isotopic fractionation since the deepest layers of the exposed target

have lower  $^{20}\text{Ne}/^{22}\text{Ne}$  ratios than the bulk sample and the surface (Fig. 2.17). If there is a sputtering effect (“erosion”), the superficial layers of the samples are removed, which contain neon enriched in light isotopes, leading to a residue that is enriched in heavy isotopes, once believed to be the SEP component. A steady state can be reached after a time that depends mainly on the sputtering rate, which is on the order of  $10^{-11}$  m  $\text{a}^{-1}$ . In our publication, we showed that the steady state  $^{20}\text{Ne}/^{22}\text{Ne}$  ratio can simply be expressed by the isotope mass ratio multiplied by the solar wind ratio, for large samples ( $>10\text{ }\mu\text{m}$ )<sup>17</sup>. Using the solar wind value of Heber *et al.* (2009), we obtain for the steady state value, a  $^{20}\text{Ne}/^{22}\text{Ne}$  ratio of 12.53, exactly the neon B value determined by Black (1972). Nevertheless, using Pepin’s recent measurement (Pepin *et al.*, 2012), the steady state  $^{20}\text{Ne}/^{22}\text{Ne}$  ratio is 12.72 (Fig. 2.18), similar to the neon isotopic ratios measured on grains from the lunar soil, which were exposed for a very long time to the solar wind (*e.g.*, Eberhardt *et al.*, 1972; Benkert *et al.*, 1993) as shown in Figure 2.19. Whatever the exact ratio of the solar wind, we proposed that the steady state value is indeed neon B, either the historical Black’s value of  $12.52\pm0.18$ , or my preferred ratio, estimated from Eberhardt’s lunar soil results, of  $\sim12.7$  (Fig. 2.19) (Eberhardt *et al.*, 1972).

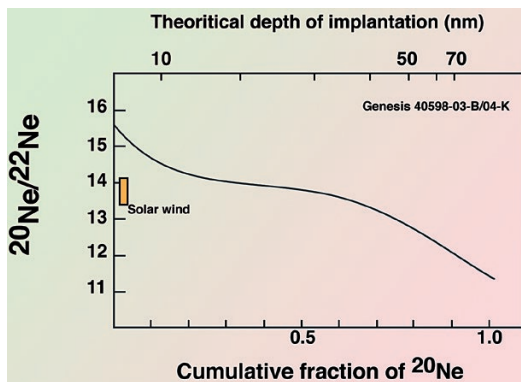


**Figure 2.17** Simplified neon profile in a Genesis glass target obtained by etching. This figure shows that the heavy neon isotopes are implanted deeper, which produces an isotopic fractionation that depends on the depth. Implantation depths are estimates according to the SRIM model (modified from Grimberg *et al.*, 2006).

17. We have shown in Raquin and Moreira (2009) that the steady state value of the solar wind implantation, coupled to sputtering is  $m_1/m_2 \cdot R_{\text{SW}}$  where  $m_1$  and  $m_2$  are the masses of the two isotopes  $N_1$  and  $N_2$  ( $R = N_1/N_2$ ).

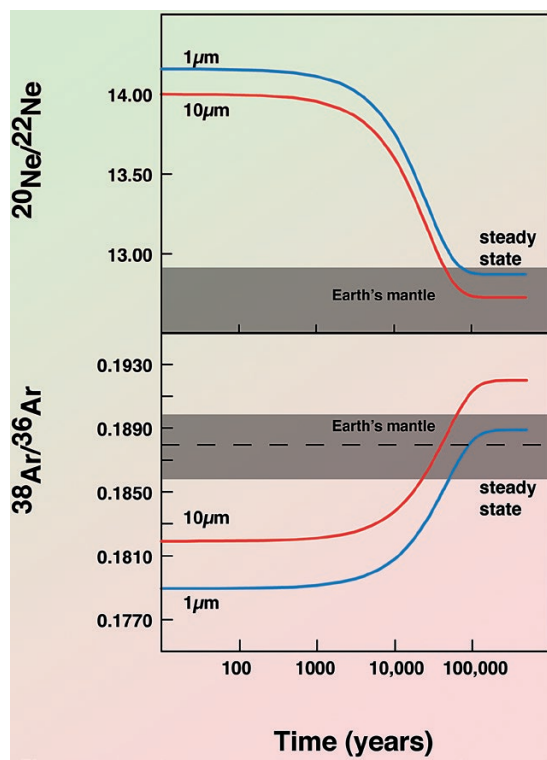


**Figure 2.18**

Example of the calculation of the implantation-sputtering model developed by Raquin and Moreira (2009). The model was applied to the  $^{20}\text{Ne}/^{22}\text{Ne}$  and  $^{38}\text{Ar}/^{36}\text{Ar}$  ratios on dust sizes of 1  $\mu\text{m}$  and 10  $\mu\text{m}$ . The steady state ratio is obtained after a few ka. The Earth's mantle domain is presented for comparison. This will be discussed in Sections 5 and 8. The "erosion" rate was assumed to be 5 nm  $\text{a}^{-1}$ .

Furthermore, the calculation supposes that the time of irradiation is sufficiently long (a few thousand years) to reach steady state, and that the samples are sufficiently large ( $>10 \mu\text{m}$ ). Otherwise, the  $^{20}\text{Ne}/^{22}\text{Ne}$  of the irradiated samples will have a  $^{20}\text{Ne}/^{22}\text{Ne}$  ratio between the theoretical neon B and the solar wind ratios as shown in Figures 2.18 and 2.20. Figure 2.18 shows that, when a grain with a depth of 1  $\mu\text{m}$  is considered rather than 10  $\mu\text{m}$ , the steady state  $^{20}\text{Ne}/^{22}\text{Ne}$  ratio is higher than for larger grains (12.87 vs 12.73, using Pepin's solar neon). This is due to the fact that the heavy neon isotopes are not implanted into the deep layers of the grain since it is too small. So these grains are enriched in light isotopes compared to larger grains. Figure 2.20 explores the possibility that the irradiation time might not be the same

for all grains of a large population. I used a Monte-Carlo technique to calculate the implanted neon isotopic ratios in 1,000 grains that had been exposed to the solar wind for times following the distribution shown in Figure 2.20. Calculation results shown in Figure 2.20 suppose two target sizes (1  $\mu\text{m}$  and 10  $\mu\text{m}$ ). The irradiation times are imposed by a normal law with a mean of 20,000 years and a standard deviation of 10,000 years, which themselves are arbitrary and used only for purposes of illustration. The obtained distributions of  $^{20}\text{Ne}/^{22}\text{Ne}$  ratios in grains of 10  $\mu\text{m}$  and 1  $\mu\text{m}$  are shown in Figure 2.20. Some grains have almost solar ratios whereas others have neon B ratios (steady state) because they were



exposed longer to solar wind. The weighted means are 12.93 and 13.04, respectively, higher than the steady state value of 12.73 obtained for long times and samples larger than 10  $\mu\text{m}$  (in this case using Pepin's solar wind ratio). This simple calculation shows that the neon B has a well-defined isotopic composition under only some simple assumptions (high exposure times and large dust size). If neon B originates from solar wind irradiation, depending on the dust size and time of irradiation, its isotopic composition can be variable with values starting from the neon B value ( $\sim 12.7$ ) to higher ratios (13). Similar calculation can be performed for the  $^{38}\text{Ar}/^{36}\text{Ar}$  ratio (Fig. 2.18) starting from the solar ratio of  $\sim 0.182$  (e.g., Pepin *et al.*, 2012). The steady state  $^{38}\text{Ar}/^{36}\text{Ar}$  ratio is then  $\sim 0.192$  for large grains (10  $\mu\text{m}$ ) and 0.189 for small grains (1  $\mu\text{m}$ ), in agreement with lunar soil grains argon ratios measured by Eberhardt *et al.* (1972) and Benkert *et al.* (1993), although in the case of argon, the cosmogenic contribution might complicate the picture (Fig. 2.21).

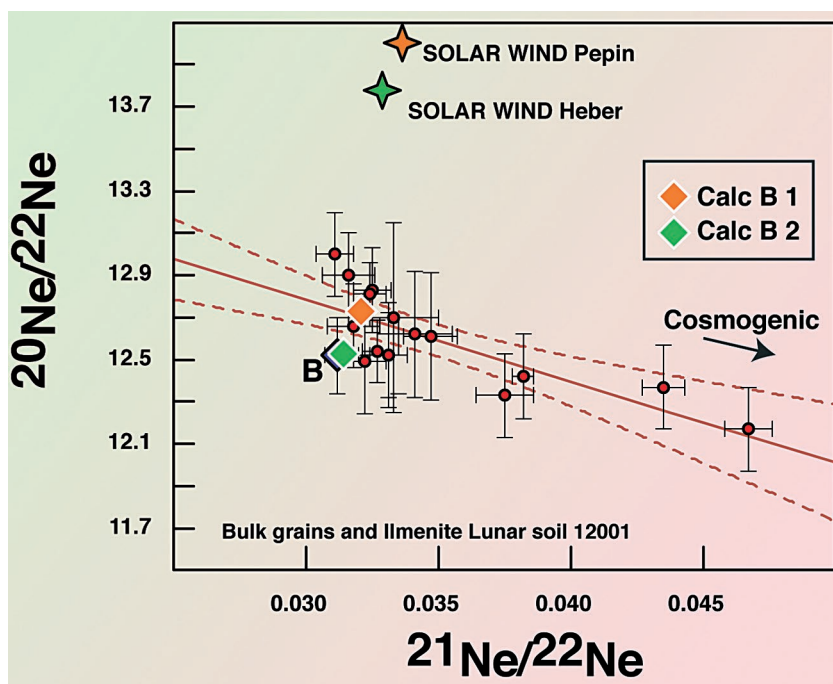


**Figure 2.19**

Neon compositions of grains from the Lunar soil 12001 (Eberhardt *et al.*, 1972). Note that Benkert *et al.* (1993) gives similar ratios for bulk lunar soil 71501 samples. Calculated B1 is the steady state value of the implantation-sputtering model of Raquin and Moreira (2009) using Pepin's neon solar wind ratios (Pepin *et al.*, 2012), whereas calculated neon B2 was obtained using isotopic ratios from Heber *et al.* (2009).



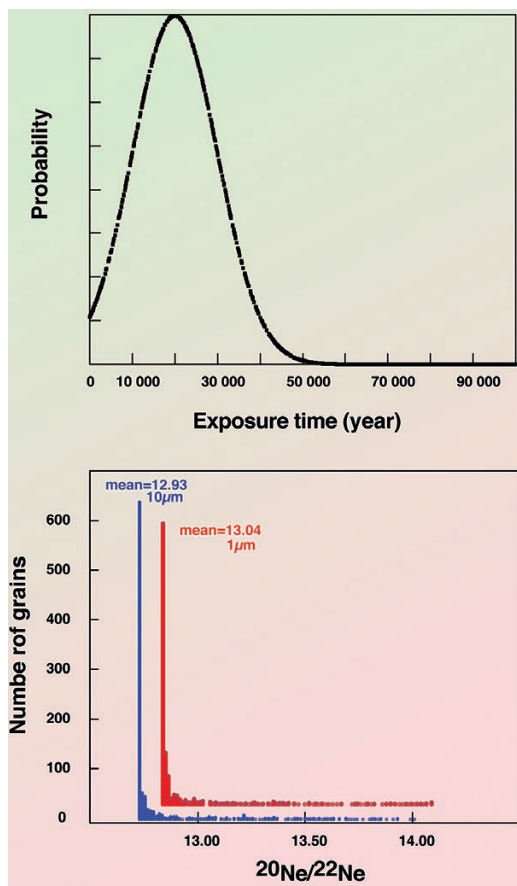


**Figure 2.20** Monte-Carlo simulation of solar wind implantation. This calculation assumes that dust grains are not all exposed to the solar wind for the duration. They have a probability of exposure corresponding to a normal law having here a mean of 20,000 and a standard deviation of 10,000 (top). The steady state ratio is obtained only for long times. Dust exposed for a short time yields a solar isotopic ratio whereas the others show the neon B value (bottom).

I suggest that taking the neon isotopic ratios measured on the lunar soil, determined by Eberhardt *et al.* (1972) for the value of the neon B, rather than Black's value, is the proper approach. It is moreover consistent with the implantation-sputtering model of Raquin and Moreira (2009), when using the recent estimate of Pepin *et al.* (2012) for the solar wind neon ratios. Therefore, I propose using  $12.73 \pm 0.02$ <sup>18</sup> for the neon-B  $^{20}\text{Ne}/^{22}\text{Ne}$  ratio, rather than the ratio of  $12.52 \pm 0.18$  determined by Black (1972). Although it might sound as if these are rather similar values, the precise determination of the neon isotopic ratio produced by the solar wind implantation is important to constrain the origin of the terrestrial neon, as some mantle-derived samples have  $^{20}\text{Ne}/^{22}\text{Ne}$  ratios close to 12.8 (e.g., Yokochi and Marty, 2004; Mukhopadhyay, 2012), higher than the previous estimate for neon B (see Section 4).

18. The uncertainty on this value directly reflects that of the measured neon isotopic ratio in the solar wind ( $\pm 0.02$  for Pepin *et al.*, 2012) but it also depends on whether all grains have the same exposure time and size (e.g., they are all at steady state).



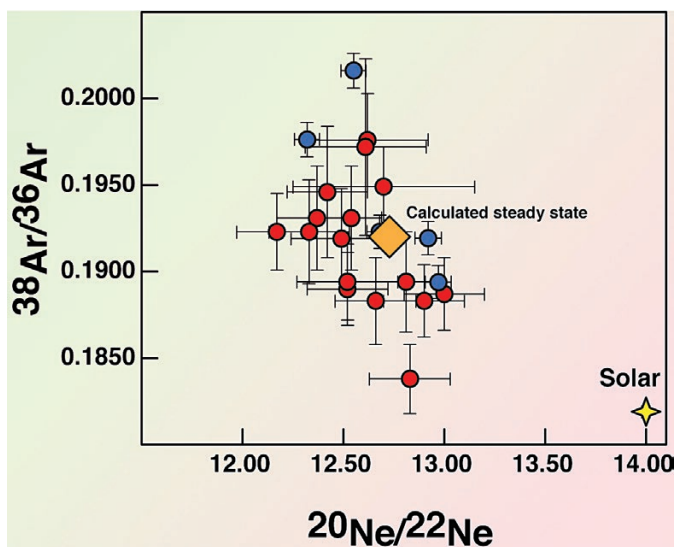


**Figure 2.21**

Ne and argon isotopic composition in the lunar soils. The calculated steady state value is also shown to illustrate the validity of the implantation-sputtering model (large grains of 10  $\mu\text{m}$ ). Lunar soil data from Eberhardt *et al.* (1972) and Benkert *et al.* (1993).

## 2.5 Martian Mantle has a Solar Xenon (or Q) and Earth-like Atmospheric Xenon

SNC meteorites<sup>19</sup> are presumed to come from Mars (Bogard and Johnson, 1983; Bogard *et al.*, 1986). They provide the unique opportunity to constrain the noble gas compositions of both the Martian atmosphere and the mantle (Bogard, 1997; Garrison and Bogard, 1998; Mathew *et al.*, 1998; Terribilini *et al.*, 1998; Mathew and Marti, 2001; Eugster *et al.*, 2002; Swindle, 2002). The Martian atmospheric xenon isotopic composition is similar to that of the Earth's atmosphere (Fig. 2.22). The major difference is for the  $^{129}\text{Xe}/^{130}\text{Xe}$  isotopic ratio, which is much higher in the Martian atmosphere, suggesting either a high  $^{129}\text{I}$  primordial content, or an early formation and degassing. The fact that the two atmospheres have the same xenon isotopic compositions will be discussed in Section 8, as it is an essential constraint on the formation and evolution of terrestrial planet atmospheres. However, what has to be considered seriously, are the results presented in Figure 2.22. These two figures present the xenon isotopic ratios in the Chassigny SNC meteorite.

19. SNC: Shergotty, Nakhla, Chassigny. These meteorites are supposed to come from Mars.



Chassigny, which fell in France in 1815, and is a dunite (olivine rich rock), containing melt inclusions in its olivines. Mathew and Marti (2001) produced a remarkable publication on the xenon isotopic composition of this meteorite. They demonstrated that a component having solar-like xenon composition is present in the Martian interior (Fig. 2.22). The component they named “Chass-S” has a xenon isotopic signature close to that of the solar wind. What I want to show on this figure is that Xe-Q is also a possible composition of the Chass-S end-member. This is particularly true for the olivine-rich samples they analysed.

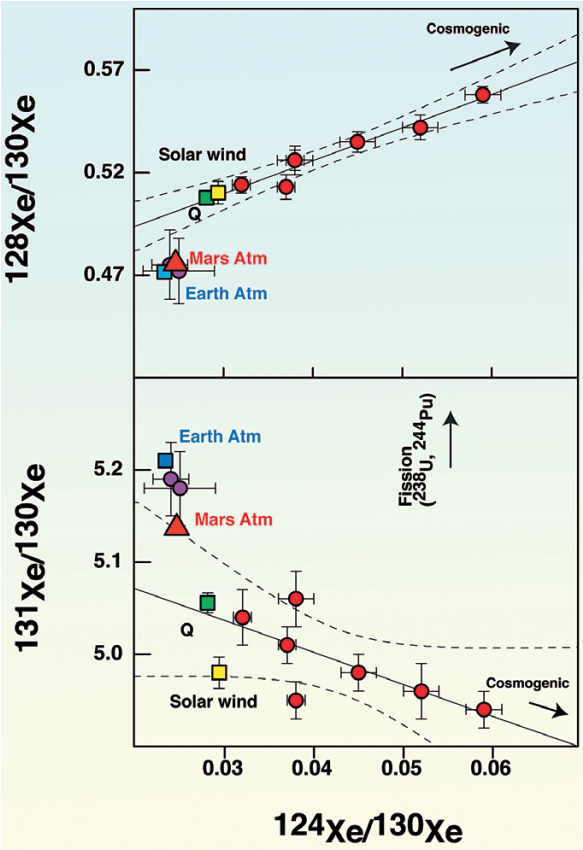


**Figure 2.22** Xenon isotopic ratios in olivines from the Chassigny SNC meteorite (red dots; violet dots are the first heating steps, contaminated by atmosphere; data from Mathew and Marti, 2001) and in the Martian atmosphere (red triangle; Swindle, 2002). This figure shows that the xenon in Mars’s interior is either solar or Q-like although most Marsophiles propose a solar composition instead of Q. The mixing lines reflects mixture between the Q or solar and cosmogenic xenon.





The reason why it is important to know if Mars's interior has a Xe-Q composition rather than solar, is that on Earth, the observation that CO<sub>2</sub>-well gases show that the Earth's mantle might have a Q composition, and not solar, at the end of the accretion before atmospheric subduction (Holland *et al.*, 2009; see Section 7).

## 2.6 Conclusions

Chondrites exhibit noble gas isotopic compositions that can be described in terms of mixture of 3 components. Ar, Kr, and Xe are mostly carried by the phase Q, which is a resistant carbonaceous phase that is degassed only at high temperature and is present in chondrites whatever their degree of metamorphism. Pre-solar grains are observed in chondrites and show very peculiar isotopic compositions (neon A, HL...) reflecting their condensation in the envelope of supernovas or red giants. These pre-solar grains are rich in neon, but it is unclear if they contribute to the bulk budget of the terrestrial rare gases (see Section 5). Fractionated solar wind resulting in ion implantation, and known as component B, is an important contributor to the He and Ne (and possibly Ar) budget in meteorites, particularly in ordinary and enstatite chondrites. Neon B has a <sup>20</sup>Ne/<sup>22</sup>Ne ratio close to 12.7, higher than the first estimate of Black who proposed 12.52±0.18 (Black, 1972). The neon B isotopic ratio is similar to the maximum observed ratios in terrestrial samples, a point which has been raised to question the existence of neon B in the deep Earth (Trieloff *et al.*, 2000). A solar Xe composition has been inferred to be present in Chassigny, an SNC meteorite from Mars (Mathew and Marti, 2001), suggesting that solar Xe could be present in Mars's interior, although the phase Q could also account for these observations.

It is therefore conceivable that phase Q was present in Earth's parent bodies and then in the Earth's primitive mantle, although this is not observed on Earth for the non-radiogenic isotopes of Kr and Xe. Only small excesses compared to the atmosphere of the non-radiogenic Kr and Xe isotopic compositions have been measured on CO<sub>2</sub>-well gases and attributed to the contribution of a component having the isotopic composition of phase Q (Cafee *et al.*, 1999; Holland and Ballentine, 2006; Holland *et al.*, 2009). The next sections will present the noble gas systematics of the Earth's mantle and discuss these observations in the light of the noble gas compositions of meteorites. A summary of all the compositions discussed in this chapter is given in Table 2.1.





**Table 2.1** Noble gas isotopic compositions in Earth's atmosphere, Mars's atmosphere, phase Q, and the solar wind. Data from Black (1972), Busemann *et al.* (2000), Eugster *et al.* (2002), Swindle (2002), Wieler (2002), and Pepin *et al.* (2012).

	20Ne/22Ne	±	21Ne/22Ne	±	38Ar/36Ar	±
Earth Atmosphere	9.80		0.0290		0.1880	
Solar wind (pepin2012)	14.00	0.02	0.0336	0.0001	0.1818	0.0002
Q	10.67	0.02	0.0294	0.0010	0.1873	0.0007
Mars Atm	10.10	0.70			0.244	0.012
B component Black1972	12.52	0.18	0.0335	0.0015	0.1862	0.0042
B component Steady state	12.73	0.02	0.0321	0.0001	0.1919	0.0002

	78Kr/84Kr	±	80Kr/84Kr	±	82Kr/84Kr	±	83Kr/84Kr	±	86Kr/84Kr	±
Earth Atmosphere	0.00610		0.0396		0.2022		0.2014		0.3052	
Solar wind	0.00640	0.00003	0.0409	0.0001	0.2048	0.0005	0.2029	0.0003	0.3024	0.0010
Q	0.00603	0.00003	0.0394	0.0001	0.2018	0.0002	0.2018	0.0002	0.3095	0.0005
Mars Atm	0.00653	0.00007	0.0417	0.0015	0.2063	0.0022	0.2042	0.0022	0.2994	0.0085

	124Xe/ 130Xe	±	126Xe/ 130Xe	±	128Xe/ 130Xe	±	129Xe/ 130Xe	±	131Xe/ 130Xe	±	132Xe/ 130Xe	±	134Xe/ 130Xe	±	136Xe/ 130Xe
Earth Atmosphere	0.0234		0.0218		0.471		6.50		5.21		6.61		2.56		2.18
Solar wind	0.0294	0.0007	0.0255	0.0008	0.510	0.005	6.27	0.04	4.98	0.02	6.02	0.03	2.21	0.01	1.80
Q	0.0281	0.0001	0.0251	0.0001	0.508	0.002	6.44	0.02	5.06	0.01	6.18	0.01	2.33	0.01	1.95
Mars Atm	0.0246	0.0013	0.0214	0.0013	0.476	0.0065	15.55	0.16	5.14	0.03	6.48	0.04	2.60	0.02	2.28

In this section, I present a brief overview of the history of the helium geochemistry in the mantle. Its interpretations will be discussed in Sections 6 and 8, in the context of the systematics of all noble gases in the Earth's mantle.

### 3.1 The Discovery of $^3\text{He}$ on Earth

Helium has only two stable isotopes,  $^3\text{He}$  and  $^4\text{He}$ . While  $^3\text{He}$  is considered as primordial,  $^4\text{He}$  is mostly radiogenic in the mantle and almost entirely of radiogenic origin in the continental crust.  $^4\text{He}$  is produced from the decay of U, Th, and (less significantly) Sm. Although helium is the second most abundant element in the universe, it is very rare on Earth. There is only  $5.24 \times 10^{-6} \text{ cm}^3 \text{ cm}^{-3}$  (~5 ppm by volume) of helium in the present-day Earth's atmosphere.  $^3\text{He}$  is even rarer since its atmospheric abundance is  $7 \times 10^{-12} \text{ cm}^3 \text{ cm}^{-3}$ . Therefore its detection is difficult and it was only in 1939 that Alvarez and Cornog discovered  $^3\text{He}$  on Earth by analysing air and gas from wells (Alvarez and Cornog, 1939a,b). In 1946, Aldrich and Nier further measured also the helium isotopic composition in well gases and observed a radiogenic ratio comparable to the atmospheric value<sup>20</sup> (Aldrich and Nier, 1946). They obtained similar results in their second and more detailed publication in 1948 (Aldrich and Nier, 1948). Their conclusion was: *"The present study can hardly be regarded as more than a preliminary exploration of a new and fascinating field of investigation. It is apparent that a far more comprehensive and systematic study will be required to definitely establish the natural sources of  $^3\text{He}$  and  $^4\text{He}$ . Included in such a program should be an investigation of the helium from the upper atmosphere and that from meteorites"*. Obviously, they could not have been more right as I will show below. The origin of the  $^3\text{He}$  on Earth remained matter of debate until 1969. For example, Morrison and Pine (1955) explained all the present-day  $^3\text{He}$  observed in the atmosphere or in terrestrial samples by nuclear reactions instead of by the remnant of a primordial gas.

The measurement of  $^3\text{He}$  excesses in seawater (Clarke *et al.*, 1969) fundamentally changed opinions. In this study, Clarke and collaborators published the first  $^3\text{He}$  excesses relative to atmospheric composition in seawater sampled at different depths in the south Kermadec trench.  $^3\text{He}/^4\text{He}$  ratios as high as 1.22 times the atmospheric ratio<sup>21</sup> were measured in deep seawater, which clearly suggests  $^3\text{He}$  degassing from the mantle. They also provided the first estimate of the  $^3\text{He}$  flux from the mantle ( $\sim 520 \text{ mol a}^{-1}$ ), which is close to modern estimates of this critical parameter. The detection of  $^3\text{He}$  in seawater was, for many workers,

20. It would correspond to  $^3\text{He}/^4\text{He} \sim 0.1\text{Ra}$  where Ra is the atmospheric isotopic ratio ( $1.384 \times 10^{-6}$ ).

21. This is the only paragraph I will be using the  $^3\text{He}/^4\text{He}$  notation, as it makes sense from an historical point of view. In the next section, the most logical notation  $^4\text{He}/^3\text{He}$  will be used.



an unambiguous signal for the existence of primordial gases in the mantle. This pioneering publication was followed by many on seawater (e.g., Fig. 3.1), but also opened a Pandora's box of helium systematics in mantle-derived samples.

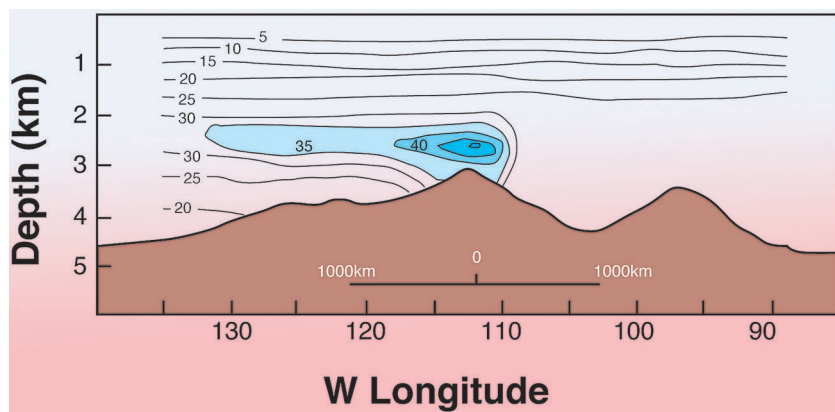


**Figure 3.1**  $^3\text{He}$  excess in seawater above the East Pacific Rise (in notation delta:  $\delta^3\text{He} = (\text{R}/\text{Ra}-1) \cdot 100$ ). The  $^3\text{He}$  plume demonstrates the supply of  $^3\text{He}$  to the oceans by degassing of the mantle. The present-day global  $^3\text{He}$  flux at ridges is estimated between 500 (Bianchi *et al.*, 2010) and 1,000  $\text{mol a}^{-1}$  (Farley *et al.*, 1995) (modified from Craig and Lupton, 1981).

Although the *Clarke's* paper is often considered to represent the first evidence for  $^3\text{He}$  from the mantle, it must be said that the “Forgotten” Russian Group of *Mamyrin* (Fig. 3.2) and *Tolstikhin* published in the same year significant  $^3\text{He}$  excesses in gases from thermal springs in south Kuriles (Fig. 3.3) (Mamyrin *et al.*, 1969a). I imagine that during the cold war, publications written in Russian were hardly accessible to US scientists. Using their cyclotron mass spectrometer, they obtained  $^3\text{He}/^4\text{He}$  ratios up to 10 times that of the atmospheric ratios, close to the Mid Ocean Ridge Basalts (MORB) ratio. Immediately after *Clarke's* publication, *Fisher* tried to detect  $^3\text{He}$  in oceanic basalts that had high  $^4\text{He}$  and  $^{40}\text{Ar}$  abundances (Fisher, 1970). Because of experimental limitations, particularly the difficulty of distinguishing the HD peak from the  $^3\text{He}$  peak, he did not find any clear  $^3\text{He}$  signal in oceanic basalts, although he did not disagree with *Clarke's* hypothesis about high  $^3\text{He}$  concentrations in the primitive mantle. The first clear evidence for high  $^3\text{He}$  abundances in rocks were the two works of *Tolstikhin et al.* (1974) and *Lupton and Craig* (1975). They both measured  $^3\text{He}/^4\text{He}$  ratios in rocks, up to 12.2 Ra in basalts from Lau Basin for *Lupton and Craig*, and up to 10 Ra in xenoliths in *Tolstikhin's* paper. They both concluded on a primordial origin for  $^3\text{He}$ .





**Figure 3.2** The “Russian noble gas group”: Igor Tolstikhin (left) and Boris Mamyrin (right) in 2000. They were among the first to analyse precisely the helium isotopes in gases and rocks. Their first works were however published in Russian, which therefore did not make an immediate impact in the Western literature.

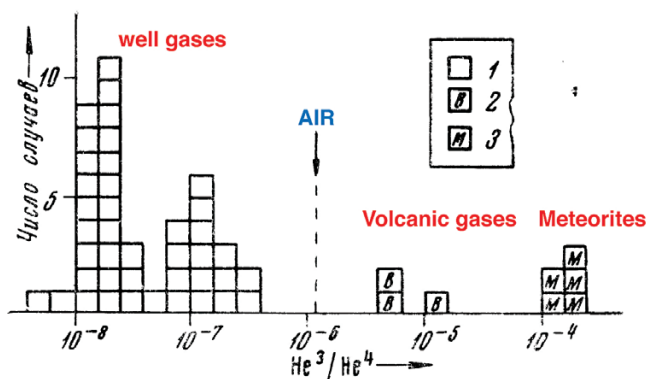
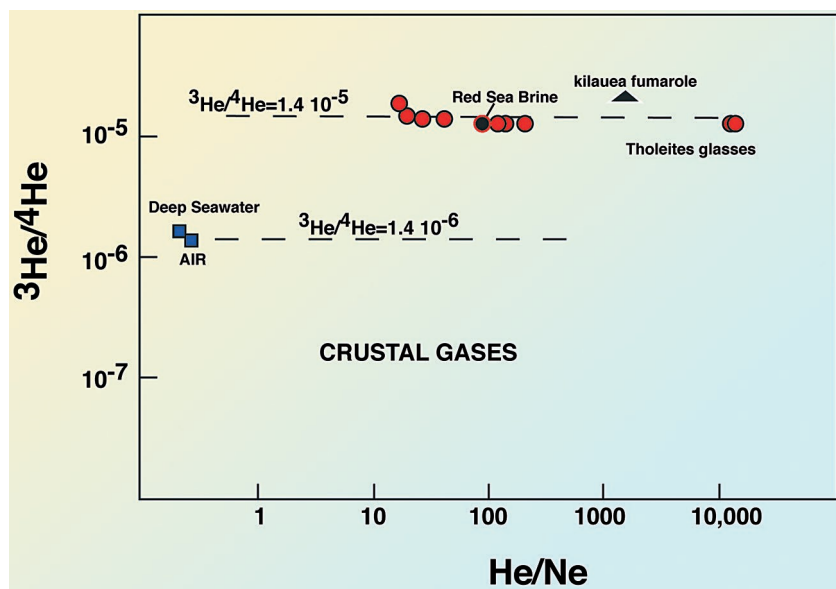


Рис. 1. Гистограмма отношений  $\text{He}^3/\text{He}^4$ , полученных: 1 — для разнообразных природных газов; 2 — для газов из вулканов (колл. Н. В. Альбинского); 3 — для метеоритов по данным (8). Стрелкой отмечено отношение  $\text{He}^3/\text{He}^4$  в воздухе

**Figure 3.3** The Russian group was among the first to show the first evidence for  $^3\text{He}$  in the mantle. Here are given the helium isotopic ratios in volcanic gases (2), meteorites (3) and well gases (1). Air is indicated with an arrow at a ratio  $\sim 10^{-6}$  (modified from Mamyrin *et al.*, 1969b).



At the end of the 1970's, it was clear that the mantle had a much higher  $^3\text{He}/^4\text{He}$  ratio than the atmosphere (see Fig. 3.4). Other studies followed, all confirming the presence of high  $^3\text{He}/^4\text{He}$  ratios in the mantle relative to the atmosphere (Craig and Lupton, 1976; Kaneoka and Takaoka, 1977; Kaneoka and Takaoka, 1978). The “industrial” approach of the helium systematics in mantle-derived samples, the fruits of which are discussed below, started in the early 1980's with Mark Kurz (Kurz and Jenkins, 1981; Kurz *et al.*, 1982a; Kurz *et al.*, 1982b; Kurz *et al.*, 1983) and others (Kaneoka *et al.*, 1983; Ozima and Zashu, 1983; Kyser and Rison, 1982; Rison and Craig, 1983; Condomines *et al.*, 1983; Porcelli *et al.*, 1986; Poreda *et al.*, 1985; Poreda *et al.*, 1986; Porcelli *et al.*, 1987).



**Figure 3.4** The first helium isotopic results in oceanic basalts. The  $^3\text{He}/^4\text{He}$  ratio corresponds to  $R/R_a = 10$  and  $^4\text{He}/^3\text{He} = 71,500$ , in good agreement recent estimates of the mean MORB ratio (modified from Craig and Lupton, 1981).

### 3.2 Helium Isotope Systematics in Oceanic Basalts

After these pioneering works, more than 30 years of helium analyses have provided many precise helium isotopic ratios of oceanic basalts (MORB and OIB). The most suitable samples for analysing helium isotopes are the glassy margins of pillow lavas (Fig. 3.5) and phenocrysts containing melt or fluid inclusions (Fig. 3.6).







Photo credit: Manuel Moreira.

**Figure 3.5**

Typical pillow lava collected on sea floor at mid ocean ridges. The glassy margin of pillow lavas formed by quenching contains vesicles that are rich in mantle-derived gases. This sample was dredged on the Pacific-Antarctic Ridge during the PAC2 cruise of the R/V Atalante to which I participated.

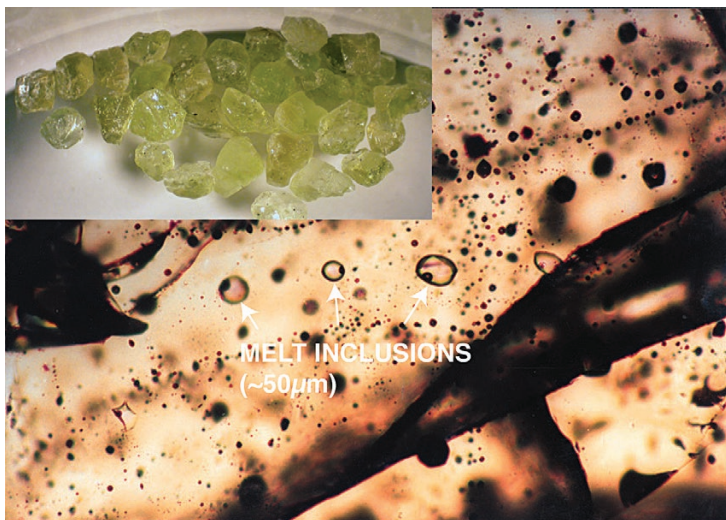
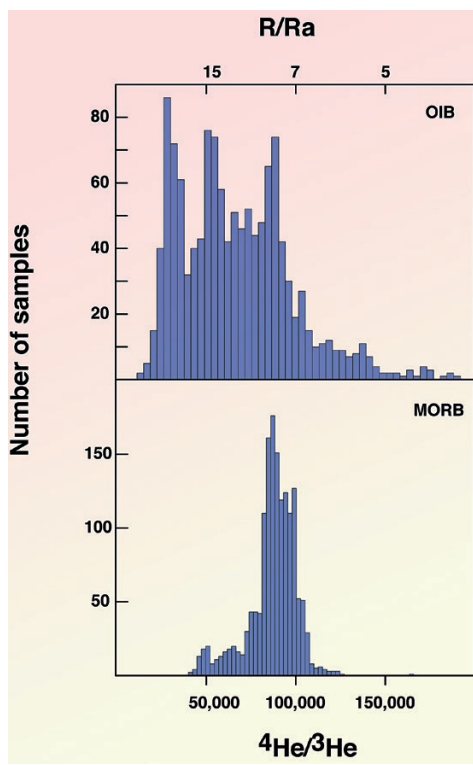


Photo credit: Manuel Moreira.

**Figure 3.6**

Melt inclusions are the main carrier of  $\text{CO}_2$  and volatiles in phenocrysts. Melt inclusions in an olivine can be observed on this picture. Typical melt inclusions are of the order of  $\sim 50 \mu\text{m}$  whereas the olivines have diameters of  $\sim 2 \text{ mm}$ . Olivines are often the only sample that can analysed for helium in Oceanic Island Basalts.



**Figure 3.7**

Histogram of the  $^4\text{He}/^3\text{He}$  ratio in Oceanic Island Basalts (OIB) (upper plot) and Mid Ocean Ridge Basalts (MORB) (lower plot). These two histograms have different shapes. Whereas the MORB histogram suggests a well-homogenised mantle and a radiogenic helium isotopic signature, the OIB histogram shows a larger dispersion, and helium isotopic ratios as low as 15,000 ( $\text{R}/\text{Ra} = 50$ ). The tailing of the MORB histogram to low values represents plume-ridge interactions with Iceland, Saint Paul-Amsterdam, Shona and Discovery topographic anomalies and therefore cannot be considered as “normal MORB” (Poreda *et al.*, 1986; Moreira *et al.*, 1995; Graham *et al.*, 1999; Sarda *et al.*, 2000).

Figure 3.7 shows a compilation of the helium isotopic ratios in OIB and MORB without discriminating between location. Only basaltic materials are represented in this figure (glass or olivine/clinopyroxene phenocrysts). Mantle xenoliths are excluded from this figure because their origin is ambiguous. Please note that I am using the  $^4\text{He}/^3\text{He}$  ratio instead of the ‘classical’  $\text{R}/\text{Ra}$  ratio, which is the  $^3\text{He}/^4\text{He}$  ratio normalised to the atmospheric ratio. The use of the former is a logical continuation of standard isotopic nomenclature, which reports the radiogenic isotope over a stable of the same element. This approach is therefore more consistent with other commonly used radiogenic isotopic systems such as  $^{87}\text{Sr}/^{86}\text{Sr}$  or  $^{206}\text{Pb}/^{204}\text{Pb}$ . However, the use of  $\text{R}/\text{Ra}$ , originally coined in the early literature persists, and for convenience I also report equivalent  $\text{R}/\text{Ra}$  values where appropriate.

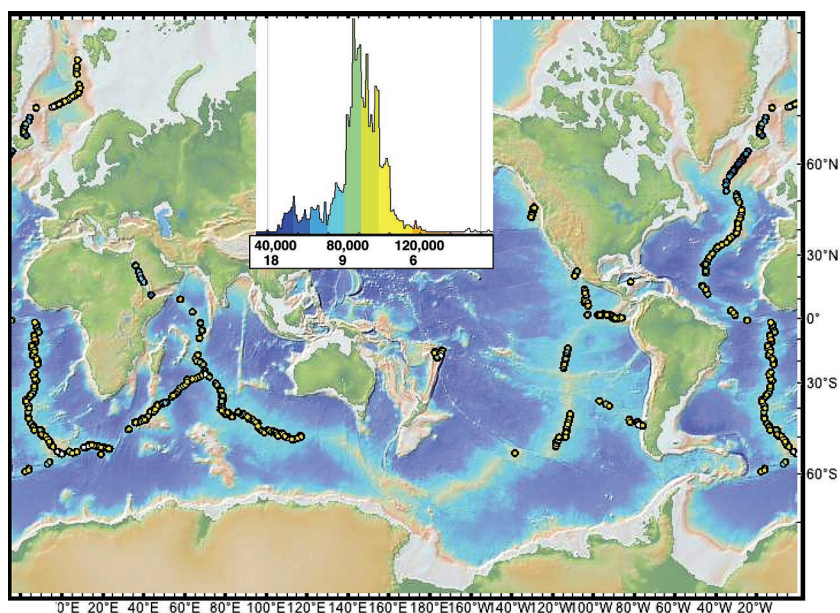
Figure 3.7 shows the large variations in the  $^4\text{He}/^3\text{He}$  ratios of oceanic island basalts, from non-radiogenic ratios (15,000;  $\text{R}/\text{Ra} = 50$ ) up to 200,000 ( $\text{R}/\text{Ra} = 3.6$ ). This contrasts with the homogeneity of MORB, which with the exception of the Reykjanes ridge, the South Atlantic ridge anomalies Shona and Discovery and the Saint Paul-Amsterdam plateau on the South East Indian Ridge, show a homogeneous ratio of  $90,000 \pm 10,000$ . The anomalously low  $^4\text{He}/^3\text{He}$  measured in samples from topographic



anomalies are often associated with plume-ridge interaction (Schilling, 1991), see Figure 3.8, and therefore cannot be considered as representative of normal MORB mantle, although this has been debated (Anderson, 2000; Meibom *et al.*, 2003). The few peaks that can be observed on the OIB histogram reflect locations that are oversampled such as Hawaii, Iceland, or Galapagos.

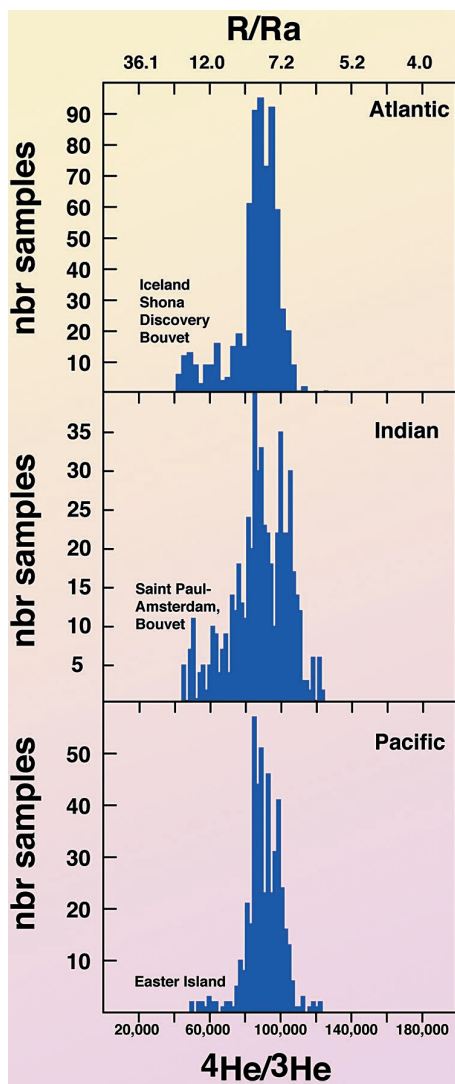
### 3.2.1 Mid ocean ridge basalts (MORB)

Figure 3.8 shows the location of those MORB samples that have been analysed for helium. With a few exceptions, this is the same data compilation used by Graham (2002), and the following discussion is similar. Note that most ridge systems have been analysed for helium with the exception of the far south Pacific-Antarctic ridge. To compare different mantle domains, Figure 3.9 shows the helium isotopic ratio histograms for the Atlantic, Indian and Pacific oceans. This figure shows that the three ridge systems have similar mean  $^4\text{He}/^3\text{He}$  ratios and dispersions. The Indian Ocean appears to show a higher dispersion for the helium isotopic ratio, likely because the Indian mantle contains the so-called DUPAL component (Dupré and Allègre, 1983; Hart, 1984b) that is rarely seen in other ridge systems.



**Figure 3.8**

MORB sample locations having published helium isotopic ratios. The value of their helium isotopic ratios is represented in the symbols using a colour scale (blue = primitive, orange is radiogenic) that given in the insert ( $^4\text{He}/^3\text{He}$  ratios).



**Figure 3.9**

Histogram (number of samples “n”) of the  $^4\text{He}/^3\text{He}$  ratio in MORB from different upper mantle domains. Samples with low  $^4\text{He}/^3\text{He}$  ratios are often associated with topographic anomalies reflecting plume-ridge interactions (a few plume-ridge interactions are given in the figure).

This DUPAL component has radiogenic helium (Mahoney *et al.*, 1989; Georgen *et al.*, 2003; Raquin and Moreira, 2009; Parai *et al.*, 2012) and is considered to result from the injection of lower crust into the Indian mantle by delamination during the breakup of Gondwana (Mahoney *et al.*, 1989; Kamenetsky *et al.*, 2001; Escrig *et al.*, 2004; Meyzen *et al.*, 2005) or from the contamination of the asthenosphere by a mantle plume or a series of mantle plumes (*i.e.* Kerguelen, Mario, Crozet *et al.*; Weis *et al.*, 1989; Mahoney *et al.*, 1992).

The similarity of the helium isotopic ratio in these three sets of mantle samples (Atlantic/Indian/Pacific) provides constraints on mantle dynamics and on the history of the depleted mantle. There are some local variations between different ridge segments. For instance, the  $^4\text{He}/^3\text{He}$  ratios are different between two segments of the Pacific Antarctic ridge delimited by the Menard fracture zone (Moreira *et al.*, 2008). There is also an abrupt increase in  $^4\text{He}/^3\text{He}$  north of the Kurchatov Fracture zone in the North Atlantic (~41 °N) (Kurz *et al.*, 1982b; Moreira and Allègre, 2002). These observations suggest that different mantle domains have slightly different  $\text{U}/^3\text{He}$  ratios, which can result from either a slightly greater degassing rate or a slight enrichment in U and Th (Moreira and Allègre, 2002). However, on the global scale, the MORB source mantle can be considered relatively homogeneous for helium as





it is for other isotopic systems, compared to OIB sources. This suggests that the MORB source is well stirred by convection (*e.g.*, Allègre and Lewin, 1995; Allègre *et al.*, 1995), and that different mantle domains are not extensively degassed compared to one another (*i.e.* have similar time integrated  $U^{235}/He$ ), otherwise the variations between different mantle MORB sources would be more significant (Moreira *et al.*, 2008).

### 3.2.2 Oceanic island basalts (OIB)

The first study on oceanic island basalts was that of Kaneoka and Takaoka who analysed phenocrysts and xenocrysts from Kilauea and Hualalai (Hawaii) (Kaneoka and Takaoka, 1977). They obtained  $^4He/^3He$  ratios as low as  $40,000 \pm 5,000$  (or up to  $R/Ra = 18$ ). This work was followed by the seminal paper of Kurz's, showing that OIB exhibit both lower and higher  $^4He/^3He$  ratios compared to MORB (Fig. 3.10) (Kurz *et al.*, 1982a). Note that OIB measurements were an analytical challenge, as unlike glassy MORB samples, they were made on olivine separates, that typically contain less than  $10^6$  atoms  $g^{-1}$  of  $^3He$ . The Paris group could not measure such low helium concentrations because of analytical issues related to the glassy housing of the ARESIBO I and II mass spectrometers, as well as the fact that the extraction and purification lines were also in glass. Helium diffuses through glass and therefore the helium blanks are too high to allow the measurement of helium in olivine samples. Moreover, these Reynolds-type glass machines cannot distinguish HD from  $^3He$ , and although background of  $H_2$  is low in these instruments, the HD peak is still too high to measure phenocrysts well compared to mass spectrometers made of stainless steel and with mass resolution higher than 600. Therefore, the helium systematics in OIB phenocrysts was performed by a few groups, and were only made in Paris after we modified the extraction and purification lines coupled to the ARESIBO mass spectrometers (Moreira *et al.*, 1999; Madureira *et al.*, 2005; Doucet *et al.*, 2006; Mata *et al.*, 2010; Mourão *et al.*, 2012).

Although OIB show  $^4He/^3He$  both higher and lower than MORB, a key observation is that most oceanic hotspots exhibit low  $^4He/^3He$  compared to MORB (Figs. 3.7 and 3.11). Hawaii, Iceland, Galapagos and La Réunion share this characteristic. The most primitive helium isotopic ratios (*i.e.* highest  $R/Ra$  or lowest  $^4He/^3He$ ) were measured on Baffin Island picrites (Stuart *et al.*, 2003). These rocks are early volcanic products of the Icelandic mantle plume, similar to the Tertiary volcanic rocks in West Greenland (Graham *et al.*, 1998). The  $^4He/^3He$  ratio is as low as 15,000 ( $R/Ra \sim 50$ ) in Baffin picrites (Stuart *et al.*, 2003). This value is radiogenic compared to the solar value (2,500;  $R/Ra \sim 290$ ), but much less radiogenic compared to the MORB ratio (90,000;  $R/Ra = 8$ ). Hawaii, Iceland and Galapagos hotspots also show primitive helium isotopic ratios, although less primitive (non-radiogenic) than the Baffin samples (Kurz *et al.*, 1983; Kurz *et al.*, 1985; Graham *et al.*, 1998; Hilton *et al.*, 1999; Kurz *et al.*, 2009). The origin of these low  $^4He/^3He$  ratios in OIB will be discussed in detail in Section 6, in the context of the noble gas systematics. Most authors, however, agree with a 'primordial'



origin of these low  $^4\text{He}/^3\text{He}$  ratios, meaning the source of this isotopic signature is rich in primordial  $^3\text{He}$ . Indeed, to produce in a 4.5 Ga closed-system a  $^4\text{He}/^3\text{He}$  ratio of 15,000, starting from the solar ratio of 2,500 with a U content similar to the primitive mantle (~20 ppb) (e.g., Allègre *et al.*, 1986), a  $^3\text{He}$  concentration of  $\sim 1.2 \times 10^{-13}$  mol g $^{-1}$  is necessary. For comparison, the MORB source has an estimated concentration of  $\sim 5 \times 10^{-15}$  mol g $^{-1}$  (Moreira *et al.*, 1998). It appears, therefore, that the MORB source is considerably more degassed than the majority, low  $^4\text{He}/^3\text{He}$  OIB sources.

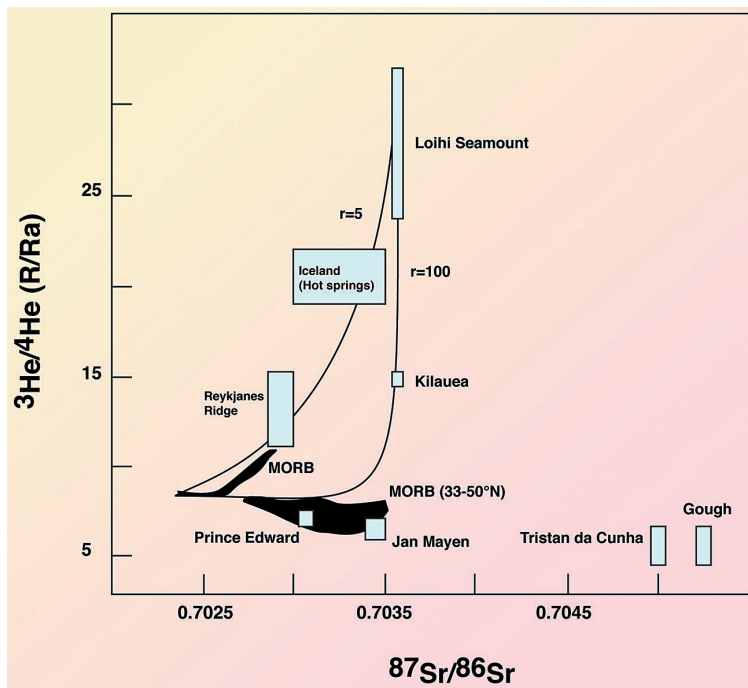


**Figure 3.10** He-Sr systematics in OIB as published by Kurz *et al.* (1982a).

A few oceanic islands do not exhibit such low, “primitive”  $^4\text{He}/^3\text{He}$  ratios (Fig. 3.11). Here, I focus on the origin of the “low  $^3\text{He}$ ” hotspots and on the question of whether they represent a mantle signature or shallow processes such as magmatic chamber degassing, radiogenic addition or crustal contamination.

Since the first paper of Kurz on OIB, it has been observed that some OIB have low  $^4\text{He}/^3\text{He}$  ratios, attributed to a primitive reservoir in the deep mantle, whereas some others have radiogenic helium ratios comparable to the mean MORB value of 90,000 ( $R/R_a = 8$ ) (Kurz *et al.*, 1982a). São Miguel (Azores archipelago), Canaries, Comoros, Gough, Tristan da Cunha, Saint Helena, Cameroon



line or Tubuai hotspots show more radiogenic helium than MORB (Kurz *et al.*, 1982a; Kurz *et al.*, 1990; Graham *et al.*, 1993; Kurz, 1993; Barfod *et al.*, 1999; Moreira *et al.*, 1999; Class *et al.*, 2005; Parai *et al.*, 2009; Day and Hilton, 2011).

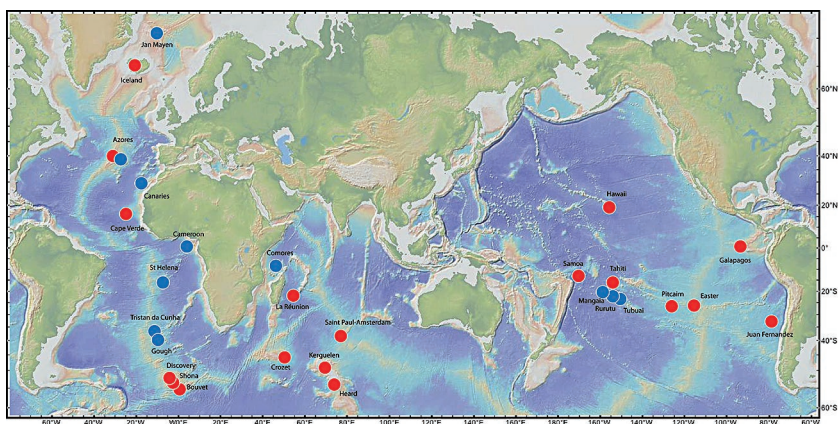


**Figure 3.11** Location of major hotspots (oceanic) analysed for helium. The red circles represent the “high  $^3\text{He}$ ” hotspots, the blue circles are the “low  $^3\text{He}$ ” hotspots.

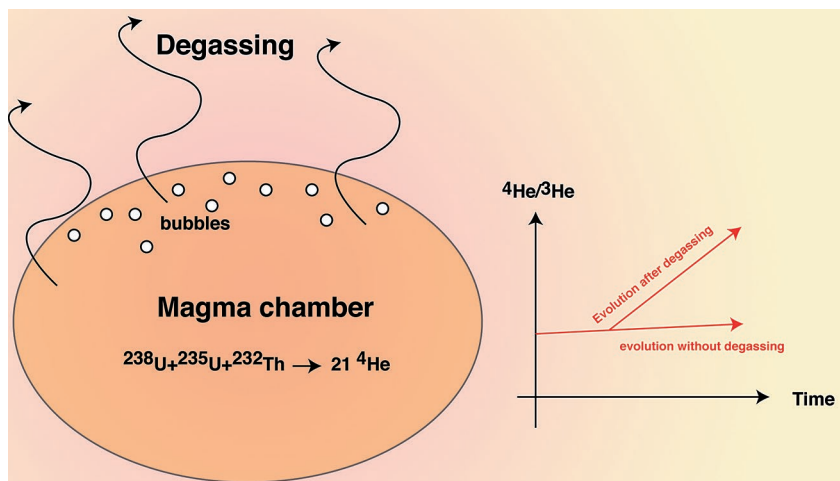


**Figure 3.12** Cartoon showing how degassing can influence the helium isotopic ratio. When  $\text{CO}_2$  is oversaturated in magma, it forms bubbles that can be degassed from the magmatic chamber. Helium has a low solubility in magmas and therefore will enter into the gas phase. The degassed magma thus has a high  $(\text{U}+\text{Th})/^3\text{He}$  ratio. In a relatively short time the magma will obtain a radiogenic helium signature.



These “low  $^3\text{He}$ ” hotspots are obviously not sampling a primordial reservoir, but a material relatively rich in radiogenic helium. In the 1980’s only a few samples from these low  $^3\text{He}$  hotspots had been analysed for helium, and their radiogenic signatures were the subject of debate. For instance, *Zindler* and *Hart* demonstrated that degassing and radiogenic production could produce radiogenic helium rapidly within magmatic chambers (Zindler and Hart, 1986b) (Fig. 3.12). This is illustrated in Figure 3.13 where the helium isotopic ratio is reported against the concentration of helium in radiogenic Pacific hotspot samples. These samples indicate magma chamber degassing, where low helium contents in the magma coupled to radiogenic decay of U and Th can produce high  $^4\text{He}/^3\text{He}$  isotopic ratios in some samples even though the original mantle source was primitive in its helium isotopic ratio (*e.g.*, low  $^4\text{He}/^3\text{He}$  ratio).

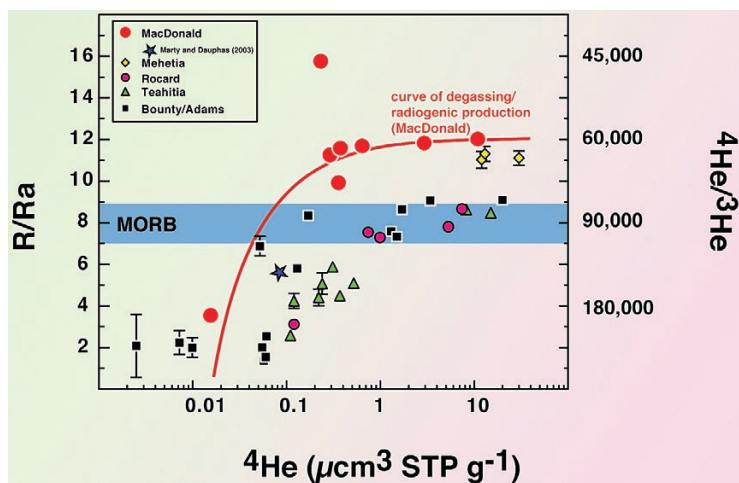


**Figure 3.13**

Helium concentration expressed in  $\mu\text{cm}^3\text{STP g}^{-1}$  ( $= 10^{-6} \text{ cm}^3$  of helium at standard pressure and temperature per gram of sample) and isotopic ratios in Pacific hotspot glasses showing that degassing and production of radiogenic  $^4\text{He}$  in the magma chamber can produce radiogenic  $^4\text{He}/^3\text{He}$  in OIB. A similar shallow origin for high  $^4\text{He}/^3\text{He}$  ratios was proposed for Heard lavas that show both high and low  $^4\text{He}/^3\text{He}$  ratios (Hilton *et al.*, 1995). Obviously, such a process will be more significant for high U and Th lavas. The red curve represents the isotopic ratios of lavas having different U/ $^3\text{He}$  ratios for a given age of 50,000 years, a Th/U ratio of 3 and a U content of 0.08 ppm. These curves can readily explain the MacDonald samples (large black dots) (modified from Moreira and Allègre, 2004).

Moreover, Hilton *et al.* (1995) observed both primitive and radiogenic helium isotopic ratios in Heard Island lavas, which were attributed to crustal assimilation of the former to produce the latter (see Fig 3.14). He therefore questioned the mantle origin of the “low  $^3\text{He}$ ” hotspots. I recall his review of my study of the Azores Archipelago in which I published helium isotopic ratios of the São



Miguel island that were extremely radiogenic. In this study I interpreted the He isotopic ratio as reflecting the source instead of shallow processes. We were both right. It has been confirmed that the São Miguel mantle source has indeed a radiogenic helium isotopic composition, but also that most of the samples contain post-eruption radiogenic helium (Moreira *et al.*, 2012). In this publication, I proposed, based on measured helium in São Miguel lava (Azores) aged for ~1 Ma, that, if olivines are used for measuring helium isotopic ratios in subaerial lavas, alpha implantation into the olivine rims from the surrounding U-rich basalts can produce radiogenic helium isotopic ratios during crushing under vacuum. This is particularly true if samples are old and depleted in mantle-derived helium (Moreira *et al.*, 2012). This process can “mask” the mantle-derived signature. It has also been observed that olivine and clinopyroxene (cpx) do not always have the same helium isotopic ratios, cpx is always more radiogenic than olivine (Marty *et al.*, 1994; Shaw *et al.*, 2006). This suggests that crustal assimilation could indeed influence the magmatic helium composition as suggested by (Hilton *et al.*, 1995) especially when the magmas are degassed. All these observations and calculations suggest that degassing, U-Th radioactive decay, post-eruption alpha implantation are processes capable of altering the magmatic helium isotopic compositions of oceanic basalts.

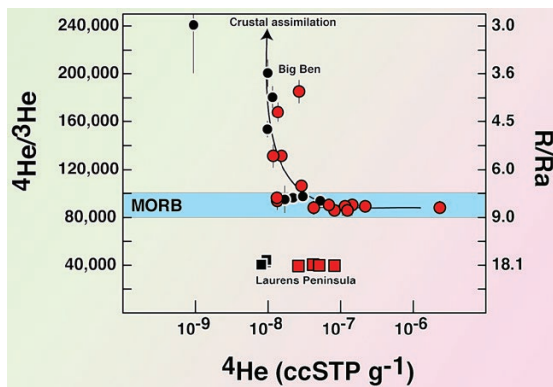


**Figure 3.14** Heard island helium isotopic ratios (data from Hilton *et al.*, 1995). Hilton *et al.* (1995) interpreted the radiogenic helium as crustal assimilation rather than the presence of radiogenic helium in the mantle source of the Big Ben series. In red: olivines. In black: clinopyroxenes.

However, a few detailed studies on the Comoros, São Miguel (Azores), Canary, Cameroon Line, Tubuai, and Mangaia, Rurutu hotspots have confirmed that some mantle sources have radiogenic helium isotopic ratios (see Figs. 3.15, 3.16 and 3.17). Shallow magma degassing and radiogenic production cannot explain the observed compositions and the correlations seen with other isotopic systems, less sensitive to degassing and contamination (Hanyu and Kaneoka, 1997; Barfod *et al.*, 1999; Moreira *et al.*, 1999; Hilton *et al.*, 2000a; Aka *et al.*, 2004; Class *et al.*, 2005; Gurenko *et al.*, 2006; Day and Hilton, 2011; Hanyu *et al.*, 2011; Moreira *et al.*, 2012). The more-radiogenic-than MORB helium isotopic ratios observed on these OIB exhibit a mantle signature, which is clearly different to the “primitive” nature of most OIB.



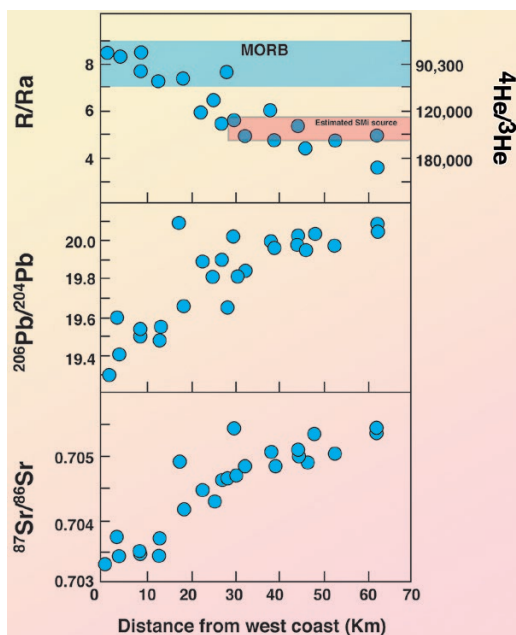


**Figure 3.15**

He-Pb-Sr variations in São Miguel island (Azores archipelago) (modified from Kurz, 1991). The correlation between all radiogenic systems suggests that the mantle source of São Miguel lavas contains radiogenic helium. These radiogenic helium isotopic ratios were confirmed by measurements on thermal springs and lavas from the Nordeste volcano (Jean-Baptiste *et al.*, 2009; Moreira *et al.*, 2012). The São Miguel source has a  $^4\text{He}/^3\text{He}$  of  $\sim 140,000$  ( $R/Ra \sim 5.3$ ) (Moreira *et al.*, 2012), which results from the melting of an enriched source recycled into the mantle more than 2.5 Ga ago (Beier *et al.*, 2007; Elliott *et al.*, 2007).

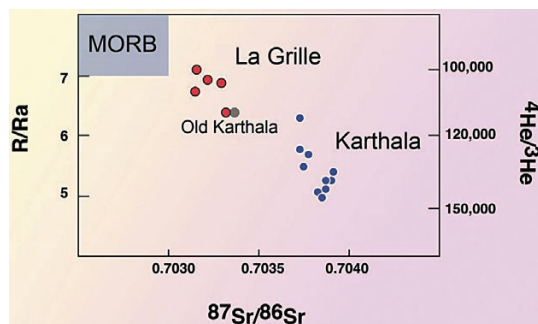


**Figure 3.16**

Helium isotopic ratios versus the strontium isotopic ratios in Comoros lavas showing the mixing between lithospheric and “plume” end-members sampled by the Karthala volcano. (Class *et al.*, 2005). The  $^4\text{He}/^3\text{He}$  ratio is  $\sim 140,000$  in the Comoros “plume” component. Comoros is a well-defined high  $^4\text{He}$  hotspot.



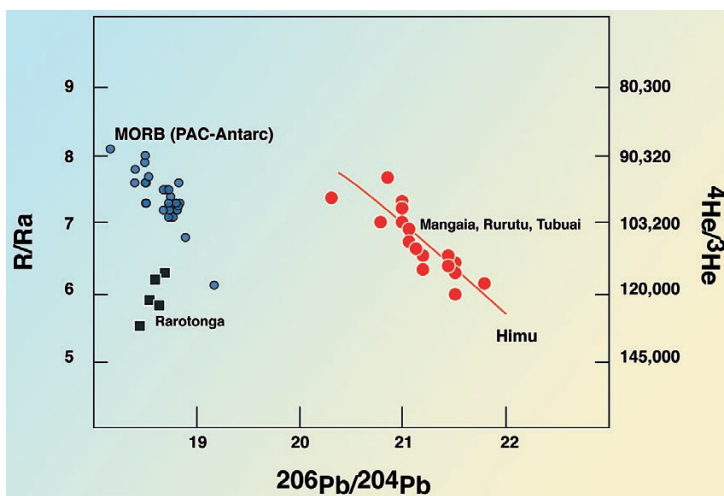


**Figure 3.17**

This figure shows that the HIMU end-member, supposed to be recycled oceanic crust, has also radiogenic helium. Data for Pacific-Antarctic ridge from Moreira *et al.* (2008) and Hamelin *et al.* (2011). The  $^{206}\text{Pb}/^{204}\text{Pb}$  ratio is a proxy for the HIMU end member (modified from Hanyu *et al.*, 2011).

Subducted material must have a high  $\text{U}/^3\text{He}$  ratio as it is degassed both during its formation (*e.g.*, at mid oceanic ridges) and during subduction when the slab is dehydrated or basalt transforms to eclogite. An increase of the  $\text{U}/^3\text{He}$  ratio by a factor of 100 for the subducted oceanic crust relative to the fresh undegassed crust will produce a  $^4\text{He}/^3\text{He}$  ratio of  $\sim 10^6$  ( $\text{R}/\text{Ra} \sim 0.7$ ) 1 Ga after subduction. This ratio is higher than the measured ratio in “low  $^3\text{He}$ ” hotspots, HIMU or EM-type, which are close to 140,000 ( $\text{R}/\text{Ra} \sim 5$ ). However, helium is certainly one of the most diffusive elements. Helium diffusion from the ambient mantle can reduce the  $^4\text{He}/^3\text{He}$  ratio in the subducted material as suggested by Hanyu and Kaneoka (1997) and Hart *et al.* (2008). Although the diffusion coefficient Hart and collaborators used is relatively high ( $10^{-6} \text{ cm}^2 \text{ s}^{-1}$ ) compared to the measured helium diffusivity in olivine ( $\sim 10^{-7} \text{ cm}^2 \text{ s}^{-1}$  at mantle temperatures<sup>22</sup>; Hart, 1984a), they propose an elegant model that can explain the helium isotopic composition in “low  $^3\text{He}$ ” hotspots. In the model the recycled oceanic crust does not yield a  $^4\text{He}/^3\text{He}$  ratio of  $10^6$  as the closed system calculation would produce, but rather shows a helium isotopic ratio of  $\sim 180,000$  ( $\text{R}/\text{Ra} \sim 3$ ), which is in closer agreement with the signature of “low  $^3\text{He}$ ” hotspots.

22. The difference between Hart *et al.* (2008) and Hart (1984a) for the helium diffusivity in the mantle is that Hart *et al.* (2008) propose that the bulk helium diffusivity in the mantle is  $\sim 10$  times higher than in a single olivine grain due to inter-grain diffusivity.

### 3.3 Conclusions

The  $^4\text{He}/^3\text{He}$  ratios of the Earth's different reservoirs exhibit a large variation as represented on Figure 3.18. The atmospheric and crustal helium isotopic ratios reflect the production of radiogenic helium by U, Th, and Sm alpha decays. There is an unambiguous primordial  $^3\text{He}$  signal in the mantle, its presence cannot

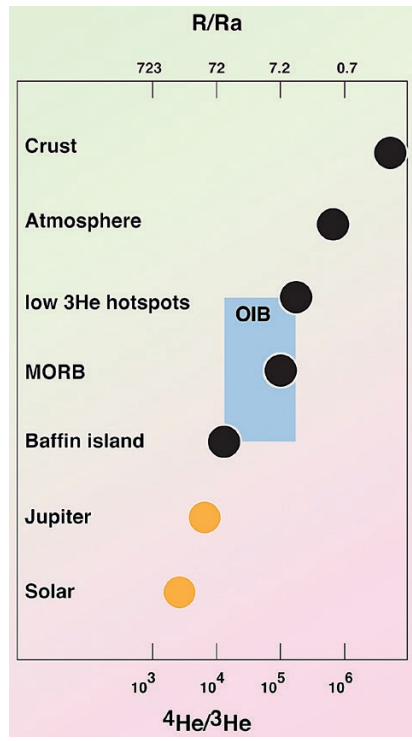


**Figure 3.18**

Helium isotopic ratios on Earth compared to solar and Jupiter, which are the probable starting helium isotopic compositions for the Earth. The atmospheric and crustal isotopic ratios reflect the helium loss to space and the addition of radiogenic helium respectively.

be accounted for nuclear reactions in the mantle. The lowest  $^4\text{He}/^3\text{He}$  ratio measured on Earth samples has been from olivines in picritic samples from Baffin Island, which represents the early products of the Icelandic mantle hotspot. MORB have a mean  $^4\text{He}/^3\text{He}$  ratio of  $\sim 90,000$  ( $R/Ra = 8$ ) and show a small dispersion, suggesting a well-homogenised reservoir due to convective stirring in the upper mantle. In contrast, the mantle sources of oceanic island basalts show a more variable  $^4\text{He}/^3\text{He}$  ratios, which is in agreement with other isotopic systems that show also a larger variability in OIB than in MORB. This helium isotopic ratio variability in OIB surely represents a mixture between a primitive material with low  $^4\text{He}/^3\text{He}$  (high  $^3\text{He}/^4\text{He}$ ) and either the ambient MORB mantle or recycled material such as oceanic crust or sediments (or both). The mechanism capable of preserving primordial helium in the deep mantle will be discussed in detail in Section 6, in the light of the noble gas systematics of terrestrial reservoirs. Here, the important message to keep in mind is that helium isotopes provide clear evidence that the mantle is not fully degassed of its primordial volatile budget, and that the mantle has a highly heterogeneous  $^4\text{He}/^3\text{He}$  ratios.



## 4. RADIOGENIC ARGON AND XENON IN THE MANTLE AND THE 'AGE' OF MANTLE DEGASSING

Similar to the case of He discussed in the last section, terrestrial Ar is dominated by its radiogenic isotope  $^{40}\text{Ar}$ , produced by the radioactive decay of  $^{40}\text{K}^{23}$ . Indeed  $^{40}\text{Ar}$  forms a significant fraction of the modern atmosphere at 0.934%, as unlike  $^4\text{He}$ , which escapes to space,  $^{40}\text{Ar}$  has accumulated over Earth history. The predominance of the radiogenic isotope in terrestrial Ar is illustrated by the reference atmospheric ratios of  $^{40}\text{Ar}/^{36}\text{Ar} = 298.6$  and  $^{38}\text{Ar}/^{36}\text{Ar} = 0.188^{24}$ . Figure 4.1 further shows the variation of these two isotopic ratios in different terrestrial reservoirs and of the Mars and Venus atmospheres.

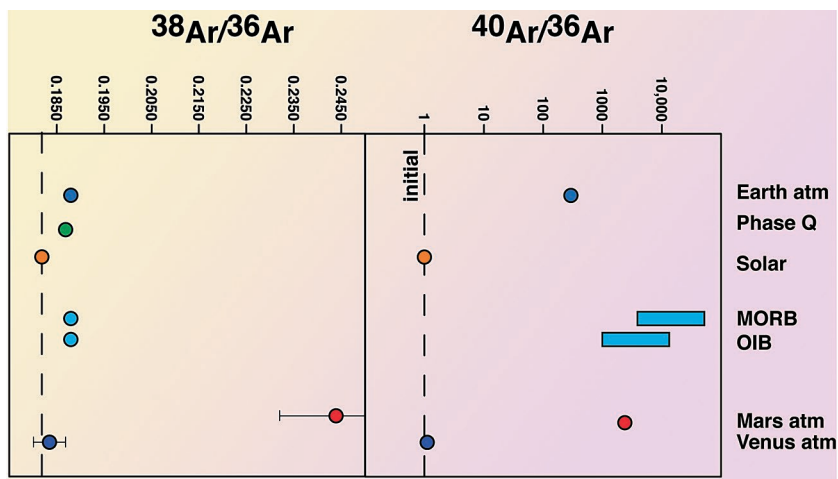


**Figure 4.1**

Variation in the isotopic ratios of argon in different reservoirs. The Earth's mantle shows very radiogenic  $^{40}\text{Ar}/^{36}\text{Ar}$  compared to the atmosphere and to the solar value. Mars and Venus ratios are taken from Wieler (2002) and Swindle (2002). Q composition is from Busemann *et al.* (2000). Regarding the  $^{38}\text{Ar}/^{36}\text{Ar}$  ratio of the Mars atmosphere, it seems that the mass spectrometer installed aboard the Opportunity rover was able in April 2013 (Press releases) to reproduce  $^{38}\text{Ar}/^{36}\text{Ar}$  ratio previously determined (Viking, SNC meteorites) with better precision. These new results confirm that a large fraction of argon was certainly lost from the Mars atmosphere, producing residual argon enriched in  $^{38}\text{Ar}$ .

23.  $^{40}\text{K}$  has two decays:  $^{40}\text{K} + e^- \rightarrow ^{40}\text{Ar}$  ( $\lambda_e = 0.581 \times 10^{-10} \text{ a}^{-1}$ ) and  $^{40}\text{K} \rightarrow ^{40}\text{Ca} + \beta^-$  ( $\lambda_\beta = 4.962 \times 10^{-10} \text{ a}^{-1}$ ).

24. The  $^{40}\text{Ar}/^{36}\text{Ar}$  ratio has been recently re-determined. The value is now 298.6 in the atmosphere (Lee *et al.*, 2006).



## 4.1 Radiogenic Argon in MORB and OIB

The radioactive decay of  $^{40}\text{K}$  to  $^{40}\text{Ar}$  has been harnessed with huge success for geochronological purposes (e.g., Dalrymple, 1969; McDougall and Harrison, 1999). Such work is not the focus of my attention here, but the difficulties encountered in the early application of K-Ar geochronology to testing the nascent theory of plate tectonics by dating basalts in the ocean basin first revealed important aspects of the Ar isotopic evolution of the Earth. Notably, attempts to date submarine basalts using the K-Ar method have resulted in unrealistic estimates as radiogenic  $^{40}\text{Ar}$  is “in excess” in the source of these lavas. For example, Funkhouser *et al.* (1968) found “K-Ar ages” up to  $690 \pm 7$  Ma in fresh MORB for East Pacific Rise (EPR). Obviously, this age is meaningless. Additionally, they observed that radiogenic argon excesses are more substantial in the glassy rim than into the more crystalline part in the interior of a pillow. The glassy margin of pillow lavas is formed by the quenching of the lava at the contact of the fresh seawater and can then trap vesicles with mantle-derived gases. The interior of the pillow is hotter, and crystallises slower, allowing its degassing and seawater assimilation. The glassy margin of pillow lavas are thus the preferred samples for analysing noble gases in oceanic basalts, even though they pose difficulties for geochronology.

Furthermore, Dalrymple and Moore (1968) made similar observations and obtained “K-Ar ages” on Kilauea (Hawaii) fresh pillow lavas of up to 43 Ma. They concluded that submarine pillows are not suitable for K-Ar dating because of this excess in radiogenic argon. Subsequently, argon systematics in submarine pillow lavas has been used to constrain the mantle-atmosphere system instead of for age dating. Since then, many publications have focused on the determination of the  $^{40}\text{Ar}/^{36}\text{Ar}$  ratios in mantle reservoirs (e.g., Fisher, 1983; Ozima and Zashu, 1983; Sarda *et al.*, 1985) and on the determination of the chronology of atmosphere formation (e.g., Ozima and Kudo, 1972; Ozima, 1975).

For example, Fisher (1975) was one of the first to analyse argon in MORB samples and he acquired  $^{40}\text{Ar}/^{36}\text{Ar}$  ratios as high as  $\sim 16,000$ . This ratio is much higher than the atmospheric value of 299, which demonstrates the significant presence of radiogenic  $^{40}\text{Ar}$  in the mantle. Later on, Ozima and Zashu (1983) analysed the five noble gases, including argon, on the same MORB samples and obtained radiogenic  $^{40}\text{Ar}/^{36}\text{Ar}$  ratios lower than 5600. In three publications, the Paris group obtained ratios as high as  $28,150 \pm 330$  (Allègre *et al.*, 1983b; Sarda *et al.*, 1985; Staudacher *et al.*, 1989) in samples from the Mid Atlantic Ridge (Fig. 4.2). Clearly, the mantle source of the mid oceanic ridge basalts has a very radiogenic argon isotopic ratio compared to the atmospheric value. Such a difference will be used to constrain the degassing history of the mantle.

Prior to the 1990's, only a few OIB were analysed for their argon isotopic ratio. As discussed in the previous section, there are few quenched glass samples of OIB available and so noble gas analyses typically need to be made on olivine phenocrysts, or entrained xenoliths, which have trapped fluid or melt inclusions. Such materials yield much smaller amounts of gas than quenched glass and





pose a greater technical challenge. Fisher (1983) analysed argon in Hawaiian ultramafic nodules and obtained  $^{40}\text{Ar}/^{36}\text{Ar}$  ratios up to 7,300. The results from three glass samples from Loihi and Hualalai (Hawaii) are given in Allègre *et al.* (1983b) with close-to-air  $^{40}\text{Ar}/^{36}\text{Ar}$  ratios ( $1,150 \pm 19$ ). Kaneoka and Staudacher with their collaborators published moderately radiogenic ratios, lower than 6,200 in dunite nodules from Loihi seamount and Réunion island (Kaneoka *et al.*, 1983; Staudacher *et al.*, 1986). Finally, Sarda and collaborators analysed by step-heating eight samples from Loihi seamount and obtained close-to-air  $^{40}\text{Ar}/^{36}\text{Ar}$  ( $<979 \pm 17$ ) (Sarda *et al.*, 1988), confirming previous analyses (Staudacher *et al.*, 1986). Although the role for air contamination could not be excluded, these measurements on OIB samples suggested that such OIB mantle reservoirs with low  $^4\text{He}/^3\text{He}$  isotopic ratios also had lower  $^{40}\text{Ar}/^{36}\text{Ar}$  than the MORB source, confirming that the MORB source is more degassed.

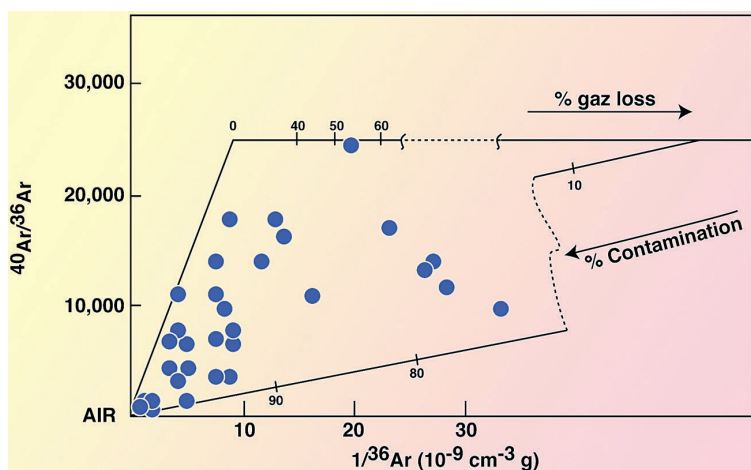


**Figure 4.2**

Argon isotopic compositions in Mid Ocean Ridge Basalts reported against  $1/^{36}\text{Ar}$ . This figure shows the two main processes that disturb the argon isotopic composition in basalts: gas loss (horizontal line because isotopic ratios are not fractionated) and air contamination (mixing with air). Because argon is not soluble in magma, it is intensely degassed during eruption and therefore is easily contaminated (modified from Sarda *et al.*, 1985).

This critical problem of atmospheric contamination (as mentioned above, the atmosphere contains ~1% argon) needed to be addressed quantitatively. By coupling Ne-Ar measurements on the same sample it is possible to correct argon for atmospheric contamination. Indeed, the mantle  $^{20}\text{Ne}/^{22}\text{Ne}$  ratio, which will be explained in more detail in the next section, is the ‘rosetta stone’ of the atmospheric contamination correction. With Joachim Kunz and Claude Allègre, I was the first to use a step crushing technique to produce, in a Ne-Ar mixing diagram (Fig. 4.4), a hyperbolic mixing curve precise enough to allow the determination

of the MORB-source  $^{40}\text{Ar}/^{36}\text{Ar}$ , before atmospheric contamination (Moreira *et al.*, 1998). Using this, we proposed a maximum  $^{40}\text{Ar}/^{36}\text{Ar}$  ratio for the MORB source of 44,000 (Fig. 4.4), assuming the mantle has a  $^{20}\text{Ne}/^{22}\text{Ne}$  ratio that is exactly solar (see Section 5 for the rationale behind this constraint). In part, the high precision obtained was possible because we used the famous sample 2 $\pi$ D43, which became known as the “ultimate popping rock”. This sample, shown on Figure 4.3, is extremely vesicular (20%), and very gas rich. To my knowledge, this is the MORB sample containing the highest amount of mantle-derived noble gases (Javoy and Pineau, 1991). This sample was collected in 1985 at 14 °N in the Atlantic, at 3,500 m depth, with the R/V Boris Petrov. It was a great opportunity for our laboratory that *Philippe Sarda* was on-board. By itself, this sample has been the subject of a large number of publications and it is often considered as a reference sample for the study of noble gases in the mantle (Staudacher *et al.*, 1989; Sarda and Graham, 1990; Javoy and Pineau, 1991; Burnard *et al.*, 1997; Kunz *et al.*, 1998; Moreira *et al.*, 1998; Kunz, 1999).

Recent studies using step heating or step crushing, and Ne and Ar measurements on single samples have been performed on MORB and OIB and it seems clear that the mantle sources of most hotpots (*e.g.*, Galapagos, Iceland, Hawaii) have  $^{40}\text{Ar}/^{36}\text{Ar}$  ratios lower than 10,000, lower than the maximum MORB ratio of ~30,000 (Hiyagon *et al.*, 1992; Honda *et al.*, 1993; Moreira *et al.*, 1995; Valbracht *et al.*, 1997; Sarda *et al.*, 2000; Tieloff *et al.*, 2000; Tieloff *et al.*, 2002; Honda and Woodhead, 2005; Hopp and Tieloff, 2005; Raquin and Moreira, 2009; Mukhopadhyay, 2012), but higher than the atmospheric ratio (299) which is the value that was proposed for the lower mantle by the Paris group in the 1980’s.

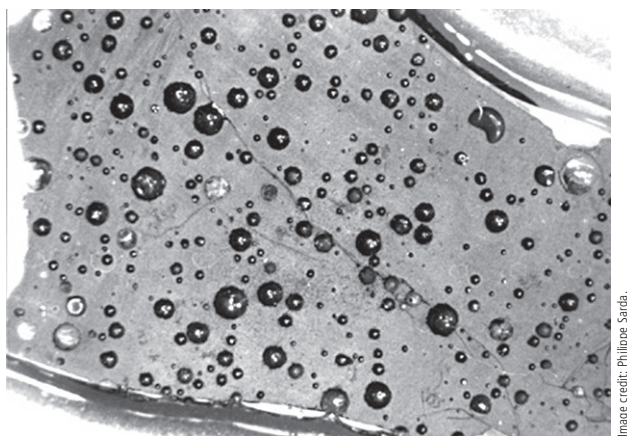
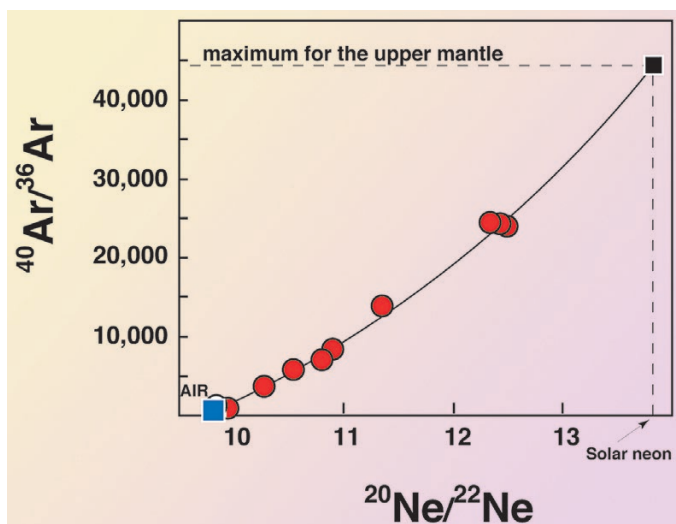


Image credit: Philippe Sarda.

**Figure 4.3**

Popping rock 2 $\pi$ D43. This exceptional sample was collected at 14 °N on the Mid Atlantic ridge. It has a vesicularity of ~20% and contains large quantities of mantle-derived gases, unfractionated by degassing. The largest vesicles are ~1 mm in this picture.





**Figure 4.4**

Mixing diagram between the neon and argon isotopic ratios obtained by step crushing of sample 2πD43. This technique allowed us to constrain the  $^{40}\text{Ar}/^{36}\text{Ar}$  in the MORB source. In such a diagram, mixing is represented by a hyperbola rather than by straight lines (modified from Moreira *et al.*, 1998).

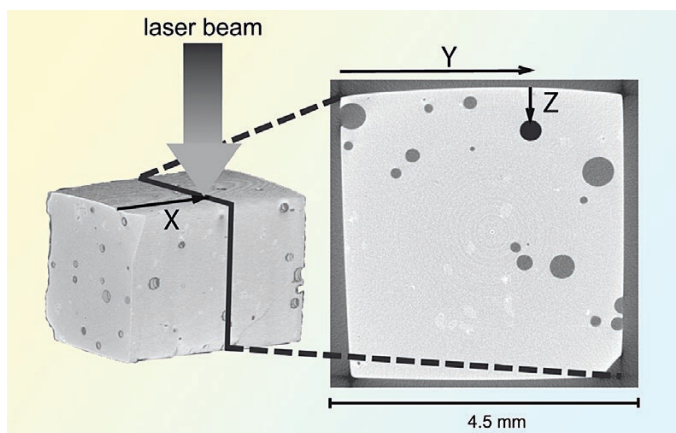


**Figure 4.5**

Figure showing the technique to open single vesicles in glassy oceanic basalt. Ultra violet photons (UVs) are focussed on the surface of the sample to ablate it until a vesicle is opened. The sample can be characterised using microtomography (from Colin *et al.*, 2013, with permission from Elsevier).

Another interesting approach used to determine the Ar isotopic composition of mantle reservoirs and document the isotopic heterogeneity of vesicles while avoiding atmospheric contamination was developed by *Pete Burnard*, now in Nancy (France) but who was then in Manchester (UK). This method consists of the extraction of the gas in a single vesicle using a laser (Burnard *et al.*, 1997; Burnard, 1999). Subsequent studies on single vesicles using laser ablation were reported by Raquin *et al.* (2008) and Colin *et al.* (2013). The traditional technique to

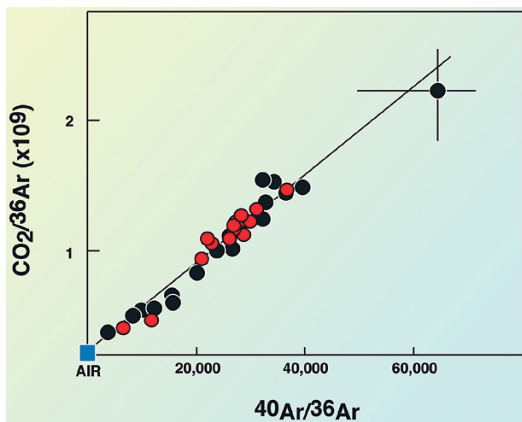


**Figure 4.6**  $^{40}\text{Ar}/^{36}\text{Ar}$  vs  $\text{CO}_2/^{36}\text{Ar}$  in single vesicles from the popping rock 2 $\pi$ D43 obtained by laser extraction techniques coupled to mass spectrometry (black dots: Burnard *et al.*, 1997; red dots: Raquin *et al.*, 2008).

extract gases from oceanic glassy samples had been either crushing or step heating of a large sample (~1 g) in order to get sufficient gas to make precise measurements. However, this crushing technique extracts gas from dozens of vesicles and possibly incorporates trapped atmospheric gas in cracks or in empty vesicles. The laser extraction method is, on paper, simple. Under vacuum, a laser beam (for example using an excimer laser) is focused on a sample and the glass is “drilled” until a vesicle is pierced, which is observed

as a pressure jump in the sample cell (Fig. 4.5). This technique was successively applied to the gas-rich sample 2 $\pi$ D43 (Fig. 4.6) by Burnard *et al.* (1997) and later on by us (Raquin *et al.*, 2008). In Burnard’s study, the analytical technique to “open” a vesicle was slightly different. In Burnard *et al.* (1997), Burnard used a YAG laser (infrared) to heat the  $\text{CO}_2$  in the vesicles, whereas now an excimer laser (193 nm) is used to open vesicles, without heating the surrounding sample. The results are given on Figure 4.6. These two studies performed on the same sample provided slightly different results on the  $^{40}\text{Ar}/^{36}\text{Ar}$  in single vesicles and on the mantle composition. The main discrepancy is the slightly lower  $^{40}\text{Ar}/^{36}\text{Ar}$  ratios we obtained on most of the vesicles compared to Burnard’s work (Fig. 4.6). The distinction might be explained by the different method of blank corrections (Raquin *et al.*, 2008). Nevertheless, with the exception of one particularly radiogenic vesicle in Burnard’s study ( $\sim 64,000 \pm 8,000$ ), both studies obtained  $^{40}\text{Ar}/^{36}\text{Ar}$  of the order of  $\sim 40,000$  in vesicles from the 2 $\pi$ D43 sample, compatible with the highest ratios measured in MORB, although higher (*e.g.*, Staudacher *et al.*, 1989).



## 4.2 The Terrestrial Argon Budget

The  $^{40}\text{Ar}/^{36}\text{Ar}$  ratio of different mantle reservoirs is a key parameter for studying mantle-atmosphere system evolution over geological times (Hart and Hogan, 1978). Another fundamental use of the K-Ar system in mantle geochemistry is terrestrial mass balance through the “argon budget”, which demonstrates that the deep mantle is not degassed (Turekian, 1959; Allègre *et al.*, 1996; Davies, 1999; Lassiter, 2004). This calculation is possible because  $^{40}\text{Ar}$  was practically non-existent in the primitive Earth, and so the current  $^{40}\text{Ar}$  budget has predominantly been produced by the decay of  $^{40}\text{K}$  during the Earth’s lifetime. Indeed the  $^{40}\text{Ar}/^{36}\text{Ar}$  ratio is lower than 1 in the gas rich meteorites<sup>25</sup>, whereas it is ~299 in the Earth’s atmosphere and more than 40,000 in the mantle (see Figs. 4.1 and 4.6). The primordial  $^{40}\text{Ar}$  is only ~0.1‰ of the present-day estimate of the Earth’s bulk  $^{40}\text{Ar}$  and can be neglected in the budget of radiogenic argon. Consequently, with a knowledge of the K content of the Bulk Silicate Earth (BSE), it is simple to calculate the total  $^{40}\text{Ar}$  that has been produced by  $^{40}\text{K}$  decay over 4.5 Ga of Earth history. This value can be compared to the argon budget in the atmosphere, crust, and mantle, all accessible reservoirs that can be sampled. This approach in “onion layers” was re-visited by Allègre *et al.* (1996) and I reproduce here their calculation albeit with an up-to-date of K estimates for the BSE.

Allègre *et al.* (1996) considered a primitive mantle having a uranium content derived from carbonaceous chondrite concentrations (~20 ppb for BSE) and a K/U of 12,700 (weight ratio) derived from Jochum *et al.* (1983). With this K content, they concluded that 50% of the  $^{40}\text{Ar}$  produced on Earth is still the lower mantle. Table 4.1 presents the U content of BSE derived using various chondrite classes and their inferred K content assuming a recently revised K/U ratio of 13,800 for the BSE (Arevalo *et al.*, 2009). The latter is higher than the previous estimate of 12,700 (Jochum *et al.*, 1983). Although the different classes of chondrites have different U contents (Wasson and Kalleyman, 1988), I correct for devolatilisation of volatile elements and core formation by using the near invariant U/Ca ratios of the meteorites and calculating the mantle U content for several estimates of BSE Ca content (2.0 and 2.5% from McDonough and Sun, 1995 and Lyubetskaya and Korenaga, 2007, respectively). In this way the U content of the BSE depends little on the chondritic parent body chosen. These new estimates confirm the calculation of Allègre *et al.* (1996) and Arevalo *et al.* (2009), in the sense of that between 35 to 60% of the  $^{40}\text{Ar}$  produced during Earth’s history is presumed to be present still in the lower mantle. These estimates are minimum values since the  $^{40}\text{Ar}$  concentration considered for the MORB source were derived from the popping rock sample 2πD43. As discussed above, this is the most gas-rich

25. Gas rich meteorites contain sufficient  $^{36}\text{Ar}$  that addition of radiogenic  $^{40}\text{Ar}$  by  $^{40}\text{K}$  radioactive decay does not affect the primordial  $^{40}\text{Ar}/^{36}\text{Ar}$  ratio.





Table 4.1

The  $^{40}\text{Ar}$  budget in the BSE assuming a K/U ratio of  $13,800 \pm 2,600$  (Arevalo *et al.*, 2009). U in BSE is determined using the Ca/U ratio in different types of chondrites (Masson and Kalleyman, 1988) and two different estimates for the Ca of the mantle (2.5% and 2%) (e.g., McDonough and Sun, 1995; Lyubetskaya and Korenaga, 2007) and from different starting compositions. The percentage of radiogenic argon in the lower mantle can vary from 35 to 60% depending of the starting composition of the Earth. This calculation assumes a homogeneous mantle with regard to its Ca content, which might not be the case (e.g., Kaminski, 2013). The argon budget in the crust and in the atmosphere is taken from Allegre *et al.*, (1996). The  $^{40}\text{Ar}$  content in the MORB source is taken at  $7 \times 10^{-6} \text{ cm}^3 \text{STP g}^{-1}$  (Moreira *et al.*, 1998).

	U BSE (Ca=2.5%)	U BSE (Ca=2.0%)	K BSE (Ca=2.5%)	K BSE (Ca=2.0%)	Ar x10 <sup>18</sup> g (Ca=2.5%)	±	Ar x10 <sup>18</sup> g (Ca=2.0%)	±	% in lower mantle (Ca=2.5%)	±	% in lower mantle (Ca=2.0%)	±
CI	22.6	17.8	311	246	174	34	137	27	53	9	40	12
CM	21.9	17.3	302	239	169	33	133	26	51	9	38	12
CO	20.8	16.5	287	227	160	31	127	25	49	10	35	13
CV	22.6	17.9	312	247	174	34	138	27	53	9	40	12
H	24.3	19.2	335	265	187	36	148	29	56	8	45	11
L	25.1	19.8	346	274	193	37	153	30	58	8	46	10
LL	25.3	20.0	349	276	195	37	154	30	58	8	47	10
EH	26.8	21.2	370	292	206	40	163	32	60	8	50	10
EL	25.0	19.8	346	273	193	37	152	30	57	8	46	10

MORB sample ever found, although it is taken to be representative of the MORB source (Staudacher *et al.*, 1989; Sarda and Graham, 1990; Javoy and Pineau, 1991; Moreira *et al.*, 1998). No higher radiogenic  $^{40}\text{Ar}$  concentrations were measured in MORB, suggesting that this particularly high concentration might be an upper limit for the MORB source concentration.

Lassiter (2004) is the last of a number of studies (*e.g.*, Albarède, 1998; Davies, 1999) to have challenged the argon budget model of Allègre and his collaborators arguing that the BSE might not have a K/U ratio as high as 13,000 but lower because recycled altered oceanic crust with low K/U has been neglected in the global K budget (Lassiter, 2004). Using a lower K/U of ~8,000 for the bulk Earth in the calculation of the radiogenic argon budget, he inferred that only a few % of the  $^{40}\text{Ar}$  is still in the lower mantle, the same fraction as in the upper mantle. Therefore, in such a scenario, there is no need for a deep reservoir rich in radiogenic argon.

As pointed out by Halliday (2013), this calculation, and the possibility that 50% of the radiogenic argon is in the lower mantle, has no relationship with the notion of a primordial reservoir in the sense of the helium or neon isotope systematics (see Sections 3, 5, 6). This reservoir could have been degassed of its primordial isotopes and then isolated from the surface where degassing occurs. What is relevant for the possibility of a deep primordial noble gas rich reservoir is the determination of noble gas isotopic ratios, including the  $^{40}\text{Ar}/^{36}\text{Ar}$ . The argon budget suggests only that the radiogenic argon produced during the Earth's history is not completely degassed.

## 4.3 Radiogenic and Fissiogenic Xenon on the Earth

### 4.3.1 Brief outlook of xenology

With an isotope spectrum comprising 9 stable isotopes (Fig. 4.7), xenon provides an abundance of riches for noble gas isotope geochemists. The most abundant isotopes are radiogenic ( $^{129}\text{Xe}$ ), derived from  $^{129}\text{I}$  or are fissiogenic ( $^{131}\text{--}^{136}\text{Xe}$ ), products of the spontaneous fission of  $^{238}\text{U}$  and  $^{244}\text{Pu}$ . The lighter stable isotopes of xenon, from mass 124 to mass 130, except  $^{129}\text{Xe}$ , are non-radiogenic. The two isotopes 124 and 126 are very rare and difficult to measure in the laboratory. As a consequence of the contrasting origins of its isotopes, xenology can be split into two main areas of interest; the first being the study of its radiogenic/fissiogenic heavy isotopes, the second the study of the mass-dependent fractionation of its non-radiogenic light isotopes either during planetary formation or during atmosphere evolution. In this section I focus on the radiogenic/fissiogenic xenon isotopes measured in oceanic basalts. The composition of the non-radiogenic xenon isotopes on Earth will be discussed in Sections 7 and 8 because it provides important constraints on the possible subduction of atmospheric noble gases into the mantle and on the origin and evolution of terrestrial volatiles.





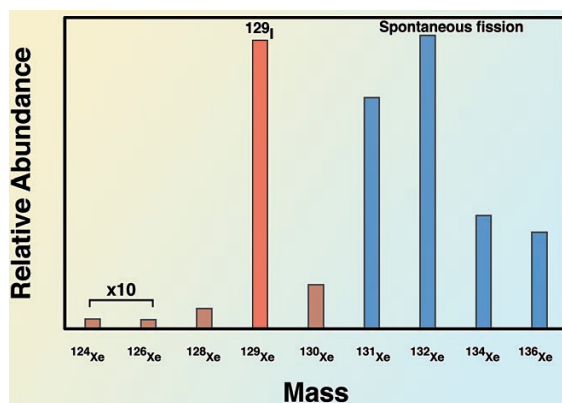


**Figure 4.7**

Relative abundances of xenon isotopes in Earth's atmosphere.  $^{129}\text{Xe}$  is partly derived from the now extinct radioactive decay of  $^{129}\text{I}$  ( $T_{1/2} = 17$  Ma).  $^{131}\text{--}^{136}\text{Xe}$  isotopes are mainly the product of the spontaneous fission of  $^{244}\text{Pu}$  ( $T_{1/2} = 82$  Ma) and  $^{238}\text{U}$ . The other isotopes are stable and non-radiogenic.

As discussed in Section 2, in 1960, *Reynolds* published his first work on the isotopic composition of xenon on a meteorite named Richardton and he showed for the first time an excess of  $^{129}\text{Xe}$  compared to the terrestrial atmosphere (Fig. 4.8). He attributed this observation to the decay of  $^{129}\text{I}$ , an isotope with a 17 Ma half-life, produced in explosive stars and injected into the Solar System shortly before its formation. Moreover, thanks to this study it was shown that the heavy isotopes of xenon have a fissionogenic origin in the Earth's atmosphere, as we will discuss below. Apart from a few studies on uranium and tellurium rich minerals, there was little analysis of xenon in terrestrial samples published before *Butler et al.* (1963). This work focused on three terrestrial samples: an eclogite, a granite and more interestingly, a gas from a  $\text{CO}_2$  well. They observed  $^{129}\text{Xe}$  anomaly in this gas sample and interpreted it as reflecting decay of  $^{129}\text{I}$ . They concluded that the Earth's mantle is not fully degassed and homogenised. This pioneering work was followed by other studies on  $\text{CO}_2$  well gases (*Boulos and Manuel, 1971; Phinney et al., 1978*); some of these works are summarised in Figure 4.9 including the  $^{129}\text{Xe}/^{130}\text{Xe}$  and  $^{136}\text{Xe}/^{130}\text{Xe}$  ratios obtained, corrected with more recent estimates of the atmospheric xenon isotopic compositions. At the same time, two studies provided xenon isotopic ratios in xenoliths and phenocrysts from Hawaii, albeit with only small isotopic xenon excesses relative to air (*Hennecke and Manuel, 1975; Kaneoka and Takaoka, 1978*).

Figure 4.9 shows the xenon isotopic ratios measured on MORB samples by *Staudacher and Allègre (1982)*. This paper is seminal for two reasons. This is the first xenon isotopic study on oceanic basalts, and secondly this is the first paper of the Paris noble gas group. By the end of the 1970's, the two ARESIBO mass spectrometers (Fig. 4.10) had been constructed at the Institut de Physique du



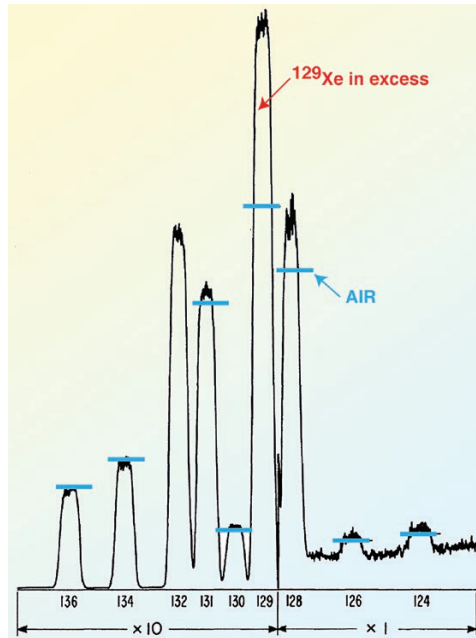


**Figure 4.8**

The xenon spectrum of the chondrite Richardton obtained by Reynolds in 1960. This is the first observation of  $^{129}\text{Xe}$  excess in meteorites suggesting that extinct  $^{129}\text{I}$  was still present during the Solar System formation.

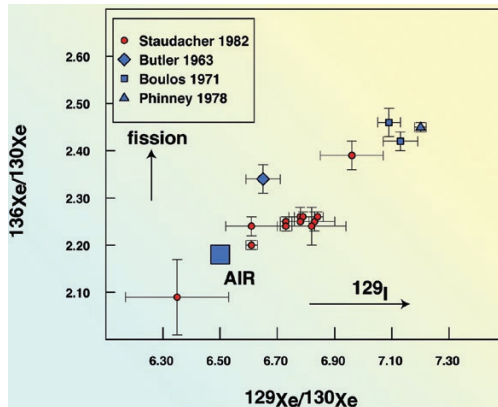


**Figure 4.9**

The first xenon analyses of mantle-derived samples showing significant excesses relative to the atmospheric composition. Staudacher and Allègre (1982) published the first  $^{129}\text{Xe}$  excesses in MORB, whereas the other publications focused on  $\text{CO}_2$ -well gases (Butler *et al.*, 1963; Boulos and Manuel, 1971; Phinney *et al.*, 1978).



Globe de Paris by *Thomas Staudacher* (Fig. 4.11), *André Lecomte* (Fig. 4.12), *Michel Girard* (Fig. 4.13), and *Claude Allègre*. These fantastic guys, to whom I add *Philippe Sarda* who arrived later, were the heart of the Paris noble gas group, the leaders in the 1980's and 1990's of (heavy) noble gas geochemistry.

The Staudacher and Allègre (1982) article is the first showing noble gas data obtained with these fantastic machines that are still working 33 years later. Figure 4.9 shows a comparison between MORB and CO<sub>2</sub>-well gases. It was already clear then that there is a <sup>129</sup>Xe excess in the mantle compared to the atmosphere. The <sup>136</sup>Xe excess in the mantle originates from spontaneous fission of both the <sup>244</sup>Pu and <sup>238</sup>U as we will see below. The simplest explanation for the high <sup>129</sup>Xe/<sup>130</sup>Xe ratio in the mantle was, and still is, the degassing of the mantle during the period in which <sup>129</sup>I was extant. The <sup>129</sup>I half-life is 17 Ma, so the <sup>129</sup>Xe excess in the mantle reflects I/Xe fractionation, resulting from mantle degassing in the first 200 Ma of earth history, although this interpretation was debated in the 1980's (Ozima *et al.*, 1985). A more detailed discussion on the degassing of the mantle based on xenon isotopes will be presented in Sections 6 and 7.

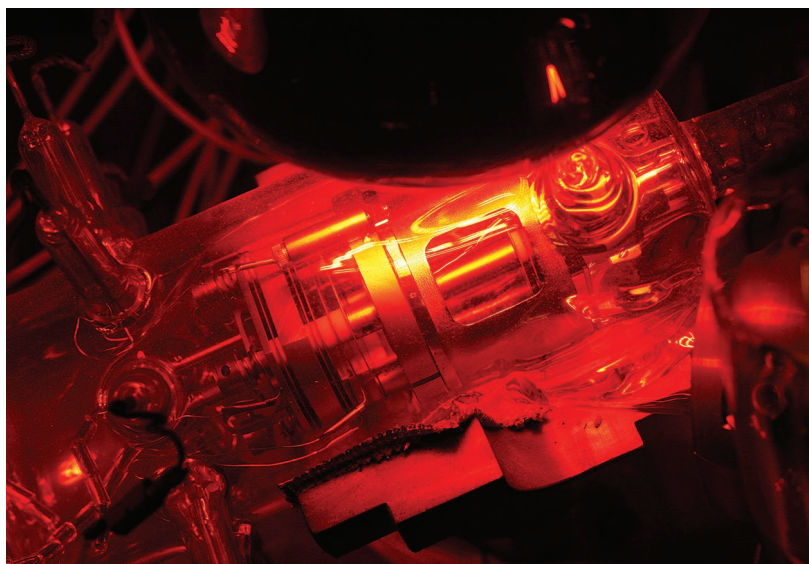


Photo credit: Joël Dyon (IPGP).

**Figure 4.10**

The ARESIBO mass spectrometer conceived by Claude Allègre at the end of the 1970's. This noble gas mass spectrometer is still working at the Institut de Physique du Globe de Paris. Its acronym is derived from the names Allègre, Reynolds, Signer, and Baur. In this image, one can see the ion source through the glass. The red colour comes from the infrared lamps that are used to desorb gases from the metallic part of the source. This technique, coupled to the use of glass, allows for very low background and memory effects in these mass spectrometers.



### 4.3.2 Radiogenic xenon from $^{129}\text{I}$ extinct radioactivity in the MORB source

Three questions arose from these first studies of xenon isotopes in mantle-derived samples published during the 1980's. Firstly, what was the exact  $^{129}\text{Xe}/^{130}\text{Xe}$  ratio of the mantle source of the mid ocean ridge basalts considering that samples may suffer atmospheric contamination or if there was subduction of atmospheric xenon? Secondly, what was the isotopic composition of the deep mantle from whence mantle plumes originated? Finally, what were the relative proportions in the mantle of xenon that originates from  $^{244}\text{Pu}$  and  $^{238}\text{U}$  spontaneous fission respectively; this is important for constraining models of the evolution of the atmosphere/mantle system. The methodology that can be used to address the first question will be discussed mainly in the next



Photo credit: Cécile Gautheron.

**Figure 4.12** André Lecomte, known as Dédé. To make it simple: Dédé knows how to do everything in the lab.



Photo credit: Manuel Moreira.

**Figure 4.11** Thomas Staudacher measuring the isotopic compositions of xenon in his house on La Réunion island.



Photo credit: André Lecomte.

**Figure 4.13** Michel Girard (on the right!). He conceived the electronics of the ARESIBO mass spectrometer. Even though he is now retired, he is still helping us with mass spectrometer issues.



section, using the neon systematics in oceanic basalts. The subduction of atmospheric xenon in the mantle and the idea of a “subduction barrier for volatiles” will be discussed in Section 7. In this section, I will discuss the origin of the fission-derived xenon to provide realistic parameters in modelling terrestrial atmosphere formation and mantle evolution. These models that will be reviewed in Sections 7 and 8.

There are only a few studies of xenon isotopes in MORB samples and I choose to discuss four of them because they offer high precision isotopic ratios, large excesses compared to air, and because noble gases were extracted from the samples using step crushing or heating techniques (Kunz *et al.*, 1998; Moreira *et al.*, 1998; Tucker *et al.*, 2012; Parai *et al.*, 2012). The xenon isotopic ratios reported in these publications are shown in Figure 4.14. Recently acquired xenon compositions from CO<sub>2</sub>-well gases are incorporated in Figure 4.14 for comparison and provide a first order method to determine the maximum  $^{129}\text{Xe}/^{130}\text{Xe}$  ratio in the MORB source (Holland and Ballentine, 2006).

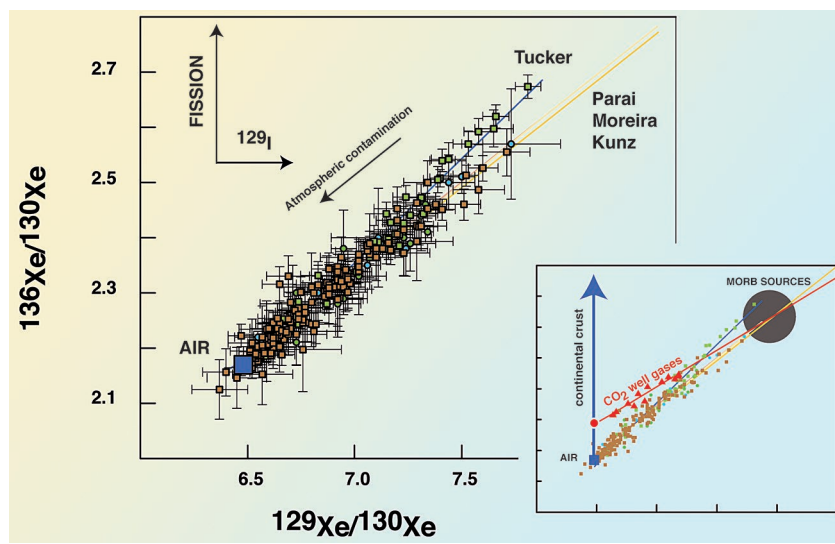


**Figure 4.14**

Recent compilation of xenon isotopic ratios in MORB. Data from Kunz *et al.* (1998), Moreira *et al.* (1998), Parai *et al.* (2012) and Tucker *et al.* (2012). The insert shows the same MORB compilation compared to CO<sub>2</sub> well gases from Holland and Ballentine (2006). The continental crust line is theoretical and assumes the production of  $^{136}\text{Xe}$  by spontaneous fission of  $^{238}\text{U}$ . CO<sub>2</sub> well gases show a mixture between MORB-like and crustal components and therefore the MORB-line and the CO<sub>2</sub> well gas line should cross at the mantle composition. This diagram provides a possible upper limit for the  $^{129}\text{Xe}/^{130}\text{Xe}$  in the MORB source (~8).



Figure 4.14 confirms previous results obtained on MORB by Staudacher and Allègre (1982) although with a much better precision and with an interesting feature reflecting possible homogeneity in the xenon isotopic composition in the MORB source. Results from the three studies (Moreira; Kunz; Parai) yield a single mixing line in the Xe-Xe diagram whereas the results from Tucker *et al.* (2012) suggest a different  $^{129}\text{Xe}/^{136}\text{Xe}$  ratio in the Equatorial Atlantic mantle compared to the North Atlantic and in the Indian mantles. CO<sub>2</sub>-well gas results are also shown in Figure 4.14 for comparison (Holland and Ballentine, 2006). CO<sub>2</sub>-well gases contain a proportion of crust-derived noble gases that explain the different slopes of the MORB and CO<sub>2</sub>-well gas mixing lines. The non-radiogenic end-member of these CO<sub>2</sub>-well gases contains fissionogenic xenon derived from the spontaneous fission of  $^{238}\text{U}$  alone, which explains the position of this first end-member above the atmospheric composition (along the blue line in Fig. 4.14). The second end-member, however, is similar for the two populations suggesting a common source, as already pointed out by Staudacher (1987). The intersection of the trends provides a constraint on the xenon isotopic composition of the mantle source of MORB and CO<sub>2</sub>-well gases.

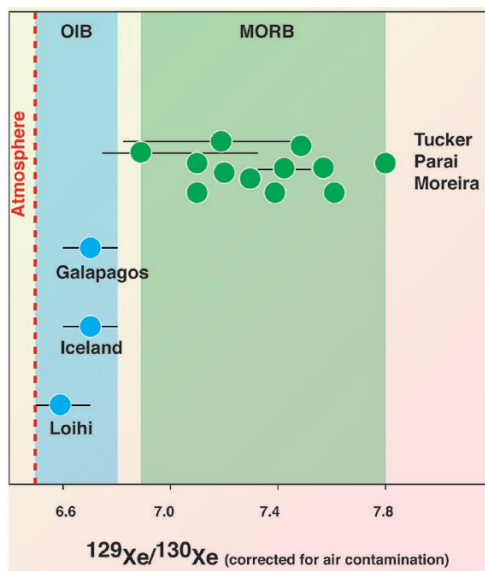


**Figure 4.15**

$^{129}\text{Xe}/^{130}\text{Xe}$  ratios in MORB, corrected for air contamination using the  $^{20}\text{Ne}/^{22}\text{Ne}$  ratio. Three primitive hotspots are shown for comparison, for which the xenon isotopic ratios are also corrected for air contamination using neon isotopes. Clearly, the  $^{129}\text{Xe}/^{130}\text{Xe}$  ratios are different between these three reservoirs. These differences reflect ancient I/Xe fractionation since the  $^{129}\text{I}$  has been extinct since at least 4 Ga. The classical interpretation of this diagram is that the MORB source was degassed early in the Earth's history, producing a relatively non-radiogenic  $^{129}\text{Xe}/^{130}\text{Xe}$  ratio in the atmosphere and a radiogenic  $^{129}\text{Xe}/^{130}\text{Xe}$  ratio in the MORB source due to a high  $^{129}\text{I}/^{130}\text{Xe}$  ratio produced by degassing. A undegassed mantle, sampled by mantle plumes, has lower  $^{129}\text{Xe}/^{130}\text{Xe}$  than the MORB source because the  $^{129}\text{I}/^{130}\text{Xe}$  ratio was small. The variation of the  $^{129}\text{Xe}/^{130}\text{Xe}$  ratio within the different MORB sources may either reflect interaction with plumes or subduction of atmospheric xenon (see Section 7).



The  $^{129}\text{Xe}/^{130}\text{Xe}$  ratio of these sources is between 7.5 and 8, agreeing with the isotopic ratios corrected for atmospheric correction using neon isotopes, as will be discussed in Section 5.

The MORB source is also heterogeneous in  $^{129}\text{Xe}/^{130}\text{Xe}$  as shown in Figure 4.15. The  $^{129}\text{Xe}/^{130}\text{Xe}$  ratio is currently stable because  $^{129}\text{I}$  is extinct. These results can be interpreted either as a recycling of atmospheric xenon or as the injection of primitive material into the upper mantle, both having low  $^{129}\text{Xe}/^{130}\text{Xe}$  ratio. This will be discussed in Section 7.

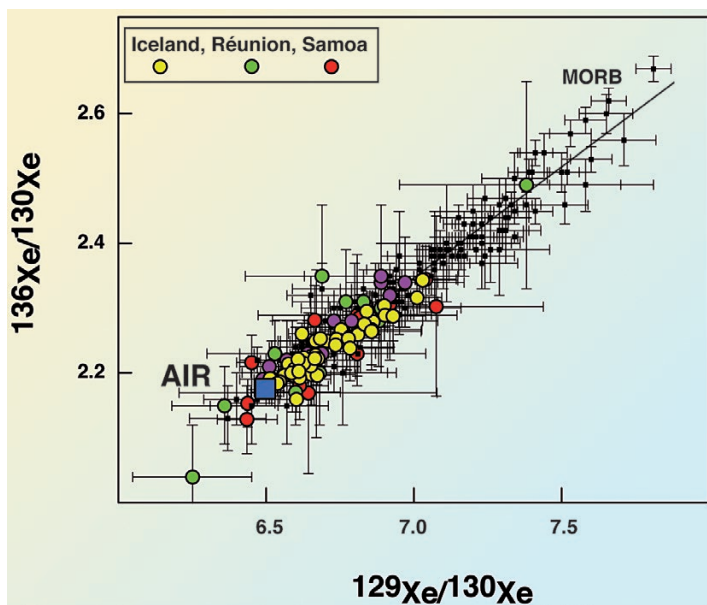


**Figure 4.16** Xenon isotopic composition in some OIB (Iceland, Samoa and La Réunion hotspots). Data from Poreda and Farley (1992), Trierloff *et al.* (2000, 2002) and Mukhopadhyay (2012). This figure shows that OIB have systematically lower xenon isotopic ratios than MORB (small black dots).

OIB show systematically lower  $^{129}\text{Xe}/^{130}\text{Xe}$  ratios than MORB (Fig. 4.16). It could be suggested that this reflects a higher atmospheric contamination of OIB because they contain less gases due to higher degassing. However, using neon isotopes, it has been demonstrated that these lower  $^{129}\text{Xe}/^{130}\text{Xe}$  ratios are indeed mantle sourced. Figure 4.15 shows recent estimates of  $^{129}\text{Xe}/^{130}\text{Xe}$  ratios in Iceland, Galapagos, and Loihi samples, three primitive hotspots for helium and neon (Valbracht *et al.*, 1997; Trierloff *et al.*, 2000; Raquin and Moreira, 2009; Mukhopadhyay, 2012). This diagram will be discussed in detail later because it provides important constraints on early mantle dynamics and the degassing





history of the mantle. What it is important to underline here is that the MORB sources exhibit higher  $^{129}\text{Xe}/^{130}\text{Xe}$  ratios than the OIB sources and the Earth's atmosphere. This clearly reflects the consequences of primordial degassing.

#### 4.4 Determination of the Composition of the Non-radiogenic Atmosphere

Based on the first measurements of light xenon isotopes in the Richardton meteorite, *Reynolds* proposed in 1960 that the atmospheric xenon composition reflects an isotopically fractionated residue of gas loss from a primitive atmosphere. Two starting compositions for the primordial atmospheric xenon can be considered, from which the present day atmosphere is ultimately derived. One is the phase Q (see Section 2); the second is solar. Because phase Q appears also to result from mass fractionation from an original solar composition, it can be considered as the starting isotopic composition of the pre-fractionation atmosphere. When reporting the atmospheric composition normalised to the solar composition, a clear trend in the non-radiogenic/fissionogenic isotopes is observed, which is consistent with a mass-dependent, Rayleigh distillation<sup>26</sup> (Fig. 4.17)

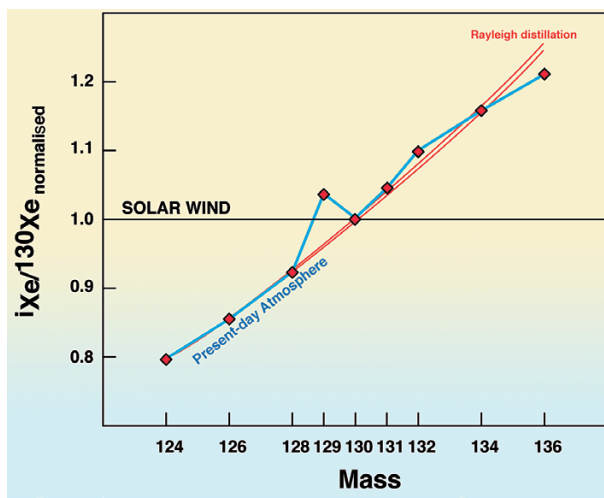


Figure 4.17

Present-day atmospheric xenon composition normalised to the solar wind. Rayleigh distillations (here the two red curves represent Rayleigh distillation with a fractionation factor in  $m_i/130$  or  $(m_i/130)^{1/2}$ ) fit the non-radiogenic xenon isotopic composition suggesting that the present-day atmosphere is the residue of a gas loss from the atmosphere. However, the figure clearly shows that there is an issue for the heavy isotopes, particularly for the  $^{136}\text{Xe}$ . This has led to the definition of a primordial xenon isotopic composition for the Solar System different from that of the present-day solar wind, depleted in heavy xenon isotopes (named U-Xe).

26. A Rayleigh distillation occurs when there is a fractionation process in which the product is removed from the system at each step of the process. Its mathematical formulation is  $R = R_0 f^{1-a}$ , where  $a$  is the fractionation factor and  $f$  is the remaining fraction of the reference isotope.



as pointed out by Reynolds (1960). However, this normalisation to the solar isotopic composition raises a problem for the heavy xenon isotopes compared to the expected compositions. In particular, this model predicts too little  $^{136}\text{Xe}$ .

This observation has led to the definition of the U-Xe (Pepin and Phinney, 1976, the most famous unpublished manuscript!), which is similar to the solar xenon other than for heavy xenon isotopes (see Fig. 4.18)<sup>27</sup>. The non-radiogenic terrestrial atmosphere composition is determined using the observed non-radiogenic isotopic fractionation, and extrapolated (using Rayleigh type fractionation) to the radiogenic/fissiogenic isotopes (Fig. 4.19). The resulting present-day atmospheric pattern shows the fissiogenic xenon excess, originating mostly from the spontaneous fission of  $^{244}\text{Pu}$  as it will be discussed in the next section, and the  $^{129}\text{Xe}$  excess, resulting from the radioactive decay of the now-extinct  $^{129}\text{I}$ .

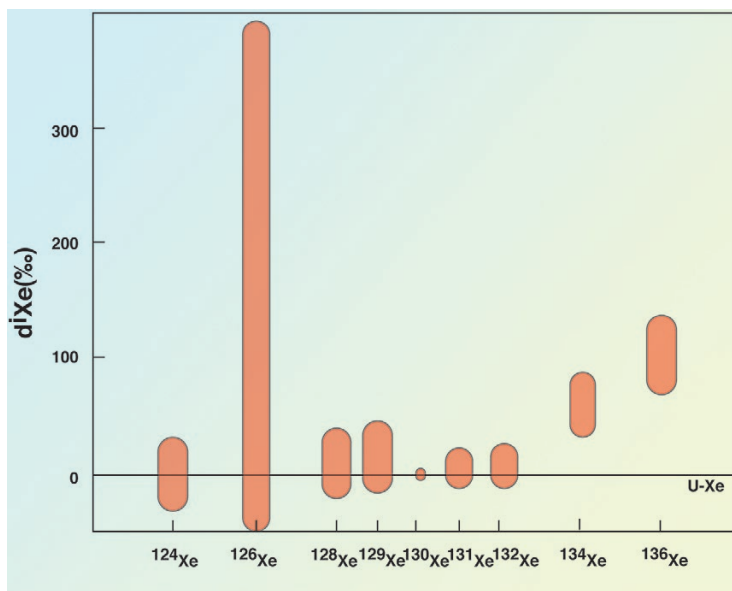


**Figure 4.18**

Figure showing the xenon isotopic excesses (in %) relative to 'U-Xe' in samples rich in implanted solar wind. The excess in  $^{134}\text{Xe}$  and  $^{136}\text{Xe}$  in solar wind rich samples is visible, albeit their origin is unclear. U-Xe is similar to the solar wind as it was determined from lunar samples, with the exception of these two heavy isotopes (adapted from Pepin *et al.*, 1995).

27. Why the sun is enriched in heavy xenon isotopes compared to U-Xe is unclear if U-Xe is the primordial xenon isotopic composition of the solar system.



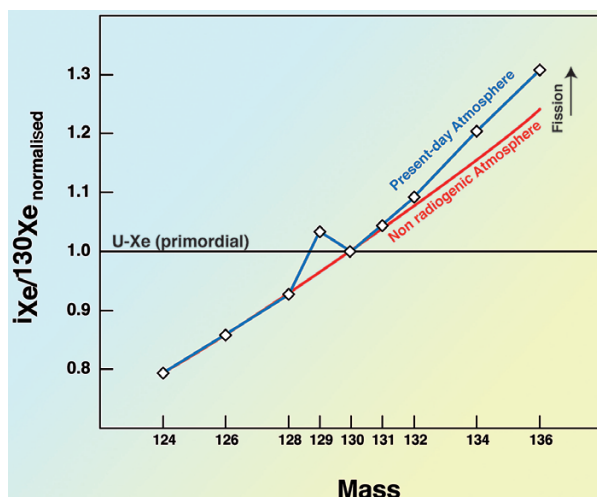


**Figure 4.19** Xenon isotopic ratios normalised to the 'U-Xe' of the present-day atmosphere and of the non-radiogenic atmosphere resulting from the mass-dependent isotopic fractionation of a primordial atmosphere having U-Xe composition (primordial – although slightly different from solar).

#### 4.4.1 Xenon from extinct $^{244}\text{Pu}$ radioactivity on Earth

The  $^{244}\text{Pu}$  atom is susceptible to spontaneous fission. It has a longer half-life (82 Ma) than the  $^{129}\text{I}$ - $^{129}\text{Xe}$  couple, and therefore can provide insights into mantle degassing on a somewhat longer time-scale than the I-Xe system. It also has the advantage that Pu is refractory, whereas iodine is volatile. To make the most of this potential chronometer requires that Pu abundance is known in the primitive bulk Earth. However, this is a system that requires high precision xenon measurements because it is necessary to distinguish the xenon produced by  $^{244}\text{Pu}$  from those isotopes produced by the spontaneous fission of the more abundant and still extant  $^{238}\text{U}$ .

#### 4.4.2 Brief history of the discovery of $^{244}\text{Pu}$ on Earth

Reynolds (1960) measured the xenon isotopic composition of the meteorite Richrardtton and used these values in order to calculate the non-radiogenic Xe inventory of the Earth. This led to the observation that the heavy xenon isotopes are in excess in the atmosphere and must have been produced by the spontaneous fission of some heavy elements, likely the lanthanides. The same year, using a simple calculation of the amount of fissionogenic  $^{136}\text{Xe}$  in the atmosphere, Kuroda (1960) postulated that  $^{244}\text{Pu}$  spontaneous fission was the source of this excess. Fields *et al.* (1966) measured the decay constant of the spontaneous and alpha

decay of  $^{244}\text{Pu}$ , followed by Alexander *et al.* (1971) who determined the fission yield by measuring xenon isotopes on 14.7 mg of  $\text{PuO}_2$  for 23 months after its precipitation and degassing.  $^{244}\text{Pu}$  was detected on Earth in the mineral bastnäsite by Hoffman *et al.* (1971). The existence of  $^{244}\text{Pu}$  was also deduced from measurement of the isotopic composition of xenon in lunar samples (Drodz *et al.*, 1972; Behrmann *et al.*, 1973). Therefore, by the end of the 1970's it was clear that  $^{244}\text{Pu}$  was still present, as was  $^{129}\text{I}$ , when the Solar System formed and that the  $^{244}\text{Pu}$ -Xe system could be used to date geological processes, in particular, atmospheric formation and its evolution. Because heavy xenon isotopes originate from both spontaneous fission of  $^{244}\text{Pu}$  and  $^{238}\text{U}$ , it is important to determine accurately the  $^{244}\text{Pu}/^{238}\text{U}$  ratio at the formation of the Solar System to assess their relative contribution. This was the goal of various studies on the xenon isotopes of Archean zircons (Honda *et al.*, 2003; Turner *et al.*, 2004; Turner *et al.*, 2007). Based on these studies of terrestrial zircons, Turner *et al.* (2007) inferred that the terrestrial  $^{244}\text{Pu}/^{238}\text{U}$  ratio calculated for an age of 4.57 Ga was  $\sim 0.008$ , close to the ratio determined from studies of xenon in meteorites (see review in Azbel and Tolstikhin, 1993). This suggests that these two elements don't fractionate during accretion and differentiation (as might be expected of incompatible, refractory lithophile elements), and that a chondritic ( $^{244}\text{Pu}/^{238}\text{U}$ ) ratio can be considered a reliable value for the Earth.

#### 4.4.3 Fissiogenic xenon in the Earth's mantle

The first publication of the xenon composition of the MORB source showing large excesses compared to the atmosphere and with sufficient precision to distinguish between  $^{244}\text{Pu}$  and  $^{238}\text{U}$  derived xenon is the one of Kunz *et al.* (1998) from the Paris group. Interesting studies such as that of the North Chile Ridge (Niedermann and Bach, 1998) have also published xenon isotopic ratios in MORB, but unfortunately these ratios were mostly atmospheric and thus inadequate for the determination of Pu/U proportion. In Paris, an electron multiplier equipped with ion counting was installed in the mid 1990's at the IPGP on the ARESIBO I mass spectrometer, allowing better precision than the analogue electron multiplier that was used previously. R. Ragetti, Thomas Staudacher, and André Lecomte performed this improvement. J. Kunz then used this new configuration to analyse MORB samples to determine the proportion of  $^{244}\text{Pu}$ -derived fissiogenic xenon in the mantle. This is an analytical challenge since the xenon fission yields between  $^{244}\text{Pu}$  and  $^{238}\text{U}$  are very close. Since the paper of Kunz and collaborators, only a few publications have been published with significant excesses compared to atmosphere and with high precision xenon measurements on MORB measured with sufficient precision to resolve the contribution of the fissiogenic products of  $^{238}\text{U}$  and  $^{244}\text{Pu}$ . The xenon isotopic ratios published in these studies were measured with a new generation of multi-collection mass spectrometer, named Noblesse from Nu Instruments© with one of them installed at Harvard University in Mukhopadhyay's laboratory (Parai *et al.*, 2012; Tucker *et al.*, 2012). A compilation of available xenon isotopes measured in pulse counting modes is shown on Figure 4.20. As discussed above (and will be further expounded in Section 5),



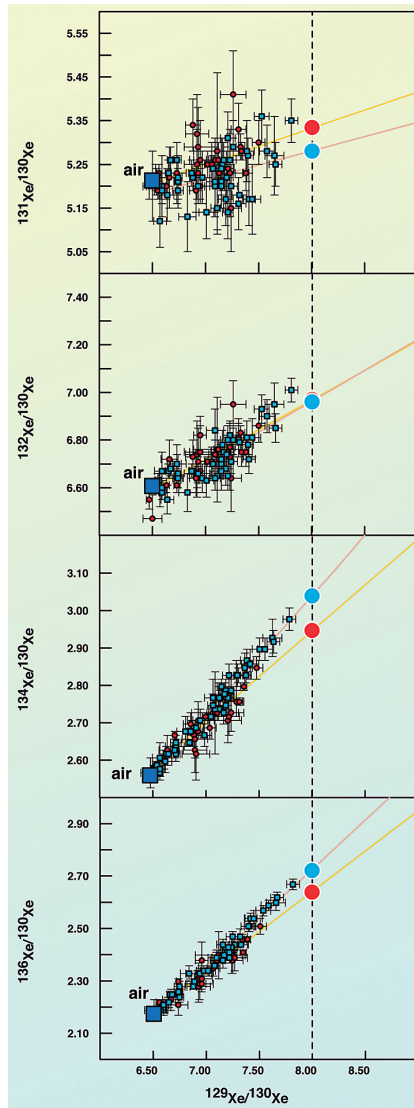


**Figure 4.20**

Fission-derived xenon isotopes measured in MORB samples. Large dots are extrapolated ratios for a  $^{129}\text{Xe}/^{130}\text{Xe}$  of 8, supposed here to be the value of the MORB source to illustrate the method of determination of the other xenon isotopic ratios (fissiogenic) in the mantle. However, as discussed in the text, the  $^{129}\text{Xe}/^{130}\text{Xe}$  may vary in the mantle (see Fig. 4.15), and therefore different  $^{129}\text{Xe}/^{130}\text{Xe}$  can be considered for the extrapolation. Data from Tucker *et al.* (2012) (blue) and Kunz *et al.* (1998) (red).



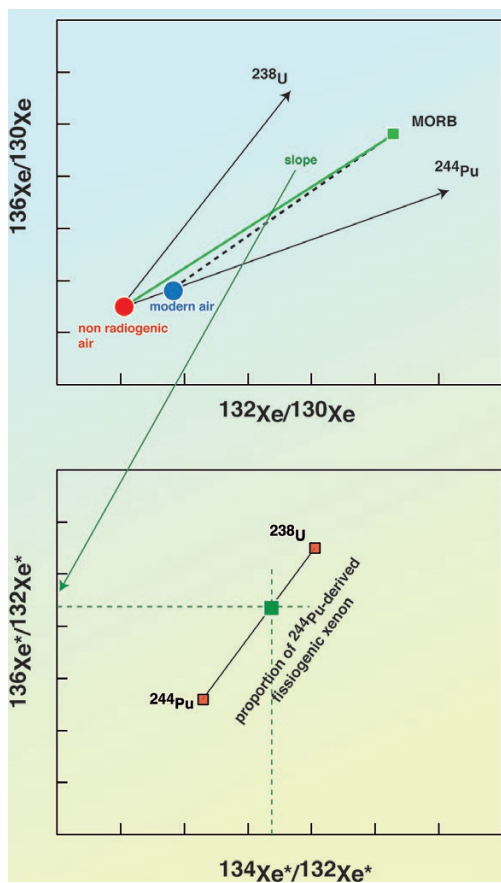


**Figure 4.21**

Explanation of the method of determination of the  $^{244}\text{Pu}$  and  $^{238}\text{U}$  derived proportions of xenon in a set of samples. In the classic three-isotope xenon diagram, the slopes defined by the MORB-Air or MORB-non-radiogenic air provide the fissionogenic isotope ratios in excess in the mantle (noted with a \*). In the bottom figure, the proportion between  $^{244}\text{Pu}$  and  $^{238}\text{U}$  spontaneous fissions can be derived because the yields of xenon isotopes are different for  $^{244}\text{Pu}$  and  $^{238}\text{U}$  spontaneous fissions.

xenon. The MORB source appears heterogeneous with respect of the proportion of the spontaneous fissions of U and Pu.

the  $^{129}\text{Xe}/^{130}\text{Xe}$  ratio of a mantle source, prior to atmospheric contamination, can be determined with coupled Ne isotope measurements (Fig. 4.15). The  $^{129}\text{Xe}/^{130}\text{Xe}$  ratio varies between 7 and 7.8 in different MORB sources. Linear mixing and extrapolation to a given  $^{129}\text{Xe}/^{130}\text{Xe}$  ratio allow determination of the other xenon isotopic compositions and their uncertainties (see Fig. 4.20 for an example using  $^{129}\text{Xe}/^{130}\text{Xe} = 8$ ). Different MORB sources for  $^{134}\text{Xe}/^{132}\text{Xe}$  and  $^{136}\text{Xe}/^{132}\text{Xe}$  ratios can then be calculated using the method shown in Figure 4.21 which is simply the determination of the slope of the mixing line between the present-day mantle compositions and either the present-day or the non-radiogenic atmosphere. These  $^{134}\text{Xe}/^{132}\text{Xe}$  and  $^{136}\text{Xe}/^{132}\text{Xe}$  ratios are subsequently compared to the production ratios of the spontaneous fissions of  $^{238}\text{U}$  and  $^{244}\text{Pu}$ . The MORB sources, corresponding to the two populations of samples, are represented in Figure 4.22. This figure shows that the fissionogenic xenon composition in the MORB source originates from both  $^{244}\text{Pu}$  and  $^{238}\text{U}$  spontaneous fission, whereas the atmosphere contains only  $^{244}\text{Pu}$ -derived



#### 4.4.4 Fissiogenic xenon isotopes in OIB: a pure $^{244}\text{Pu}$ signature and the evidence for an isolation of the OIB source since 4.4Ga

Mukhopadhyay (2012) has provided new precise xenon measurements of one glassy Iceland sample<sup>28</sup>, named DICE. This is the OIB equivalent of 2πD43 and is sufficiently gas rich to allow the proportion of  $^{244}\text{Pu}$  and  $^{238}\text{U}$  derived xenon to be determined for Iceland using the same method as described for MORB above. The results of the estimate of the  $^{136}\text{Xe}^*/^{132}\text{Xe}^*$  and  $^{134}\text{Xe}^*/^{132}\text{Xe}^*$  ratios (using a non-radiogenic air end-member) are represented in Figure 4.22 and compared to MORB, to the present-day atmosphere and to the theoretical production ratio from spontaneous fission of  $^{244}\text{Pu}$  and  $^{238}\text{U}$ . The results show that the fissiogenic xenon in the Icelandic source is mostly derived from  $^{244}\text{Pu}$  as suggested by Mukhopadhyay (2012), with no contribution of  $^{238}\text{U}$ -derived xenon.

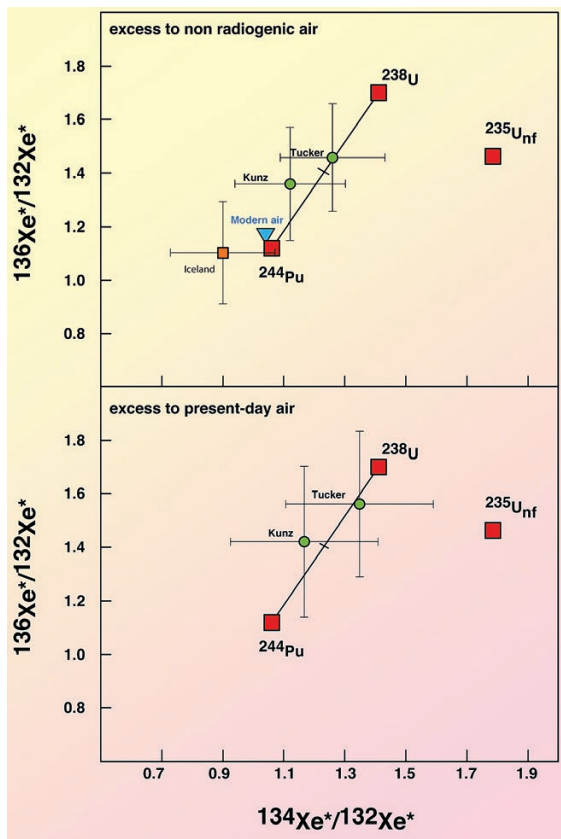


Figure 4.22

Pu-U derived xenon in the MORB sources, the Iceland source and in modern air. Central Atlantic MORBs show a higher proportion of  $^{238}\text{U}$ -derived xenon (Tucker *et al.*, 2012). The modern atmosphere contains pure  $^{244}\text{Pu}$ -derived fissiogenic xenon compared to the non-radiogenic air. Fissiogenic xenon in the Iceland mantle source is derived from pure  $^{244}\text{Pu}$ , suggesting the Icelandic mantle plume is an undegassed reservoir where the  $^{238}\text{U}/^{130}\text{Xe}$  is low compared to the MORB source.  $^{235}\text{U}_{\text{nf}}$  represents the neutron-induced fission, which is not a significant contributor to the fissiogenic xenon in the mantle.

28. This sample comes from the glassy margin of a pillow lava formed during the eruption under ice, rather than at the bottom of the ocean. The pressure is high enough that these samples are not degassed in contrast to subaerial lavas.





This can be interpreted as the Iceland mantle source being undegassed. For the closed system evolution of the terrestrial mantle, the contribution from  $^{244}\text{Pu}$  dominates the budget of fissionogenic Xe isotopes (Fig. 4.23). This is also true for the atmosphere, which has accumulated the majority of xenon during mantle degassing, including the early produced fission products of  $^{244}\text{Pu}$ . The influence of the spontaneous fission of  $^{238}\text{U}$  is only evident if this early-produced ‘plutogenic’ component is lost by degassing. This is the case for MORB (see Fig. 4.23). Thus the evidence in Figure 4.22 for an undegassed, OIB source (Iceland) but a degassed MORB source supports the inferences made independently from  $^{129}\text{Xe}$  (Fig. 4.15).

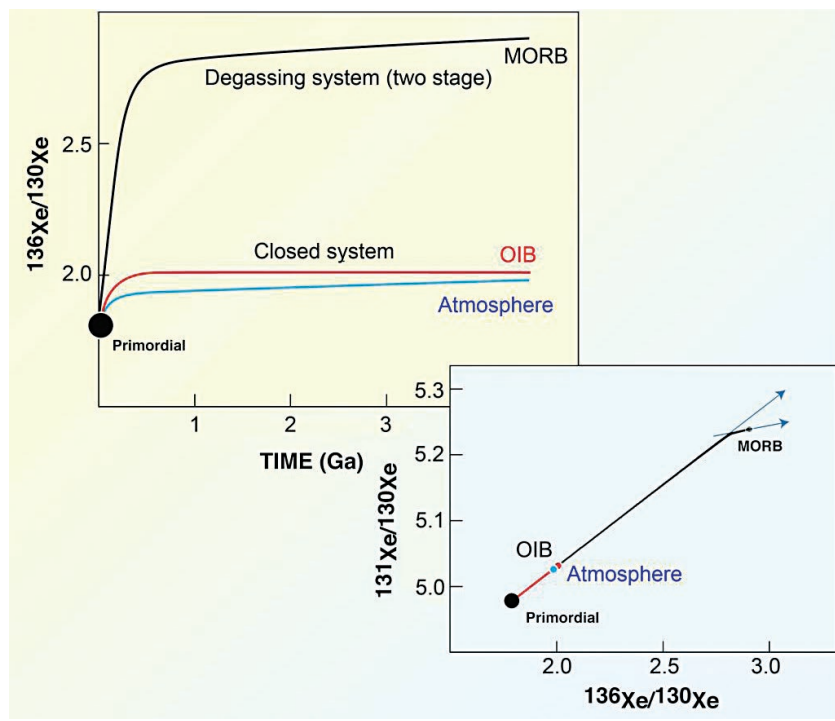


**Figure 4.23**

The temporal  $^{136}\text{Xe}/^{130}\text{Xe}$  evolution in a degassing reservoir (the MORB source) and in an undegassed reservoir (the OIB source). The bottom-right figure shows the same calculation for two isotopic ratios to illustrate influence of  $^{238}\text{U}$  after  $^{244}\text{Pu}$  was extinct. The MORB evolution shows a deviation from the  $^{244}\text{Pu}$  production line that is not observed in the closed-system reservoir. This is due to the fact that the  $^{238}\text{U}/^{130}\text{Xe}$  is low in the OIB source and high in the MORB source because of the degassing. The degassing model is based on the following assumptions. It is a two stage degassing model (see Section 8),  $[\text{U}] = 20$  ppb in the bulk Earth,  $(\text{Pu}/\text{U})_0 = 0.008$ ,  $^{130}\text{Xe}$  is  $4.5 \times 10^{-16} \text{ mol g}^{-1}$  in the primitive mantle. This calculation is meant to be illustrative rather than definitive.



## 4.5 Conclusions

---

Argon and xenon are extremely powerful tracers of atmospheric formation and mantle evolution. This is particularly the case for xenon that has both isotopes originating from short-lived radiogenic decay (e.g.,  $^{129}\text{Xe}$ , the daughter of  $^{129}\text{I}$ ), and fissionogenic isotopes of short ( $^{244}\text{Pu}$ -derived fission) and long-term processes ( $^{238}\text{U}$ -derived fission). Argon is also radiogenic, the daughter of the (relatively) slowly decaying radiogenic  $^{40}\text{K}$  and has the advantage of not having a primordial radiogenic argon contribution. This allows simple budgets to be constrained, providing the bulk K/U of the Earth is known with reasonable accuracy. The argon budget suggests that ~50% of the argon produced in 4.5 Ga is still in the lower mantle. By coupling argon and xenon, and the other rare gases (He, Ne), it is possible to model the evolution of the mantle and the atmosphere. Further details will be examined in Sections 6, 7, and 8.

Several important issues, however, remain including the possibility of subduction of rare gases into the upper mantle or into the mantle source of oceanic islands, which will be examined in Section 7. We have good constraints on the composition of radiogenic isotopes in the mantle, even if there still are a few unresolved issues including the variability and maximum values of the radiogenic isotopic ratios in the upper mantle and in mantle source of oceanic islands.

In the next section, I will address topics that use the non-radiogenic isotopes of the neon and the argon to understand the primordial mantle composition and the origin of noble gases on Earth. Non-radiogenic isotopes of krypton and the xenon will be discussed in Sections 7 and 8.



## 5. SOLAR NEON AND ARGON IN THE MANTLE AND THE CONSTRAINTS ON THE ORIGIN OF NOBLE GASES ON EARTH

### 5.1 The Discovery of Solar-like Neon in the Mantle

An important aspect of noble gas geochemistry is the discovery of non-atmospheric neon isotopic ratios in mantle-derived samples, including basalts or diamonds. Neon has three isotopes,  $^{20}\text{Ne}$ ,  $^{21}\text{Ne}$ , and  $^{22}\text{Ne}$  with isotopic ratios of 9.8 and 0.029 in the atmosphere, for  $^{20}\text{Ne}/^{22}\text{Ne}$  and  $^{21}\text{Ne}/^{22}\text{Ne}$ , respectively. There are two main difficulties in analysing precisely these two isotopic ratios in mantle-derived rocks. The first is the peak superposition of  $^{40}\text{Ar}^{++}$  and  $\text{CO}_2^{++}$ , two abundant elements in mantle-derived gas, which requires efficient gas purification, *e.g.*, perfect separation between neon and argon and low memory effects of  $\text{CO}_2$  and argon in the mass spectrometer. Charcoal at liquid nitrogen temperature can minimise argon and  $\text{CO}_2$  in the flight tube. An advantage having a glass mass spectrometer, such as the ARESIBO machines hosted at *institute de Physique du Globe de Paris*, is the possibility of degassing the ion source overnight using infrared lamps. This baking creates a low background. The second important issue to determine the neon isotopic ratios in mantle-derived samples is the blank correction. Samples having low neon abundances often have high blank contributions. Moreover,  $^{21}\text{Ne}$  is very rare in these samples (it is only  $\sim 0.3\%$  of total Neon

and occurs at abundances of  $10^6$  atom  $\text{g}^{-1}$  in these samples) and is therefore difficult to detect. These constraints probably explain why the mantle neon isotopic composition was accurately analysed later than the other noble gases. Indeed, the first analyses of Ne in oceanic basalts were conducted as recently as 1976 (Craig and Lupton, 1976). One has to wait until the late eighties to get precise measurements, starting with the work of *Philippe Sarda* (Fig. 5.1 in 1988). Prior to this remarkable publication, only few articles were published showing neon isotopic ratios higher than those of air in mantle-derived rocks (*e.g.*, Kyser and Rison, 1982; Ozima and Zashu, 1983; Poreda and Radicati di Brozolo, 1984) but uncertainties were large and the excesses compared to air were difficult to interpret. A brief neon history is provided in Moreira and



Photo credit: Cécile Gautheron.

**Figure 5.1** Picture of *Philippe Sarda*. He published a remarkable publication on neon isotopes in oceanic basalts in 1988.



Allègre (1998), where we review the distinct neon isotopic ratios measured in oceanic samples prior to this publication.

For me, neonology of Earth's mantle started with Sarda *et al.* (1988). The  $^{20}\text{Ne}/^{22}\text{Ne}$  ratio measured in one sample was as high as 13, which even considering its relatively large error of  $\pm 1$  is still one of the highest MORB vales measured (Fig. 5.2). This work provides the first clear excesses of  $^{20}\text{Ne}$  and  $^{21}\text{Ne}$  compared to air in oceanic basalts. The same year, Ozima and Zashu published the

neon isotopic ratios of Zaire cubic diamonds, which also show excesses of  $^{20}\text{Ne}$  and  $^{21}\text{Ne}$  compared to air (Ozima and Zashu, 1988). Independently of each other, these two studies made two important observations. The first is the presence of solar-like neon in the mantle, particularly in the MORB source, which implies that the atmosphere is not simply the complementary reservoir of the depleted MORB source. The second is the  $^{21}\text{Ne}$  excess in the MORB source compared to both the atmosphere and the solar composition.  $^{20}\text{Ne}$  and  $^{22}\text{Ne}$  are considered as non-radiogenic in the mantle, which is not the case in crustal rocks, whereas  $^{21}\text{Ne}$  is nucleogenic, which implies it can be produced by reactions such as  $^{18}\text{O}(\alpha, n)^{21}\text{Ne}$  or  $^{24}\text{Mg}(n, \alpha)^{21}\text{Ne}$ . The three Ne isotopes are produced during nucleogenic reactions, but the production rate is negligible for the two most abundant isotopes in the mantle. However, the three isotopes are produced up to 1,000 times more rapidly in crustal rocks than in the mantle because of higher U and Th concentrations (Yatsevich and Honda, 1997). Crustal rocks exhibit low  $^{20}\text{Ne}/^{22}\text{Ne}$  and high  $^{21}\text{Ne}/^{22}\text{Ne}$  ratios compared to air (Zadnik and Jeffery, 1985; Kennedy *et al.*, 1990; Azuma *et al.*, 1993).

The  $^{20}\text{Ne}/^{22}\text{Ne}$  ratio is stable with time in the mantle and therefore the solar-like neon observed in the MORB source, and later on in all mantle-derived samples, does reflect a primordial component with a solar-like signature, different from the atmospheric one. Here on the notion of “solar-like” ratio is used because the measured compositions can reflect either a pure solar value (with more or less subduction of atmospheric neon, see Section 7 or for example the discussion in Kendrick *et al.*, 2011) or the neon B value, discussed in Section 2. In the 90's and beginning of 2000's, we were talking about solar neon in the mantle, but now I

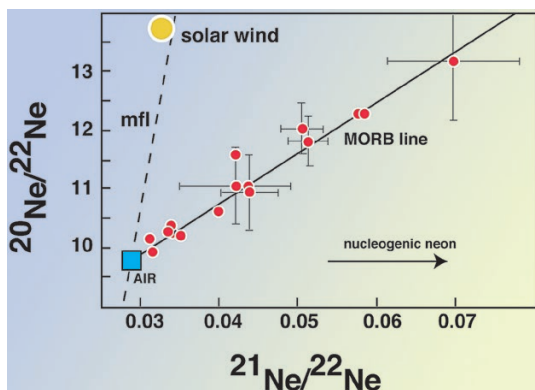
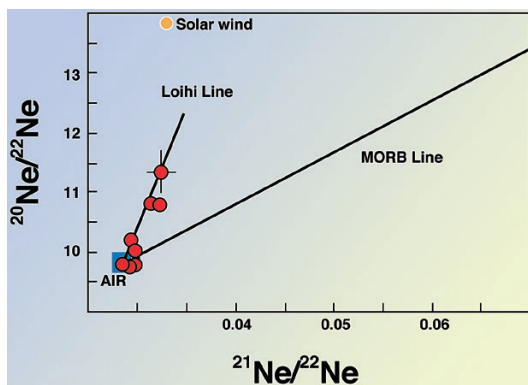


Figure 5.2

Three neon isotope diagram showing MORB samples analysed by Sarda *et al.* (1988). The present-day atmosphere (AIR), solar wind, and mass fractionation line (mfl) are also shown. This work was the first clear evidence for solar-like neon in the mantle.



prefer to discuss the neon ratio in terms of solar-like neon to leave open the exact value of the mantle neon. This is important for the discussion of the mechanism of noble gas incorporation in Earth building blocks. The  $^{21}\text{Ne}/^{22}\text{Ne}$  variations in mantle-derived samples are explained by nucleogenic  $^{21}\text{Ne}$  addition in a degassed



**Figure 5.3** Neon isotopes in Loihi samples (Hawaii) analysed by Honda *et al.* (1991). This publication is the first to propose that the OIB source has solar neon.

reservoir, in a similar way the  $^4\text{He}/^3\text{He}$  and  $^{40}\text{Ar}/^{36}\text{Ar}$  ratios are radiogenic in the degassed MORB source compared to the primordial composition (Sections 3 and 4).

Discussions in the middle of 1990's concerned the neon composition in the OIB sources. Sarda *et al.* (1988) had measured samples from Loihi seamount and asserted they observed atmospheric neon, which retrospectively was not correct since some samples presented excesses of  $^{20}\text{Ne}$  and  $^{21}\text{Ne}$  relative to the atmosphere (see also the debate about the OIB Ar isotopic ratio in the previous section). At that time the Paris group believed that the atmospheric neon observed in the Loihi source reflected the primordial composition in its source. This suggestion also explained the atmosphere composition: it was degassed from the mantle and therefore the undegassed reservoir and the atmosphere should have the same composition for non-radiogenic isotopic ratios. Allègre *et al.* (1993) proposed that the solar-like neon in the MORB source could reflect incorporation into the upper mantle of cosmic dust having a solar composition.

These ideas were not shared by other noble gas groups, particularly those of Honda, Hiyagon (Hiyagon *et al.*, 1992) or Poreda (Poreda and Farley, 1992). Three studies showing solar-like neon in OIB (Fig 5.3) were published in 1991 and 1992 (Honda *et al.*, 1991; Hiyagon *et al.*, 1992; Poreda and Farley, 1992), but the results were interpreted by the Paris group as reflecting isotopic fractionation of the neon. Their argument was that the slope in the three-neon isotope diagram of the Loihi line is close to the neon mass fractionation line (mfl) suggesting isotopic fractionation. It turned out that Honda was right.

Claude Allègre, Thomas Staudacher and Philippe Sarda only changed their minds about the solar-like neon in the OIB sources in the middle of the 90's thanks to the work of Peter Valbracht and myself (see below). In 1998, when we worked on the paper entitled "Helium - Neon systematics and the structure



of the mantle" (Moreira and Allègre, 1998), I compiled neon isotopic ratios in oceanic samples, and then I realised that *Thomas Staudacher* had reported solar-like neon in OIB before others in his paper on Réunion Island (1990), but did not interpret these neon results in term of solar neon in the mantle.

In 1995, we published the neon isotope measurements on samples from the Shona ridge anomaly, which is a topographic high located on the South Atlantic ridge at ~52 °S, having non-radiogenic helium isotopic ratios (Moreira *et al.*, 1995). The results are shown on Figure 5.4, together with the results we obtained with *Philippe Sarda* on the topographic anomaly named Discovery, located north of Shona, which also has non-radiogenic helium. Both locations show non-nucleogenic neon characteristics, similar to Loihi neon (Sarda *et al.*, 2000). This was the first time that mixing between two components was observed for neon and that a clear correlation between the  $^{21}\text{Ne}/^{22}\text{Ne}$  and the  $^4\text{He}/^3\text{He}$  ratios had been seen. Two years later, *Peter Valbracht* analysed neon and argon isotopes in newly dredged Loihi samples (Valbracht *et al.*, 1997). These new results confirmed the works of *Honda* and his group (Honda *et al.*, 1991, 1993), and of *Hiyagon* and collaborators (Hiyagon *et al.*, 1992) suggesting that all mantle reservoirs have a solar-like neon isotopic composition.

Therefore, in 1995, it was clear to everybody that the mantle had a solar-like  $^{20}\text{Ne}/^{22}\text{Ne}$  ratio, and that the difference in  $^{21}\text{Ne}/^{22}\text{Ne}$  between the MORB and the OIB sources was due to a higher  $(\text{U}+\text{Th})/^{22}\text{Ne}$  in the MORB source induced by its degassing. Since this time, discussions focused on the exact value of the  $^{20}\text{Ne}/^{22}\text{Ne}$  ratio in the mantle. Is it exactly solar or lower? If so, is it indicative of the neon B value, or is it induced by subduction of atmospheric neon? The difficulty for answering these questions is the ubiquitous presence of atmospheric contamination in the samples, which is a process that was not understood. Another difficulty is the precise determination of neon isotopes with mass spectrometry in samples that are not contaminated by atmosphere. Mantle-derived neon abundances are low in these samples and obtaining high precision is therefore difficult. Modifications to the extraction and purification lines of the mass spectrometers resulted in improvements in blank,  $\text{CO}_2$  and  $^{40}\text{Ar}^{++}$  corrections and detection limits and better precisions to be obtained.

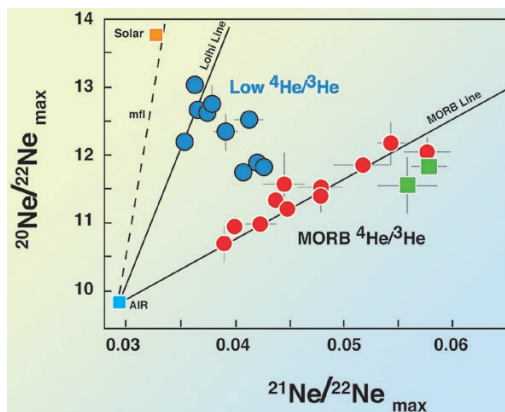


**Figure 5.4**

Neon isotopes in South Atlantic samples: Shona and Discovery ridge anomalies (Moreira *et al.*, 1995; Sarda *et al.*, 2000). Neon shows the mixing between MORB and primitive components.



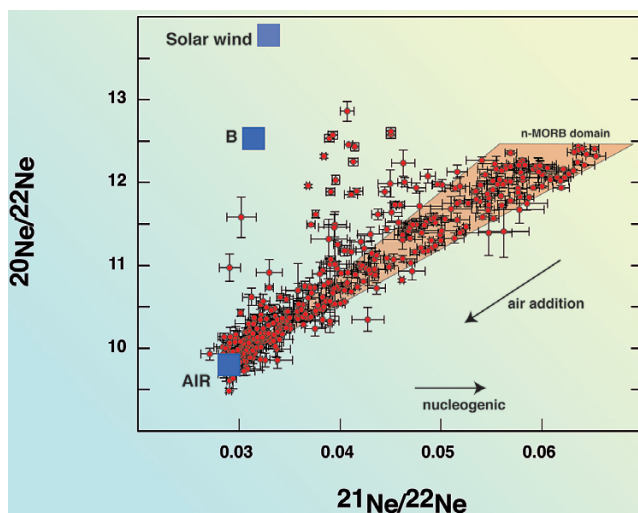


**Figure 5.5**

Neon isotopic compositions measured in MORB. The dot entitled “B” is the composition of neon B, measured in gas rich meteorites and on the lunar soil (see Section 2). It might represent the primordial neon composition, although some authors suggest that the primordial mantle had a solar composition.  $^{21}\text{Ne}$  is produced by nucleogenic reactions (e.g.,  $^{18}\text{O}(\alpha, n)^{21}\text{Ne}$ ). Air contamination decreases both ratios.

Figure 5.5 shows a recent compilation of all available neon isotopic ratios in MORB. Please note that in this diagram I consider only samples with an uncertainty lower than 5% on their  $^{20}\text{Ne}/^{22}\text{Ne}$  and  $^{21}\text{Ne}/^{22}\text{Ne}$  ratios. Higher ratios have been published, but these have large uncertainties. All crushing or heating steps are represented here. Most of the samples fall on a mixing trend between the atmosphere and a component having  $^{20}\text{Ne}/^{22}\text{Ne}$  and  $^{21}\text{Ne}/^{22}\text{Ne}$  ratios of  $\sim 12.5$  and  $\sim 0.060$ . This up-to-date correlation is grossly similar to the mixing line determined by Sarda *et al.* (1988) (Fig. 5.2). The samples lying above this MORB line are samples from the EPR at 17 °S and have non-radiogenic helium, although there is no evidence for the presence of a hotspot (Niedermann *et al.*, 1997; Kurz *et al.*, 2005). This peculiar neon signature for MORB is very similar to those observed in the South Atlantic on Shona and Discovery ridge anomalies (Fig. 5.4), except in the latter cases are associated to topographic anomalies (Moreira *et al.*, 1995; Sarda *et al.*, 2000). The second new observation on the neon in MORB is the broad variation of  $^{21}\text{Ne}/^{22}\text{Ne}$  ratios for a given  $^{20}\text{Ne}/^{22}\text{Ne}$  ratio (for example at 12.5), which was not seen in Sarda *et al.* (1988). The  $^{21}\text{Ne}/^{22}\text{Ne}$  ratio varies from 0.055 up to 0.068, which suggests heterogeneous (U+Th)/ $^{22}\text{Ne}$  in the MORB-source<sup>29</sup>.

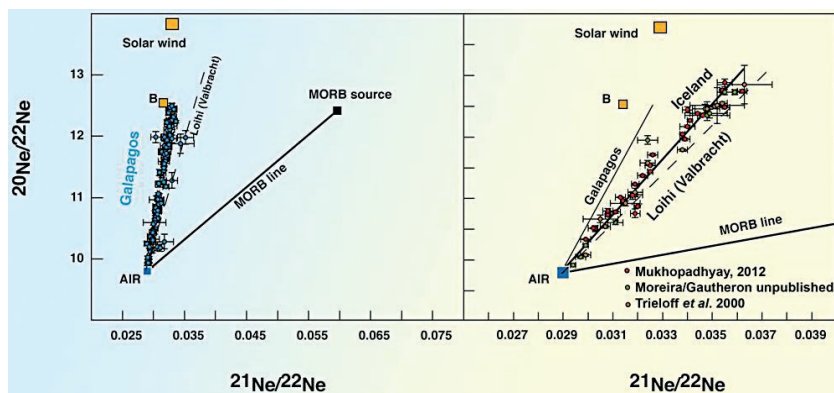
29. The range in (U+Th)/ $^3\text{He}$  ratio of the MORB source inferred from variability in the helium isotopic ratio is similar.





Figure 5.5 shows that the  $^{20}\text{Ne}/^{22}\text{Ne}$  ratios in MORB sampled far from hotspots are systematically lower than 12.5, which therefore could be the value of the MORB source mantle. Such a value was also suggested based on a completely different approach by Ballentine *et al.* (2005). These authors have analysed noble gas isotopes in  $\text{CO}_2$  well gases from New Mexico (USA) and concluded that the neon isotopic composition reflects the mixture of air, crustal-derived neon and mantle-derived neon. They have successfully deconvoluted the measured neon isotope signal to determine the  $^{20}\text{Ne}/^{22}\text{Ne}$  ratio of the mantle-derived neon. They calculated a  $^{20}\text{Ne}/^{22}\text{Ne}$  ratio of  $12.20 \pm 0.05$  for the mantle, similar to the maximum ratio measured in MORB.

To analyse neon isotopes in terrestrial samples, it is preferable to have glass samples although measurements of sufficient precision can sometimes be made on phenocryst or xenolith olivines (see Section 3). Thus there are many fewer Ne analyses on OIB than MORB. In the remainder of this section I will only consider high precision analyses made on basaltic glass samples, and as a result I am restricted to the neon isotopic compositions of four OIB, the Galapagos, Iceland, Samoa and Hawaii. Other hotspots have been investigated, *e.g.*, the Azores or Tubuai hotspots, but the analyses were not performed on glass (Madureira *et al.*, 2005; Jackson *et al.*, 2009; Parai *et al.*, 2009; Hanyu *et al.*, 2011). The two most recently studied hotspots are Iceland and the Galapagos islands for which I give the neon isotopic results in Figure 5.6.



**Figure 5.6**

Neon isotopes in Galapagos and Icelandic glass samples, two OIB with the primitive neon isotopic signature. Data from Trierloff *et al.* (2000), Kurz *et al.* (2009), Raquin and Moreira (2009) and Mukhopadhyay (2012). The MORB line was determined by Sarda *et al.* (1988). As in the previous figure, the observed trends reflect atmospheric contamination. For comparison, the Loihi Line determined by Valbracht *et al.* (1997) is given.

The objective of these studies on Galapagos and Iceland samples were twofold (Harrison *et al.*, 1999; Dixon *et al.*, 2000; Trierloff *et al.*, 2000; Moreira *et al.*, 2001; Dixon, 2003; Kurz *et al.*, 2009; Mukhopadhyay, 2012): firstly to verify if OIB



source has less nucleogenic neon than the MORB source and secondly to determine the  $^{20}\text{Ne}/^{22}\text{Ne}$  ratio of this reservoir. The first objective has been met since the results from these two hotspots confirm those of Hawaii and Samoa (Honda *et al.*, 1991; Poreda and Farley, 1992; Honda *et al.*, 1993; Valbracht *et al.*, 1997; Jackson *et al.*, 2009). The  $^{21}\text{Ne}/^{22}\text{Ne}$  ratio is clearly lower in the source of oceanic islands than in the MORB source. It should be noted the un-nucleogenic neon in Galapagos that is close to the solar value or to the neon B. The Iceland hotspot has also a very primitive in neon isotopic signature as shown in Figure 5.6, although slightly more nucleogenic than the Galapagos hotspot, in agreement with the more radiogenic helium isotopic ratio of the Iceland lavas ( $^4\text{He}/^3\text{He}$  ~42,000; R/Ra ~17 for Iceland against  $^4\text{He}/^3\text{He}$  ~31,000 or R/Ra = 22 for Galapagos). The maximum measured  $^{20}\text{Ne}/^{22}\text{Ne}$  is close to 12.5 for Galapagos, whereas it is 12.75 for Iceland samples, slightly above the neon B ratio determined by Black, (1971, 1972) but in agreement with measured neon ratio on Lunar soil or with the calculated isotopic ratio of implanted solar wind (see Section 2).

## 5.2 Atmospheric Contamination in Oceanic Samples

Only a few studies on oceanic basalts provide neon isotopic ratios with enough precision to allow a discrimination between their “neon B” ratios. Determining the mantle neon isotopic ratio is fundamental to understanding the mechanism of incorporation of noble gases in the silicate Earth as it will be discussed in Section 8. Solar-like  $^{20}\text{Ne}/^{22}\text{Ne}$  (~13.8) would suggest the dissolution of Ne in a molten Earth from a solar-like dense primordial atmosphere, whereas a ratio close to neon B would suggest that neon was incorporated into the parent bodies by solar wind irradiation during planetary accretion.

In order to discuss the actual  $^{20}\text{Ne}/^{22}\text{Ne}$  ratio of the mantle, it is essential to understand the physical process behind what has been called the atmospheric contamination and so be able to distinguish between a mantle-derived signature and any shallow contamination process. Step-crushing or step-heating often shows the presence of an atmospheric component in samples (Fig. 5.7), for both isotopic and elemental ratios, although sometimes the rare gases are elementally fractionated (Harrisson *et al.*, 2003). I published one example of such step-crushing in 1998 on the popping rock sample 2πD43 (Moreira *et al.*, 1998). Figure 5.7 shows the neon isotopic composition and concentration during step crushing. It can be easily seen that atmospheric neon is associated with high neon concentrations and is mainly found during the first crushing steps. Similar observations have been seen in other studies where samples were step crushed (Trieloff *et al.*, 2000, 2002; Mukhopadhyay, 2012; Parai *et al.*, 2012; Tucker *et al.*, 2012). A few key remarks can be made about this phenomenon. The first one is that such an important atmospheric component is mainly observed in vesicle-rich samples (Fig. 5.8) (Ballentine and Barfod, 2000). The second is that the blanks measured prior to analyses of these gas-rich samples are generally much higher than for typical samples, suggesting (atmospheric) gas is leaking out of the sample. Blanks



decrease after the first crushing steps. Finally, the recent study of Raquin *et al.* (2008) on noble gas analyses of single vesicles has shown that atmospheric gases are at atmospheric pressure, not at crustal or mantle pressures.

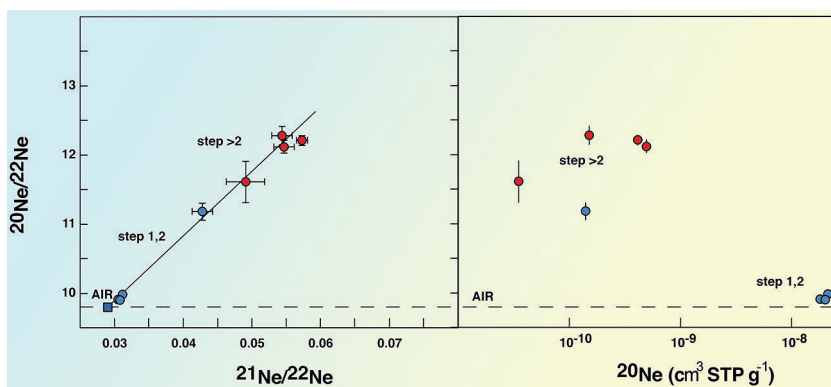


**Figure 5.7** Neon concentration and isotopic ratios in the 2πD43 popping rock sample (Moreira *et al.*, 1998). This study shows that during step crushing, the atmospheric gases are liberated first.

All these observations suggest that the air component observed in oceanic basalts reflects atmospheric contamination and that this air fills empty vesicles during storage in the laboratory (Fig. 5.9). We have to suppose that some empty vesicles are connected to the atmosphere through thin channels, formed by a fracture in the glass. Such a simple explanation accounts for all the observations. An empty vesicle filled with air can contain  $\sim 10^{-8}$  cm<sup>3</sup>STP of <sup>20</sup>Ne (for a radius of 500 μm), which is of the order of the measured value in the popping rock or other gas rich samples. Vacuum is reached prior to analysing samples (12 to 36 hours at  $\sim 100$  °C), so the gas in these vesicles connected to surface should be pumped. High blanks observed before the analysis of these samples indeed suggest this is the case. However, it takes time to pump such small volumes if the channels have small diameter (*e.g.*,  $\sim \mu\text{m}$ ) and overnight appears to be not long enough to pump out all the atmospheric gases.

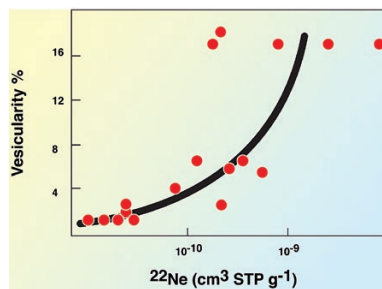


**Figure 5.8** Figure showing the relationship between the vesicularity and the neon concentration, taken here as a proxy of atmospheric contamination. High vesicularity seems to entrain high atmospheric contamination (modified from Ballentine and Barford, 2000).



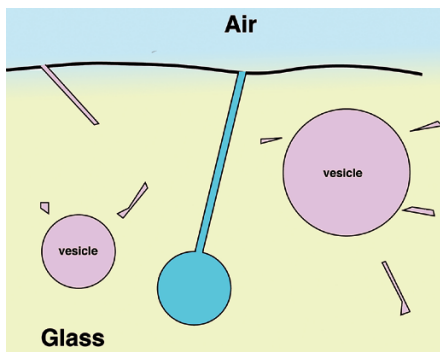


**Figure 5.9**

Cartoon explaining the atmospheric composition observed in oceanic basalts. Air can enter empty vesicles during storage in the laboratory. High vesicularity samples can therefore be rich in atmospheric gases as observed by Ballentine and Barfod (2000) and baking overnight under vacuum might not be long enough to fully outgas these vesicles.

Although contamination by hydrothermal alteration is a viable mechanism (e.g., Patterson *et al.*, 1990), I am convinced that the atmospheric component observed in most samples reflects atmospheric contamination in the laboratory during storage, as suggested by (Ballentine and Barfod, 2000; Tieloff *et al.*, 2003; Raquin *et al.*, 2008). This is different from the interpretation of Sarda (2004) who proposed that this component instead reflects atmospheric subduction in the mantle, through the recycling of altered oceanic crust (see Section 7).

Atmospheric contamination is present in most of the samples and therefore the determination of the maximum  $^{20}\text{Ne}/^{22}\text{Ne}$  ratio in the mantle source of these samples is difficult. One can never be sure

that the maximum ratio measured in a sample is really the mantle signature free of atmospheric contamination. Step crushing or step heating is an analytical method that could minimise this uncertainty but does not provide an undisputed mantle signature. Laser ablation on single vesicles such as presented in Section 4 is also a powerful technique allowing the measurement of atmospheric-free noble gases, although the precision is less good than for bulk sample analyses.

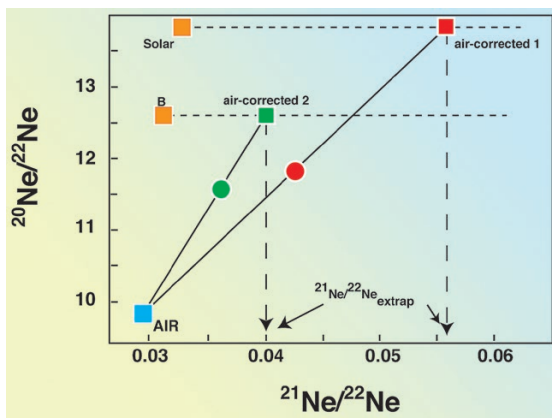


**Figure 5.10**

Method of correction for atmospheric contamination using either a solar or neon B  $^{20}\text{Ne}/^{22}\text{Ne}$  ratio for the mantle. The  $^{21}\text{Ne}/^{22}\text{Ne}$  ratio can then be derived assuming a simple binary mixing between the uncontaminated magma and an atmospheric component. This method is slightly different from the one proposed by Honda *et al.* (1993).



### 5.3 Atmospheric Contamination Correction for Determination of All Noble Gas Isotopic Ratios

Neon systematics can be used to correct for atmospheric contamination of the heavy noble gases in order to obtain their isotopic compositions in the mantle sources free of atmospheric contamination, as already alluded to in Section 4. The method assumes that a measurement is a mixture between the atmospheric and the magmatic components. Since the  $^{20}\text{Ne}/^{22}\text{Ne}$  ratio is “known” (assumed to be solar-like, either solar or neon B), non-radiogenic and stable, we can easily derive the  $^{21}\text{Ne}/^{22}\text{Ne}$  ratio (Figs. 5.10 and 5.11), and the other rare gas isotopic ratios (Fig. 5.12) are corrected for the contamination by finding the point at which the extrapolation of the air-sample mixing line intersects the solar-like value of the  $^{20}\text{Ne}/^{22}\text{Ne}$ . This approach was pioneered by Honda *et al.* (1993), although in a slightly different way, by considering the slope for neon in the Ne-Ne diagram as a proxy of the “primitive” nature of the reservoir source rather than to use the method given here.

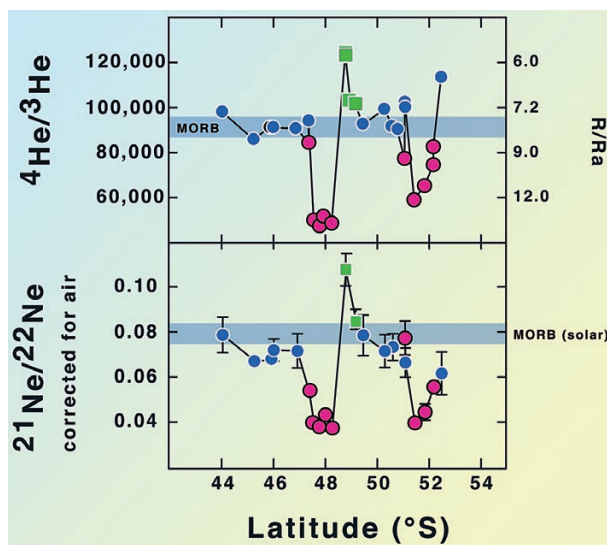


**Figure 5.11**

$^4\text{He}/^3\text{He}$  and  $^{21}\text{Ne}/^{22}\text{Ne}$  ratios (corrected for air contamination) in samples from Shona and Discovery ridge anomalies, which are located on the South Atlantic Ridge. The perfect correlation between the two isotopic ratios suggests that the method for correcting the  $^{21}\text{Ne}/^{22}\text{Ne}$  ratio from the atmospheric contamination presented in the previous figure is correct (modified from Sarda *et al.*, 2000).

In the first publications on He-Ne systematics, a solar neon composition in the mantle was used to correct for atmospheric neon (*e.g.*, Honda *et al.*, 1993; Moreira *et al.*, 1995). This choice made in the late 1990's may be incorrect if the



$^{20}\text{Ne}/^{22}\text{Ne}$  ratio is lower in the mantle (12.5, for example, close to “neon B”, see Section 2). Therefore, correction of isotopic ratios of heavy noble gases using neon imposes a choice between solar or “B” neon, a choice that could be different for MORB or OIB if these sources have different  $^{20}\text{Ne}/^{22}\text{Ne}$  ratios, as discussed later. Furthermore, this method of correction implies that atmospheric neon is not subducted into the mantle, as we will discuss in Section 7. The validation of the method of correction for atmospheric contamination is for instance provided on Figure 5.11 derived from Sarda *et al.* (2000). In this publication on MORB from the South Atlantic Ridge, we used a solar  $^{20}\text{Ne}/^{22}\text{Ne}$  ratio for the atmospheric neon correction, which explains why the  $^{21}\text{Ne}/^{22}\text{Ne}$  ratio is 0.08 in MORB-like samples rather than  $\sim 0.06$  as observed in Figure 5.5. If I had to correct the data today, I would use a ratio of 12.5 instead. Nevertheless, the agreement between the  $^4\text{He}/^3\text{He}$  and  $^{21}\text{Ne}/^{22}\text{Ne}$  ratio variations along the ridge axis clearly suggests that the correction is indeed appropriate. A similar approach has been conducted on the helium and neon isotopic variation along the EPR at  $\sim 17^\circ\text{S}$  (Kurz *et al.*, 2005), which convinced Mark Kurz of the validity of this method, something of which I am proud.

This method of correction using either solar-like  $^{20}\text{Ne}/^{22}\text{Ne}$  ratio can also be applied to derive the isotopic compositions of the other noble gases, particularly Ar and Xe isotopic ratios (Farley and Poreda, 1993). However, in this case, the method of correction is slightly more difficult since mixing is not linear as shown on Figure 5.10, but hyperbolic<sup>30</sup>. Step crushing allows well-constrained hyperbolae to be determined and therefore precise extrapolation to solar-like ratios. Parai *et al.* (2012) used recently this method to determine the  $^{40}\text{Ar}/^{36}\text{Ar}$  compositions of the magma sources of MORB from the South West Indian Ridge (SWIR). They observed important variations of the  $^{40}\text{Ar}/^{36}\text{Ar}$  ratio (12,000 up to 50,000) along the SWIR, suggesting that the mantle might not be homogeneous for the radiogenic argon composition (Parai *et al.*, 2012). However, as said earlier, such a correction supposes homogeneous  $^{20}\text{Ne}/^{22}\text{Ne}$  ratio in the mantle, which might not be the case, especially in the Indian Ocean where the DUPAL anomaly is strongly influencing the chemical and isotopic compositions of the oceanic basalts (Dupré and Allègre, 1983).

Another example of the use of neon to correct for air contamination is given in Figure 5.12 that shows the xenon isotopic ratios as a function of the  $^{20}\text{Ne}/^{22}\text{Ne}$  ratio in a few MORB samples from the Atlantic Ridge (Moreira *et al.*, 1998; Tucker *et al.*, 2012). In this figure, I plot four samples measured by step crushing including the popping rock 2πD43 we had measured in 1998. I also chose three samples measured by Tucker *et al.* (2012) to illustrate how the  $^{129}\text{Xe}/^{130}\text{Xe}$ , corrected for

30. In general, mixing arrays in isotopic space are hyperbolic, with a curvature determined by the abundance ratio of the denominator nuclides in the end-members. In the case of the Ne-Ar system, for example, the hyperbola is defined by the ( $^{36}\text{Ar}/^{22}\text{Ne}$ ) ratio of the two end-members. In the special case of diagrams with two isotopic ratios of the same element with a common denominator the mixing is linear as seen in the  $^{20}\text{Ne}/^{22}\text{Ne}$  and  $^{21}\text{Ne}/^{22}\text{Ne}$  plots earlier in this section.



atmospheric contamination using the neon B composition for the mantle, varies in the mantle source of MORB (see data from this approach used in Fig. 4.15). Note the contrasting curvature of the mixing relative to argon, which results from deficit of the xenon in the atmosphere, and then in a low Xe/Ne in the atmosphere relative to the mantle, producing the observed hyperbolae. The discussion on this variation in the  $^{129}\text{Xe}/^{130}\text{Xe}$  ratio was initiated in Section 4, and will be discussed into more detail in Sections 7 and 8.

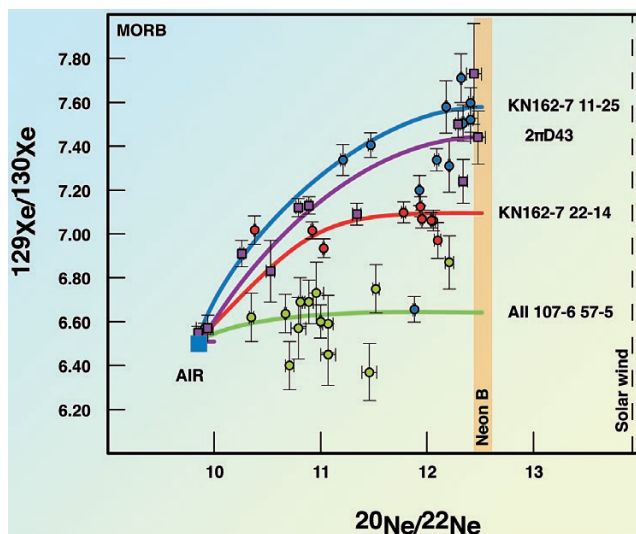


**Figure 5.12**

$^{20}\text{Ne}/^{22}\text{Ne}$  plotted against  $^{129}\text{Xe}/^{130}\text{Xe}$  in a suite of MORB samples from the Atlantic. Neon isotopic ratios allow the determination of the uncontaminated  $^{129}\text{Xe}/^{130}\text{Xe}$  ratio of the magma source of these samples by extrapolating to a  $^{20}\text{Ne}/^{22}\text{Ne}$  ratio of 12.5, the supposed mantle ratio. This figure shows heterogeneous  $^{129}\text{Xe}/^{130}\text{Xe}$  ratios in the mantle source of MORB. Data from Tucker *et al.* (2012) and Moreira *et al.* (1998).

## 5.4 The He-Ne Correlation in the Mantle and the Unique Primitive Source

On a global scale, there is a correlation in oceanic basalts between the  $^{21}\text{Ne}/^{22}\text{Ne}$  (corrected for air contamination) and the  $^4\text{He}/^3\text{He}$  ratios (*e.g.*, Honda's publications) (Fig. 5.13). Samples with MORB helium have MORB-neon and samples with less radiogenic helium show un-nucleogenic  $^{21}\text{Ne}/^{22}\text{Ne}$  ratios (Honda *et al.*, 1991; Honda *et al.*, 1993; Moreira *et al.*, 1995; Moreira *et al.*, 1996; Valbracht *et al.*, 1996; Valbracht *et al.*, 1997; Moreira and Allègre, 1998; Sarda *et al.*, 2000; Trierloff *et al.*, 2000; Moreira *et al.*, 2001; Trierloff *et al.*, 2002; Dixon, 2003; Hopp *et al.*, 2004; Yokochi and Marty, 2004; Hopp and Trierloff, 2005; Madureira *et al.*, 2005; Doucet





*et al.*, 2006). This correlation is expected because most of the  $^{21}\text{Ne}$  derives from  $(n,\alpha)$  and  $(\alpha,n)$  reactions<sup>31</sup>. The  $^4\text{He}/^{21}\text{Ne}$  production ratio should be homogenous in the mantle, and have a value of  $\sim 4.5 \times 10^{-8}$  (Yatsevich and Honda, 1997). The correlation between the  $^{21}\text{Ne}/^{22}\text{Ne}$  (corrected for air contamination) and the  $^4\text{He}/^3\text{He}$  ratios reflects a mixture between two components, one being the MORB source, the other one being an undegassed/Primitive reservoir. Moreover, these two components have also different  $^3\text{He}/^{22}\text{Ne}$  ratios, as shown by the hyperbolic mixing in the  $^{21}\text{Ne}/^{22}\text{Ne}$ - $^4\text{He}/^3\text{He}$  diagram of Figure 5.13. The interpretation of this diagram will be discussed in Section 6 on the origin of the primordial signature in OIB.

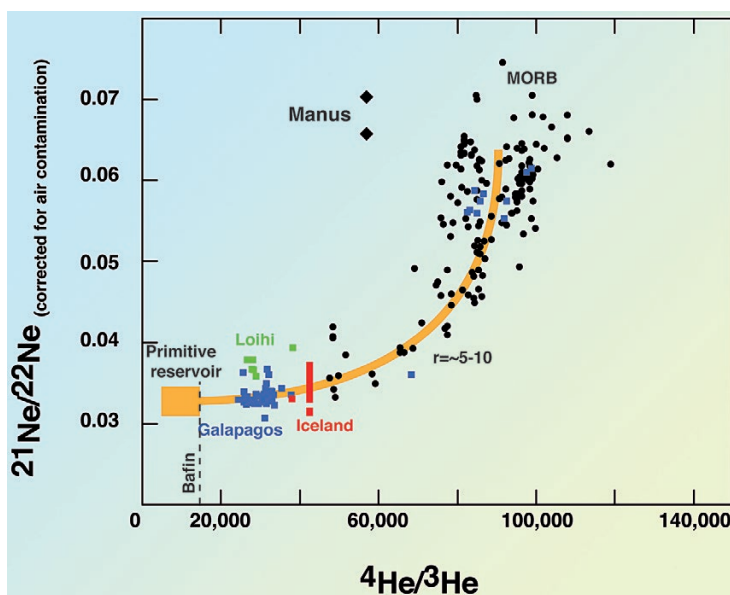


**Figure 5.13**

$^4\text{He}/^3\text{He}$ - $^{21}\text{Ne}/^{22}\text{Ne}$  (corrected for air contamination using  $^{20}\text{Ne}/^{22}\text{Ne} = 12.5$ ) in oceanic basalts. This mixing curve shows that most of the oceanic samples are a mixture between two components: MORB and a primitive reservoir having low helium and neon isotopic ratios. Baffin samples have the most primitive helium ratios on Earth (but no neon was measured in these non-glassy samples), and provide a limit for the helium isotopic ratio of the primitive reservoir ( $\sim 15,000$ ;  $R/R_a \sim 50$ ) (Stuart *et al.*, 2003). Manus samples are back arc basalts showing non-radiogenic helium, but nucleogenic neon (Shaw *et al.*, 2001). Any mixing array with the primitive mantle must have different  $r = (^3\text{He}/^{22}\text{Ne})_{\text{MORB}}/(^3\text{He}/^{22}\text{Ne})_{\text{primitive}}$  in this case.

31. A small fraction of the neutrons and the alpha particles produced during U and Th radioactive decays can form nucleogenic  $^{21}\text{Ne}$ . The  $^4\text{He}/^{21}\text{Ne}$  production ratio is estimated at  $\sim 5 \times 10^{-8}$  (Yatsevich and Honda, 1997).



However, in a few locations, nucleogenic neon is not always associated with radiogenic helium and vice versa (Shaw *et al.*, 2001; Kurz *et al.*, 2005; Tucker *et al.*, 2012). For instance, Shaw has measured MORB-like neon in samples with low  $^4\text{He}/^3\text{He}$  (down to 57,000;  $\text{R}/\text{Ra} = 12.7$ ) from Manus Back Arc Basin (Shaw *et al.*, 2001). Recently, Tucker *et al.* (2012) have measured samples on the Mid Atlantic ridge with nucleogenic neon ( $^{21}\text{Ne}/^{22}\text{Ne} \sim 0.065$ ) associated with “normal” helium isotopic ratio (80,000;  $\text{R}/\text{Ra} = 9$ ) and samples with un-nucleogenic Ne (0.055) coupled to radiogenic helium (95,000;  $\text{R}/\text{Ra} = 7.6$ ). Such decoupling between helium and neon certainly reflects fractionation between helium and neon during degassing or melting.

## 5.5 Solar Argon in the Mantle?

Whatever the neon isotopic ratio in the mantle (solar or neon B), the logical continuation of the search for solar noble gases in the mantle is the study of the non-radiogenic argon isotopic ratio,  $^{38}\text{Ar}/^{36}\text{Ar}$ . Similarly to neon, the  $^{38}\text{Ar}/^{36}\text{Ar}$  ratio could be solar, chondritic (Q) or argon B in the mantle at the end of the accretion. The search for a solar-type argon for the mantle, in my opinion, started really with the work of Peter Valbracht on Loihi samples in 1997 (Valbracht *et al.*, 1997). Peter Valbracht came to IGP to do his post-doc in particular on this topic with new samples recently dredged on Loihi. I was a PhD student when he made the analysis on the ARESIBO mass spectrometers. The problem that arose at that time was a

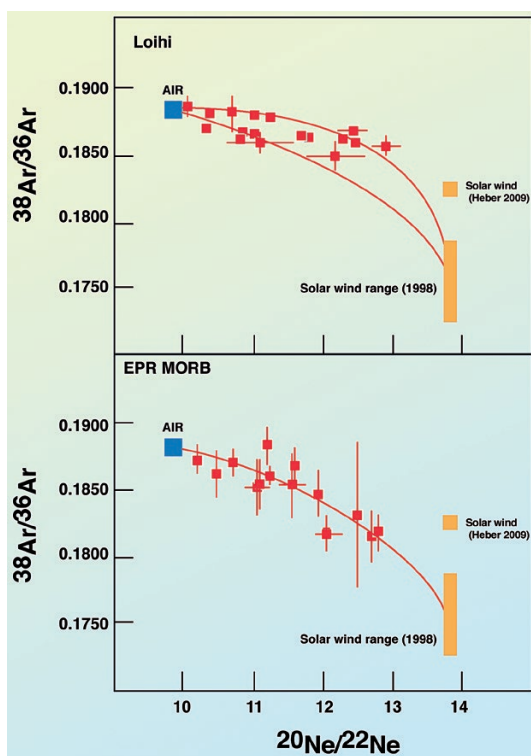


Figure 5.14

Pepin used noble gas measurements in Loihi and EPR from Valbracht *et al.* (1997) and Niedermann *et al.* (1997) to propose that the  $^{38}\text{Ar}/^{36}\text{Ar}$  is solar in the mantle. However, this interpretation has been challenged and some analytical issues can be the origin of the low  $^{38}\text{Ar}/^{36}\text{Ar}$  ratios (see text) (modified from Pepin, 1998).



problem of gas purification. He used the step heating to remove the atmospheric contamination at low temperatures and at high temperature steps the mantle-derived gases. The problem that we had observed at this time was the release of impurities after purification with hot Ti getters because the crucible of the furnace was still hot and was probably still outgassing chlorine or hydrocarbons. This disturbed the argon analyses. Valbracht *et al.* (1997) found  $^{38}\text{Ar}/^{36}\text{Ar}$  isotopic ratios lower than air, but I am still very suspicious about these data because of the pollution associated with the outgassing of the molybdenum crucible. Figure 5.14 is a reproduction of a figure from an article of Pepin (1998) that used data of Valbracht *et al.* (1997) and those of Niedermann *et al.* (1997) on the East Pacific Rise to show that the  $^{38}\text{Ar}/^{36}\text{Ar}$  is solar in the Earth's mantle. The new value for solar wind argon obtained by Heber and colleagues in 2009 is included in this figure (Heber *et al.*, 2009).

The hypothesis of solar argon in the mantle was challenged by further work in Paris (Kunz, 1999; Raquin and Moreira, 2009). Both studies suggest that the mantle has a  $^{38}\text{Ar}/^{36}\text{Ar}$  similar to that of the atmosphere, using the neon systematics and paying a careful attention to the gas purification and to the tailing effect under mass 38, which can be an issue for high  $^{40}\text{Ar}/^{36}\text{Ar}$  samples. Kunz, and then Raquin and I used the  $^{20}\text{Ne}/^{22}\text{Ne}$ - $^{40}\text{Ar}/^{36}\text{Ar}$  diagram to show a hyperbolic mixing between atmosphere and the mantle to derive the  $r$  parameter of

the hyperbolae ( $r = (^{36}\text{Ar}/^{22}\text{Ne})_1 / (^{36}\text{Ar}/^{22}\text{Ne})_2$ ). Then, a theoretical mixing hyperbolae was constructed using this  $r$  value for the  $^{20}\text{Ne}/^{22}\text{Ne}$ - $^{38}\text{Ar}/^{36}\text{Ar}$  diagram to show that  $^{38}\text{Ar}/^{36}\text{Ar}$  is not solar in the present-day mantle. Examples of this method are given on Figures 5.15 and 5.16 for MORB and Galapagos samples. This is also true for the La Réunion hotspot (Trieloff *et al.*, 2002) and Iceland (Trieloff *et al.*, 2000; Mukhopadhyay, 2012). Based on these recent measurements on MORB and on Galapagos and Iceland hotspots, which best represent the primitive reservoir, it seems clear that the mantle has a present day  $^{38}\text{Ar}/^{36}\text{Ar}$  composition close to the atmospheric composition, different from the solar ratio. The early analyses of Valbracht *et al.* (1997) and Niedermann *et al.* (1997) probably

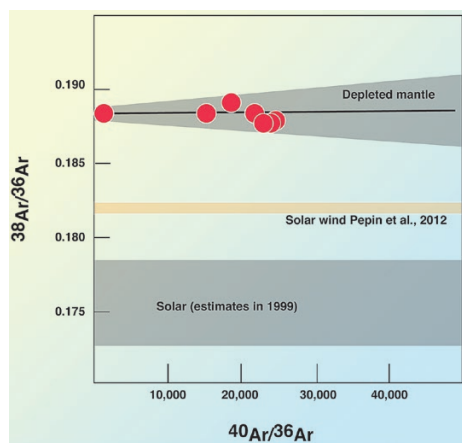


**Figure 5.15**

Joachim Kunz proposed in 1999 that  $^{38}\text{Ar}/^{36}\text{Ar}$  is not solar in the MORB source. This figure shows that for a large range of  $^{40}\text{Ar}/^{36}\text{Ar}$  ratios, the  $^{38}\text{Ar}/^{36}\text{Ar}$  is atmospheric in the MORB sample 2πD43. Kunz proposed that the mantle has a  $^{38}\text{Ar}/^{36}\text{Ar}$  ratio similar to the one of the atmosphere (modified from Kunz, 1999).



reflect analytical problems such as either incomplete purification or improper base-line correction. It should be also said that *Ballentine and Holland* established also that the  $^{38}\text{Ar}/^{36}\text{Ar}$  ratio is atmospheric-like in the mantle source of  $\text{CO}_2$ -well gases. For a large range of  $^{40}\text{Ar}/^{36}\text{Ar}$  (air to  $\sim 30,000$ ), the  $^{38}\text{Ar}/^{36}\text{Ar}$  is constant at an atmospheric ratio and does not show any mixing with solar-like argon (Ballentine and Holland, 2008), which is consistent with the Ar systematics in oceanic basalts.

In Section 8, I will discuss the origin of this composition in the Earth's mantle, which could reflect massive atmospheric subduction, the chondritic composition or solar wind implantation.

## 5.6 Conclusions about the Neon and Argon Isotopic Composition in the Mantle

The non-radiogenic neon and argon isotopic compositions in the mantle ( $^{20}\text{Ne}/^{22}\text{Ne}$  and  $^{38}\text{Ar}/^{36}\text{Ar}$ ) provide essential constraints on the mechanism of noble gas incorporation in the Earth's mantle. The present-day composition appears to be different from the solar composition for both the  $^{20}\text{Ne}/^{22}\text{Ne}$  and  $^{38}\text{Ar}/^{36}\text{Ar}$  ratios. The  $^{20}\text{Ne}/^{22}\text{Ne}$  ratio is solar-like but with values of  $\sim 12.5$  in the MORB source and between 12.5 (Galapagos) and  $\sim 12.8$  (Iceland) in OIB sources.

These ratios resemble the implanted solar wind (neon B like,  $^{20}\text{Ne}/^{22}\text{Ne} \sim 12.7$ , see Section 2) rather than true the solar values ( $^{20}\text{Ne}/^{22}\text{Ne} = 14.0$ ; Pepin *et al.*, 2012). Precise determinations of the  $^{38}\text{Ar}/^{36}\text{Ar}$  suggest that the mantle has a composition very analogous to that of the atmosphere ( $0.188$ ), or chondritic ( $Q = 0.1875 \pm 0.0005$ ), different from the solar ratio ( $0.1819$ ; Pepin *et al.*, 2012). The interpretations that can be derived from such information will be reviewed in Section 8.

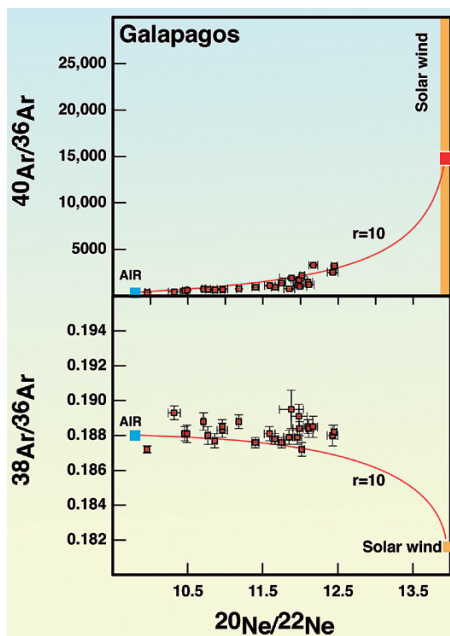


Figure 5.16

Neon-argon in Galapagos samples (Raquin and Moreira, 2009 and unpublished data). The  $r$  parameter is defined by  $(^{36}\text{Ar}/^{22}\text{Ne})_1 / (^{36}\text{Ar}/^{22}\text{Ne})_2$  and is determined using the  $^{20}\text{Ne}/^{22}\text{Ne}$ - $^{40}\text{Ar}/^{36}\text{Ar}$  mixing diagram (top). The same  $r$  has to be used for  $^{20}\text{Ne}/^{22}\text{Ne}$ - $^{38}\text{Ar}/^{36}\text{Ar}$  (bottom). This shows that the solar component can barely be the end-member of the mixing. The solar value is derived from Pepin *et al.* (2012).



## 6. THE EXISTENCE OF THE PRIMITIVE NOBLE GAS RESERVOIR

We have seen in the previous sections that the radiogenic, nucleogenic and fissiogenic isotopic ratios of helium, neon, argon, and xenon suggest contrasting mantle sources of MORB and OIB. Such differences in  $^4\text{He}/^3\text{He}$ ,  $^{21}\text{Ne}/^{22}\text{Ne}$ ,  $^{40}\text{Ar}/^{36}\text{Ar}$  and  $^{129-136}\text{Xe}/^{130}\text{Xe}$  require chemical fractionation processes to have occurred over geological time scales because the parental isotopes ( $^{232}\text{Th}$ ,  $^{235}\text{U}$ ,  $^{238}\text{U}$  and  $^{40}\text{K}$ ) have long half-lives ( $>700$  Ma). For the rare gas systems, fractionation of lithophile parents from atmophile (volatile) daughters is readily related to degassing processes, which we know occur on a planetary scale as a result of on-going mantle convection and plate creation at ridges (see Section 3). In this section, I will discuss several scenarios that may explain the different noble gas isotopic compositions of the two reservoirs that generate MORB and OIB.

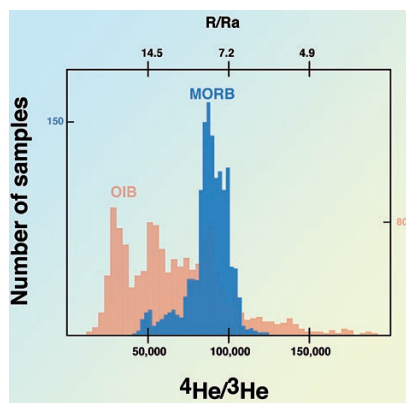


Figure 6.1

Histogram of the  $^4\text{He}/^3\text{He}$  isotopic ratios in oceanic basalts, showing the dichotomy between MORB ( $n = 1576$ ) and OIB ( $n = 1500$ ). The MORB source is more homogenous with a mean ratio of  $\sim 90,000$ , whereas OIB show both lower and higher  $^4\text{He}/^3\text{He}$  (although it should be noted that while the MORB are all essentially zero age some of the OIB are as old as a few Ma).  $R/R_a$  is the other notation for the helium isotopic ratio ( $R = ^3\text{He}/^4\text{He}$  and  $R_a$  is the atmospheric ratio).

### 6.1 Noble Gases Suggest a Deep “Primitive” Reservoir for the OIB Source

As a first step I will focus only on helium and neon to interpret the existence of a primitive reservoir and make the assumption that these interpretations should be applicable to the heavy rare gases.

The  $^4\text{He}/^3\text{He}$  ratio is systematically lower in OIB compared to MORB (Fig. 6.1), with a few exceptions such as discussed in Section 3. This is also the case for neon for which the  $^{21}\text{Ne}/^{22}\text{Ne}$  ratio, corrected for any atmospheric contamination, is also systematically less nucleogenic in OIB (e.g., Fig. 5.6), although for the analytical reasons discussed in the last section there are fewer Ne data and the high  $^4\text{He}/^3\text{He}$  OIB are not well represented. In addition,  $^{21}\text{Ne}/^{22}\text{Ne}$  and  $^4\text{He}/^3\text{He}$  ratios in oceanic basalts are correlated (Fig. 5.13), defining a hyperbolic mixing array with a hyperbolic parameter (curvature) near 5 (e.g., Moreira and Allègre, 1998). This suggests that the  $^3\text{He}/^{22}\text{Ne}$  ratio is different in these two sources,



and provides additional constraints on the composition of the OIB reservoir. The He-Ne correlation observed on Figure 5.13 suggests a common, low (U+Th)/<sup>3</sup>He, (U+Th)/<sup>22</sup>Ne source for all OIB, and different mixing proportions between this source and MORB.

Interpretations of the origin of the low (U+Th)/<sup>3</sup>He and (U+Th)/<sup>22</sup>Ne mantle source and the time of its isolation has varied. This bears on its character and likely locations. Perhaps the majority of scientists have suggested that the OIB source is an undegassed source enriched in <sup>3</sup>He and <sup>22</sup>Ne (see also the evidence from Xe in Section 4), resulting in low (U+Th)/<sup>3</sup>He and (U+Th)/<sup>22</sup>Ne ratios, whereas others suggest that on contrary the OIB source has low (U+Th)/<sup>3</sup>He and (U+Th)/<sup>22</sup>Ne ratios because during melting, U and Th are more incompatible than He and Ne. In this model low <sup>4</sup>He/<sup>3</sup>He and <sup>21</sup>Ne/<sup>22</sup>Ne reflect the isotopic compositions of ancient, “frozen-in” melt residues, rather than undegassed or even primitive reservoirs.

## 6.2 The Canonical Model: the Two-layer Mantle

Since the discovery of lower <sup>4</sup>He/<sup>3</sup>He ratios in OIB compared to MORB, it has been suggested that OIB are the expression at the surface of a mantle plume derived from the lower mantle (Kaneoka, 1981; Kurz *et al.*, 1982a; Kaneoka, 1983; Kurz *et al.*, 1983). The bulk lower mantle was proposed by many authors to be entirely primitive for noble gases, whereas the upper mantle is degassed. In such a scenario, mantle plumes can derive from either the 670 km boundary layer or from the core-mantle boundary layer. In the case where mantle plumes are issued from the boundary between the upper and the lower mantles, entrainment of a few % of lower mantle material can explain their primitive noble gas compositions (Allègre and Moreira, 2004). However, this simplest two-layer mantle has been criticised because of the seismic observation that slabs penetrate into the lower mantle (*e.g.*, Grand *et al.*, 1997; Van der Hilst *et al.*, 1997) and the implication that the consequent counter flow would, to some extent, mix upper and lower mantles. Whether or not this convective exchange is sufficient to rule out the lower mantle as a whole for the source of noble gases has been addressed in several modelling studies (*e.g.*, Van Keken *et al.*, 1997; Gonnerman and Mukhadopyay, 2009). It has further been suggested that the modern observations of slab penetration into the lower mantle reflect a recent change in style of convection and that for most of Earth history, the whole lower mantle has in fact been isolated (Allègre, 2002).

Although it has some flaws, this two-layer model had a large impact on the chemical geodynamics, and is still, for me, a reference model. Moreover, this model is adaptable and has been modified to place the lower layer, not at the 670 km boundary, but as a stealth layer deeper in the lower mantle or in a region corresponding to the core-mantle boundary (*e.g.*, Tolstikhin and Hofmann, 2005). These more recent versions of the layered mantle have also



been examined numerically by Xie and Tackley (2004), Samuel and Farnetani (2003) and Deschamps *et al.* (2011), and show promise given a suitably higher density lower layer.

### 6.3 The Basal Magma Ocean (BMO) Model

A recent variant of the two layered mantle model is to relate the lower layer to a largely crystallised deep melt layer, residual to a terrestrial magma ocean formed during terrestrial accretion. I reproduce in Figure 6.2 this basal magma ocean model (BMO) of Labrosse *et al.* (2007). This interesting model can be described in four stages. The first step is the existence of a planetary-wide magma ocean potentially resulting from the Moon forming impact. Such a magma ocean may crystallise from the middle, leaving a molten mantle at the surface and also a BMO, which itself continues to crystallise. As the BMO crystallises (over billions of years), the crystals can be introduced into the convective mantle but the incompatible elements will remain in the residual liquid. The liquid also becomes iron-rich, ultimately to the point that the crystals are too dense to be further convectively entrained and they consequently form piles of crystals above pockets of magma. Mantle plumes can entrain a certain percentage of these crystals and we will later see that they could have a suitable noble gas isotope signature.

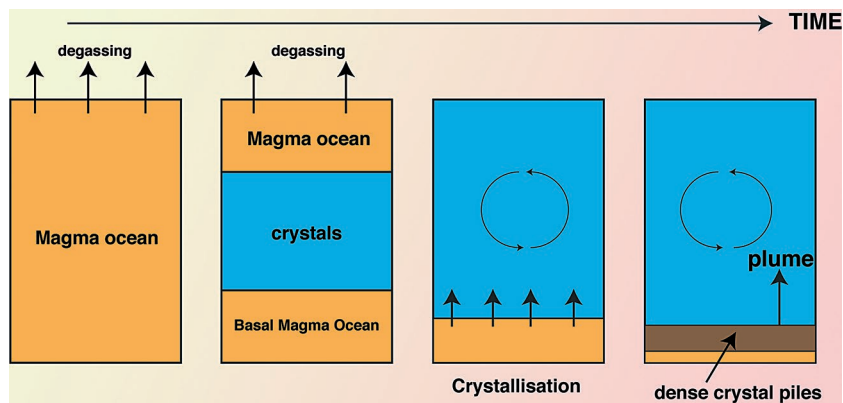


**Figure 6.2** The BMO model of Labrosse *et al.* (2007). Crystallisation of a basal magma ocean produces piles of dense crystals sited above residual enriched melt. Mantle plumes can entrain these crystals that contain primordial isotopic composition for noble gases.

An important point of this model is that degassing initially occurs in the first phase when the Earth is molten, but it continues throughout the history of Earth in the convective mantle by the formation of oceanic crust. However, the BMO cannot be degassed because it is not in contact with the atmosphere.





It is therefore enriched in noble gases in the same manner as for other incompatible elements. The differences between noble gases and other lithophile elements rest in the fact that the rest of the mantle is strongly degassed, and so produces a large contrast of concentration between the deep melt and the convecting mantle. Figure 6.3 shows the calculated concentrations of elements in the crystallising basaltic melt and in the crystals assuming fractional crystallisation. If we assume<sup>32</sup> that the noble gas partition coefficients between perovskite and the melt are between  $10^{-2}$  and  $10^{-3}$ , then the crystals can be enriched in noble gases compared to the degassed mantle. The pile of crystals, if sampled by mantle plume, can provide the “primitive” noble gas signatures in OIB (Coltice *et al.*, 2011). This is achieved even more easily (in terms of mass balance) if this is the melt layer itself sampled by mantle plumes, as it is enriched in noble gases by a few orders of magnitude compared to the MORB-source mantle (Fig. 6.3).

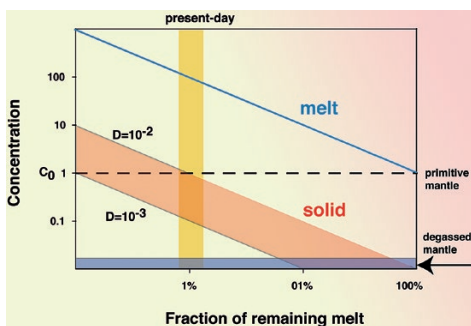


**Figure 6.3**

Simple calculation of fractional crystallisation showing how the melt and the crystals can be enriched in noble gases if they have partition coefficient between  $10^{-2}$  and  $10^{-3}$  between perovskite and melt (inspired by Coltice *et al.*, 2011).

This model is theoretical and makes many assumptions, both geophysical (relative density of melt and crystals; for example) and geochemical (partition coefficient; for example). However, I find this model attractive because it provides a physical framework to the noble gas systematics.

## 6.4 The Core

The ultimate deep-layer of a two-layer model explaining noble gas systematics is the core. Indeed, it has also been proposed that primordial noble gases are concentrated in the core, assuming they are more soluble in metal than their parent (U, K, Th). Porcelli and Halliday (2001) have evaluated the possibility that non-radiogenic helium is sited in the core. I recount a similar discussion below. No data for noble gas partitioning between silicate and metal exist at the pressures of formation of the core (~50 GPa, 1300 km; Siebert, 2012), but at lower pressure, the partition coefficients are always below 0.1 and decrease with pressure down to  $3 \times 10^{-4}$  at  $P = 10$  GPa (Matsuda *et al.*, 1993) (Fig. 6.4). The present day<sup>3</sup>He

32. No experimental data exists on such partition coefficients. This needs to be performed in the next years to test the BMO model.



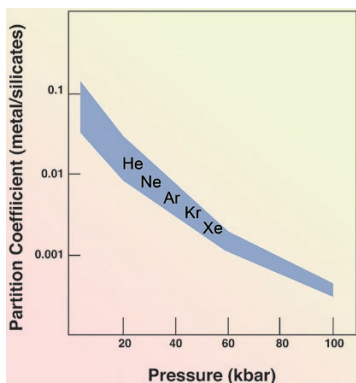


**Figure 6.4** Noble gas partition coefficient for metal/silicate determined for pressure up to 100 kbars (modified from Matsuda *et al.*, 1993).

concentration of the MORB source can be estimated to be  $\sim 10^{-10} \text{ cm}^3 \text{STP g}^{-1}$  (Moreira *et al.*, 1998). I assume here that the whole mantle has this concentration. I also assume the core has an isotopic composition similar to the primordial Earth ( $^4\text{He}/^3\text{He} \sim 5000$ ;  $\text{R}/\text{Ra} \sim 140$ ; see Section 2), implying that the gas was sequestered during core formation with no associated U, Th or Sm. To produce a ratio of 20,000 in a mantle plume by solid mixing of core material with MORB mantle like material, the  $^3\text{He}$  concentration in the core has to be  $\sim 500$  times the present-day concentration in the MORB source. I assume here that only 1% of the material in the plume is derived from the core to illustrate my point, although even this amount of core material is unlikely to be directly entrained given the constraints provided by W isotope systematics (see Scherstén *et al.*,

2004). This issue was also raised by Porcelli and Halliday (2001). So, the  $^3\text{He}$  concentration in the core has to be, at minimum,  $\sim 5 \times 10^{-8} \text{ cm}^3 \text{STP g}^{-1}$ . Bearing in mind that the partition coefficient between melt and silicate is  $3 \times 10^{-4}$  or lower (Matsuda *et al.*, 1993), the primordial  $^3\text{He}$  concentration in the Earth before core formation would have been higher than  $1.5 \times 10^{-4} \text{ cm}^3 \text{STP g}^{-1}$ ,  $10^6$  times the present day concentration in the MORB source. This model is unlikely because such a high concentration (possibly even higher since the mantle might have been degassed by more than 99%) is not observed in meteorites.

A second scenario can be envisaged involving noble gases in the core. It consists of a diffusive flux of  $^3\text{He}$  (and other noble gases) from the core to the bottom of the mantle, again assuming the core is rich enough in  $^3\text{He}$  and sufficiently poor in U and Th, to avoid a radiogenic helium signature developing in the core itself. As above, the helium concentration in the core is taken to reflect the equilibrium between the primitive material and the metal with a partitioning value similar to those measured by (Matsuda *et al.*, 1993). Let us propose a simple calculation in which helium is diffusing out of the core and is incorporated into silicates in the thermal boundary layer above. The concentration in the boundary layer is given by:

$$C_{bl}(t) = \frac{C_{core}(t)}{k}$$

where  $k$  is the metal/silicate partition coefficient ( $\sim 3 \times 10^{-4}$ ; Matsuda *et al.*, 1993) and  $C_{core}(t)$  is the concentration in the core at a time  $t$ . Note that it is not only the concentration gradient that determines the helium flux, but also the ability of helium to enter into silicate phase. If we suppose that the life of this thermal boundary layer is  $\sim 1 \text{ Ga}$ , then one can write the following mass balance:



$$\frac{4}{3}\pi a^3 [C_{core}(\tau) - C_0] = 4\pi a^2 \sqrt{D\tau} \frac{C_{core}(t)}{\kappa}$$

where  $a$  is the radius of the core. Note that  $(D\tau)^{1/2}$  is the thickness of the silicate “helium layer”. The core is supposed to be well mixed.

Figure 6.5 shows the calculated concentrations in the core and in the thermal boundary layer as a function of the helium diffusivity. The starting bulk Earth  $^3\text{He}$  concentration used is  $10^{-8} \text{ cm}^3\text{STP cm}^{-3}$ , similar to chondritic  $^3\text{He}$  concentrations. This simple calculation illustrates that under certain conditions of diffusivity, the boundary layer can be significantly re-enriched in helium by diffusion out of the core. If the core doesn’t contain U and Th (in the order of the ppt), the primitive helium signature observed in OIB could potentially reflect this mechanism. Figure 6.6 is a cartoon showing the scenario of the primitive reservoir being located in the core. Mantle plumes sample the boundary layer and therefore could have a primordial helium signature. However, the “helium” boundary layer is thin, on the order of  $\sim 2 \text{ km}$  with  $D = 10^{-6} \text{ cm}^2 \text{ s}^{-1}$  (and 1 Ga as the residence time for the boundary layer), compared to the thermal boundary layer ( $\sim 50 \text{ km}$ ). Therefore, it is not clear if this layer enriched in helium could be entrained in mantle plumes and if this is an important contributor to the bulk helium budget of the plume or if it can be sampled preferentially during melting at surface. This short discussion on the possibility that primitive helium might be sited in the core needs further work, either from experimental or modelling point of view.

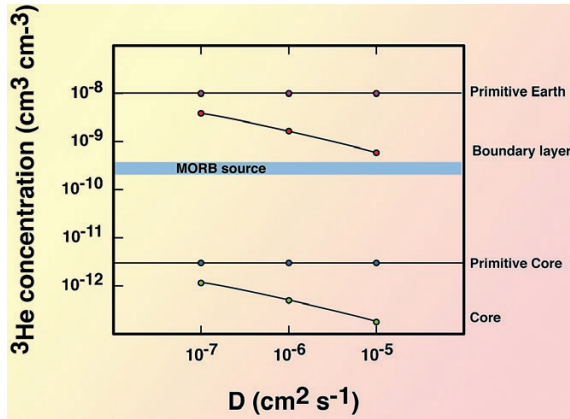


**Figure 6.5**

Results from a model of the concentration in the core and in a boundary layer assuming helium diffuses out of the core. The core is in equilibrium in this calculation with a mantle having  $10^{-8} \text{ cm}^3\text{STP/ cm}^3$   $^3\text{He}$  and a pressure formation of 100 kbars. This simplistic calculation demonstrates that the core could be the source of primordial helium as suggested by Porcelli and Halliday (2001) considering the existing partitioning data. Indeed, even if the concentration in the core is low compared to the primitive mantle, when helium diffusion out of the core occurs (because helium is much more soluble in silicates), there is a “pumping effect” into the boundary layer, and therefore the thermal boundary layer can be very rich in helium, providing the primitive helium in the plume source.



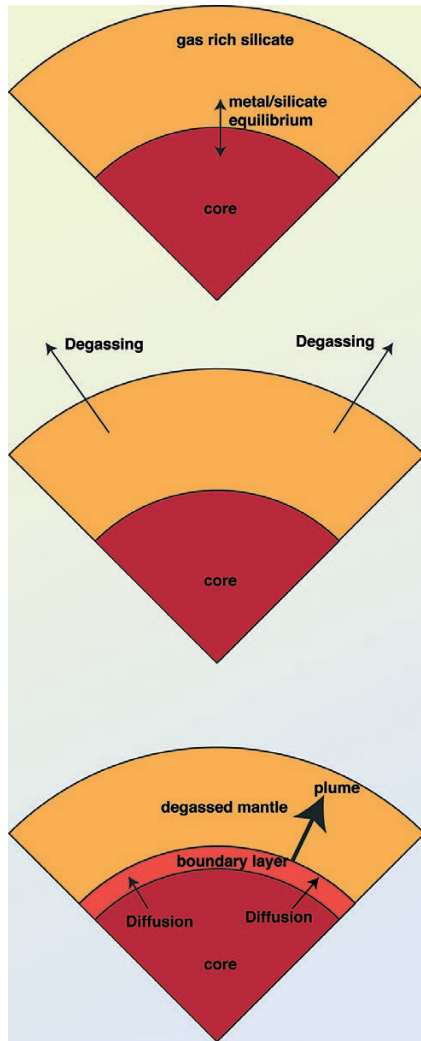


**Figure 6.6**

Cartoon explaining how a model in which primordial noble gases are sited in the core can explain the primitive signatures measured in OIB. During core formation, noble gases are partitioned between the mantle and the core according to their partitioning silicate/metal coefficients. Later, diffusion out of the core allows replenishment of a boundary layer in noble gases. Diffusion is favoured because noble gases are lithophile. Mantle plumes entrain this boundary layer, which is rich in primordial noble gases. At the moment, such a model has to be considered to be speculative but it cannot be excluded (e.g., Porcelli and Halliday, 2002).



## 6.5 Anderson's Revolt

The classical models described above generate the non-degassed noble gas signatures by convective isolation of a deep layer. This implicitly requires active upwelling to deliver this material to the surface, thereby linking OIB to mantle plumes (Morgan, 1971). Others have disputed that OIB are the surface expression of mantle plumes derived from the deep mantle. This then requires a different origin for the distinct noble gas signatures of OIB. As a long term sceptic of mantle plumes, in the 90's *Don Anderson* developed alternative explanations of low  $^4\text{He}/^3\text{He}$  ratios that did not require, deep non-degassed reservoir (Anderson, 1993, 1998, 2000; Meibom *et al.*, 2003).

An important point repeatedly raised by *Anderson* is the so-called "helium paradox", which notes that submarine glass samples in low  $^4\text{He}/^3\text{He}$  hotspots and erupted deep enough (or under glaciers) to avoid massive degassing contain significantly less helium than MORB which the opposite is expected from their isotope systematics (Kurz *et al.*, 1983; Honda *et al.*, 1991, 1993; Moreira *et al.*, 1995; Harrison *et al.*, 1999; Breddam *et al.*, 2000; Dixon *et al.*, 2000; Moreira and Sarda, 2000; Trieloff *et al.*, 2000; Moreira *et al.*, 2001; Kurz *et al.*, 2009; Mukhopadhyay, 2012). To counter this dilemma it has been suggested that the helium loss is pre-eruptive (Hopp and Trieloff, 2008) or that hotspot lavas contain less helium because they contain more water and  $\text{CO}_2$ , favouring more extreme degassing than in a ridge setting (Hilton *et al.*, 2000b; Yamamoto and Burnard, 2005; Gonnermann and Mukhopadhyay, 2007).

*Anderson* has proposed some alternatives to the classical two-reservoir model involving a non-degassed reservoir sampled by mantle plumes. Because one obvious idea is that low  $^4\text{He}/^3\text{He}$  ratios are low because they sample an ancient reservoir with no U and Th, the lithospheric mantle is a good target. Lithospheric mantle is a residue of melting; U and Th are very incompatible; therefore these two elements should be very depleted in a dunitic/harzburgitic mantle. The relative enrichment in He can have two possible origins. Either helium is compatible or moderately incompatible during melting in contrast to its highly incompatible parents (*e.g.*, Parman *et al.*, 2005), or there is a process that could enrich the mantle in helium that is decoupled of the strict solid/melt partitioning.

The second scenario was explored in an experiment of *Pierre Schiano* illustrated in Figure 6.7, which shows that during melt migration within an olivine induced by a temperature gradient, the  $\text{CO}_2$  fluid can be separated from the melt and can be "trapped" within the olivine (Schiano *et al.*, 2007). If noble gases are concentrated into the  $\text{CO}_2$  fluid, dunitic or harzburgitic mantle can then be enriched in volatiles, including noble gases. This process of trapping  $\text{CO}_2$  bubbles within the lithospheric mantle has been proposed by Anderson (1998). With *Philippe Sarda*, we have also suggested such a process to explain the low  $^3\text{He}/^{22}\text{Ne}$  and  $^4\text{He}/^{40}\text{Ar}$  ratios in mantle xenoliths because this process mimics an open system vesiculation (Moreira and Sarda, 2000). However, such a mechanism fails to explain the primitive helium and neon signatures in OIB. Whilst some



portions of the continental lithospheric mantle can meet the criteria of being depleted in U and Th, and being old, the  $^4\text{He}/^3\text{He}$  ratios measured in rocks derived from the continental mantle (either xenoliths or mafic volcanism) don't show an unradiogenic  $^4\text{He}/^3\text{He}$  ratio (Fig. 6.8; Gautheron and Moreira, 2002; Dunai and Porcelli, 2002). This peculiar helium isotopic signature in continental-derived samples reflects the evolution of a reservoir having a  $(\text{U}+\text{Th})/^3\text{He}$  ratio typically higher than the MORB and most OIB. The subcontinental lithosphere therefore cannot explain the non-radiogenic  $^4\text{He}/^3\text{He}$  helium isotopic ratios in OIB.

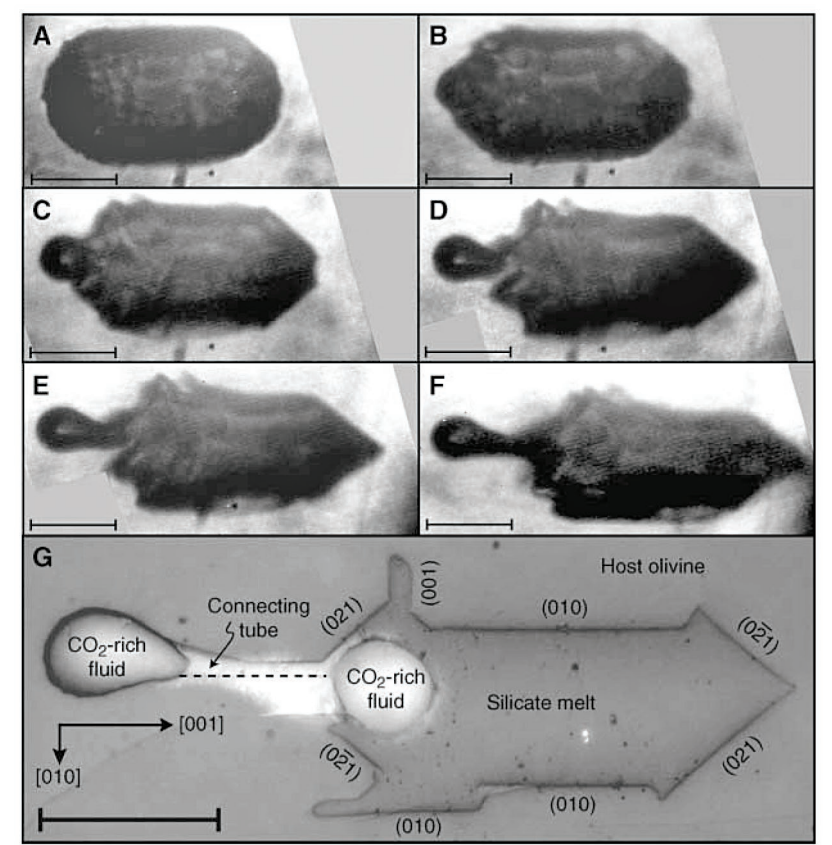


**Figure 6.7** Experimental melt percolation in an olivine showing the disconnection of the CO<sub>2</sub>-rich fluid from the melt during melt transport in an olivine. This process could explain how to enrich the lithospheric mantle in CO<sub>2</sub> and noble gases relative to lithophile elements, which are transported to the surface with the melt (from Schiano *et al.*, 2007, with permission from Science).

The CO<sub>2</sub> trapping within the present-day oceanic lithosphere also fails to explain the primitive helium isotopic ratios in OIB. A simple calculation can be used to show this hypothesis is untenable. If unradiogenic  $^4\text{He}/^3\text{He}$  helium in OIB is derived from the oceanic lithosphere by “freezing” the helium isotopic signature in CO<sub>2</sub> bubbles trapped in the lithosphere, then the mantle must have had such an unradiogenic helium ratio at the time of the formation of this lithosphere. The upper mantle does indeed increase its  $^4\text{He}/^3\text{He}$  with time as a coupled consequence of degassing and decay of U+Th, but in recent times the rate of change has been quite small. Helium from sufficiently long ago needs to be trapped to record sufficiently low  $^4\text{He}/^3\text{He}$  for many OIB. To quantify these effects, showing how far back in time He (with no associated U and Th) would need to have been trapped to mimic the most non-radiogenic OIB signatures, the evolution with time of the mantle helium isotopic ratio is represented in Figure 6.9 (see similar calculation in Porcelli and Elliott, 2008). Two model parameter sets are used in Figure 6.9, which require any trapped gas to be at least 700 Ma and plausibly much older. Yet the oceanic lithosphere is a maximum of ~180 Ma and cannot reproduce the helium isotopic signatures seen at Hawaii, Iceland or Galapagos.

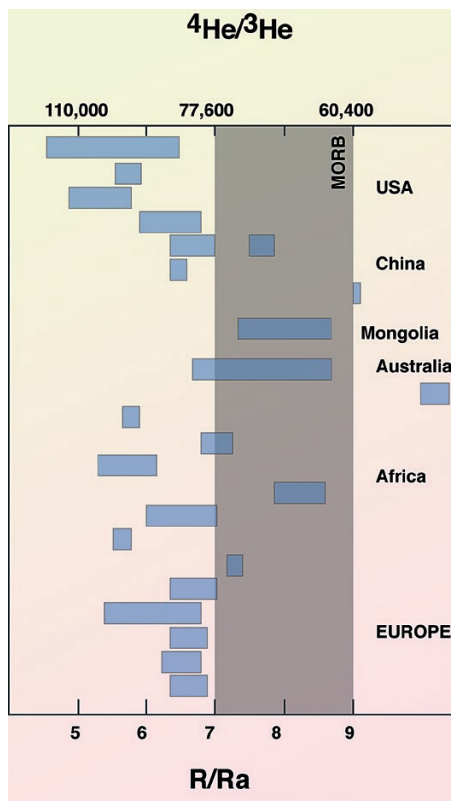


**Figure 6.8**

Helium isotopic composition in samples from the lithospheric mantle (phenocrysts, xenoliths). Most of the samples show relatively radiogenic helium isotopic ratios compared to the MORB mean value. This suggests that the sub-continental lithospheric mantle typically has a higher (U+Th)/<sup>3</sup>He ratio than the MORB and most OIB sources. This reservoir can hardly be the source of low  $^4\text{He}/^3\text{He}$  hotspots. It could potentially be involved, however, in the genesis of “low  $^3\text{He}$ ” hotspots such as the Canaries, Cameroon line, or Comoros (Barfod *et al.*, 1999; Hilton *et al.*, 2000a; Class *et al.*, 2005) (modified from Hilton and Porcelli, 2003).





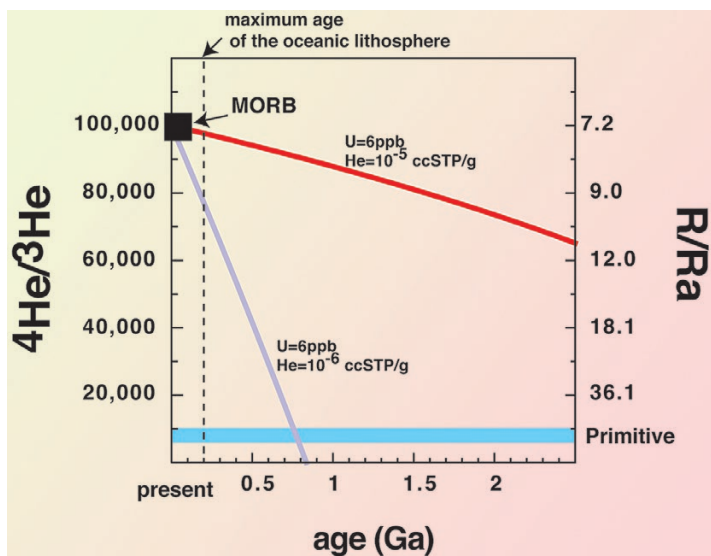


**Figure 6.9**

Evolution with age of the helium isotopic ratio in the MORB source. Two extreme helium concentrations are considered for the calculation ( $10^{-5}$  and  $10^{-6} \text{ cm}^3\text{STP g}^{-1}$ ). The upper value is derived from the gas rich popping rock 2 $\pi$ D43 (Moreira *et al.*, 1998). This model includes also  $^3\text{He}$  degassing at a rate of  $1000 \text{ mol a}^{-1}$  (e.g., Farley *et al.*, 1995). U content is taken as 6 ppb, typical of the depleted mantle. This simple calculation shows that oceanic lithosphere (with a maximum age of 180 Ma) cannot have been isolated sufficiently long ago to preserve a He isotope ratio comparable to that of the most unradiogenic OIB. Therefore, such OIB must be derived from an older (deeper) reservoir than the oceanic lithosphere.

## 6.6 Is the Low $^4\text{He}/^3\text{He}$ Reservoir a Residue of Melting?

A related mechanism to account for the “primitive” noble gases in OIB is that OIB sample a residue of melting. In this case, rather than trapping gas rich samples in modern lithosphere, it is assumed that noble gases are less incompatible than their parents (U, Th, K). This is an idea particularly driven by *Don Anderson* or more recently by Coltice and Ricard (1999), Parman *et al.* (2005) and Class and Goldstein (2005). Indeed, if helium is less incompatible than uranium during partial melting, the residue will have a  $U/^3\text{He}$  ratio lower than that of the crust and mantle. If this process is old (the calculations shown in Fig. 6.7 also pertain to this model) then it will show a helium isotopic ratio less radiogenic in the residue than in the mantle. A possible scenario proposed is the recycling of depleted, oceanic lithosphere, which can be much older than extant lithosphere, considered in the previous paragraph (Coltice and Ricard, 1999; Parman *et al.*, 2005; Class and Goldstein, 2005).



The determination of the relative partition coefficients of uranium, thorium, and helium has been a quest for many researchers, culminating in the most recent work by Heber *et al.* (2007). A number of studies on helium partition coefficients between olivine/cpx and melt showed that it was small enough to consider helium as an incompatible element (Hiyagon and Ozima, 1986; Marty and Lussiez, 1993). However, it is the value of this coefficient compared to that of uranium and thorium that is critical (Fig. 6.10). Considerable attention has also been focussed on experimental determination of U and Th partitioning (see review in Blundy and Wood, 2003), but sadly simultaneous determination of the partitioning of all three elements is not practical. The different datasets have been considered together in Figure 6.10. With these data, no large fractionations between (U+Th) and He can be produced without generating a source with very little He that would easily be perturbed by other components evident in OIB (Porcelli and Elliott, 2008).

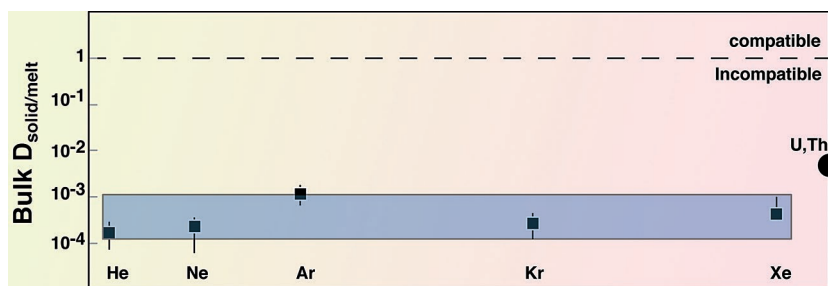


**Figure 6.10**

Partition coefficients during melting calculated assuming 60% olivine and 40% clinopyroxene in the mantle. Noble gas data from Heber *et al.* (2007). Noble gases are highly incompatible elements. Although very incompatible in olivine, U and Th are less incompatible in cpx (e.g., Blundy and Wood, 2003) and therefore their bulk D are higher than the partitioning coefficients of the noble gases.

A scenario with a residual mantle created a long time ago and stored in the deep mantle to become the source of mantle plumes can also be investigated for Ne isotopes (Kurz *et al.*, 2009). Galapagos lavas show the most primitive neon signature on Earth (Kurz *et al.*, 2009; Raquin and Moreira, 2009) and Figure 6.11 shows the time evolution of the <sup>21</sup>Ne/<sup>22</sup>Ne ratio in the mantle. If the source of Galapagos lavas represents a melt residue, the model age of this melting event is >4.3 Ga as demonstrated by Kurz *et al.* (2009). Similarly, Porcelli and Elliott (2008) quantified that, even if U+Th and He could be appropriately fractionated, the most unradiogenic OIB <sup>4</sup>He/<sup>3</sup>He isotope ratios required isolation for >3 Ga. In conclusion, if OIB don't sample a primitive reservoir, the "age" of this reservoir is old enough that it can be considered as primordial for the isotopic ratios.



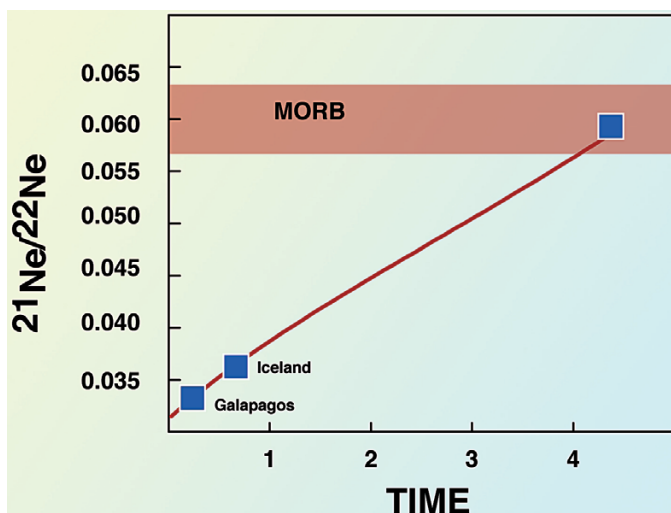


**Figure 6.11** Neon evolution of the mantle and the “model ages” of Galapagos and Iceland hotspots. This model considers a  $(\text{U}+\text{Th})/^{22}\text{Ne}$  ratio such as the present-day MORB composition is obtained in 4.5 Ga (modified from Kurz *et al.*, 2009; Iceland and Galapagos data from Trieloff *et al.*, 2000; Moreira *et al.*, 2001; Kurz *et al.*, 2009; Raquin and Moreira., 2009). Time in Ga.

## 6.7 Relationship with Lithophile Elements and the Question of a Non-chondritic Earth

One of the issues regarding the classical two-layer mantle with a lower mantle being undifferentiated is that OIB with non-radiogenic helium does not have a chondritic neodymium isotopic ratio and  $^{87}\text{Sr}/^{86}\text{Sr}$  close to the expected bulk silicate Earth. Although correlations between helium and Pb, Sr or Nd can be observed at the scale of a single oceanic island (*e.g.*, Kurz *et al.*, 1987; Kurz *et al.*, 1990; Kurz *et al.*, 2004; Jackson *et al.*, 2007), at a global scale the relationship between helium and the other isotopic systems shows a more complicated pattern (Fig. 6.12). However, what Figure 6.12 demonstrates is the probable existence of a common end-member<sup>33</sup> for all OIB having a low  $^4\text{He}/^3\text{He}$  (high  $^3\text{He}/^4\text{He}$ ) ratios and unradiogenic strontium, radiogenic neodymium, and moderately radiogenic lead, unlike bulk silicate Earth. Recent work on the  $^{142}\text{Nd}/^{144}\text{Nd}$  ratios of terrestrial samples has shown an early terrestrial fractionation producing positive excesses of  $^{142}\text{Nd}$  in ~3.8 Ga samples from Isua (Greenland) (Harper and Jacobsen, 1992;

33. Stan Hart observed this common end-member in the isotopic ratio space and named it FOZO for focal zone (Hart *et al.*, 1992).



Boyet *et al.*, 2003; Caro *et al.*, 2003; Boyet and Carlson, 2005) and negative  $^{142}\text{Nd}$  in similarly ancient samples from Nuvvuagituk, Quebec (O'Neil *et al.*, 2008; Roth *et al.*, 2013), compared to homogenous present day mantle-derived samples. This suggests an efficient mixing by convection of all primordial isotopic heterogeneities produced by melting during the Hadean.

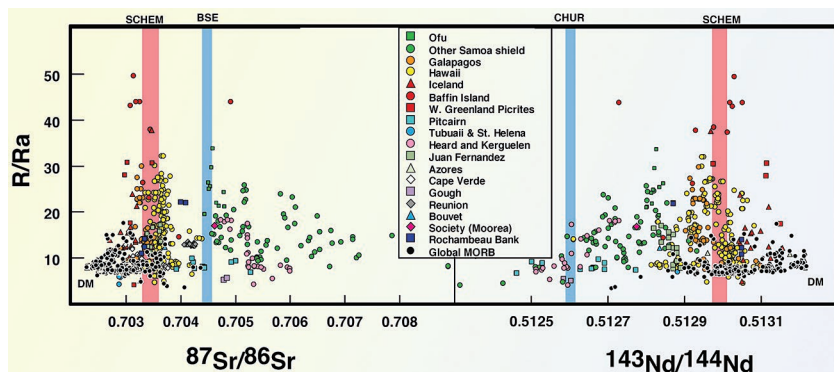


**Figure 6.12**  $R/Ra$  versus Sr and Nd isotopic ratios in MORB and OIB. The SCHEM composition (Super-Chondritic Earth Model) is taken from Caro and Bourdon (2010) and is supposed to represent the bulk Earth Nd isotopic composition if Earth is non-chondritic for the Sm/Nd system (modified from Jackson *et al.*, 2007).

Perhaps the most interesting aspect of the terrestrial  $^{142}\text{Nd}$  systematics is the observation that accessible Earth does not have a chondritic  $^{142}\text{Nd}/^{144}\text{Nd}$  ratio (Boyet and Carlson, 2005). Several explanations have been proposed to explain this unexpectedly, non-chondritic terrestrial Sm/Nd ratio inferred from isotopes. The first one is the presence of a complementary, deep mantle reservoir, enriched, with low  $^{142}\text{Nd}/^{144}\text{Nd}$  ratio, but never sampled. Indeed, the BMO model described above was developed to explain such a reservoir (Labrosse *et al.*, 2007), but for the case of Nd, the entrained crystals that carry the noble gas signature contain too little Nd to be evident against the higher Nd concentration of the ambient mantle. A second model is that crusts of accreting proto-planets were eroded by impacts during planetary accretion, leaving the Earth depleted in incompatible elements and non-chondritic ratios for some element pairs (Campbell and O'Neil, 2012).

Whatever the exact nature of the process that produces a non-chondritic  $^{142}\text{Nd}/^{144}\text{Nd}$  ratio, the inferred  $^{146}\text{Sm}/^{144}\text{Nd}$  fractionation can be applied to the  $^{147}\text{Sm}/^{144}\text{Nd}$  ratio and corresponding present-day  $^{143}\text{Nd}/^{144}\text{Nd}$  calculated for this non-chondritic Bulk Silicate Earth. The resulting  $^{143}\text{Nd}/^{144}\text{Nd} \sim 0.5130$ , is typical of the ratio measured in very low  $^4\text{He}/^3\text{He}$  ratio samples (high  $R/Ra$ ) (Caro and Bourdon, 2010; Jackson and Carlson, 2011). Therefore, the unradiogenic noble gas reservoir could be a primitive non-chondritic mantle. Ironically, the need for a strictly primitive mantle source, demanded by the classical two-layer model has meanwhile been explained by a variety of other models, as elaborated above.



## 6.8 Conclusions

---

Noble gases provide evidence for at least two reservoirs in the mantle. The first one is the source of MORB, and is strongly degassed as seen in Section 4 to explain the high  $^{129}\text{Xe}/^{130}\text{Xe}$  ratios and will be discussed further in Section 8. This early degassing cannot have been complete and a gas rich reservoir was retained, potentially isolated deep in the mantle. Many mantle plumes need to sample such a reservoir. However its location is still unknown. This gas-rich reservoir can be the bulk lower mantle (the canonical two-layer mantle model), the D'' layer or possibly the core itself. Further work on the noble gas partitioning between the different phases of the lower mantle, or between silicate and iron, are required to provide an answer to this question.



The issue of recycling volatile elements back into the mantle is a leitmotif of geochemistry. Carbon, water and perhaps even the halogens are often identified as volatile elements which are recycled into the mantle, with their current abundances possibly at steady state, *e.g.*, where recycled and degassing fluxes are equal (Jambon, 1994). Of course, the question arises, what about the noble gases? The one major difference is that they are chemically inert and do not form phases by themselves, in contrast to, for example, CO<sub>2</sub>, the key constituent of carbonate. The second obvious question that arises is, when was the onset of subduction on Earth? Finally, we must also ask if the recycling of atmospheric noble gases affects the composition of OIB, supposedly primitive for noble gases. In this Section I will discuss the arguments for a “subduction barrier” and for the recycling of atmospheric noble gases into the upper mantle and OIB sources.

It is critical to know what happens in the subduction zone itself and during slab dehydration in particular. It is understood that large fractions of subducted atmospheric gases are transported back to the surface via dehydration and arc volcanism, and one may wonder how much remains in the slab that continues into the mantle. This is currently an issue that I believe is not resolved.

Only a few groups have focused on the issue of recycling of atmospheric noble gases back to the mantle. One of the most active is the group of Manchester directed by *Chris Ballentine*. *Philippe Sarda* also often promoted recycling in the mantle (Sarda *et al.*, 1998; Sarda, 2004). One of the major difficulties in addressing this problem is the atmospheric contamination of oceanic basalt samples. We have discussed this problem in Section 5.

Another significant challenge, especially for krypton and xenon, is identifying the composition of the primordial krypton and xenon isotopes in the deep mantle. This question was also posed for argon as we have seen in Section 5. To reiterate, did Ar have a solar composition at the end of accretion, which subsequently became atmospheric in isotopic composition by subduction of atmospheric argon? This possibility, however, requires significant isotopic fractionation of the atmospheric noble gases (*e.g.*, Pepin, 1998). Or else did it have a primordial Phase-Q or/and implanted solar argon composition, in which case no subduction is required, and no isotopic fractionation is necessary to modify the atmospheric argon isotopic composition (*e.g.*, Kunz, 1999; Raquin and Moreira, 2008)?



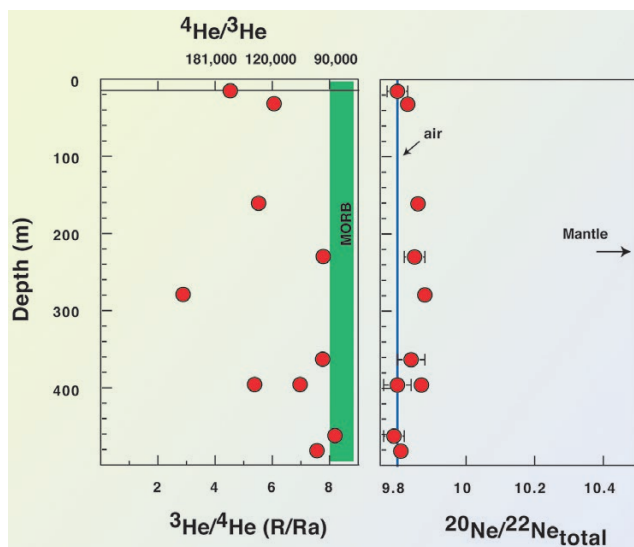


**Figure 7.1**

Depth profile in a section of 11 Ma oceanic crust showing its helium and the neon isotopic compositions (Moreira *et al.* 2003). This figure shows that the neon isotopic composition is atmospheric whereas the helium is radiogenic compared to the MORB ratio, which should therefore be true of the input to subduction zones

## 7.1 Subducting Material

Material that enters the subduction zones is clearly enriched in atmospheric noble gases. Aged oceanic crust has atmospheric isotopic ratios for all noble gases except helium, which shows radiogenic isotopic ratios compared to the mantle (*e.g.*, Fig. 7.1) (Staudacher and Allègre, 1988; Kumagai *et al.*, 2003; Moreira *et al.*, 2003). Serpentine is also enriched in atmospheric noble gases (Kendrick *et al.*, 2011) as too are oceanic sediments (Staudacher and Allègre, 1988) (Fig. 7.2). Such samples can be 100 times more concentrated in  $^{36}\text{Ar}$  than the present-day mantle. Assuming that all the subducting mantle lithosphere is serpentinised and has a  $^{36}\text{Ar}$  content of  $10^{-8} \text{ cm}^3 \text{ g}^{-1}$  (Fig. 7.2), the atmospheric  $^{36}\text{Ar}$  subducted through this carrier is a massive  $2 \times 10^{14} \text{ mol Ga}^{-1}$ , compared to the present day  $^{36}\text{Ar}$  budget in the upper mantle of  $9 \times 10^{12} \text{ moles}$  and the present-day degassing rate of  $\sim 2 \times 10^{12} \text{ mol Ga}^{-1}$ <sup>34</sup>. Obviously, there are some assumptions that are not correct in this simple calculation and we can suggest that either the oceanic lithosphere is not fully serpentinised or that an important argon loss from the slab occurs during

34. Calculated using a  $^3\text{He}$  flux out of the mantle of 1000 mole/year (Farley *et al.*, 1995) and a  $^3\text{He}/^{36}\text{Ar}$  ratio of 0.5 in the mantle (Moreira *et al.*, 1998).





subduction. This process of dehydration, known as the “subduction barrier”, was studied by *Staudacher* and *Allègre* for noble gases in general and xenon and argon in particular (Staudacher and Allègre, 1988) but the concept of this barrier can be extended to other volatiles. Staudacher *et al.* (1989) calculated that at least 98% of the noble gases are extracted from the slab and re-injected into atmosphere as a consequence of subduction zone processes. Dixon *et al.* (2002) proposed that more than 92% of water is extracted from the lithosphere during subduction dehydration.

Clearly a large fraction of the volatiles are removed from the slab and not introduced into the deep mantle. However, the fraction remaining after this subduction barrier, particularly for cold subduction, could be potentially high enough to modify the isotopic composition of the noble gases in the mantle as suggested by Porcelli and Wasserburg (1995), *Ballentine's* group (Holland and Ballentine, 2006; Holland *et al.*, 2009) and *Kendrick* (Kendrick *et al.* 2011).

We also proposed in 1998, that atmospheric argon is subducted into the mantle (Sarda *et al.*, 1998). This suggestion was deduced from the  $^{40}\text{Ar}/^{36}\text{Ar} - ^{206}\text{Pb}/^{204}\text{Pb}$  correlation we observed on MORB (Fig. 7.3) and that we interpreted as the mixture between normal depleted mantle, having a radiogenic  $^{40}\text{Ar}/^{36}\text{Ar}$  and unradiogenic lead ratios, and a component assumed to be ancient, altered, recycled oceanic crust, having atmospheric argon and radiogenic lead isotope ratios. This

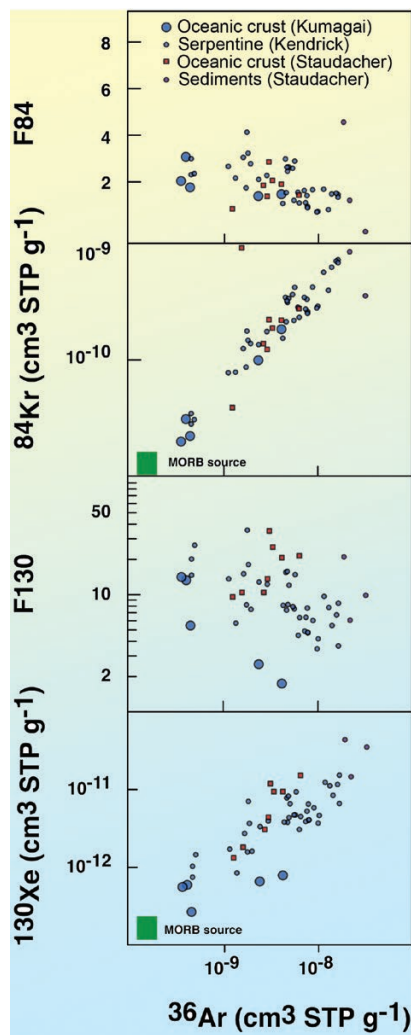


**Figure 7.2**

Kr and Xe concentrations and  $^{84}\text{Kr}/^{36}\text{Ar}$  and  $^{130}\text{Xe}/^{36}\text{Ar}$  ratios normalised to atmospheric ratios, noted as F84 and F130 respectively, reported against the  $^{36}\text{Ar}$  abundance measured in high temperature steps in serpentine samples (Kendrick *et al.*, 2011), bulk aged oceanic crust (Staudacher and Allègre 1988; Kumagai *et al.* 2003) and sediments (Staudacher and Allègre, 1988).



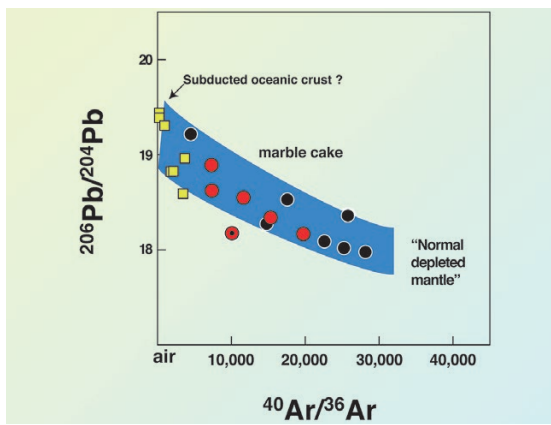


**Figure 7.3**

The “Paris group” vision of noble gas subduction into the mantle. Radiogenic lead is often associated with subducted oceanic crust, which also has low  $^{40}\text{Ar}/^{36}\text{Ar}$ . This figure can be interpreted in the light of the marble cake mantle model that suggests that the mantle contains two components: peridotite and pyroxenite, which represents recycled oceanic crust (e.g., Allègre and Turcotte, 1986).

version of the marble cake mantle<sup>35</sup> (Allègre and Turcotte, 1986) for noble gases was challenged by Burnard (1999) who judiciously proposed that this correlation is induced because high  $^{206}\text{Pb}/^{204}\text{Pb}$  ratios are often observed on bathymetric anomalies, and therefore argon should be more degassed and influenced by atmospheric contamination. However, our study raised the question of the possible deep subduction of noble gases into the mantle beyond the “subduction barrier”.

## 7.2 Chondritic Noble Gases in the Primitive Mantle?

Subduction of noble gases has been often invoked, but in my opinion the most noteworthy argument for this process is the discovery of isotopic compositions of non-radiogenic xenon ( $^{124}\text{Xe}$ ,  $^{126}\text{Xe}$ ,  $^{128}\text{Xe}$ ,  $^{130}\text{Xe}$ ) that are different in the atmosphere and in  $\text{CO}_2$  well gases (Cafee *et al.*, 1999; Holland and Ballentine, 2006).

These non-radiogenic isotopes, particularly  $^{124}\text{Xe}$  and  $^{126}\text{Xe}$  are very rare and difficult to determine precisely in oceanic basalts (Fig. 7.4). Indeed, their abundances are only  $\sim 700,000$  atoms  $\text{g}^{-1}$  even in an undegassed MORB sample, such as the popping rock  $2\pi\text{D43}$  (Staudacher *et al.*, 1989; Kunz *et al.*, 1998; Moreira *et al.*, 1998). However, most of the oceanic basalts are degassed and because it is the least soluble in melts of the noble gases, mantle-derived xenon, and particularly these two isotopes, is extremely rare and hardly detectable with mass spectrometry. Therefore, only a few studies had focused their attention on the  $^{124}\text{Xe}/^{130}\text{Xe}$  and  $^{126}\text{Xe}/^{130}\text{Xe}$  ratios in mantle-derived samples before the precise measurements of Cafee *et al.* (1999) and Holland and Ballentine (2006) on  $\text{CO}_2$  well gases. Figure 7.5 shows the  $^{124}\text{Xe}/^{130}\text{Xe}$  and  $^{126}\text{Xe}/^{130}\text{Xe}$  ratios measured on  $\text{CO}_2$  well gas samples, which contain other noble gas isotope ratios involving mantle-derived gases (Staudacher, 1987). Cafee *et al.* (1999) and Holland and

35. The marble cake mantle is an expression, coined by Claude Allègre, to describe a mantle comprised of peridotite and recycled material that has been stirred and thinned by the mantle convection to resemble the said pâtisserie.



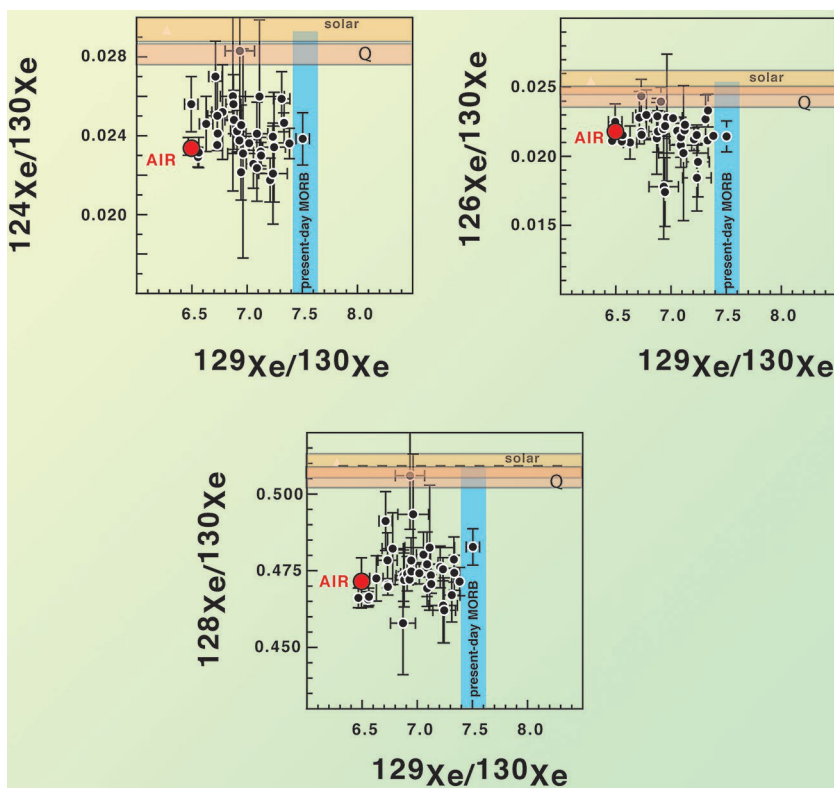


**Figure 7.4**

Non-radiogenic xenon isotopes in MORB reported against  $^{129}\text{Xe}/^{130}\text{Xe}$ . Data from (Kunz *et al.*, 1998). The present-day  $^{129}\text{Xe}/^{130}\text{Xe}$  ratio in the MORB source is close to 7.5, suggesting that non-radiogenic xenon isotopic ratios have neither chondritic nor solar compositions.

Ballentine (2006) observed slight differences between the non-radiogenic Xe isotope ratios between the well-gases and air, which can be interpreted as the result of the mixing between air and a component that could be either solar or chondritic. A bulk chondritic (AVCC) component <sup>36</sup> was proposed to be the second end-member based on measured excesses of krypton isotopic compositions in the CO<sub>2</sub> well gases (Holland *et al.*, 2009) (Fig. 7.5). An end-member having the composition of phase Q exclusively was not considered by Holland *et al.* (2009) because it did not lie on the CO<sub>2</sub> well gas mixing line. Because most of the non-radiogenic isotopic compositions of Xe and the  $^{86}\text{Kr}/^{84}\text{Kr}$  ratios of phase Q are

<sup>36</sup>. The estimate for the AVCC Kr composition can be found in Pepin (2003).



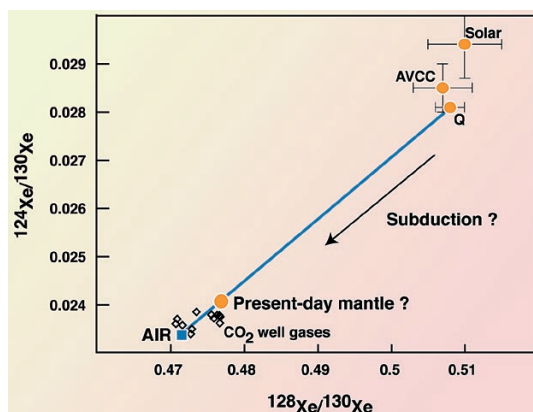


**Figure 7.5**

Non-radiogenic xenon isotopic ratios in CO<sub>2</sub> well gases. Data of CO<sub>2</sub> well gases are from Holland and Ballentine (2006). The Q composition is derived from Busemann *et al.* (2000) and the AVCC-Xe is from Pepin (2003). The correlation observed on CO<sub>2</sub>-well gases reflects the mixing between the atmosphere and a component having the Q-Xe (or AVCC) composition or being eventually solar. Holland and Ballentine proposed that the primitive mantle had the Q (or solar) composition and that subduction has modified this ratio down to the present-day composition, which is close to the atmospheric value.

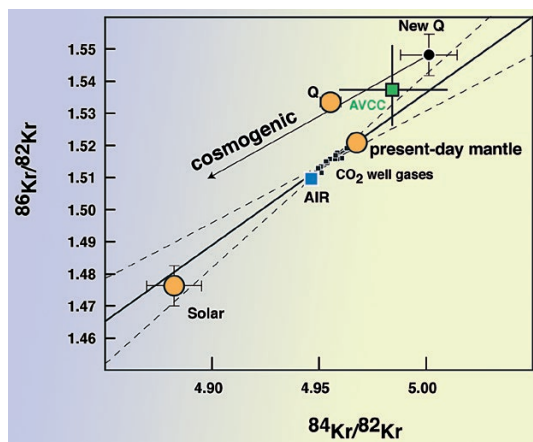


**Figure 7.6**

Kr isotopes in CO<sub>2</sub> well gases (Holland *et al.*, 2009) showing that the mantle is surprisingly non-atmospheric for Kr. The Q composition (orange dot) is from Busemann *et al.* (2000) but is probably over-estimated for <sup>82</sup>Kr due to cosmogenic reactions. The end member "New-Q" is the calculated Q composition assuming a mass fractionation in *m*<sub>1</sub>/*m*<sub>2</sub> from solar (see Section 2, Fig. 2.9). The uncertainty on this New-Q estimate stems from the uncertainty on the solar wind composition. The value for AVCC is derived from Pepin (2003). Whatever the value of phase Q is, it is clear the mantle contains chondritic Kr (expressed by AVCC or New Q), rather than solar.



close to the ratio produced by an isotopic fractionation of the solar wind ratios with a law of the type  $m_1/m_2$  (see Section 2), it can be proposed that the  $^{84}\text{Kr}/^{82}\text{Kr}$  and  $^{86}\text{Kr}/^{84}\text{Kr}$  ratios of phase Q presented on Figure 7.6 is underestimated and should be where is the “New-Q” end-member is plotted on the figure. A further constraint in determining an appropriate Q end-member may come from the fact that  $^{82}\text{Kr}$  is produced by spallation reactions in meteorites and therefore the estimate of  $^{82}\text{Kr}/^{84}\text{Kr}$  for the phase Q composition could have been previously slightly overestimated, although this requires further work to confirm this hypothesis.

From the  $\text{CO}_2$  well gas data, it appears that the mantle has a chondritic composition contribution, which is isotopically distinct from atmosphere. The interpretation, but not the only one, is that the mantle was initially chondritic for Kr and Xe, and that subduction of atmospheric Kr and Xe has modified this primordial composition to the present-day composition observed in  $\text{CO}_2$ -well gases (*e.g.*, Holland *et al.*, 2009).

Such a scenario can also be applied to the non-radio-genic neon and argon isotope ratios ( $^{20}\text{Ne}/^{22}\text{Ne}$  and  $^{38}\text{Ar}/^{36}\text{Ar}$ ). However, if the starting composition is Argon-Q, then mixing will not be detectable for argon because the phase Q has a  $^{38}\text{Ar}/^{36}\text{Ar}$  ratio close to the present-day atmospheric composition. If the primordial  $^{38}\text{Ar}/^{36}\text{Ar}$  and  $^{20}\text{Ne}/^{22}\text{Ne}$  ratios were solar, because it corresponds to a primordial solar atmosphere dissolved in the magma ocean, then the recycling of atmospheric neon and argon could to explain the present-day composition of the MORB and OIB sources (Fig. 7.7).

The interpretation of Holland and collaborators is not unique. We can also imagine that the primordial bulk Earth had isotopic ratios of Kr and Xe similar to the present-day atmospheric composition. In this case the isotopic compositions of the Earth's atmosphere must have been produced during

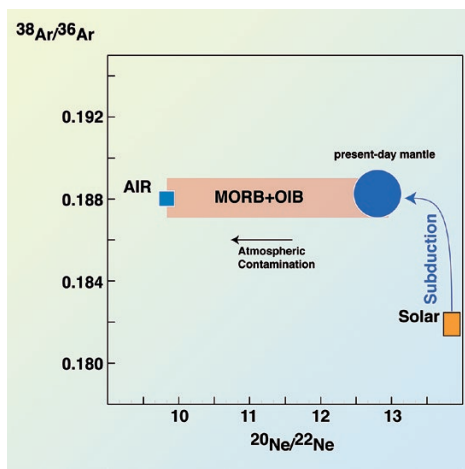


**Figure 7.7**

A model of subduction into the mantle of atmospheric Ne and Ar, assuming the primordial mantle isotopic compositions were solar at the end of the accretion. This model is required if the noble gases were incorporated into the mantle by the dissolution of gases from a dense primordial solar atmosphere into the magma ocean. Otherwise, if the primordial compositions were not solar, but chondritic (*e.g.*, neon-B), this subduction is not necessary to explain the present-day isotopic composition of Ne and Ar (figure modified from Moreira and Raquin, 2007).



planetary formation and not after differentiation. Then, the late veneer of chondritic material, which is invoked to account for the Earth's siderophile element abundances and isotope ratios, was incorporated into the Earth's upper mantle, producing the isotopic composition currently observed in the CO<sub>2</sub>-well gases by mixing with the existing 'air' component. An argument for an early isotopic fractionation of xenon is the observation that the present-day atmospheric Xe composition of Mars is identical to the Earth's atmosphere. It is difficult to understand how Mars and Earth, two planets with different masses, could have produced the same xenon isotopic signature by xenon loss to space during geological times. This discussion on the origin of the isotopic fractionation will be further detailed in the last Section.

### 7.3 Subduction-Degassing Model and the "Xenon Replenishment" of the Mantle

Numerous models have been used to test the idea of recycling atmospheric noble gases into the deep mantle. A relatively detailed model should take into account subduction, a flux from the lower mantle (or deeper reservoir) to the upper mantle, and a degassing term to the surface. As discussed in the Section 8, it might be also indispensable to consider that the atmospheric isotopic composition changes over geological time, even in its non-radiogenic isotope ratios, due to gas loss to space. Of course, the difficulty lies in determining the parameters of subduction and mantle degassing. Even if the current degassing term can be determined by measuring the flux of <sup>3</sup>He at ridges, the fact remains that the subduction term is very difficult to estimate. It is a free parameter that must be evaluated in order to estimate the feasibility of a possible recycling of atmospheric noble gases in the mantle. I will not repeat here the model of Porcelli and Wasserburg (1995) on the mantle evolution assuming the mantle is in steady state. This model, although an influential benchmark study, has some inconsistencies in the composition of xenon inferred for the deep mantle. Namely, if the mantle is in the steady state<sup>37</sup>, this means that to obtain the radiogenic <sup>129</sup>Xe/<sup>130</sup>Xe in the upper mantle, a flux of material having a high <sup>129</sup>Xe/<sup>130</sup>Xe is required to compensate for the subduction of atmospheric xenon, since the production of <sup>129</sup>Xe is now stopped. One implication of this model is that the deep mantle has a <sup>129</sup>Xe/<sup>130</sup>Xe ratio that needs to be much greater than recent measurements have documented for the source of OIB (Fig. 4.16).

Therefore, I discuss below a simple model of subduction-degassing to assess the isotopic ratio <sup>129</sup>Xe/<sup>130</sup>Xe in the mantle over geologic time. I'm assuming here that the primitive mantle had xenon-Q value. In addition, I assume that

37. In this steady state model, outgassing fluxes balanced inputs from subduction and a lower mantle reservoir to give modern upper mantle noble gas compositions.



subduction began only 2.5 Ga ago. This calculation is just to illustrate the feasibility and the difficulties inherent in such a model. A more detailed approach is necessary to address fully the issue of the noble gas subduction in the mantle.

The temporal evolution of a non-radiogenic and stable isotope is given

by:  $\frac{dN}{d\tau} = +\Phi(\tau) \cdot N - \delta(\tau) \cdot C_1$ , where  $\Phi$  is the degassing term ( $\text{year}^{-1}$ ) and  $\delta(\tau)$

is the mass of material subducted each year. The signs in the equation are such because the equation is written in terms of age.  $C_1$  is the concentration of a given isotope in the subducting material.  $N$  is the total number of moles of a given isotope in the upper mantle. The simplest case is when  $\Phi$  and  $\delta$  are independent of the time.  $\Phi$  can be determined using the present day  $^3\text{He}$  flux and the total  $^3\text{He}$  quantity in the upper mantle. The degassing constant  $\Phi$  is  $2.2 \times 10^{-10} \text{ a}^{-1}$  using  $1,000 \text{ mol a}^{-1}$  for the  $^3\text{He}$  flux at ridges (Farley *et al.*, 1995) and a  $^3\text{He}$  concentration of  $4.5 \times 10^{-15} \text{ mol g}^{-1}$  in the upper mantle (Moreira *et al.*, 1998). The parameter  $\Phi$  is independent of the gas chosen for the calculation since it reflects a melting flux (and it is assumed that all noble gases reasonably approximate to perfectly incompatible and completely degassing species).

I illustrate this model using xenon isotopes. The present-day isotopic compositions are taken to be the highest isotopic ratios measured in  $\text{CO}_2$  well gases (Holland and Ballentine, 2006). Figure 7.8 shows the results for the  $^{129}\text{Xe}/^{130}\text{Xe}$  and  $^{124}\text{Xe}/^{130}\text{Xe}$  ratios using a constant  $^{130}\text{Xe}$  subduction flux of  $2.2 \text{ mol a}^{-1}$ . This flux was adjusted so that the  $^{124}\text{Xe}/^{130}\text{Xe}$  was Q-like in the mantle at 2.5 Ga. The calculation with this  $^{130}\text{Xe}$  flux shows that at 2.5 Ga, the mantle had a Q- $^{124}\text{Xe}/^{130}\text{Xe}$  ratio by hypothesis, but a  $^{129}\text{Xe}/^{130}\text{Xe}$  ratio of  $\sim 25$ , much more radiogenic than the present-day value ( $\sim 8$ ). A lower  $^{130}\text{Xe}$  subduction flux cannot produce the necessary changes in the isotopic composition, the flux being too small. In contrast, higher fluxes lead to a mantle having a Q composition only a few million years ago, which suggests a massive recent recycling of the atmospheric noble gases.

A total  $^{130}\text{Xe}$  subduction flux of  $2.2 \text{ mol a}^{-1}$  calculated for the model shown in Figure 7.8 has to be considered in the light of the material that currently subducts into the mantle. The flux of subducted sediment is  $\sim 0.1 \times 10^{16} \text{ g a}^{-1}$  (Plank and Langmuir, 1998). The flux of oceanic crust is  $5 \times 10^{16} \text{ g a}^{-1}$  and the lithosphere flux is  $\sim 50 \times 10^{16} \text{ g a}^{-1}$ . Assuming only one of these materials carries the atmospheric xenon, in order to provide the flux of  $2.2 \text{ mol a}^{-1}$ , they need to have the following concentrations:  $5 \times 10^{-11}$ ,  $1 \times 10^{-12}$  and  $1 \times 10^{-13} \text{ cm}^3 \text{ g}^{-1}$  for sediment, crust, lithospheric mantle, respectively. These numbers are not unrealistic although, they contravene the hypothesis of a subduction barrier. Indeed, Staudacher and Allègre (1988) measured  $^{130}\text{Xe}$  concentrations to be on the order of a few  $10^{-11} \text{ cm}^3 \text{ STP g}^{-1}$  in sediments and in altered oceanic crust. However, it is possible that the mantle wedge itself is the vector for transfer of noble gases into the wider mantle. Namely, volatiles extracted from the slab into mantle wedge may not be returned to the atmosphere but instead carried into the mantle beyond by convective mixing. At this point, the discussion is highly speculative, and requires further work to be considered as a viable scenario.





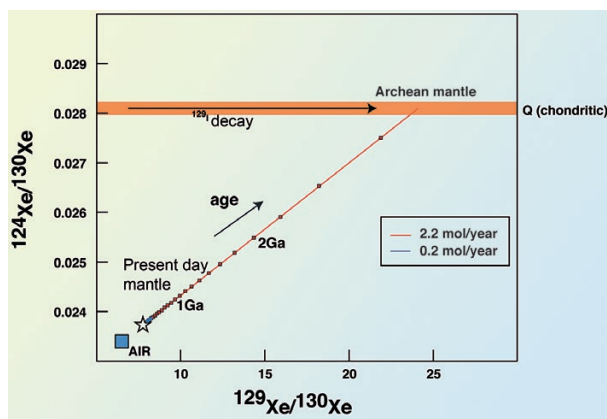


**Figure 7.8**

Temporal evolution of the xenon isotopic composition of the mantle using a model assuming that xenon with an atmospheric isotopic composition is subducted into the upper mantle, which is also degassed at mid oceanic ridges. Such a model is required if the primordial isotopic composition was chondritic for xenon. The model is modified from Moreira and Raquin (2007).

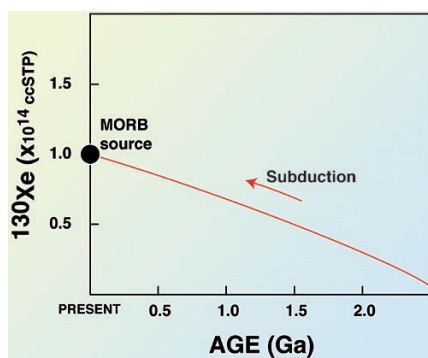


**Figure 7.9**

Temporal evolution of the amount of  $^{130}\text{Xe}$  into the upper mantle using the model of subduction-degassing presented in Figure 7.8 that explains the present-day xenon isotopic composition of the mantle. The amount of xenon increases with time in the mantle, which is not expected since the mantle is supposed to degas. This can be called the “replenishment” of the mantle. However, in this model, the mantle was strongly degassed during accretion. The introduction of atmospheric xenon started with subduction.

Nevertheless, if we accept that the subduction of atmospheric noble gases is responsible for the close-to-air xenon isotopic ratios in the mantle, then the upper mantle had a radiogenic  $^{129}\text{Xe}/^{130}\text{Xe}$  ratio ( $\sim 25$ ) and contained 10 times less  $^{130}\text{Xe}$  a few billion years ago (Fig. 7.10), before subduction started. The required very radiogenic  $^{129}\text{Xe}/^{130}\text{Xe}$  ratio in the mantle, after a massive degassing and before the subduction of atmospheric xenon, was argued by Staudacher and Allègre (1988) as consistent with the subduction barrier and against subduction of atmospheric noble gases. However, from a theoretical point of view, such a radiogenic ratio is possible. Let us consider that a single stage of fast degassing occurred early in



the Earth history for a period of 50 Ma, during the ocean magma stage, when  $^{129}\text{I}$  was still alive. Two equations can be derived (one for the mantle and one for the atmosphere) to model the evolution of the xenon isotopic ratio:

$$R_{\text{mantle}}(t) = R_0 + \frac{\lambda \mu_0}{\lambda - \Phi} (1 - e^{-(\lambda - \Phi)t})$$

$$R_a(t) = R_0 + \frac{m_0 (\lambda (e^{-\Phi t} - 1) + \Phi (1 - e^{-\lambda t}))}{(\Phi - \lambda)(1 - e^{-\lambda t})}$$

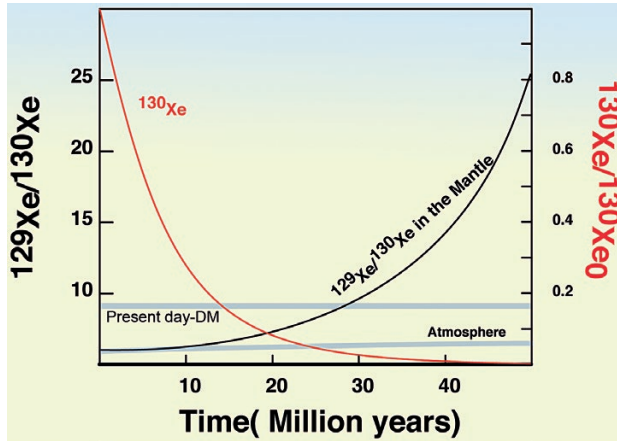


**Figure 7.10**

A model of mantle and atmosphere evolution in the early degassing stage that can produce a high  $^{129}\text{Xe}/^{130}\text{Xe}$  of ~25 in the early mantle required if xenon is subducted into the mantle (Fig. 7.8). Here the  $^{130}\text{Xe}$  concentration in the mantle is assumed to decrease exponentially because of the degassing to the atmosphere (red curve). For the calculation, I use  $^{130}\text{Xe} = ^{130}\text{Xe}(0) \cdot \exp(-\Phi t)$  where  $\Phi$  is the degassing term ( $\text{year}^{-1}$ ). Then, in the mantle,  $^{129}\text{Xe}/^{130}\text{Xe} = R(t) = R(0) + \mu_0 \lambda / (\lambda - \Phi) \cdot \exp[-(\lambda - \Phi)t]$  where  $\lambda$  is the decay constant of  $^{129}\text{I}$  and  $\mu_0$  is the initial  $^{129}\text{I}/^{130}\text{Xe}$  ratio. A similar equation can be given for the evolution of the isotopic ratio in the atmosphere. The parameters of the model ( $\mu_0$  and  $\Phi$ ) are adjusted in order to produce a  $^{129}\text{Xe}/^{130}\text{Xe}$  of 25 after the first 50 million years of Earth history starting from a solar  $R(0)$  of 6 in the mantle, and of 6.5 in the atmosphere. To explain the high  $^{129}\text{Xe}/^{130}\text{Xe}$  in the primordial mantle, the degassing has to be important (>99% in 37 Ma).

It is possible to produce both a mantle  $^{129}\text{Xe}/^{130}\text{Xe}$  ratio of 25 and an atmospheric ratio of 6.5 in 50 Ma with  $\Phi = 1.24 \times 10^{-7} \text{ a}^{-1}$  and  $\mu_0 = (^{129}\text{I}/^{130}\text{Xe})_0 = 0.63$ . This suggests that the degassing of the mantle was fast and efficient (99% of primordial xenon is degassed in 37 Ma), and that the  $^{130}\text{Xe}$  was depleted in the mantle at the end of this degassing stage ( $\sim 5 \times 10^{-14} \text{ cm}^3 \text{ g}^{-1}$ ) (Fig. 7.10).



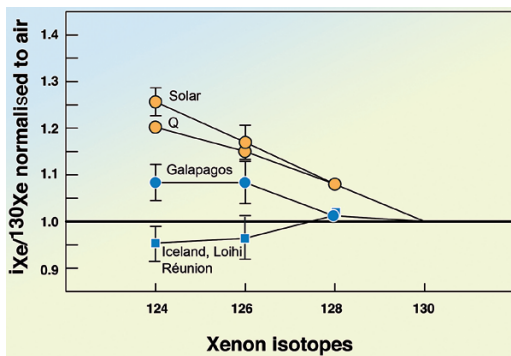


**Figure 7.11** Non-radiogenic xenon isotopes of Loihi, Iceland, Réunion and Galapagos basalts corrected for atmospheric contamination using neon. Modified from (Trieloff *et al.*, 2002), data from Galapagos from the author.

It is also important to observe that, if the Earth's primordial composition was chondritic for Kr and Xe (Holland and Ballentine, 2006; Holland *et al.*, 2009), the subduction of atmospheric noble gases also affected the OIB source since it has been shown that the non-radiogenic isotopic xenon compositions of Iceland, Galapagos, Réunion, Hawaii mantle sources are close to atmospheric, distinct from the Q or solar Xe compositions (Fig. 7.11) (Trieloff *et al.*, 2002).

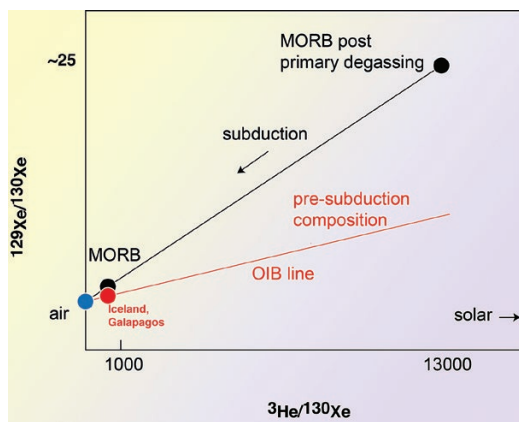


**Figure 7.12** Mixing diagram showing the difference between the  $^{129}\text{Xe}/^{130}\text{Xe}$  ratio of MORB and OIB before the subduction of atmospheric Xe, if primordial xenon composition was chondritic, requiring a very radiogenic  $^{129}\text{Xe}/^{130}\text{Xe}$  in the Hadean mantle. Adapted from Mukhopadhyay (2012).

It was emphasised by Mukhopadhyay (2012) that the OIB xenon is not a mixture of MORB and atmosphere xenon (Fig. 7.12). However, recycling of atmospheric xenon into the plume source would require that it also had a high initial  $^{129}\text{Xe}/^{130}\text{Xe}$  ratio, suggesting a possible early degassing of this reservoir; a hypothesis that needs to be discussed in the light of all noble gases

Moreover, in such a scenario, the xenon isotopic fractionation that occurred in the Earth's atmosphere either early or during geological times has still an unknown origin, which will be discussed in the next section.



## 7.4 Conclusions

---

I have tried in this section to develop the arguments suggesting that subduction of atmospheric rare gases, in particular the heavy rare gases such as krypton and xenon, is possible under certain conditions. The subduction of atmospheric xenon in the MORB source implies a very radiogenic  $^{129}\text{Xe}/^{130}\text{Xe}$  ( $>25$ ) 4.4 Ga ago. The high  $^{129}\text{Xe}/^{130}\text{Xe}$  ratios required by this assumption were the reason the concept of subduction barrier was developed by Staudacher and Allègre (1988), who believed such values implausible. However, radiogenic  $^{129}\text{Xe}/^{130}\text{Xe}$  can be obtained under certain conditions, namely a massive primordial degassing of xenon, which increases significantly the  $^{129}\text{I}/^{130}\text{Xe}$  ratio. A calculation of atmospheric xenon subduction shows that it takes a fair amount of atmospheric xenon to pollute the mantle. This would suggest that the volatile subduction barrier is not very effective, in contrast to what has been previously thought. The values of the Kr and Xe isotopic ratios of  $\text{CO}_2$  well gases give evidence supporting atmospheric recycling into the deep mantle. To conclude this section, if the notion of subduction of atmospheric noble gases in the mantle is reasonable, additional work must be performed to confirm or refute this model. In particular, it is important to understand the behaviour of the noble gases during subduction.



In the previous sections, I endeavoured to describe the current state of understanding of the geochemistry of noble gases in the mantle compared to the elemental and isotopic compositions of the Sun and chondritic meteorites. The modest knowledge of the Martian interior and its atmosphere, thanks to analyses of SNC meteorites, also offers an essential constraint on the origin of volatiles in terrestrial planets. In the following, I will provide general ideas about the origin of noble gases on Earth, and the evolution of the mantle/atmosphere system. Understanding of origin of volatiles in terrestrial planet atmospheres has been explored extensively in the publications of *R. Pepin* (e.g., Pepin and Porcelli, 2006; Pepin, 2003; Pepin, 1997; Pepin, 1991) and *J. Pollack* (Pollack and Black, 1979; 1982). Moreover, two excellent reviews have been recently published on this topic, and I recommend these two articles for a more detailed discussion of the origin of volatiles on Earth and the terrestrial planets (Marty, 2012; Halliday, 2013).

### 8.1 Summary of the Previous Sections and General Remarks

---

Noble gases provide clear evidence for at least two reservoirs in the Earth's mantle, with different elemental and isotopic compositions. One is sampled by MORB. Mantle plumes producing oceanic islands sample the second, whose exact location is still subject to debate. The first reservoir has more radiogenic, fissiogenic and nucleogenic isotopic ratios of all the noble gases relative to the oceanic islands reservoir. In contrast, many non-radiogenic isotopic ratios appear to be identical in the two reservoirs.

The isotopic ratios of helium and neon in OIB show the existence of an ancient (possibly primordial) reservoir in the deep Earth, either in the lower mantle or possibly in the core. This reservoir has been isolated since at least 4.4 Ga as suggested by the non-nucleogenic  $^{21}\text{Ne}/^{22}\text{Ne}$  ratios in Iceland and Galapagos lavas (Kurz *et al.*, 2009). The radiogenic isotopic ratios of argon and xenon measured in MORB suggest that their source is more degassed than the OIB sources. The core as the source of primordial noble gases cannot be excluded, but for the moment, has to be considered as speculative because of unknown silicate/metal partitioning at high pressure and uncertain mechanisms of incorporation into the plume source. Xenon isotope systematics (particularly the  $^{129}\text{Xe}$ ) suggests that the primordial material in the plume source has been isolated since 4.4 Ga, in agreement with Kurz's argument using the  $^{21}\text{Ne}/^{22}\text{Ne}$  ratio. The exact location of the primordial reservoir is still a major question of mantle geodynamics. Anyhow, the source of OIB samples is a reservoir containing sufficient primordial rare gases to provide primitive isotopic ratios without being affected by radiogenic rare gases present in recycled material rich in U and K, as suggested by other non-volatile isotopic systems (e.g., Sr, Nd, Pb).



Additionally, the results of measurements of rare gases in meteorites show that heavy rare gases in chondrites are carried by a carbonaceous phase, called phase Q, which can be degassed only at high temperatures. It is therefore possible that the early Earth had this composition for Kr and Xe, as suggested recently by Holland *et al.* (2009). This primordial Q composition in the mantle would then have been modified by subduction of atmospheric noble gases, in the *whole* mantle (both OIB and MORB sources). However, this then raises the question of the origin of the isotopic fractionation in atmospheric xenon (on Earth and Mars) and krypton, as well as the chronology of this isotopic fractionation.

A composition similar to the implanted solar wind can explain the isotopic composition of neon in the Earth's mantle. This component, named "B" historically by Black (1971), has a  $^{20}\text{Ne}/^{22}\text{Ne}$  ratio around 12.5-12.7. In Section 2, I proposed a method to revise Black's proposed value of 12.52 to a new value of 12.72, on the basis of measurements made on samples of lunar soils analysed after the Apollo mission recoveries. This "B" component is present in all classes of meteorites and is more abundant relative to other components in reduced chondrites, formed close to the Sun, and therefore it is plausible that the primitive mantle has this neon B composition. However, a solar neon isotopic ratio in the primitive mantle (as opposed to the implanted solar value of neon B) cannot be excluded on the basis of the neon measurements in oceanic basalts only since atmospheric contamination is ubiquitous in those samples and/or because subduction of atmospheric neon has decreased the solar ratio to its present value. The  $^{38}\text{Ar}/^{36}\text{Ar}$  ratio in the mantle is not solar but again, subduction of atmospheric argon into the mantle could have changed this from a primordial solar composition. Nevertheless, the  $^{38}\text{Ar}/^{36}\text{Ar}$  ratio in the mantle and in the atmosphere is very close to that measured in phase Q or is also close to the composition of argon from solar wind implanted in dust, as calculated using a model of implantation-sputtering (Section 2). Therefore, for argon, the chondritic composition appears to be the most credible starting isotopic composition for the Earth. This is important since a primordial chondritic composition does not require an isotopic fractionation of the atmospheric argon as it would if the starting composition was solar (*e.g.*, Pepin, 1991; Pepin, 1998), which would have been then followed by subduction of atmospheric argon into the whole mantle.

Finally, an important observation is that the Martian atmosphere has a xenon isotopic composition very close to that of the Earth (Fig. 8.1). Additionally, the krypton isotopic composition of Mars's atmosphere shows an isotopic composition very similar to the solar one (Fig. 8.2) (compositions from Eugster *et al.*, 2002), and different from the Earth's atmosphere. These observations are important in order to understand when the isotopic fractionation of xenon occurred in the atmosphere and what is the possible physical mechanism behind the xenon isotopic fractionation without fractionating the Kr and Ar. Indeed, Mars and Earth have different sizes and ages of formation, and were not accreted at the same location in the disk, and probably not by the same process, if Mars is a planetary embryo (Dauphas and Pourmand, 2011). The xenon isotopic fractionation from the atmospheres of Mars and the Earth has therefore to be either mass-or-planet



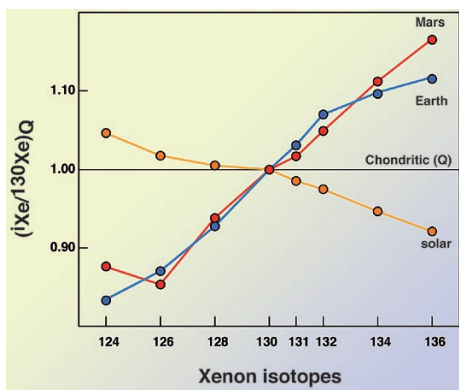


**Figure 8.1**

Xenon isotopic composition of Mars's atmosphere compared to Earth's atmosphere, solar and chondritic compositions. The isotopic ratios are normalised to  $^{130}\text{Xe}$  and to the Q composition. The  $^{129}\text{Xe}$  is excluded in this figure.

independent, or have occurred before or during the planet formations, and also without affecting the other noble gases

Another statement that can be usefully made in this preamble is that it seems problematic for the Earth's mantle noble gas compositions to reflect the dissolution of solar noble gases in a magma ocean. Indeed, Figure 8.3 shows that if a Jupiter-type solar atmosphere was dissolved in a magma ocean, the pattern of rare gases would show a depletion in heavy rare gases because they are less soluble in the magmas than helium and neon (Fig. 8.3). This is not the case in the Earth's mantle, that rather shows enrichment in heavy noble gases similar

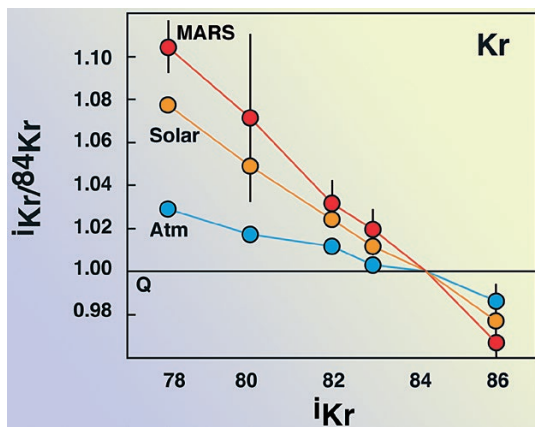


**Figure 8.2**

Krypton isotope abundances in the Martian atmosphere compared to the terrestrial atmosphere and the Sun, normalised to phase Q Kr composition (modified from Busemann *et al.*, 2000). Martian atmospheric krypton is very close to the solar composition. The Earth's atmosphere is either fractionated from solar or represents a mixture between chondritic (Q – corrected as discussed in Fig. 7.6 caption), possibly derived from the degassing of the mantle, and solar. Mars' atmospheric composition is taken from (Eugster *et al.*, 2002).  $i\text{Kr}$  refers to the isotopes (78, 80...).





to chondrites (Moreira *et al.*, 1998; Ballentine *et al.*, 2005). Therefore, the scenario of dissolution of solar noble gases from a dense solar atmosphere seems less probable than considering they were present in parent bodies on the Earth either in phase Q for Kr and Xe, or were incorporated by another mechanism such as solar wind implantation for He, Ne and possibly Ar.

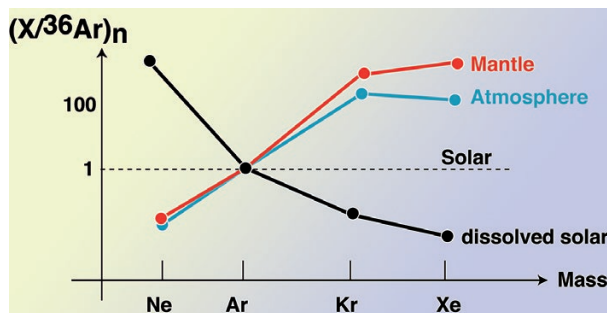


**Figure 8.3**

Cartoon showing the noble gas elemental pattern in a magma ocean in equilibrium with a dense atmosphere having a solar composition, compared to the mantle and the atmosphere patterns. The noble gas solubilities considered here are solubilities in tholeiite (Jambon *et al.*, 1986), which indicate that heavy noble gases are less soluble than the light ones. This implies that dissolution of a dense primordial solar atmosphere would lead to a depletion in the magma of heavy noble gases.

The origin of noble gases on terrestrial planets can obviously be related to the origin of other volatiles such as water, N or C, although this is not obligatory. For example, solar wind implantation is a physical process able to enrich the noble gases without significantly changing the budget of the most abundant volatiles (see Section 2). However, if volatile-rich material such as comets or carbonaceous chondrites can explain the abundances of major volatiles, there are unknowns about their contribution for noble gases, in terms of elemental and isotopic compositions. Figure 8.4 shows the volume of material (cometary material or chondrite CI) that is necessary to add to the Earth to explain its water budget (mantle + oceans). These volumes are relatively small compared to the size of Earth and models of planetary formation such as the “Nice” model can easily explain how volatile-rich material is delivered at the end of the accretion (Walsh *et al.*, 2011).

However, noble gases have never been measured on cometary ice – only on refractory grains from the 81P/Wild2 comet (Marty *et al.*, 2008). Marty and co-workers suggested that neon in those grains have an isotopic composition close to the one of the phase Q, different from the solar composition and different from the mantle neon. However the grains collected on Wild2 were refractory grains, and may not represent the bulk comet. The simplest assumption that can be made is that noble gases trapped in cometary ice have a solar isotopic



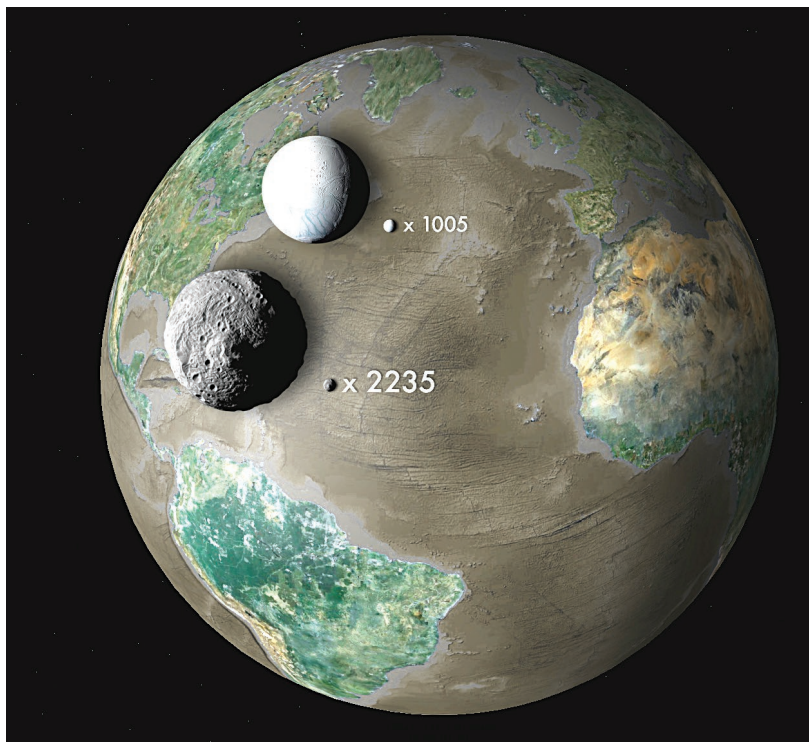


Photo credit: Antoine Pitrou (IGP).

**Figure 8.4**

Mass of the water on Earth represented as spheres depending on different concentrations. The white object would be cometary material (100%  $\text{H}_2\text{O}$ ) whereas the rocky object represents the equivalent sphere when using a chondritic concentration (~15%  $\text{H}_2\text{O}$ ). Next to the spheres are given the number of objects with a radius of 100 km that would be necessary for the Earth's water budget. Note that an enstatite chondrite concentration (0.05%  $\text{H}_2\text{O}$ ) leads to a sphere with the same radius as Earth. A small fraction of cometary or carbonaceous chondritic material among the parent bodies will provide enough water on Earth. The question that arises is the time constraint of this process.

composition because ice reflects the condensation of nebular gas. However, this has to be considered as speculative until new measurements are performed on real material. Laboratory experiments of noble gas trapping on ice at low temperature have demonstrated an interesting feature. The elemental pattern of ice formed from a gas having a solar composition shows a remarkable coincidence with the elemental pattern of the Earth's atmosphere (Fig. 8.5). Experiments on noble gas trapping on ice at low temperature suggest that atmospheric noble gases may derive both from comets and from degassing of the Earth's interior (the Dauphas dual origin of the atmosphere) (Owen *et al.*, 1992; Owen and Bar-Nun, 1996; Bar-Nun and Owen, 1998; Dauphas *et al.*, 2000; Dauphas, 2003). Such a



model could explain the Kr isotopic compositions of the terrestrial and Martian atmospheres since they both show a solar contribution in their isotopic signatures (Fig. 8.2). Earth's atmospheric krypton could then be the mixture of these solar-gas rich comets and degassing of Q-Kr from the mantle, that could have had this Q composition at the end of accretion (Holland *et al.*, 2009) (Section 7). This scenario is however not possible in such a simple way for the xenon, as we will discuss below.

The issues I am going to address in this last Section are:

- What is the exact neon isotopic ratio in the mantle: solar or neon B?
- How and when did mantle degassing occur ?
- Was the atmosphere always a closed system for noble gases? Were there any late additions or gas losses to space?
- What is the general picture of the origin and evolution of noble gases on Earth?

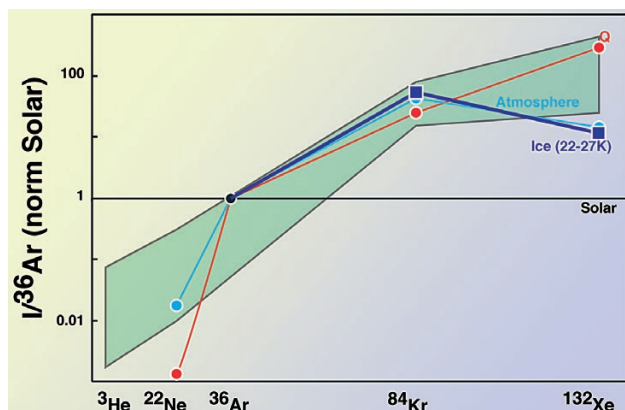


**Figure 8.5**

Elemental noble gas pattern of the phase Q, the atmosphere and solar noble gases trapped on ice at 22-27 °K (Notesco *et al.* 2003). The green field represents bulk carbonaceous chondrites from Mazor *et al* (1970).

## 8.2 Neon B or Solar Neon in the Mantle?

An important constraint on the mechanism of noble gas incorporation in the Earth's interior is the Ne isotopic composition. Neon is depleted in the phase Q, the main carrier of heavy noble gases in chondrites, relative to the heavy noble gases. Therefore, it seems unlikely that the neon is derived from phase Q in Earth. Moreover, the  $^{20}\text{Ne}/^{22}\text{Ne}$  isotopic ratio in the mantle suggests that neon is derived from a solar-like component. Two possibilities can explain the high  $^{20}\text{Ne}/^{22}\text{Ne}$



ratios observed in the mantle. The first one is that the primordial mantle had a ratio that is exactly solar ( $\sim 14$ ), and the second scenario is that it is close to the so-called neon B present in chondrites and which reflects solar wind implantation (see Section 2). These isotopic ratios reflect different mechanisms of neon incorporation into the primitive mantle. Solar neon can be inherited from the dissolution of a dense primordial atmosphere with solar elemental and isotopic compositions. However, as discussed earlier, the noble gas elemental pattern is not fully coherent with such a hypothesis. Neon B reflects solar irradiation of dust before accretion of parental bodies. The Earth is accreted closer to the Sun than most chondrites, with the exception of enstatite chondrites. It is therefore credible that Earth's parent bodies contain more implanted solar wind than do carbonaceous or ordinary chondrites like enstatite chondrites (see section 2), suggesting that Earth could have been formed from bodies that acquired their neon by solar wind implantation, assuming that sputtering was associated with implantation as suggested by Raquin and Moreira (2009).

Determining the exact neon isotopic composition of the mantle is therefore fundamental to constrain the mechanism of noble gas incorporation in the primordial Earth. In Section 5, I described the neon isotopic compositions in oceanic basalts and I have shown that most of the samples with precise measurements have  $^{20}\text{Ne}/^{22}\text{Ne}$  ratios lower than 12.8 in the OIB source and 12.6 in the MORB source. However, atmospheric contamination at the surface could have systematically lowered the mantle-derived ratio from the solar ratio ( $\sim 14$ ; Grimberg *et al.*, 2006; Grimberg *et al.*, 2008; Heber *et al.*, 2009; Pepin *et al.*, 2012) to the present-day  $^{20}\text{Ne}/^{22}\text{Ne}$  maximum values of the samples of  $\sim 12.7$ . However, Ballentine *et al.* (2005) have also concluded that the shallow mantle  $^{20}\text{Ne}/^{22}\text{Ne}$  ratio is close to 12.5, based on the measurements of  $\text{CO}_2$  well gases, using a method allowing correction for air contamination. Therefore, the systematic contamination of oceanic basalts is not a viable explanation.

Such a ratio of  $\sim 12.7$ , lower than the solar value, could also represent subduction of atmospheric neon as discussed in Section 7. However, the similarity between the determination of the present-day neon isotopic ratio of the mantle and the neon B is a strong argument suggesting that subduction of atmospheric neon is negligible and that step-crushing or step-heating techniques have successfully removed the atmospheric contamination. This scenario excludes an exactly solar composition in the primordial mantle.

Nevertheless, it must be noted that Yokochi and Marty (2004) and Ballentine *et al.* (2005), and more recently Mukhopadhyay (2012), have proposed that plume source has a solar isotopic ratio, and not neon B. Indeed, Yokochi and Marty (2004) have measured a  $^{20}\text{Ne}/^{22}\text{Ne}$  of  $13.04 \pm 0.40$  ( $2\sigma$ ) in one crushing step on a magnetite sample from plume-related Devonian rocks from Kola (Russia). Similarly, Mukhopadhyay (2012) has measured a ratio of  $12.88 \pm 0.06$  in one crushing-step on a glass sample from Iceland. This value is close to the



neon B ratio of 12.72 proposed in Section 2, although outside the reported errors. Further neon analyses are required in oceanic basalts to conclude about the “true”  $^{20}\text{Ne}/^{22}\text{Ne}$  ratio in the mantle.

Unless future results show clearer evidence for a solar neon ratio in mantle-derived samples, I consider that the most probable origin for helium and neon in the Earth’s mantle is the solar wind irradiation on dust that will accrete to form the Earth’s building blocks, in keeping with inferences from well gas measurements (Ballentine *et al.*, 2005). The origin of Ar-Kr-Xe is more complex, and certainly involves a significant contribution from the phase Q, enriched in those noble gases relatively to He and Ne.

### 8.3 Mantle Degassing

The large amount of  $^{40}\text{Ar}$  present in the atmosphere is an argument suggesting that mantle is degassed, although not completely, as discussed in Section 4.  $^3\text{He}$  is still degassing at a rate of 500 to 1000 mol  $\text{a}^{-1}$ , which is an unambiguous proof of degassing (Craig and Lupton, 1981; Farley *et al.*, 1995; Bianchi *et al.*, 2010). It is therefore clear from noble gas systematics that degassing of the mantle has formed a large part of the atmosphere, if not all of it.

The chronology of this degassing can be discussed using models of mantle degassing applied to the radiogenic and the non-radiogenic noble gases. Moreover, the completeness of mantle degassing can be examined in the light of the MORB-OIB isotopic dichotomy shown in previous sections. Indeed, the difference between the MORB and OIB sources is observed not only for the helium isotopic ratio but also for all noble gas radiogenic isotopic ratios as discussed in Sections 3, 4 and 5. These different isotopic ratios reflect distinct parent/daughter ratios (*e.g.*,  $\text{K}/^{36}\text{Ar}$ ,  $\text{U}/^3\text{He}$  etc) and time of fractionation. Noble gas degassing induces parent/daughter fractionation. Since Shillibeer and Russell (1955), many publications have discussed coherent models of mantle/atmosphere evolution able to explain the isotopic ratios of the mantle reservoirs (*e.g.*, Ozima, 1973; Schwartzman, 1973; Ozima, 1975; Tolstikhin, 1975; Hamano and Ozima, 1978; Staudacher and Allègre, 1982; Allègre *et al.*, 1983b; Sarda *et al.*, 1985; Allègre *et al.*, 1986; Kunz *et al.*, 1998; Tolstikhin and Marty, 1998).

They all use the simple concept expressed by the following differential equations describing the evolution of a radiogenic noble gas isotope in the mantle and in the atmosphere ( $F$  and  $F_{\text{atm}}$ ):

$$\begin{aligned}\frac{dF}{dt} &= -\text{deg} + \text{prod} \\ \frac{dF_{\text{atm}}}{dt} &= +\text{deg}\end{aligned}$$



Here *deg* is a degassing term that depends of the time and *prod* is the radiogenic production, which itself depends on the time evolution of the radioactive parent concentration induced by the continental crust extraction, slab subduction, etc.

Similar equations can be written for non-radiogenic isotopes (e.g.,  $^{130}\text{Xe}$ ,  $^3\text{He}$  etc.), without the production term, of course. Complex modelling can obviously be performed, including gas loss to space with or without mass fractionation as discussed later in this section, subduction of atmospheric noble gases into the mantle (as seen in Section 7), a late veneer of chondritic or cometary material (Marty, 2012), continental crust extraction, hidden reservoirs, etc.

Figure 8.6 shows a cartoon describing different fluxes that are needed to develop a comprehensive model of the mantle/atmosphere evolution. The expert of such complex modelling is *Igor Tolstikhin* (see Section 3 and Azbel and Tolstikhin, 1993; Tolstikhin and Marty, 1998), and it is always a great fun to attend to his oral presentations! I recommend this.

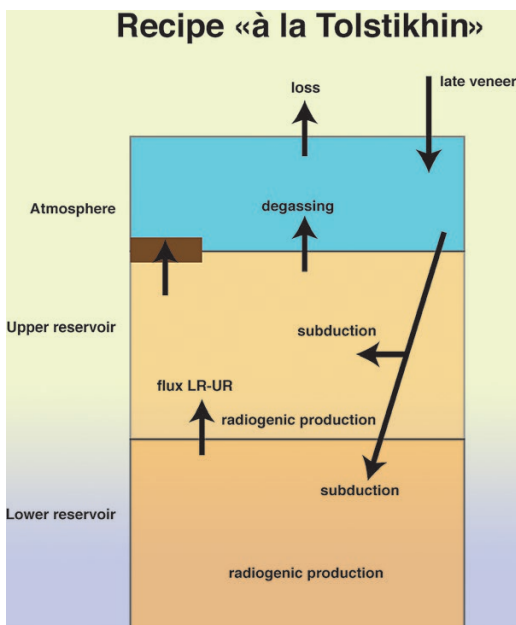


**Figure 8.6**

Cartoon showing fluxes between reservoirs that have to be considered in order to describe the mantle/atmosphere evolution with time. The expert of such multi-parameter models is our colleague Igor Tostikhin.

It is beyond the scope of this article to give a solution to such a complicated modelling but I want to stress here that the degassing term is the fundamental parameter that explains the noble gas isotopic compositions in the MORB and



OIB sources. Indeed, degassing is the physical mechanism able to significantly fractionate the parent/daughter ratios of the different noble gas isotopic systems. This is particularly true for any primordial degassing that occurred if the Earth's mantle was molten in the early Hadean. Degassing of a magma ocean cannot be simulated numerically due to its very high Rayleigh number, but it seems certain that a magma ocean was efficiently degassed of its noble gases.

The present-day degassing flux (e.g.,  $\sim 500\text{--}1,000 \text{ mol a}^{-1}$  of  $^3\text{He}$ ; Farley *et al.*, 1995; Bianchi *et al.*, 2010) is not high enough to have produced a large  $^4\text{He}/^3\text{He}$  (and other noble gas isotopic ratios) dichotomy between MORB and OIB in 4.5 Ga (see Section 3 for the helium isotopic observations in oceanic basalts). This is true even if one considers the depletion by continental crust extraction in very incompatible elements such as U and K of the MORB source. Moreover, the different  $^{129}\text{Xe}/^{130}\text{Xe}$  isotopic ratios between the MORB and OIB sources suggests an early separation of these two reservoirs (Section 4), as well as an early degassing of the xenon, before  $^{129}\text{I}$  was extinct ( $\sim 170 \text{ Ma}$ ) (e.g., Fig. 8.7).

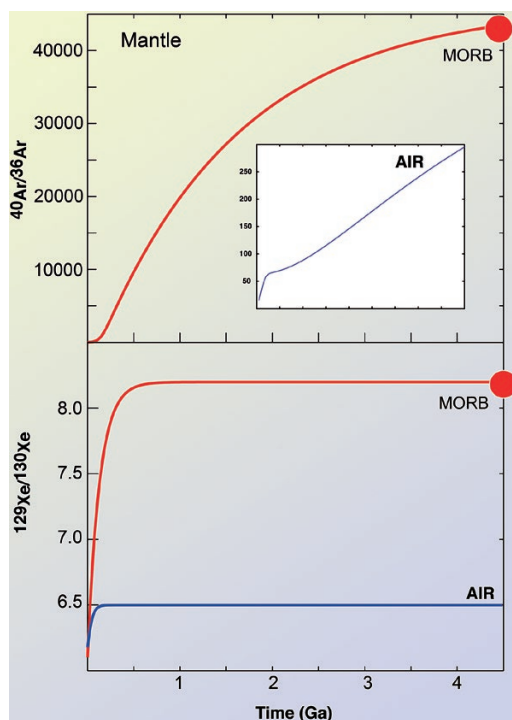


**Figure 8.7**

Result of a two stage degassing model applied to the mantle/atmosphere system and to the two isotopic systems  $^{129}\text{I}$ - $^{129}\text{Xe}$  and  $^{40}\text{K}$ - $^{40}\text{Ar}$ . To produce the present-day atmosphere and mantle isotopic ratios, the degassing constants have been fitted and are then used to produce the evolution of the concentration in Figure 8.8. MORB ratios are derived from Section 4.





The incorporation of all the radiogenic noble gases in a degassing model, and not only the use of just one noble gas such as helium, necessitates the use of a minimum of two degassing stages (*e.g.*, Allègre *et al.*, 1986). Without any equation, this can be easily understood if we consider that, in order to produce variations in the  $^{129}\text{Xe}/^{130}\text{Xe}$  ratio, an early degassing is necessary. However in order to have radiogenic argon in the atmosphere (which was produced throughout the Earth history), and to produce the observed  $^3\text{He}$  flux at ridges, a more recent degassing is required. Such a simple argument is confirmed by modelling, which also provides better time constraints and predicts the relative proportion of these two degassing stages.

The simplest model that can explain the noble gas isotopic ratios on Earth can be expressed with an equation having the following form:

$$\frac{S(t)}{S_0} = Ae^{-\alpha t} + (1 - A)e^{-\beta t},$$

where  $S(t)$  represents the number of moles of a stable and non-radiogenic isotope in the mantle (*e.g.*,  $^3\text{He}$ ,  $^{36}\text{Ar}$ ,  $^{130}\text{Xe}$ ),  $S_0$  being the initial content in the mantle. This model assumes that the mantle is degassed in two stages, but it neglects subduction of atmospheric noble gases into the mantle. It also supposes no gas loss to space. The previous sections have shown that this can be questioned, but such a simple calculation can provide essential ideas about the mantle degassing before studying more complex models. The model can be applied to the  $^{129}\text{I}$ - $^{129}\text{Xe}$  and  $^{40}\text{K}$ - $^{40}\text{Ar}$  systems, which are both short and long half-lived isotopic systems. For the radiogenic isotopes, and assuming the same degassing process, one can write the following equation:

$$\frac{dF}{dt} = -\Psi(t)F + \lambda P$$

with  $\Psi(t) = \frac{\alpha Ae^{-\alpha t} + (1 - A)\beta e^{-\beta t}}{Ae^{-\alpha t} + (1 - A)e^{-\beta t}}$  being the degassing term (used for  $S(t)$ ), and

the second term of the equation is the radiogenic production from the parent  $P$ . Detailed calculations from such models can be found in few publications such as Sarda *et al.* (1985; Allègre *et al.* (1986), Coltice *et al.* (2009) and Turner (1989) with more or less detail. The term  $A$  in the previous equation is a constant that gives the “proportion” between the two stages of degassing. The terms  $\alpha$ ,  $\beta$  are constants in  $\text{year}^{-1}$  that describe the vigour of each of the degassing.  $P(t)$  is the evolution of the concentration in the mantle of the radioactive parent isotopes such as  $\text{K}$ ,  $\text{U}$  etc. Finally, similar equations can be written for the evolution of stable and non-radiogenic isotopes and also for the radiogenic isotopes in the atmosphere. The constraints to obtain the values of the different constants are the isotopic ratios of the mantle and of the atmosphere. Figure 8.7 shows an example of results of such a calculation applied to the  $^{40}\text{Ar}/^{36}\text{Ar}$  and  $^{129}\text{Xe}/^{130}\text{Xe}$  ratios in the MORB source and in the atmosphere. The deduced evolution of their



concentrations in the mantle, which reflects the evolution from degassing, is given in Figure 8.8. It clearly shows that in the context of this two-step degassing, the major step of degassing occurred during the first 100 Ma, when Earth was still accreting, and possibly molten at its surface, favouring degassing. Rates of degassing decreased at 4.4 Ga and a more “tranquil” period of degassing started, which is plausibly linked with plate tectonics.

To conclude on mantle degassing and the formation of the atmosphere, it seems clear that massive degassing of the mantle occurred very early in Earth history and rapidly produced a large part of the atmosphere. The residual quantity of primordial noble gases was in the order of 1%. This process provides an explanation for the high  $^{129}\text{Xe}/^{130}\text{Xe}$  ratios measured in MORB compared to the atmosphere. A stronger degassing would have had to occur during this period if we assume subduction of atmospheric xenon into the mantle as discussed in the previous Section. On the contrary, to explain high  $^{40}\text{Ar}/^{36}\text{Ar}$  ratios in MORB, the degassing has to be continuous and later since the  $^{40}\text{Ar}$  is dominantly present from the decay of the relatively long-lived (1.3 Ga)  $^{40}\text{K}$  in the Earth history, and this degassing is still happening as illustrated by the  $^3\text{He}$  flux at ridges. This is linked to the plate tectonic regime of the Earth’s mantle convection. Therefore, a two-stage degassing model is needed in order to explain the noble gas systematics on Earth. It has to be mentioned that this first-order model has neglected important fluxes of noble gases to the atmosphere such as a late veneer of cometary or chondritic material and has also assumed the atmosphere did not lose noble gases to space, which might be questioned as discussed below. The question of the subduction of atmospheric noble gases has been addressed in the Section 7, and remains one of the major open questions in the noble gas geochemistry. Therefore, progress in improving our understanding of the mantle/atmosphere system requires the inclusion of these new terms in the models.

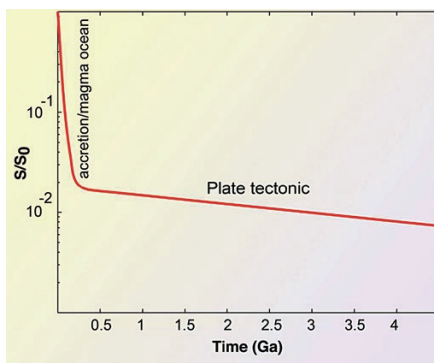


**Figure 8.8**

A two-stage degassing model that is able to produce the present-day radiogenic isotopic compositions of He, Ne, Ar and  $^{129}\text{Xe}/^{130}\text{Xe}$  (represented in Fig. 8.7). The first stage consists of a strong degassing of the mantle, probably because it was molten, whereas the second stage corresponds to the plate tectonic regime. The first stage is very early (> 4.4 Ga ago) and therefore the primordial atmosphere might have been sensitive to elemental and isotopic fractionation due to external conditions in the Solar System. Please note that in such a simple model, there is no gas loss to Space, nor gain, and that subduction is neglected.



## 8.4 Atmosphere: a Closed System (Loss or Addition)?

As discussed above, a part of the atmosphere derives from the degassing of the mantle. It is not however clear if the present noble gas budget represents the totality of what has been degassed. In this section, I discuss the possibility that either noble gases were added to the atmosphere by extra-terrestrial sources after mantle degassing (solar krypton?), or that noble gases were lost to the space, particularly the neon, but also, as it will be discussed in the next section, xenon.

### 8.4.1 Late veneer of chondritic material in order to explain (or not) the atmospheric neon

Marty (2012) has recently repropose (he first suggested this idea in 1989) that the neon composition of the atmosphere ( $^{20}\text{Ne}/^{22}\text{Ne} \sim 9.8$ ) reflects a late addition of material having the “planetary” component (“A”,  $^{20}\text{Ne}/^{22}\text{Ne} \sim 8.5$ ) to a primordial atmosphere with solar neon ( $^{20}\text{Ne}/^{22}\text{Ne} \sim 14$ ). In his exposition he notes that the solar composition (also his primordial mantle and atmosphere), the present day MORB source (Depleted mantle DM), the present-day atmosphere and the planetary end-member (component “A”) are on the same mixing line, suggesting a possible mixture between solar and chondritic (Marty, 2012) (Fig. 8.9). This could suggest that a late veneer of chondritic gas into the atmosphere changed its neon isotopic composition, which was supposed here to be solar at the end of accretion.

However, statistically, the neon composition of the incoming material as sampled by present-day falling meteorites appears to have a composition intermediate between neon “A” ( $^{20}\text{Ne}/^{22}\text{Ne} \sim 8.5$ ) and neon B ( $^{20}\text{Ne}/^{22}\text{Ne} \sim 12.5$ ) instead of the component “A” alone (Section 2; Ott, 2002). Moreover, the component “A” used by Marty was shown to be in fact the mixture of the two components P3 and HL (*e.g.*, review in Ott, 2002), both being pre-solar diamonds, and it is clear that heavy noble gases (*e.g.*, Ar) in chondrites are carried by phase Q, which has then to be considered in this scenario.

On Figure 8.9, I use the same reasoning as Marty, using recent estimates of solar, Q, P3 (A2) compositions (*e.g.*, Ott, 2002; Heber *et al.*, 2009)) in order to find the possible composition of the material that was possibly accreted on Earth after the atmosphere was created. I assume here that a chondrite is a mixture of three components: Q (the carrier of heavy noble gases) and HL-P3 (pre-solar material). Neon B is excluded as a possible component (if late veneer material is constituted of CI, for instance, see Section 2). If neon B is a major component in the late veneer material this scenario becomes untenable. In this conceptual model, neon is mostly carried by HL and P3 components whereas argon is carried by the phase Q. The  $^{36}\text{Ar}/^{22}\text{Ne}$  of this late veneer material is then  $\sim 32$ , close to the atmospheric ratio (Fig. 8.9 top). Figure 8.9 (bottom) represents the  $^{38}\text{Ar}/^{36}\text{Ar}$  plotted against the  $^{22}\text{Ne}/^{36}\text{Ar}$  for the same components. Starting from a primordial composition that is also solar for argon, most of the argon in the atmosphere and the mantle would derive from the late chondritic veneer. Thus this scenario



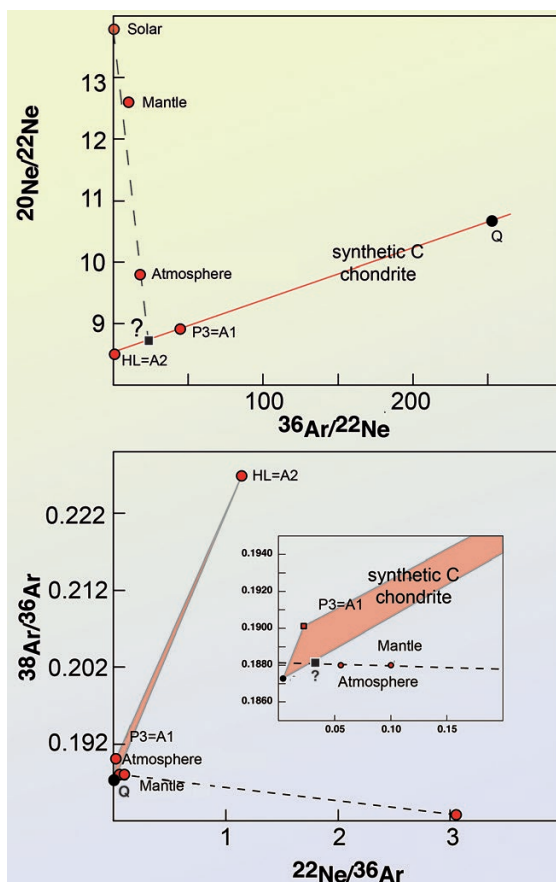


**Figure 8.9**

Model of Marty (2012) proposing that atmospheric neon reflects the addition of a late veneer of chondritic material. Here, his model is modified using a different composition for the late veneer. Instead of taking the neon A composition (comprised of pre-solar diamond components HL and P3, labelled A1 and A2, a mixture between pre-solar diamonds and phase Q is preferred. Atmosphere is supposed to be a mixture between a primordial solar (or neon B) atmosphere and chondritic material derived from the late veneer. In his model, Marty (2012) does not consider that the late veneer could have a neon B contribution. In the bottom figure, the model is applied to the argon isotopic composition. The "?" marks the theoretical composition of the late veneer that is necessary to explain the atmospheric composition.

implies an important subduction of neon and argon from the late veneer material into the mantle in order to modify the primordial solar argon composition of the mantle to the observed isotopic compositions. As sketched in Figure 7.7,



the curvature of mixing for this subducted material may be such that only the mantle Ar isotope ratio is significantly influenced. The scenario of a late chondritic veneer of noble gases developed by *Marty* is an elegant explanation for the neon isotopic composition of the atmosphere but makes an important assumption by considering that the material of the late veneer does not have a neon B contribution, which is however observed in most chondrite classes (Section 2)<sup>38</sup>.

Another scenario can explain the non-solar neon isotopic composition of the Earth's atmosphere. Neon loss from atmosphere accompanied with mass fractionation might be also a viable explanation. A model that may elucidate this isotopic fractionation is the hydrodynamic escape model of Hunten *et al.* (1987). Although there are many unknown (but adjustable) parameters in this model, it offers a physical process able to fractionate neon isotopes (and maybe those of other noble gases). This theory proposes that a EUV flux at high altitude drives thermal loss of H<sub>2</sub>, which allows entrainment of heavier species such as the noble gases. If we follow Hunten *et al.* (1987) or Pepin (1991), we can assume there is a UV flux such that the critical mass  $m_c$ , below which the species cannot escape is 25 amu, so we don't lose the heavy noble gases. We can therefore estimate that the neon isotopic ratio can decrease from the solar or neon B values to the present day atmospheric ratio of 9.8 by this process with only a loss of 40% loss of the <sup>22</sup>Ne (30% if we start from neon B). This neon loss is compatible with the present-day neon inventory.

Therefore, we have two possible explanations for the peculiar neon isotopic composition of present day atmosphere, starting initially with either a solar or neon B isotopic composition, two scenarios are offered. One is a late veneer of "chondritic" material that does not contain solar-like neon and argon, as suggested by Marty (1989, 2012), and the second scenario is a neon loss to space accompanied with mass fractionation (*e.g.*, Hunten *et al.*, 1987). In both cases, the atmosphere cannot be considered as a closed system and either neon was lost or was gained.

#### 8.4.2 A different atmospheric xenon composition in the Archean

Another observation showing that the Earth's atmosphere is not a closed system, is the fundamental observation that the xenon isotopic composition of the atmosphere has changed with time, not just as a result of radiogenic and fissogenic contributions (Pujol *et al.*, 2009; Holland *et al.*, 2013). This observation can be coupled with the measurements of Kr and Xe in CO<sub>2</sub> well gases (Cafee *et al.*, 1999; Holland and Ballentine, 2006; Holland *et al.*, 2009), which show that the primordial mantle seems to have been chondritic rather than atmospheric in its Kr and Xe isotopic compositions (non -radiogenic). As discussed in Section 7, this scenario implies however the subduction of Kr and Xe into the whole mantle, in disagreement with the "subduction barrier" hypothesis.

38. Except maybe Cl.



Figure 8.10 shows the interpretation of Pujol *et al.* (2011) of the isotopic composition of Archean atmospheric xenon. They analysed xenon in fluid inclusions trapped in quartz, sampled from a drill core in a 3.5 Ga aged terrain in Western Australia. Although the interpretation is difficult because they needed to correct for a) the addition of  $^{130}\text{Xe}$  due to the double electron capture of  $^{130}\text{Ba}$ , a rare nuclear process but one that can play a role in such ancient samples (Hennecke *et al.*, 1975; Bryman and Picciotto, 1978; Kirsten *et al.*, 1983; Moreira, 2007) and b) for the fission-derived xenon on the heavy isotopes  $^{131-136}\text{Xe}$ . After correcting the measured xenon isotope abundances for these two effects, they derived the isotopic composition of the atmosphere 3.5 Ga ago, which yields a xenon isotope pattern different from the one of the present-day atmosphere (Fig. 8.10). They proposed that the Archean atmosphere had a xenon isotopic composition similar to either the chondritic composition or to the solar one. However, they do not provide a physical mechanism able to fractionate significantly only the xenon isotopic composition without affecting the lighter noble gas isotopic fractionation, including the krypton. Pujol *et al.* (2011) however noticed that xenon has a low first energy ionisation compared to the other noble gases, which could suggest that ionisation of the atmosphere could play a role in this fractionation of the xenon. This was clearly illustrated by Halliday in a figure from his recent review in which he represents the first potential ionisation energy as a function of the

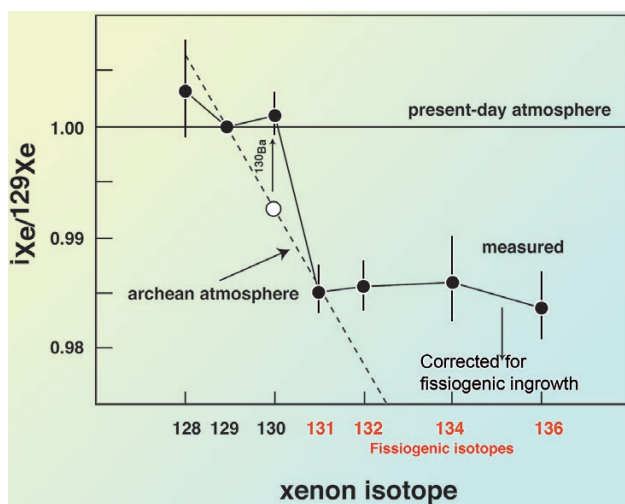


**Figure 8.10**

Xenon isotope spectrum in fluid inclusions from core drilled in the 3.5 Ga-old terrain at North Pole, (Western Australia). After correction for double electron capture of  $^{130}\text{Ba}$  and for the spontaneous fission from U, Pujol *et al.* (2011) propose that the xenon composition of the atmosphere was different in the Archean compared to that of today.



normalised abundances of noble gases and other volatiles on Earth (Halliday, 2013). A limit of ~13.5 eV for the first potential ionisation energy separates the Xe and other volatiles from the lighter noble gases. This limit maybe has a physical sense in terms of irradiation in the Solar System, but this requires further work.

The issue of the chronology of this important isotopic fractionation of the xenon also has also to be addressed (Fig. 8.11). Pujol *et al.* (2011) propose this is a continuous process (Fig. 8.12), although in my opinion, this is still subject to debate because the methodology to obtain the isotopic composition in Archean rocks is accompanied by large uncertainties (Fig. 8.10) (see Pepin, 2013 for a comment of the Pujol's paper). Beside the fact that there are still issues to be addressed, this observation is extremely important for understanding the formation of the atmosphere, and the depletion in xenon of the atmosphere. Xenon was probably lost from the atmosphere, at some moment in the Earth's history, and this was accompanied by an important isotopic fractionation, without affecting the other noble gases (Kr, see Fig. 8.2, or argon if its primordial isotopic composition was Q-like or solar wind implanted). It is useful to repeat here, that Mars' atmosphere shares the same xenon isotopic composition as the Earth's atmosphere and also has a similar depletion in xenon compared to other noble gases and to the chondritic elemental compositions. This suggests that if the xenon was lost from the atmosphere, the physical process that produced this loss is not dependent of the planet size.

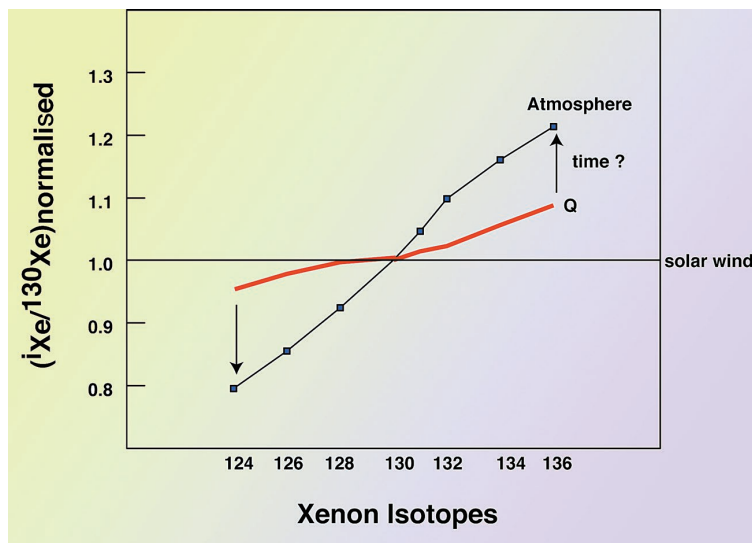


**Figure 8.11**

Schematic interpretation of the evolution of the atmospheric xenon, starting from a chondritic isotopic composition. The issue that needs to be addressed here is the source and the chronology of this important isotopic fractionation, which is also observed on the Mars atmosphere.





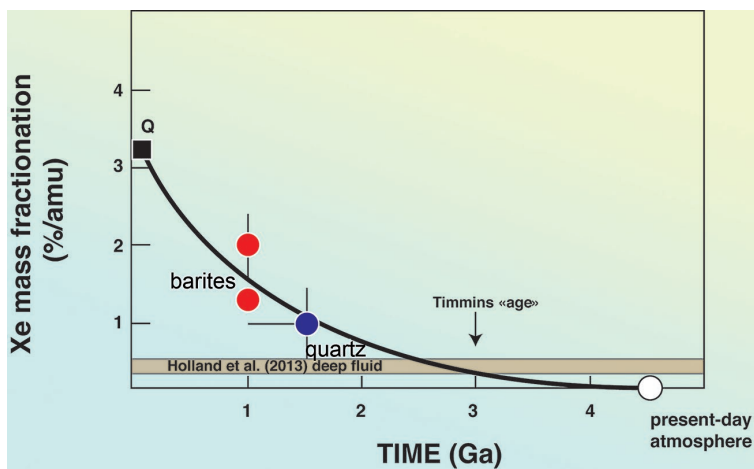


**Figure 8.12**

Pujol *et al.* (2011) have suggested that the isotopic fractionation of the xenon is continuous over the age of the Earth, suggesting xenon loss from the atmosphere by an unknown physical process. This figure is modified from Pujol *et al.* (2011). Dots represent barites and quartz samples from the Archean. The brown area represents the xenon compositions in fluids from Timmins (Canada) that have been isolated from the surface since at least 1.5 Ga (Holland *et al.*, 2013). The Timmins “age” is the in situ radiogenic age determined using radiogenic/fissionogenic ages based on U-Th-K concentrations of the crystalline basement. This very recent work (published during the editing of this book) is the first confirmation of the Pujol’s observation of the xenon isotopic evolution of the Earth’s atmosphere.

## 8.5 The Krypton-Xenon Systematics and the Dual Origin of the Atmosphere

Krypton isotopes provide another constraint on the origin of volatiles. Figure 8.13 shows the isotopic pattern for the atmosphere and of the Sun, normalised to the Q composition. This figure shows that the Earth’s atmosphere (and also the mantle, although it displays a little difference compared to air; Holland *et al.*, 2009) has an isotopic composition intermediate between the solar and this major chondritic composition. This is obviously quite different from the xenon isotopic pattern (Fig. 8.13, bottom) where the Q-composition is intermediate between solar and the Earth’s atmospheric xenon isotopic composition. Isotopic fractionation during gas loss, starting from the Q composition, should deplete the residual atmosphere in the light Kr isotopes preferentially, like for xenon. This is not the case and therefore it has to be proposed that krypton did not suffer the isotopic fractionation experienced by xenon (see above the discussion on the first ionisation energy). On the contrary, the simplest explanation to produce



the krypton pattern is the addition of solar krypton to a Q-like krypton, as for Mars' atmosphere (Fig. 8.2). Adding solar xenon into a chondritic-atmosphere through cometary material cannot be excluded since they have close isotopic patterns. Moreover, the xenon is subsequently isotopically fractionated, and such a fractionation has “erased” the primordial atmosphere composition. The atmospheric krypton isotopic signature can then be interpreted as the mixture between Q-krypton degassed from the mantle and solar-Kr rich material, which could be cometary (Fig. 8.13) as suggested by Dauphas (2003). Subsequent subduction of atmospheric krypton into the mantle would have “atmospherised” the mantle krypton (Holland *et al.*, 2009).

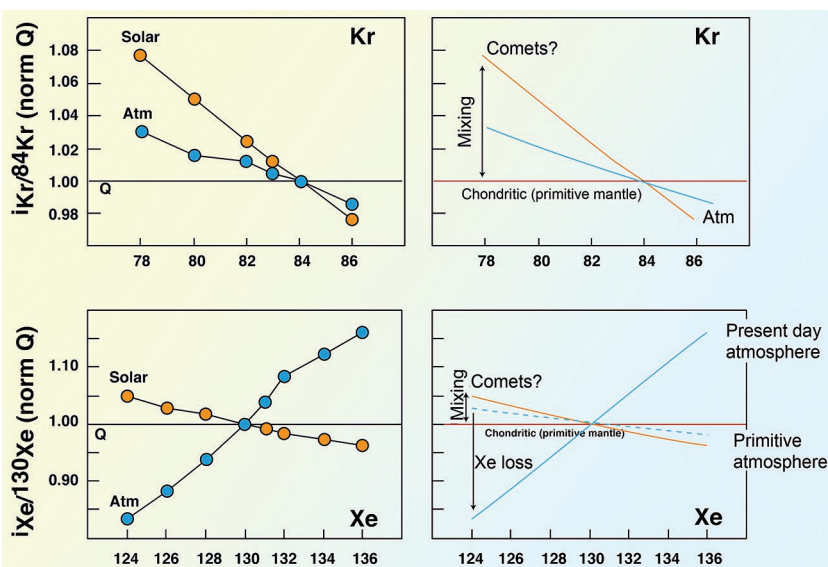


**Figure 8.13** Kr and Xe isotopic patterns in the Earth's atmosphere and their possible interpretation in terms of a mixture between Q and Solar (comets?) subsequently followed by an isotopic fractionation of the xenon (“à la Dauphas”). Here it is assumed that the primitive mantle (and therefore the primitive atmosphere formed by degassing) has a chondritic Kr and Xe isotopic composition (Holland *et al.*, 2009). The value used here for the isotopic composition of phase Q is derived from Busemann *et al.* (2000), except for  $^{82}\text{Kr}$  as it has been discussed in Figure 7.6.  $i_{\text{Kr}}$  and  $i_{\text{Xe}}$  refers to the isotopes of Kr and Xe, respectively.

Another possible scenario is that atmospheric krypton could simply be a mixture of solar and Q *already* in the parent bodies, and then it is logical to observe similar krypton isotopic ratios in the mantle and in the atmosphere, without the need for subduction (Tieloff and Kunz 2005). Then, the difference between air and the source of  $\text{CO}_2$ -well gases for the krypton (Holland *et al.*, 2009) could reflect late addition into the mantle of chondritic late veneer as already suggested in the previous section.



## 8.6 Conclusions

Radiogenic noble gas systematics suggest that a fraction of the Earth's atmosphere was formed by degassing of the mantle in two stages, the first stage corresponding to the accretion period, when the Earth was partially molten whereas the second stage reflects the more continuous processes associated with plate tectonics, in particular the degassing at mid oceanic ridges.

Mantle neon has a  $^{20}\text{Ne}/^{22}\text{Ne}$  composition close to  $\sim 12.6$ - $12.8$  (see Section 5). This neon isotopic composition either reflects the subduction of atmospheric neon into a primitive mantle having solar composition or it could reflect solar wind implantation in parent body's precursors as discussed in Sections 2 and 5. A similar interpretation can be proposed for argon. The  $^{38}\text{Ar}/^{36}\text{Ar}$  ratio in the mantle is identical to the atmospheric ratio (Kunz 1999; Ballentine and Holland, 2008; Raquin and Moreira, 2009; Mukhopadhyay, 2012). This can be interpreted either by the fact that the atmosphere was degassed from a mantle having a primordial composition that is a mixture of chondritic (Q) and solar implanted argon or solar, or by assuming subduction of atmospheric argon in the whole mantle that had previously solar isotopic composition. The atmospheric argon is therefore the result of either an isotopic fractionation accompanying a gas loss (Pepin, 1998) or to the addition of a chondritic late veneer (Marty, 2012). The present-day krypton and xenon isotopic compositions (non-radiogenic isotopes) are (almost) atmospheric in the mantle. Again, this could reflect the subduction of atmospheric Kr and Xe into a mantle that had, at the end of accretion, a chondritic isotopic signature (Holland *et al.*, 2009). Xenon is highly isotopically fractionated in Earth's atmosphere; it is enriched in heavy isotopes compared to solar or chondritic. Krypton does not show the same feature. Atmospheric krypton isotopic signatures seem to reflect the mixing of material having solar and chondritic compositions and do not show an isotopic fractionation that could have had enriched the atmosphere in heavy Kr isotopes (like for xenon).

The process that has fractionated the xenon isotopes is however unknown but it is identical for the atmospheres of Mars and Earth. The chronology of the fractionation is also unknown. Pujol *et al.* (2011) suggest is a continuous process that spreads all over the Earth history. Moreover, xenon could be the only noble gas to have been fractionated isotopically because it has the lowest potential ionisation energy (*e.g.*, Halliday, 2013).

Knowing these constraints on the noble gas signatures, I propose here two possible scenarios for the origin of noble gases on Earth. They are illustrated on Figure 8.14. There are obviously many other possibilities, and I just want to provide the reader with a general idea of the possible scenarios based on the noble gas systematics on Earth.

- a) The Earth's primordial noble compositions were chondritic, which includes neon B and a minor contribution of argon B and Kr and Xe with a Q-composition. Earth is built from such material and therefore this hypothesis is realistic. A fraction of the atmosphere was



then degassed from the mantle producing a primordial atmosphere with a composition similar to the mantle (*e.g.*, chondritic). Addition of cometary material (*e.g.*, Dauphas, 2003) can produce the krypton isotopic ratios of the present-day atmosphere, which shows a solar contribution. Xenon was then lost to space, accompanied by enrichment in Xe heavy isotopes (Pujol *et al.*, 2011). In this scenario, to explain the Kr and Xe isotopic composition of the mantle, subduction of atmospheric Kr and Xe is necessary (Holland and Ballentine, 2006; Holland *et al.*, 2009). Such a scenario has one major unknown, which is the origin and the chronology of the xenon isotopic fractionation and one important hypothesis, which is the subduction of noble gases. Ionisation of the atmospheric xenon appears to be involved in the fractionation process since it concerns only the xenon, but it raises the question of why Mars' atmosphere has the same xenon isotopic composition as the Earth, despite having only ~10% of its mass.

- b) A second scenario that can be proposed suggests that the “atmospheric” Kr and Xe isotopic compositions were already present in the Earth's parent bodies, and that the chondritic contribution observed in the mantle, as sampled by CO<sub>2</sub> well gases reflects chondritic material addition to the mantle. Such a scenario does not require atmospheric subduction and neither requires xenon loss to space accompanied with isotopic fractionation, but this model raises the question of the origin of the atmospheric Kr and Xe compositions in the parent bodies, which are not observed in meteorites. If addition of solar and chondritic Kr can produce the “atmospheric” Kr isotopic composition, there is still a question about how the xenon isotopic composition was obtained in these parent bodies since addition of solar and chondritic cannot produce the atmospheric xenon isotopic composition (Fig. 8.13).

An important constraint that requires confirmation is the observation that the Martian mantle Xe seems to have solar (or Q eventually) isotopic compositions (Matthew and Marti, 2001; Section 2), suggesting that Martian parent bodies did not have an “atmospheric” xenon isotopic signature, which is however observed in the Mars's atmosphere. If this observation of solar-like xenon in the Martian interior is confirmed, then the first scenario is clearly more realistic than the second and requires that the Martian atmospheric xenon is isotopically fractionated compared to its interior. A better understanding of the xenon isotopic fractionation in planetary atmospheres is however required, as well as the quantification of the noble gas subduction into the mantle in the case of Earth. Such work is in progress in different laboratories and answers to these two issues will (hopefully) come soon.



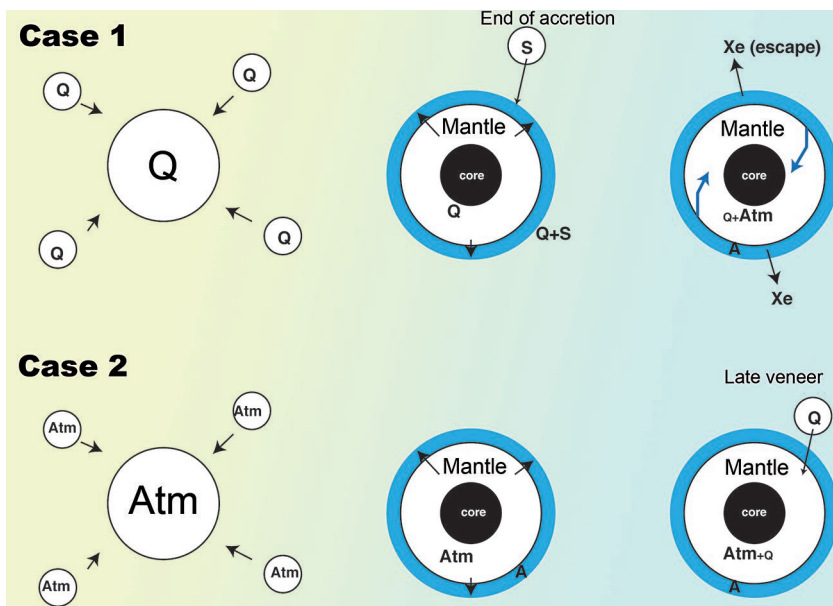


**Figure 8.14**

Two extreme scenarios can be proposed in order to reproduce on the first order observations on the noble gas isotopic compositions of the Earth. The first one (case 1) is based on the assumption that Earth had a chondritic composition (Q) (which includes the contribution of neon B and argon B). To explain the atmospheric krypton, cometary material with a solar isotopic composition can be added to the atmosphere (originally degassed from the mantle with a chondritic signature) at the end of the accretion (e.g., Walsh *et al.*, 2011). Xenon has to be lost and this is accompanied with an important mass fractionation in order to produce the observed xenon isotopic composition (and the xenon deficit in the atmosphere). Subduction of atmospheric noble gases is required to explain the present-day Kr-Xe isotopic compositions in the mantle (Holland and Ballentine, 2006; Holland *et al.*, 2009). Case 2 supposes that the chondritic contribution observed in CO<sub>2</sub> well gases represents the addition of a post-accretion veneer of chondritic material to the mantle. In such a model, the fractionated terrestrial noble gas isotopic signatures were already present in the parent bodies ('Atm'). Neon was modified in the atmosphere either by gas loss, either by addition of chondritic material having the neon A signature, without affecting the Kr and Xe isotopic compositions as suggested by Marty (1989; 2012).

I hope the reader will have been convinced that noble gases provide important constraints on the mantle structure and on the origin of volatiles on terrestrial planets. I have attempted to give the reader some information on how noble gases are essential, although not unique of course, to address the issue of the origin of planetary atmospheres (here, terrestrial planets, but also giant planets). Some results and interpretation can be considered as established and unanimously accepted by the community; some others are still debated and require further work to be confirmed or invalidated. Below is a series of questions that, to my opinion, need to be answered or confirmed in order to provide a comprehensive model of the origin of volatiles on terrestrial planets. Some will have an answer certainly in the next few years, some others will need more time, and will certainly require new samples or new analytical procedures.

- a) Where is the “primordial” reservoir sampled in OIB located? Core, D”, piles or lower mantle? Is the canonical two-layer mantle model coherent with all the geochemical and geophysical observations? New high-pressure experiments are required to determine the partitioning of noble gases in the different lower mantle phases.
- b) How effective is noble gas subduction in the mantle? Are the atmospheric noble gases subducted into the whole mantle? Is there a fractionation between noble gases during subduction?
- c) What is the physical process producing the observed isotopic fractionation of xenon in Mars and Earth atmospheres? Is it affecting only xenon? When did it occur? What is the time evolution of the xenon isotopic signature of the atmosphere?
- d) Is the neon isotopic ratio solar (and not B) in the mantle source of OIB? Answering this question will provide important constraints on the mechanism of incorporation of volatiles into the deep mantle (solar wind implantation vs. dissolution).
- e) What is the noble gas composition of Mars’ interior (chondritic, solar)? Although having the same answer for Venus would be great, I have to be reasonable! Earth’s mantle appears to have a chondritic composition for Kr and Xe. Why would Mars have a solar signature as suggested by the Chassigny meteorite? Then, why do Earth and Mars atmospheres have the same xenon isotopic compositions which are different from any other known object in the Solar System?
- f) What are the elemental and isotopic compositions of cometary material? Is it solar for the noble gas isotopic compositions? Does this material contribute significantly to the planetary noble gas budget?



- g) What is the origin of the isotopic composition of the phase Q in meteorites (solar wind implantation or adsorption under special physical conditions of irradiation)?
- h) Was there a late veneer of volatile-rich material in the Earth's atmosphere? Is it required for noble gases?







# REFERENCES

- AKA, F.T., NAGAO, K., KUSAKABE, M., SUMINO, H., TANYILEKE, G., ATEBA, B., HELL, J. (2004) Symmetrical helium isotope distribution on the Cameroon Volcanic Line, West Africa. *Chemical Geology* 203, 205-223.
- ALBARÈDE, F. (2009) Volatile accretion history of the terrestrial planets and dynamic implications. *Nature* 461, 1227-1233.
- ALDRICH, L.T., NIER, A.O. (1946) The abundance of  $^3\text{He}$  in atmospheric and well helium. *Physical Review* 70, 983-986.
- ALDRICH, L.T., NIER, A.O. (1948) The Occurrence of  $\text{He}^3$  in Natural Sources of Helium. *Physical Review* 74, 1590-1594.
- ALEXANDER, E.C., LEWIS, R.S., REYNOLDS, J.H., MICHEL, M. (1971) Plutonium-244: confirmation as an extinct radioactivity. *Science* 172, 837-840.
- ALLÈGRE, C.J. (1982) Chemical Geodynamics. *Tectonophysics* 81, 109-132.
- ALLÈGRE, C.J. (1987) Isotope geodynamics. *Earth and Planetary Science Letters* 86, 175-203.
- ALLÈGRE, C.J. (2002) The evolution of mantle mixing. *Philosophical Transactions of the Royal Society of London* 360, 2411-2431.
- ALLÈGRE, C.J., TURCOTTE, D. (1986) Implications of a two-component marble-cake mantle. *Nature* 323, 123-127.
- ALLÈGRE, C.J., LEWIN, E. (1995) Isotopic systems and stirring times of the Earth's Mantle. *Earth and Planetary Science Letters* 136, 629-646.
- ALLÈGRE, C.J., MOREIRA, M. (2004) Rare gas systematics and the origin of oceanic islands: the key role of entrainment at the 670 km boundary layer. *Earth and Planetary Science Letters* 228, 85-92.
- ALLÈGRE, C.J., BRÉVART, O., DUPRÉ, B., MINSTER, J.F. (1980) Isotopic and chemical effects produced in a continuously differentiating convecting Earth mantle. *Philosophical Transactions of The Royal Society of London* A297, 447-477.



- ALLÈGRE, C.J., HART, S.R., MINSTER, J.F. (1983a) Chemical structure and evolution of the mantle and continents determined by inversion of Nd and Sr isotopic data, I. Theoretical methods, II. Numerical experiments and discussion. *Earth and Planetary Science Letters* 66, 177-180, 191-213.
- ALLÈGRE, C.J., STAUDACHER, T., SARDA, P., KURZ, M.D. (1983b) Constraints on evolution of Earth's mantle from rare gas systematics. *Nature* 303, 762-766.
- ALLÈGRE, C.J., STAUDACHER, T., SARDA, P. (1986) Rare gas systematics, formation of the atmosphere, evolution and structure of the Earth's mantle. *Earth and Planetary Science Letters* 81, 127-150.
- ALLÈGRE, C.J., SARDA, P., STAUDACHER, T. (1993) Speculations about the cosmic origin of He and Ne in the interior of the Earth. *Earth and Planetary Science Letters* 117, 229-233.
- ALLÈGRE, C.J., MOREIRA, M., STAUDACHER, T. (1995) 4He/3He dispersion and mantle convection. *Geophysical Research Letters* 22, 2325-2328.
- ALLÈGRE, C., HOFMANN, A., O'NIONS, K. (1996) The argon constraints on mantle structure. *Geophysical Research Letters* 23, 3555-3557.
- ALVAREZ, L.W., CORNOG, R. (1939a) He3 in helium. *Physical Review* 56, 379.
- ALVAREZ, L.W., CORNOG, R. (1939b) Helium and hydrogen of mass 3. *Physical Review* 56, 613.
- AMELIN, Y., KROT, A., HUTCHEON, I.D., ULYANOV, A. (2002) Lead Isotopic Ages of Chondrules and Calcium-Aluminum-Rich Inclusions. *Science* 297, 1678-1683.
- ANDERSON, D.L. (1993) Helium-3 from the mantle: primordial signal or cosmic dust? *Science* 261, 170-176.
- ANDERSON, D.L. (1998) A model to explain the various paradoxes associated with mantle noble gas geochemistry. *Proceedings of the National Academy of Sciences of the United States of America* 95, 9087-9092.
- ANDERSON, D.L. (2000) The statistics and distribution of helium in the mantle. *International Geology Review* 42, 289-311.
- AREVALO, R., McDONOUGH, W.F., LUONG, M. (2009) The K/U ratio of the silicate Earth: Insights into mantle composition, structure and thermal evolution. *Earth and Planetary Science Letters* 279, 361-369.
- ARMSTRONG, R.L. (1968) A model for Pb and Sr isotope evolution in a dynamic earth. *Reviews of Geophysics* 6, 175-199.
- AZBEL, I., TOLSTIKHIN, I.N. (1993) Accretion and early degassing of the earth: Constraints from Pu-U-I-Xe isotopic systematics. *Meteoritics* 28, 609-621.
- AZUMA, S., OZIMA, M., HIYAGON, H. (1993) Anomalous neon and xenon in an archean anorthosite from west Greenland. *Earth and Planetary Science Letters* 114, 341-352.
- BALLENTINE, C.J., BARFOD, D. (2000) The origin of air-like noble gases in MORB and OIB. *Earth and Planetary Science Letters* 180, 39-48.
- BALLENTINE, C.J., HOLLAND, G. (2008) What CO<sub>2</sub> well gases tell us about the origin of noble gases in the mantle and their relationship to the atmosphere. *Philosophical Transactions Royal Society of London A* 366, 4183-4203.
- BALLENTINE, C.J., MARTY, B., SHERWOOD-LOLLAR, B., CASSIDY, M. (2005) Neon isotopes constrain convection and volatile origin in the Earth's mantle. *Nature* 433, 33-38.
- BARFOD, D.N., BALLENTINE, C.J., HALLIDAY, A.N., FITTON, J.G. (1999) Noble gases in the Cameleon line and He, Ne and Ar isotopic composition of high  $\mu$  (HIMU) mantle. *Journal of Geophysical Research* 104, 29509-29527.
- BAR-NUN, A., OWEN, T. (1998) Trapping of gases in water ice and consequences to comets and the atmospheres of the inner planets. In: Schmitt, B.B., de Bergh, C., Festou, M. (Eds.) *Solar System Ices*. Kluwer Academic, Dordrecht, pp. 353-366.
- BEHRMANN, C. J., DRODZ, R., HOHENBERG, C. (1973) Extinct lunar radioactivities: xenon from 244Pu and 129I in Apollo 14 breccias. *Earth and Planetary Science Letters* 17, 446-455.



- BEIER, C., STRACKE, A., HAASE, K. (2007) The peculiar geochemical signatures of São Miguel (Azores) lavas: Metasomatised or recycled mantle sources? *Earth and Planetary Science Letters* 259, 186-199.
- BENKERT, J.-P., BAUR, H., SIGNER, P., WIELER, R. (1993) He, Ne and Ar from the Solar Wind and Solar Energetic Particles in lunar ilmenites and pyroxenes. *Journal of Geophysical Research* 98, 13147-13162.
- BERNATOWICZ, T., FAHEY, A. (1986) Xe isotopic fractionation in a cathodeless glow discharge. *Geochimica et Cosmochimica Acta* 50, 445-452.
- BERNATOWICZ, T., HAGEE, B.E. (1987) Isotopic fractionation of Kr and Xe implanted in solids at very low energy. *Geochimica et Cosmochimica Acta* 51, 1599-1611.
- BIANCHI, D., SARMIENTO, J.L., GNANADESIKAN, A., KEY, R.M., SCHLOSSER, P., NEWTON, R. (2010) Low helium flux from the mantle inferred from simulations of oceanic helium isotope data. *Earth and Planetary Science Letters* 297, 379-386.
- BLACK, D.C. (1971) Trapped neon-argon isotopic correlations in gas rich meteorites and carbonaceous chondrites. *Geochimica et Cosmochimica Acta* 35, 230-235.
- BLACK, D.C. (1972) On the origins of trapped helium, neon and argon isotopic variations in meteorites, II. Carbonaceous chondrites. *Geochimica et Cosmochimica Acta* 36, 377-394.
- BLUNDY, J., WOOD, B. (2003) Mineral-melt partitioning of uranium, thorium and their daughters. In: Bourdon, B., Henderson, G., Lundstrom, C., Turner, S. (Eds) Uranium series geochemistry, Reviews in Mineralogy and Geochemistry, Vol. 52. Mineralogical Society of America, Washington, D.C., pp. 59-123.
- BOGARD, D.D. (1997) A reappraisal of the Martian  $^{36}\text{Ar}/^{38}\text{Ar}$ . *Journal of Geophysical Research* 102, 1653-1661.
- BOGARD, D.D., JOHNSON, H. (1983) Martian gases in an Antarctic meteorite? *Science* 221, 651-654.
- BOGARD, D.D., HORZ, F., JOHNSON, P. (1986) Shock-implanted noble gases: An experimental study with implications for the origin of Martian gases in shergottite meteorites. *Journal of Geophysical Research* 91 (Suppl.), E99-E114.
- BOULOS, M.S., MANUEL, O.K. (1971) The Xenon Record of Extinct Radioactivities in the Earth. *Science* 4016, 1334-1336.
- BOYET, M., CARLSON, R.W. (2005)  $^{142}\text{Nd}$  Evidence for Early (>4.53 Ga) Global Differentiation of the Silicate Earth. *Science* 309, 576-581.
- BOYET, M., Blichert-Toft, J., ROSING, M., STOREY, M., TÉLOUK, P., ALBARÈDE, F. (2003)  $^{142}\text{Nd}$  evidence for early Earth differentiation. *Earth and Planetary Science Letters* 214, 427-442.
- BRANDON, A. (2011) Planetary science: Building a planet in record time. *Nature* 473, 460-461.
- BREDDAM, K., KURZ, M.D., STOREY, M. (2000) Mapping out the conduit of the Iceland mantle plume with helium isotopes. *Earth and Planetary Science Letters* 176, 45-55.
- BROWN, H. (1949) Rare gases and the formation of the Earth's atmosphere. In: Kuiper, E.G. (Ed.) The Atmospheres of the Earth and Planets. University of Chicago Press, Chicago, pp. 258-266.
- BURNARD, P.G. (1999) Origin of Argon-lead isotopic correlation in basalts. *Science* 286, 871a.
- BURNARD, P., GRAHAM, D., TURNER, G. (1997) Vesicle-specific noble gas analyses of « popping rock »: implications for primordial noble gases in the Earth. *Science* 276, 568-571.
- BUSEMANN, H., EUGSTER, O. (2002) The trapped noble gas component in achondrites. *Meteoritics and Planetary Science* 37, 1865-1891.
- BUSEMANN, H., BAUR, H., WIELER, R. (2000) Primordial noble gases in “phase Q” in carbonaceous and ordinary chondrites studied by closed-system stepped etching. *Meteoritics and Planetary Science* 35, 949-973.
- BUTLER, W.A., JEFFERY, P. M., REYNOLDS, J.H. (1963) Isotopic Variations in Terrestrial Xenon. *Journal of Geophysical Research* 68, 3283-3291.
- BRYMAN, D., PICCIOTTO, C. (1978) Double beta decay. *Reviews of Modern Physics* 50, 11-21.



- CAFEÉ, M.W., HUDSON, G.P., VELSKO, C., HUSS, G.R., ALEXANDER, E.C., CHIVAS, R. (1999) Primordial noble gases from earth's mantle: identification of primitive volatile component. *Science* 285, 2115-2118.
- CAMPBELL, I.H., O'NEIL, H.C.O. (2012) Evidence against a chondritic Earth. *Nature* 483, 553-558.
- CARO, G., BOURDON, B. (2010) Non-chondritic Sm/Nd ratio in the terrestrial planets: Consequences for the geochemical evolution of the mantle crust system. *Geochimica et Cosmochimica Acta* 74, 3333-3349.
- CARO, G., BOURDON, B., BIRCK, J.-L., MOORBATH, S. (2003)  $^{146}\text{Sm}$ - $^{142}\text{Nd}$  evidence from Isua metamorphosed sediments for early differentiation of the Earth's mantle. *Nature* 423, 428-432.
- CHASE, C.G. (1981) Oceanic island Pb: Two-stage histories and mantle evolution. *Earth and Planetary Science Letters* 52, 277-284.
- CHAUVEL, C.A., HOFMANN, W., VIDAL, P. (1992) HIMU-EM: the French Polynesian connection. *Earth and Planetary Science Letters* 110, 99-119.
- CLARKE, W.B., BEG, M.A., CRAIG, H. (1969) Excess  $^3\text{He}$  in the sea: evidence for terrestrial primordial helium. *Earth and Planetary Science Letters* 6, 213-220.
- CLASS, C., GOLDSTEIN, S. (2005) Evolution of helium isotopes in the Earth's mantle. *Nature* 436, 1107-1112.
- CLASS, C., GOLDSTEIN, S., STUTE, M., KURZ, M.D., SCHLOSSER, P. (2005) Grand Comore island: a well-constrained "low  $^3\text{He}/^4\text{He}$ " mantle plum. *Earth and Planetary Science Letters* 233, 391-409.
- COHEN, R.S., O'NIONS, R. K. (1982) Identification of recycled continental material in the mantle from Sr, Nd and Pb isotope investigations. *Earth and Planetary Science Letters* 61, 73-84.
- COLIN, A., BURNARD, P., MARTY, B. (2013) Mechanisms of magma degassing at mid-oceanic ridges and the local volatile composition ( $^4\text{He}$ - $^{40}\text{Ar}$ - $\text{CO}_2$ ) of the mantle by laser ablation analysis of individual MORB vesicles. *Earth and Planetary Science Letters* 361, 183-194.
- COLTICE, N., RICARD, Y. (1999) Geochemical observations and one layer mantle convection. *Earth and Planetary Science Letters* 174, 125-137.
- COLTICE, N., MARTY, B., YOKOCHI, R. (2009) Xenon isotope constraints on the thermal evolution of the early Earth. *Chemical Geology* 266, 4-9.
- COLTICE, N., MOREIRA, M., LABROSSE, S., HERNLUND, J.W. (2011) Crystallization of a basal magma ocean recorded by Helium and Neon. *Earth and Planetary Science Letters* 308, 193-199.
- CONDOMINES, M., GRÖNVOLD, K., HOOKER, P.J., MUEHLENBACHS, K., O'NIONS, R.K., OSKARSSON, N., OXBURGH, E.R. (1983) Helium, oxygen, strontium and neodymium isotopic relationships in Icelandic volcanic. *Earth and Planetary Science Letters* 66, 125-136.
- CRAIG, H., LUPTON, J. (1976) Primordial neon, helium, and hydrogen in oceanic basalts. *Earth and Planetary Science Letters* 31, 369-385.
- CRAIG, H., LUPTON, J.E. (1981) Helium-3 and mantle volatiles in the ocean and the oceanic crust. In: Emiliani, C. (Ed.) *The Sea*, Vol. 7: The Oceanic Lithosphere. Harvard University Press, Cambridge, pp. 391-428.
- CROWTHER, S.A., GILMOUR J.D. (2012) Measuring the elemental abundance and isotopic signature of solar wind xenon collected by the Genesis mission. *Journal of Analytical Atomic Spectrometry* 27, 256-269.
- DALRYMPLE, G.B. (1969)  $^{40}\text{Ar}/^{36}\text{Ar}$  analyses of historic lava flows. *Earth and Planetary Science Letters* 6, 47-55.
- DALRYMPLE, G.B., MOORE, J.G. (1968) Argon-40: Excess in submarine pillow basalts from Kilauea Volcano, Hawaii. *Science* 161, 1132-1135.
- DAUPHAS, N. (2003) The dual origin of the terrestrial atmosphere. *Icarus* 165, 326-339.
- DAUPHAS, N., POURMAND, A. (2011) Hf-W-Th evidence for rapid growth of Mars and its status as a planetary embryo. *Nature* 473, 489-492.



- DAUPHAS, N., ROBERT, F., MARTY, B. (2000) The late asteroidal and cometary bombardment of Earth as recorded in water deuterium to protium ratio. *Icarus* 148, 508-512.
- DAVILLE, A. (1999) Two-layer thermal convection in miscible viscous fluids. *Journal of Fluid Mechanics* 379, 223-253.
- DAVIES, G. (1999) Geophysically constrained mantle mass flows and the  $^{40}\text{Ar}$  budget: A degassed lower mantle? *Earth and Planetary Science Letters* 166, 149-162.
- DAY, J.M.D., HILTON, D.R. (2011) Origin of  $^3\text{He}/^4\text{He}$  ratios in the HIMU-type basalts constrained from canary Island lavas. *Earth and Planetary Science Letters* 305, 226-234.
- DE PAOLO, D.J., WASSERBURG, G.J. (1976) Nd isotopic variations and petrogenetic models. *Geophysical Research Letters* 3, 249-252.
- DE PAOLO, D.J., WASSERBURG, G.J. (1979) Sm-Nd age of the Stillwater Complex and the mantle evolution curve for neodymium. *Geochimica et Cosmochimica Acta* 43, 999-1008.
- DESCHAMPS, F., KAMINSKI, E., TACKLEY, P.J. (2011) A deep mantle origin for the primitive signature of ocean island basalts. *Nature Geoscience* 4, 879-882.
- DIXON, E. (2003) Interpretation of helium and neon isotopic heterogeneity in Icelandic basalts. *Earth and Planetary Science Letters* 206, 83-99.
- DIXON, E., HONDA, M., MCDOUGALL, I., CAMPBELL, I., SIGURDSSON, I. (2000) Preservation of near-solar isotopic ratios in Icelandic basalts. *Earth and Planetary Science Letters* 180, 309-324.
- DIXON, J.E., LEIST, L., LANGMUIR, C., SCHILLING, J.-G. (2002) Recycled dehydrated lithosphere observed in plume-influenced mid-oceanic ridge basalt. *Nature* 420, 385-389.
- DOUCET, S., MOREIRA, M., WEIS, D., SCOATES, J.S., GIRET, A., ALLÈGRE, C.J. (2006) Primitive neon and helium isotopic compositions of high-MgO basalts from the Kerguelen Archipelago, Indian Ocean. *Earth and Planetary Science Letters* 241, 65-79.
- DRODZ, R., HOHENBERG, C., RAGAN, D. (1972) Fission xenon from extinct  $^{244}\text{Pu}$  in 14301. *Earth and Planetary Science Letters* 15, 338.
- DUNAI, T.J., PORCELLI, D. (2002) Storage and transport of noble gases in the subcontinental lithosphere. In: Porcelli, D., Ballentine, C.J., Wieler, R. (Eds.) *Noble Gases in Geochemistry and Cosmochemistry, Reviews in Mineralogy and Geochemistry*, Vol. 47. Mineralogical Society of America, Washington, D.C., pp. 371-409.
- DUPRÉ, B., ALLÈGRE C.J. (1980) Pb-Sr-Nd isotopic correlation and the chemistry of the north atlantic mantle. *Nature* 286, 17-22.
- DUPRÉ, B., ALLÈGRE, C.J. (1983) Pb-Sr isotope variation in Indian Ocean basalts and mixing phenomena. *Nature* 303, 142-146.
- EBERHARDT, P., GEISS, J., GRAF, H., GRÖGLER, N., MENDIA, M.D., MÖRGELI, M., SCHWALLER, H., STETTLER, A., KRÄHENBÜHL, U., VON GUNTEN, H.R. (1972) Trapped solar wind noble gases in Apollo 12 lunar fines 12001 and Apollo 11 breccia 10046. Physikalisches Institut, Bern.
- ELLIOTT, T., BLICHERT-TOFT, J., HEUMANN, A., KOETSIER, G., FORJAZ, V.-H. (2007) The origin of enriched mantle beneath São Miguel, Azores. *Geochimica et Cosmochimica Acta* 71, 219-240.
- ESCRIG, S., CAPMAS, F., DUPRÉ, B., ALLÈGRE, C.J. (2004) Osmium isotopic constraints on the Nature of the Dupal anomaly from Indian mid-ocean-ridge basalts. *Nature* 431, 59-63.
- EUGSTER, O., BUSEMANN, H., LORENZETTI, S., TERRIBILINI, D. (2002) Ejection ages from krypton-81-krypton-83 dating and pre-atmospheric sizes of martian meteorites. *Meteoritics and Planetary Science* 37, 1345-1360.
- FARLEY, K.A., POREDA, R. J. (1993) Mantle neon and atmospheric contamination. *Earth and Planetary Science Letters* 114, 325-339.
- FARLEY, K.A., NATLAND, J.H., CRAIG, H. (1992) Binary mixing of enriched and undegassed (primitive?) mantle components (He, Sr, Nd, Pb) in Samoan lavas. *Earth and Planetary Science Letters* 111, 183-199.



- FARLEY, K.A., MAIER-REIMER, E., SCHLOSSER, P., BROECKER, W.S. (1995) Constraints on mantle  $^3\text{He}$  fluxes and deep-sea circulation from an oceanic general circulation model. *Journal of Geophysical Research* 100, 3829-3839.
- FIELDS, P.R., FRIEDMAN, A.M., MILSTED, J., LERNER, J., STEVENS, C.M., METTA, D., SABINE, W.K. (1966) Decay properties of plutonium-244, and comments on its existence in Nature. *Nature* 212, 131-134.
- FISHER, D.E. (1970) Search for  $^3\text{He}$  in deep-sea basalts. *Earth and Planetary Science Letters* 8, 77-78.
- FISHER, D.E. (1975) Trapped helium and argon and the formation of the atmosphere by degassing. *Nature* 256, 113-114.
- FISHER, D.E. (1983) Rare gases from the undepleted mantle? *Nature* 305, 298-300.
- FUNKHOUSER, J. G., FISHER, D.E., BONATTI, E. (1968) Excess argon in deep sea rocks. *Earth and Planetary Science Letters* 5, 95-100.
- GANNOUN, A., BOYET, M., RIZO, H., EL GORESY, A. (2011)  $^{146}\text{Sm}$ - $^{142}\text{Nd}$  systematics measured in enstatite chondrites reveals a heterogeneous distribution of  $^{142}\text{Nd}$  in the solar nebula. *PNAS* 108, 7693-7697.
- GARDINIER, A., DERENNE, S., ROBERT, F., BEHAR, F., LARGEAU, C., MAQUET, J. (2000) Solid state CP/MAS  $^{13}\text{C}$  NMR of the insoluble organic matter of the Orgueil and Murchison meteorites: quantitative study. *Earth and Planetary Science Letters* 184, 9-21.
- GARRISON, D.H., BOGARD, D.D. (1998) Isotopic composition of trapped and cosmogenic noble gases in several martian meteorites. *Meteoritics and Planetary Science* 33, 721-736.
- GAUTHERON, C., MOREIRA, M. (2002) Helium signature of the subcontinental lithospheric mantle. *Earth and Planetary Science Letters* 199, 39-47.
- GEISS, J., BUEHLER, F., CERUTTI, H., EBERHARDT, P., FILLEAUX, C.H. (1972) Solar wind composition experiments. *Appollo 15 Preliminary Scientific Report*, N.A.S.A.
- GEORGEN, J.E., KURZ, M., DICK, H.J.B., LIN, J. (2003) Low  $^3\text{He}/^4\text{He}$  ratios in basalt glasses from the western Southwest Indian Ridge (10-24°E). *Earth and Planetary Science Letters* 206, 509-528.
- GILLMANN, C., LOGNONNÉ, P., MOREIRA, M. (2011) Volatiles in the atmosphere of Mars: The effects of volcanism and escape constrained by isotopic data. *Earth and Planetary Science Letters* 303, 299-309.
- GONNERMANN, H.M., MUKHOPADHYAY, S. (2007) Non-equilibrium degassing and a primordial source for helium in ocean-island volcanism. *Nature* 449, 1037-1040.
- GONNERMANN, H.M., MUKHOPADHYAY, S. (2009) Preserving noble gases in a convecting mantle. *Nature* 459, 560-564.
- GRAHAM, D.W. (2002) Noble Gas Isotope Geochemistry of Mid-Ocean Ridge and Ocean Island Basalts: Characterization of Mantle Source Reservoirs. In: Porcelli, D., Ballentine, C.J., Wieler, R. (Eds.) *Noble Gases in Geochemistry and Cosmochemistry, Reviews in Mineralogy and Geochemistry*, Vol. 47. Mineralogical Society of America, Washington, D.C., pp. 247-318.
- GRAHAM, D.W., HUMPHRIS, S.E., JENKINS, W.J., KURZ, M.D. (1993) Helium isotope geochemistry of some volcanic rocks from Saint Helena. *Earth and Planetary Science Letters* 110, 121-131.
- GRAHAM, D.W., JOHNSON, K.T.M., DOUGLAS PRIEBE, L., LUPTON, J.E. (1999) Hotspot-ridge interaction along the Southeast Indian Ridge near Amsterdam and St Paul islands: helium isotope evidence. *Earth and Planetary Science Letters* 167, 297-310.
- GRAHAM, D.W., LARSEN, L.M., HANAN, B.B., STOREY, M., PEDERSE, A.K., LUPTON, J.E. (1998) Helium isotope composition of the early Iceland mantle plume inferred from the Tertiary picrites of West Greenland. *Earth and Planetary Science Letters* 160, 241-255.
- GRAND, S.P., VAN DER HILST, R.D., WIDIYANTORO, S. (1997) Global seismic tomography; a snapshot of convection in the Earth. *GSA Today* 7, 1-7.





- GREVESSE, N., ASPLUND, M., SAUVAL, A.J. (2005) The new solar chemical composition. In: Alecian, G., Richard, O., Vauclair, S. (Eds.) *Element Stratification in Stars: 40 Years of Atomic Diffusion. EAS Publications Series* 17, 21–30.
- GRIMBERG, A., BAUR, H., BOCHSLER, P., BUHLER, F., BURNETT, D.S., HAYS, C.C., HEBER, V.S., JUREWICZ, A.J.G., WIELER, R. (2006) Solar wind neon from genesis: implications for the Lunar noble gas record. *Science* 314, 1133–1135.
- GRIMBERG, A., BAUR, H., BÜHLER, F., BOCHSLER, P., WIELER, R. (2008) Solar wind helium, neon and argon isotopic and elemental composition: data from the metallic glass flown on NASA's Genesis mission. *Geochimica et Cosmochimica Acta* 72, 626–645.
- GURENKO, A.A., HOERNLE, K.A., HAUFF, F., SCHMINCKE, H.-U., HAN, D., MIURA, Y.N., KANEOKA, I. (2006) Major, trace element and Nd–Sr–Pb–O–He–Ar isotope signatures of shield stage lavas from the central and western Canary Islands: Insights into mantle and crustal processes. *Chemical Geology* 233, 75–112.
- HALLIDAY, A. (2013) The origins of volatiles in the terrestrial planets. *Geochimica et Cosmochimica Acta* 105, 146–171.
- HAMANO, Y., OZIMA, M. (1978) Earth-atmosphere evolution model based on Ar isotopic data. In: Alexander, E.C., Ojima, M. (Eds.) *Terrestrial rare gases*. Japan Scientific Societies Press, Tokyo, pp. 155–171.
- HAMELIN, C., DOSSO, L., HANAN, B., MOREIRA, M., KOSITSKY, A.P., THOMAS, M.Y. (2011) Geochemical portray of the Pacific Ridge: New isotopic data and statistical techniques. *Earth and Planetary Science Letters* 302, 154–162.
- HANYU, T., KANEOKA, I. (1997) The uniform and low  $^3\text{He}/^4\text{He}$  ratios of HIMU basalts as evidence for their origin as recycled materials. *Nature* 390, 273–276.
- HANYU, T., TATSUMI, Y., KIMURA, J.-I. (2011) Constraints on the origin of the Himu reservoir from He–Ne–Ar isotope systematic. *Earth and Planetary Science Letters* 307, 377–386.
- HARPER, C. L., AND S. B. JACOBSEN (1992) Evidence from coupled  $^{147}\text{Sm}$ – $^{143}\text{Nd}$  and  $^{146}\text{Sm}$ – $^{142}\text{Nd}$  systematics from very early (4.5-Gyr) differentiation of the Earth's mantle. *Nature* 360, 728–732.
- HARRISON, D., BURNARD, P., TURNER, G. (1999) Noble gas behaviour and composition in the mantle: constraints from the Iceland Plume. *Earth and Planetary Science Letters* 171, 199–207.
- HARRISON, D., BURNARD, P., TRIELOFF, M., TURNER, G. (2003) Resolving atmospheric contaminants in mantle noble gas analyses. *Geochemistry Geophysics Geosystems* 4.
- HART, R., HOGAN, L. (1978) Earth degassing models and the heterogeneous vs homogeneous mantle. In: Alexander, E.C., Ojima, M. (Eds.) *Terrestrial rare gases*. Japan Scientific Societies Press, Tokyo, pp. 193–206.
- HART, S.R. (1984a) He diffusion in olivine. *Earth and Planetary Science Letters* 70, 297–302.
- HART, S.R. (1984b) A large-scale isotope anomaly in the Southern Hemisphere mantle. *Nature* 309, 753–757.
- HART, S.R., SCHILLING, J.G., POWELL, J. L. (1973) Basalts from Iceland and along the Reykjanes ridge: Sr isotope geochemistry. *Nature* 246, 104–107.
- HART, S.R., HAURI, E.H., OSCHMANN, L.A., WHITEHEAD, J.A. (1992) Mantle plumes and entrainment: isotopic evidence. *Science* 256, 517–520.
- HART, S., KURZ, M.D., WANG, Z. (2008) Scale length of mantle heterogeneities: Constraints from helium diffusion. *Earth and Planetary Science Letters* 269, 508–517.
- HAWKESWORTH, C.J., NORRIS, M.J., RODDICK, J.C., VOLLMER, R. (1979)  $^{143}\text{Nd}/^{144}\text{Nd}$  and  $^{87}\text{Sr}/^{86}\text{Sr}$  ratios from the Azores and their significance in LIL-element enriched mantle. *Nature* 280, 28–31.
- HEBER, V.S., BROOKER, R.A., KELLEY, S.P., WOOD, B.J. (2007) Crystal-melt partitioning of noble gases (helium, neon, argon, krypton, and xenon) for olivine and clinopyroxene. *Geochimica et Cosmochimica Acta* 71, 1041–1061.



- HEBER, V.S., WIELER, R., BAUR, H., OLINGER, C., FRIEDMANN, A., BURNETT, D.S. (2009) Noble gas composition of the solar wind as collected by the Genesis mission. *Geochimica et Cosmochimica Acta* 73, 7414-7432.
- HEBER, V.S., BAUR, H., MCKEEGAN, K., NEUGEBAUER, M., REISENFELD, D., WIELER, R., WIENS, R. (2012) Isotopic fractionation of solar wind: evidence from fast and slow solar wind collected by the Genesis Mission. *The Astrophysical Journal* 759, 121-133.
- HENNECKE, E.W., MANUEL, O.K. (1975) Noble gas in Hawaiian xenolith. *Nature* 257, 778-780.
- HENNECKE, E.W., MANUEL, O.K., SABU, D.D. (1975) Double beta decay of  $^{128}\text{Te}$ . *Physical Review C* 11, 1378-1384.
- HILTON, D.R., PORCELLI D. (2003) Noble Gases as Mantle Tracers. In: Carlson, R.W. (Ed.) Treatise on Geochemistry, Vol. 2. Elsevier-Pergamon, Oxford, pp. 277-318.
- HILTON, D.R., BARLING, J., WHELLER, G.E. (1995) Effect of shallow-level contamination on the helium isotope systematics of ocean-island lavas. *Nature* 373, 330-333.
- HILTON, D.R., GRÖNVOLD, K., MACPHERSON, C., CASTILLO, P. (1999) Extreme  $^3\text{He}/^4\text{He}$  ratios in northwest Iceland: constraining the common component in mantle plumes. *Earth and Planetary Science Letters* 173, 53-60.
- HILTON, D.R., MACPHERSON, C.G., ELLIOTT, T.R. (2000a) Helium isotope ratios in mafic phenocrysts and geothermal fluid from La Palma, the Canary Islands (Spain): Implications for HIMU mantle sources. *Geochimica et Cosmochimica Acta* 64, 2119-2132.
- HILTON, D.R., THIRLWALL, M.F., TAYLOR, R.N., MURTON, B.J., NICHOLS, A. (2000b) Controls on magmatic degassing along the Reykjanes Ridge with implications for the helium paradox. *Earth and Planetary Science Letters* 183, 43-50.
- HIYAGON, H., OZIMA, M. (1986) Partition of gases between olivine and basalt melt. *Geochimica et Cosmochimica Acta* 50, 2045-2057.
- HIYAGON, H., OZIMA, M., MARTY, B., ZASHU, S., SAKAI, H. (1992) Noble gases in submarine glasses from mid-oceanic ridges and Loihi seamount: constraints on the early history of the Earth. *Geochimica et Cosmochimica Acta* 56, 1301-13016.
- HOFMANN, A.W., WHITE, W.M. (1982) Mantle plumes from ancient oceanic crust. *Earth and Planetary Science Letters* 57, 21-436.
- HOFFMAN, D.C., LAWRENCE, F.O., MEWHERTER, J.L., ROURKE, F.M. (1971) Detection of Plutonium-244 in Nature. *Nature* 234, 132-134.
- HOLLAND, G., BALLENTINE C.J. (2006) Seawater subduction controls the heavy noble gas composition of the mantle. *Nature* 441, 186-191.
- HOLLAND, G., CASSIDY, M., BALLENTINE C.J. (2009) Meteorite Kr in Earth's Mantle Suggests a Late Accretionary Source for the Atmosphere. *Science* 326, 1522-1525.
- HOLLAND, G., SHERWOOD-LOLLAR, B., LI, L., LACRAMPE-COULOUME, G., SLATER, G.F., BALLENTINE, C.J. (2013) Deep fracture fluids isolated in the crust since the Precambrian era. *Nature* 497, 357-360.
- HONDA, M., WOODHEAD, J. D. (2005) A primordial solar-neon enriched component in the source of EM-I-type ocean island basalts from the Pitcairn Seamounts, Polynesia. *Earth and Planetary Science Letters* 236, 597-612.
- HONDA, M., MCDUGALL, I., PATTERSON, D.B., DOULGERIS, A., CLAGUE, D. (1991) Possible solar noble-gas component in Hawaiian basalts. *Nature* 349, 149-151.
- HONDA, M., MCDUGALL, I., PATTERSON, D. B., DOULGERIS, A., CLAGUE, D. (1993) Noble gases in submarine pillow basalt glasses from Loihi and Kilauea, Hawaii: A solar component in the Earth. *Geochimica et Cosmochimica Acta* 57, 859-874.
- HONDA, M., NUTMAN, A., BENNETT, V. (2003) Xenon compositions of magmatic zircons in 3.64 and 3.81Ga meta-granitoids from Greenland-a search for extinct  $^{244}\text{Pu}$  in ancient terrestrial rocks. *Earth and Planetary Science Letters* 207, 69-82.



- HOPP, J., TRIELOFF, M. (2005) Refining the noble gas record of the Réunion mantle plume source: Implications on mantle geochemistry. *Earth and Planetary Science Letters* 240, 573-588.
- HOPP, J., TRIELOFF, M. (2008) Helium deficit in high  $^3\text{He}/^4\text{He}$  parent magmas: Predegassing fractionation, not a "helium paradox". *Geochemistry, Geophysics, Geosystems* 9.
- HOPP, J., TRIELOFF, M., ALTHERR, R. (2004) Neon isotopes in mantle rocks from the Red Sea region reveal large-scale plume-lithosphere interaction. *Earth and Planetary Science Letters* 219, 61-76.
- HUNTEN, D.M., PEPIN, R.O., WALKER, J.C.B. (1987) Mass fractionation in hydrodynamic escape. *Icarus* 43, 22-28.
- HUSS, G.R., LEWIS, R.S., HEMKIN, S. (1996) The 'normal planetary' noble gas component in primitive chondrites: compositions, carrier, and metamorphic history. *Geochimica et Cosmochimica Acta* 60, 3311-3340.
- HUSS, G.R., MESHNIK, A., SMITH, J.B., HOHENBERG, C. (2003) Presolar diamond, silicon carbide, and graphite in carbonaceous chondrites: Implications for thermal processing in the solar nebula. *Geochimica et Cosmochimica Acta* 67, 4823-4848.
- JACKSON, M.G., CARLSON, R.W. (2011) An ancient recipe for flood-basalt genesis. *Nature* 476, 316-319.
- JACKSON, M.G., KURZ, M.D., HART, S., WORKMAN, R. (2007) New Samoan lavas from Ofu Island reveal a hemispherically heterogeneous high  $^3\text{He}/^4\text{He}$  mantle. *Earth and Planetary Science Letters* 264, 360-374.
- JACKSON, M.G., KURZ, M.D., HART, S.R. (2009) Helium and neon isotopes in phenocrysts from Samoan lavas: Evidence for heterogeneity in the terrestrial high  $^3\text{He}/^4\text{He}$  mantle. *Earth and Planetary Science Letters* 287, 519-528.
- JAMBON, A. (1994) Earth degassing and large-scale geochemical cycling of volatile elements In: Carroll, M.R., Holloway, J.R. (Eds.) *Volatiles in Magma, Reviews in Mineralogy and Geochemistry*, Vol. 30. Mineralogical Society of America, Washington, D.C., pp. 479-517.
- JAMBON, A., WEBER, H., BRAUN, O. (1986) Solubility of He, Ne, Ar, Kr and Xe in a basalt melting in the range 1250-1600 °C. Geochemical Implications. *Geochimica et Cosmochimica Acta* 50, 401-408.
- JAVOY, M., PINEAU, F. (1991) The volatiles record of a « popping » rock from the Mid-Atlantic Ridge at 14 °N : chemical and isotopic composition of gas trapped in the vesicles. *Earth and Planetary Science Letters* 107, 598-611.
- JEAN-BAPTISTE, P., ALLARD, P., COUTINHO, R., FERREIRA, T., FOURRE, E., QUEIROZ, G., GASPAR, J.L. (2009) Helium isotopes in hydrothermal volcanic fluids of the Azores archipelago. *Earth and Planetary Science Letters* 281, 70-80.
- JOCHUM, K.P., HOFMANN, A.W., ITO, E., SEUFERT, H.M., WHITE, W.M. (1983) K, U, and Th in mid-ocean ridge basalt glasses and heat production, K/U and K/Rb in the mantle. *Nature* 306, 431-436.
- KAMENETSKY, V.S., MAAS, R., SUSHCHEVSKAYA, N.M., NORMAN, M.D., CARTWRIGHT, I., PEYVE, A. (2001) Remnants of Gondwanan continental lithosphere in oceanic upper mantle: Evidence from the South Atlantic Ridge. *Geology* 29, 243-246.
- KAMINSKI, E., JAVOY, M. (2013) A two-stage scenario for the formation of the Earth's mantle and core. *Earth and Planetary Science Letters* 365, 97-107.
- KANEOKA, I. (1981) Noble gas constraints on the layered structure of the mantle. *Rock Magnetism and Paleogeophysics* 8, 94-99.
- KANEOKA, I. (1983) Noble gas constraints on the layered structure of the mantle. *Nature* 302, 698-700.
- KANEOKA, I., TAKAOKA, N. (1977) Excess  $^{129}\text{Xe}$  and high  $^3\text{He}/^4\text{He}$  ratios in olivine phenocrysts of Kapuho lava and xenolithic dunites from Hawaii. *Rock Magnetism and Paleogeophysics* 4, 139-143.



- KANEOKA, I., TAKAOKA, N. (1978) Excess  $^{129}\text{Xe}$  and high  $^3\text{He}/^4\text{He}$  ratios in olivine phenocrysts of Kapuho Lava and xenolithic dunites from Hawaii. *Earth and Planetary Science Letters* 39, 382-386.
- KANEOKA, I., TAKAOKA, N., CLAGUE, D. (1983) Noble gas systematics for coexisting glass and olivine crystals in basalts and dunite xenoliths from Loihi Seamount. *Earth and Planetary Science Letters* 66, 427-437.
- KANEOKA, I., TAKAOKA, N. (1978) Excess  $^{129}\text{Xe}$  and high  $^3\text{He}/^4\text{He}$  ratios in olivine phenocrysts of Kapuho Lava and xenolithic dunites from Hawaii. *Earth and Planetary Science Letters* 39, 382-386.
- KANEOKA, I., TAKAOKA, N., CLAGUE, D. (1983) Noble gas systematics for coexisting glass and olivine crystals in basalts and dunite xenoliths from Loihi Seamount. *Earth and Planetary Science Letters* 66, 427-437.
- KENDRICK, M. A., M. SCAMBELLURI, M. HONDA, PHILLIPS, D. (2011) High abundances of noble gas and chlorine delivered to the mantle by serpentine subduction. *Nature Geoscience* 4, 807-812.
- KENNEDY, B.M., HIYAGON, H., REYNOLDS, J.H. (1990) Crustal neon: a striking uniformity. *Earth and Planetary Science Letters* 98, 277-286.
- KIRSTEN, T., RICHTER, H., JESSBERGER, E.K. (1983) Double beta decay of  $^{128}\text{Te}$  and  $^{130}\text{Te}$ : Improved limit on the Neutrino restmass. *Zeitschrift für Physik C Particles and Fields* 16, 189-196.
- KLEINE, T., TOUBOUL, M., BOURDON, B., NIMMO, F., MEZGER, K., PALME, H., JACOBSEN, S.B., YIN, Q., HALLIDAY, A. (2009) Hf-W chronology of the accretion and early evolution of asteroids and terrestrial planets. *Geochimica et Cosmochimica Acta* 73, 5150-5188.
- KOGISCO, T., TATSUMI, Y., SHIMODA, G., BARSCZUS, H. (1997) High  $\mu$  (HIMU) ocean islands in southern Polynesia: New evidence for whole mantle scale recycling of subducted oceanic crust. *Journal of Geophysical Research* 102, 8085-8103.
- KUMAGAI, H., DICK, H., KANEOKA, I. (2003) Noble gas signatures of abyssal gabbros and peridotites at an Indian Ocean core complex. *Geochemistry, Geophysics, Geosystems* 4, 9107.
- KUNZ, J. (1999) Is there solar argon in the Earth's mantle? *Nature* 399, 649-650.
- KUNZ, J., STAUDACHER, T., ALLÈGRE, C.J. (1998) Plutonium-Fission Xenon Found in Earth's Mantle. *Science* 280, 877-880.
- KURODA, P. K. (1960) Nuclear Fission in the Early History of the Earth. *Nature* 187.
- KURZ, M.D. (1991) Noble gas isotopes in oceanic basalts: controversial constraints on mantle models. *Mineralogical Association Canada short course* 19, 259-286.
- KURZ, M.D. (1993) Mantle heterogeneity beneath oceanic islands: some inferences from isotopes. *Philosophical Transactions of the Royal Society A* 342, 91-103.
- KURZ, M.D., JENKINS, W.J. (1981) The distribution of helium in oceanic basalt glasses. *Earth and Planetary Science Letters* 53, 41-54.
- KURZ, M.D., JENKINS, W.J., HART, S.R. (1982a) Helium isotopic systematics of oceanic islands and mantle heterogeneity. *Nature* 297, 43-47.
- KURZ, M.D., JENKINS, W.J., SCHILLING, J.-G., HART, S.R. (1982b) Helium isotopic variation in the mantle beneath the central North Atlantic Ocean. *Earth and Planetary Science Letters* 58, 1-14.
- KURZ, M.D., JENKINS, W.J., HART, S.R., CLAGUE, D. (1983) Helium isotopic variations in volcanic rocks from Loihi Seamount and the island of Hawaii. *Earth and Planetary Science Letters* 66, 388-406.
- KURZ, M.D., MEYER, P.S., SIGURDSSON, H. (1985) Helium isotopic systematics within the neovolcanic zones of Iceland. *Earth and Planetary Science Letters* 74, 291-305.
- KURZ, M.D., GARCIA, M.O., FREY, F.A., O'BRIEN, P.A. (1987) Temporal helium isotopic variations within hawaiian volcanoes. *Geochimica et Cosmochimica Acta* 51, 2905-2914.
- KURZ, M.D., KAMMER, D.P., GULESSARIAN, A., MOORE, R.B. (1990) Isotopic variations within oceanic islands: He, Sr and Pb isotopes in basalts from São Miguel, Azores. *EOS* 71, 657.



- KURZ, M.D., CURTICE, J., LOTT III, D.E., SOLOW, A. (2004) Rapid helium isotopic variability in Mauna Kea shield lavas from the Hawaiian Scientific Drilling Project. *Geochemistry Geophysics Geosystems* 5.
- KURZ, M.D., MOREIRA, M., CURTICE, J., LOTT III, D.E., MAHONEY, J.J., SINTON, J.M. (2005) Correlated helium, neon, and melt production on the super-fast spreading East Pacific Rise near 17 °S. *Earth and Planetary Science Letters* 232, 125-142.
- KURZ, M.D., CURTICE, J., FORNARI, D., GEIST, D., MOREIRA, M. (2009) Primitive neon from the center of the Galapagos hotspot. *Earth and Planetary Science Letters* 286, 23-34.
- KYSER, T.K., RISON, W. (1982) Systematics of rare gas isotopes in basic lavas and ultramafic xenoliths. *Journal of Geophysical research* 87, 5611-5630.
- LABROSSE, S., HERNLUND, J.W., COLTICE, N. (2007) A Crystallising dense magma ocean at the base of Earth's mantle. *Nature* 450, 866-869.
- LASSITER, J. C. (2004) Role of recycled oceanic crust in the potassium and argon budget of the Earth: Toward a resolution of the "missing argon" problem. *G-cube* 5.
- LEE, J.-Y., MARTI, K., SEVERINGHAUS, J. P., KAWAMURA, K., YOO, H.-S., LEE, J., KIM, J. (2006) A redetermination of the isotopic abundances of atmospheric Ar. *Geochimica et Cosmochimica Acta* 70, 4507-4512.
- LEWIS, R.S., SRINIVASAN, B., ANDERS, E. (1975) Host phase of a strange xenon component in Allende. *Science* 190, 1251-1262.
- LEWIS, R.S., AMARI, S., ANDERS, E. (1993) Interstellar grains in meteorites: II. SiC and its noble gases. *Geochimica et Cosmochimica Acta* 58, 471-494.
- LUPTON, J.E., CRAIG, H. (1975) Excess  $^3\text{He}$  in oceanic basalts: evidence for terrestrial primordial helium. *Earth and Planetary Science Letters* 26, 133-139.
- LYUBETSKAYA, T., KORENAGA, J. (2007) Chemical composition of Earth's primitive mantle and its variance: 1. Method and results. *Journal of Geophysical research* 112, B03211.
- MADUREIRA, P., MOREIRA, M., MATA, J., ALLÈGRE, C.J. (2005) Primitive helium and neon isotopes in Terceira island (Azores archipelago). *Earth and Planetary Science Letters* 233, 429-440.
- MAHAFFY, P.R., DONAHUE, T.M., OWEN T.C., NIEMANN, H.B., ATREYA, S.K. (1998) Galileo probe measurements of D/H and  $^3\text{He}/^4\text{He}$  in Jupiter's atmosphere. *Space Science Reviews* 84, 251-263.
- MAHONEY, J.J., NATLAND, J.H., WHITE, W.M., POREDA, R., BLOOMER, S.H., FISHER, R.L., BAXTER, A.N. (1989) Isotopic and Geochemical Provinces of the Western Indian Ocean Spreading Centers. *Journal of Geophysical Research* 94 No B4, 4033-4052.
- MAHONEY, J., LEROUX, A.P., PENG, Z., FISHER, R.L., NATLAND, J.H. (1992) Southwestern Limits of Indian Ocean Ridge Mantle and the Origin of Low  $^{206}\text{Pb}/^{204}\text{Pb}$  Mid-Ocean Ridge Basalt: Isotope Systematics of the Central Southwest Indian Ridge (17°-50°E). *Journal of Geophysical Research* 97, 19771-19790.
- MAMYRIN, B.A., TOLSTIKHIN, I., ANUFRIEV, G.S., KAMENSKIY, I.L. (1969a) Anomalous isotopic composition of helium in volcanic gases. *Dokl. Akad. Nauk SSSR* 184, 1197-1199.
- MAMYRIN, B.Z., TOLSTIKHIN, I.N., ANUFRIEV, G.S., KAMENSKIY, I.L. (1969b) Isotopic analysis of terrestrial helium on a magnetic resonance mass spectrometer. *Geochemistry International* 6, 517-524.
- MARROCCHI, Y., RAZAFITIANAMAHARAVO, A., MICHOT, L., MARTY, B. (2005) Low-pressure adsorption of Ar, Kr and Xe on carbonaceous materials (kerogen and carbon blacks), ferrihydrite and montmorillonite: Implications for the trapping of noble gases onto meteoritic matter. *Geochimica et Cosmochimica Acta* 69, 2419-2430.
- MARROCCHI, Y., MARTY, B., REINHARDT, P., ROBERT, F. (2011) Adsorption of xenon ions onto defects in organic surfaces: Implications for the origin and the Nature of organics in primitive meteorites. *Geochimica et Cosmochimica Acta* 75, 6255-6266.



- MARTY, B. (1989) Neon and xenon isotopes in MORB: implications for the Earth-atmosphere evolution. *Earth and Planetary Science Letters* 94, 45-56.
- MARTY, B. (2012) The origins and concentrations of water, carbon, nitrogen and noble gases on Earth. *Earth and Planetary Science Letters* 313-314, 56-66.
- MARTY, B., TRULL, T., LUSSIEZ, P., BASILE, I., TANGUY, J.C. (1994) He, Ar, O, Sr and Nd isotope constraints on the origin and evolution of Mount Etna magmatism. *Earth and Planetary Science Letters* 126, 23-39.
- MARTY, B., PALMA, R.L., PEPIN, R.O., ZIMMERMANN, L., SCHLUTTER, D.J., BURNARD, P., WEST-PHAL, A.J. (2008) Helium and Neon Abundances and Compositions in Cometary Matter. *Science* 319, 75-78.
- MATA, J., MORAIS, L., DOUCELANCE, R., ADER, M., SILVA, L.C. (2010) Noble gases and carbon isotopic signatures of Cape Verde oceanic carbonatites: implications of carbon provenance. *Earth and Planetary Science Letters* 291, 70-83.
- MATHEW, K.J., MARTI, K. (2001) Early evolution of martian volatiles: nitrogen and noble gas components in ALH84001 and Chassigny. *Journal of Geophysical Research* 106, 1401-1422.
- MATHEW, K.J., KIM, J.S., MARTI, K. (1998) Martian atmospheric and indigenous components of xenon and nitrogen in the Shergotty, Nakhla, and Chassigny group meteorites. *Meteoritics and Planetary Science* 33, 655-664.
- MAZOR, E., HEYMAN, D., ANDERS, E. (1970) Noble gases in carbonaceous chondrites. *Geochimica et Cosmochimica Acta* 34, 781-824.
- MCDONOUGH, W. F., SUN, S.-S. (1995) Composition of the Earth. *Chemical Geology* 120, 223-253.
- MCDUGALL, I., HARRISON, T.M. (1999) *Geochronology and Thermochronology by the  $^{40}\text{Ar}/^{39}\text{Ar}$  Method*. Oxford University Press.
- MEIBOM, A., ANDERSON, D.L., SLEEP, N.H., FREL, R., PAGE CHAMBERLAIN, C., HREN, M.T., WOODEN, J.L. (2003) Are high  $^3\text{He}/^4\text{He}$  ratios in oceanic basalts an indicator of deep-mantle plume components? *Earth and Planetary Science Letters* 208, 197-204.
- MESHIK, A., MABRY, J., HOHENBERG, C., MARROCCHI, Y., PRAVDIVTSEVA, O., BURNETT, D., OLINGER, C., WIENS, R., REISENFELD, D., ALLTON, J., MCNAMARA, K., STANSBERY, E., JUREWICZ, A.J.G. (2007) Constraints on neon and argon isotopic fractionation in solar wind. *Science* 318, 433-435.
- MEYZEN, C., LUDDEN, J., HUMLER, E., LUAIS, B., TOPLIS, M.J., MÉVEL, C., STOREY, M. (2005) New insights into the origin and distribution of the DUPAL isotope anomaly in the Indian Ocean mantle from MORB of the Southwest Indian Ridge. *Geochemistry, Geophysics, Geosystems* 6, 11.
- MOREIRA, M. (2007) Constraints on the origin of the  $^{129}\text{Xe}$  on Earth using the tellurium double beta decay. *Earth and Planetary Science Letters* 264.
- MOREIRA, M., ALLÈGRE, C.J. (1998) Helium - Neon systematics and the structure of the mantle. *Chemical Geology* 147, 53-59.
- MOREIRA, M., SARDA, P. (2000) Noble gas constraints on degassing processes. *Earth and Planetary Science Letters* 176, 375-386.
- MOREIRA, M., ALLÈGRE, C.J. (2002) Rare gas systematics on Mid Atlantic Ridge (37°-40°). *Earth and Planetary Science Letters* 198, 401-416.
- MOREIRA, M., ALLÈGRE, C.J. (2004) Helium isotopes on the Macdonald seamount (Austral chain): constraints on the origin of the superswell. *Comptes Rendus Geosciences* 336, 983-990.
- MOREIRA, M., RAQUIN, A. (2007) Noble gas subduction in the mantle: the "subduction barrier" revisited. *Comptes Rendus Geosciences* 339, 937-945.
- MOREIRA, M., STAUDACHER, T., SARDA, P., SCHILLING, J.-G., ALLÈGRE, C.J. (1995) A primitive plume neon component in MORB: The Shona ridge-anomaly, South Atlantic (51-52 °S). *Earth and Planetary Science Letters* 133, 367-377.



- MOREIRA, M., VALBRACHT, P., STAUDACHER, T., ALLÈGRE, C.J. (1996) Rare gas systematics in Red Sea Ridge Basalts. *Geophysical Research Letters* 23, 2453-2456.
- MOREIRA, M., KUNZ, J., ALLÈGRE, C.J. (1998) Rare gas systematics on popping rock : estimates of isotopic and elemental compositions in the upper mantle. *Science* 279, 1178-1181.
- MOREIRA, M., DOUCELANCE, R., DUPRÉ, B., KURZ, M., ALLÈGRE, C.J. (1999) Helium and lead isotope geochemistry in the Azores archipelago. *Earth and Planetary Science Letters* 169, 189-205.
- MOREIRA, M., BREDDAM, K., CURTICE, J., KURZ, M. (2001) Solar neon in the Icelandic mantle: evidence for an undegassed lower mantle. *Earth and Planetary Science Letters* 185, 15-23.
- MOREIRA, M., BLUSZTAJN, J., CURTICE, J., HART, S., DICK, H., KURZ, M.D. (2003) He and Ne isotopes in oceanic crust: implications for noble gas recycling in the mantle. *Earth and Planetary Science Letters* 216, 635-643.
- MOREIRA, M., DOSSO, L., ONDRÉAS, H. (2008) Helium isotopes on the Pacific-Antarctic ridge (52.5°-41.5 °S). *Geophysical Research Letters* 35, L10306.
- MOREIRA, M., KANZARI, A., MADUREIRA, P. (2012) Helium and neon isotopes in São Miguel island basalts, Azores Archipelago: New constraints on the “low  $^3\text{He}$ ” hotspot origin. *Chemical Geology* 322–323, 91-98.
- MOURÃO, C., MOREIRA, M., MATA, J., RAQUIN, A., MADEIRA, J. (2012) Primary and secondary processes constraining the noble gas isotopic signatures of carbonatites and silicate rocks from Brava Island : evidence for a lower mantle origin of the Cape Verde plume. *Contributions to Mineralogy and Petrology* 163, 995–1009.
- MOUREU, C. (1913) Recherche sur les gaz rares des sources thermales. Leurs enseignements concernant la radioactivité et la physique du globe. *Journal de Chimie Physique* 11, 63-152.
- MOUREU, C. (1927) Discours et conférences sur la science et ses applications. Gauthier-Villars, Paris, pp. 369.
- MOUREU, C., LEPAPE, A. (1914) Les gaz rares des grisous. In: Extrait des Annales des Mines, Dunod, H. et Pinat, E., Editeurs, Paris.
- MUKHOPADHYAY, S. (2012) Early differentiation and volatile accretion recorded in deep mantle Neon and Xenon. *Nature* 486, 101-104.
- NIEDERMANN, S., BACH, W. (1998) Anomalously nucleogenic neon in North Chile Ridge basalt glasses suggesting a previously degassed mantle source. *Earth and Planetary Science Letters* 160, 447-462.
- NIEDERMANN, S., BACH, W., ERZINGER, J. (1997) Noble gas evidence for a lower mantle component in MORB from the southern East Pacific Rise: Decoupling of Helium and neon isotope systematics. *Geochimica et Cosmochimica Acta* 61, 2697-2715.
- NOTESCO, G., BAR-NUN, A., OWEN, T. (2003) Gas trapping in water ice at very low deposition rates and implications for comets. *Icarus* 162, 183-189.
- OKAZAKI, R., TAKAOKA, N., NAGAO, K., NAKAMURA, T. (2010) Noble gases in enstatite chondrites released by stepped crushing and heating. *Meteoritics and Planetary Science* 45, 339-360.
- O’NEIL, J., CARLSON, R.W., FRANCIS, D., STEVENSON, R.K. (2008) Neodymium-142 evidence for Hadean mafic crust. *Science* 321, 1828–1831.
- O’NIONS, R.K., EVENSEN, N.M., HAMILTON, P.J. (1979) Geochemical modeling of mantle differentiation and crustal growth. *Journal of Geophysical Research* 84, 6091-6101.
- OTT, U. (2002) Noble gases in meteorites - trapped components. In: Porcelli, D., Ballentine, C.J., Wieler, R. (Eds.) Noble Gases in Geochemistry and Cosmochemistry, Reviews in Mineralogy and Geochemistry, Vol. 47. Mineralogical Society of America, Washington, D.C., pp. 71-100.
- OTT, U., MACK, R., CHANG, S. (1981) Noble gas-rich separates from the Allende meteorites. *Geochimica et Cosmochimica Acta* 45, 1751-1788.





- OWEN, T., BAR-NUN, A. (1996) Comets, Meteorites and Atmospheres. In: Rickman, H., Valtonen, M.J. (Eds.) *Worlds in Interaction: Small Bodies and Planets of the Solar System*. Springer, pp.425-432.
- OWEN, T., BAR-NUN, A., KLEINFELD, I. (1992) Possible cometary origin of heavy noble gases in the atmospheres of Venus, Earth and Mars. *Nature* 358, 43-46.
- OZIMA, M. (1973) Was the Evolution of the Atmosphere Continuous or Catastrophic? *Nature Physical Science* 246, 41-42.
- OZIMA, M. (1975) Ar isotopes and Earth-atmosphere evolution models. *Geochimica et Cosmochimica Acta* 39, 1127-1134.
- OZIMA, M., KUDO, K. (1972) Excess Argon in Submarine Basalts and an Earth-Atmosphere Evolution Model. *Nature Physical Science* 239, 23-24.
- OZIMA, M., ZASHU, S. (1983) Noble gases in submarine pillow-glasses. *Earth and Planetary Science Letters* 62, 24-40.
- OZIMA, M., ZASHU, S. (1988) Solar-type Ne in Zaire cubic diamonds. *Geochimica et Cosmochimica Acta* 52, 19-25.
- OZIMA, M., PODOZEK, F.A., IGARASHI, G. (1985) Terrestrial xenon isotope constraints on the early history of the Earth. *Nature* 315, 471-474.
- PALMIERI, L. (1881) Della riga dell'Helium apparsa in una recente sublimazione Vesuviana. *Rendiconto dell'Accademia delle Scienze Fisiche e Matematiche Serie I*, vol XX, 150-172.
- PARAI, R., MUKHOPADHYAY, S., LASSITER, J. C. (2009) New constraints on the HIMU mantle from neon and helium isotopic compositions of basalts from the Cook-Austral Islands. *Earth and Planetary Science Letters* 277, 253-261.
- PARAI, R., MUKHOPADHYAY, S., STANDISH, J.J. (2012) Heterogeneous upper mantle Ne,Ar and Xe isotopic compositions and a possible Dupal noble gas signature recorded in basalts from the Southwest Indian Ridge. *Earth and Planetary Science Letters* 359-360, 227-239.
- PARMAN, S.W., KURZ, M.D., HART, S.R., GROVE, T.L. (2005) Helium solubility in olivine and implications for high  $^3\text{He}/^4\text{He}$  in ocean island basalts. *Nature* 437, 1140-1143.
- PATTERSON, D.B., HONDA, M., MCDUGALL, I. (1990) Atmospheric contamination: a possible source for heavy noble gases basalts from Loihi seamount, Hawaii. *Geophysical Research Letters* 17, 705-708.
- PATZER, A., SCHULTZ, L. (2001) Noble gases in enstatite chondrites I: Exposure ages, pairing, and weathering effects. *Meteoritics and Planetary Science* 36, 947-961.
- PATZER, A., SCHULTZ, L. (2002) Noble gases in enstatite chondrites II: The trapped component. *Meteoritics and Planetary Science* 37, 601-612.
- PEPIN, R.O. (1997) Evolution of Earth's noble gases: consequences of assuming hydrodynamic loss driven by giant impact. *Icarus* 126, 148-156.
- PEPIN, R.O. (1998) Isotopic evidence for a solar argon component in the Earth's mantle. *Nature* 394, 664-667.
- PEPIN, R.O. (2003) On Noble Gas Processing in the Solar Accretion Disk. *Space Science Reviews* 106, 211-230.
- PEPIN, R.O. (2013) Reply to comment on "Chondritic-like xenon trapped in Archean rocks: A possible signature of the ancient atmosphere" by Pujol, M., Marty, B., Burgess, R. (*Earth and Planetary Science Letters* 308 (2011) 298-306). *Earth and Planetary Science Letters* 371-372, 296-298.
- PEPIN, R.O., PORCELLI, D. (2006) Xenon isotope systematics, giant impacts, and mantle degassing of the early Earth. *Earth and Planetary Science Letters* 250, 470-485.
- PEPIN, R.O., BECKER, R.H., RIDER, P.E. (1995) Xenon and krypton isotopes in extraterrestrial regolith soils and in the solar wind. *Geochimica et Cosmochimica Acta* 59, 4997-5022.



- PEPIN, R.O., SCHLUTTER, D.J., BECKER, R.H., REISENFELD, D.B. (2012) Helium, neon, and argon composition of the solar wind as recorded in gold and other Genesis collector materials. *Geochimica et Cosmochimica Acta* 89, 62-80.
- PLANK, T., LANGMUIR, C. (1998) The chemical composition of subducting sediment and its consequences for the crust and mantle. *Chemical Geology* 145, 325-394.
- POLLACK, J.B., BLACK, D.C. (1979) Implications of the gas compositional measurements of Pioneer Venus for the origin of planetary atmospheres. *Science* 205, 57-59.
- POLLACK, J.B., BLACK, D.C. (1982) Noble gases in planetary atmospheres: implications for the origin and evolution of atmospheres. *Icarus* 51, 169-198.
- PORCELLI, D., WASSERBURG, G.J. (1995) Mass transfer of xenon through a steady-state upper mantle. *Geochimica et Cosmochimica Acta* 59, 1991-2007.
- PORCELLI, D., HALLIDAY, A. (2001) The core as a possible source of mantle helium. *Earth and Planetary Science Letters* 192, 45-56.
- PORCELLI, D., ELLIOTT, T. (2008) The evolution of He Isotopes in the convecting mantle and the preservation of high  $^3\text{He}/^4\text{He}$  ratios. *Earth and Planetary Science Letters* 269, 175-185.
- PORCELLI, D.R., O'NIONS, R.K., O'REILLY, S.Y. (1986) Helium and strontium isotopes in ultramafic xenoliths. *Chemical Geology* 54, 237-249.
- PORCELLI, D.R., STONE, J.O.H., O'NIONS, R.K. (1987) Enhanced  $^3\text{He}/^4\text{He}$  ratios and cosmogenic helium in ultramafic xenoliths. *Chemical Geology* 64, 25-33.
- POREDA, R. (1985) Helium-3 and deuterium in back-arc basalts: Lau Basin and the Mariana Trough. *Earth and Planetary Science Letters* 73, 244-254.
- POREDA, R.J., FARLEY, K.A. (1992) Rare gases in Samoan xenoliths. *Earth and Planetary Science Letters* 113, 129-144.
- POREDA, R., RADICATI DI BROZOLO, F. (1984) Neon isotope variations in Mid-Atlantic Ridge basalts. *Earth and Planetary Science Letters* 69, 277-289.
- POREDA, R., SCHILLING, J.G., CRAIG, H. (1986) Helium and hydrogen isotopes in ocean-ridge basalts north and south of Iceland. *Earth and Planetary Science Letters* 78, 1-17.
- PUJOL, M., MARTY, B., BURGESS, R. (2011) Chondritic-like xenon trapped in Archean rocks: A possible signature of the ancient atmosphere. *Earth and Planetary Science Letters* 308, 298-306.
- RAMSAY, W. (1904) The Rare Gases of the Atmosphere. Nobel Lecture [http://www.nobelprize.org/nobel\\_prizes/chemistry/laureates/1904/ramsay-lecture.html](http://www.nobelprize.org/nobel_prizes/chemistry/laureates/1904/ramsay-lecture.html).
- RAQUIN, A., MOREIRA, M. (2009) Air  $^{38}\text{Ar}/^{36}\text{Ar}$  in the mantle: implication on the Nature of the parent bodies of the Earth. *Earth and Planetary Science Letters* 287, 551-558.
- RAQUIN, A., MOREIRA, M., GUILLON, F. (2008) He, Ne and Ar systematics in single vesicles: Mantle isotopic ratios and origin of the air component in basaltic glasses. *Earth and Planetary Science Letters* 274, 142-150.
- RAYLEIGH, J. (1894) On an Anomaly encountered in Determinations of the Density of Nitrogen Gas. *Proceedings of the Royal Society* 4, 340.
- RAYLEIGH, J., RAMSAY, W. (1895) Argon, A new constituent of the Atmosphere. *Proceedings of the Royal Society* 57, 265-287.
- REYNOLDS, J. H. (1960) determination of the age of the elements. *Physical Review Letters* 4, 8-10.
- RICHARD, P., SHIMIZU, N., ALLÈGRE, C.J. (1976)  $^{143}\text{Nd}/^{144}\text{Nd}$  a natural tracer: an application to oceanic basalt. *Earth and Planetary Science Letters* 31, 269-278.
- RIDER, P.E., PEPIN, R.O., BECKER, R.H. (1995) Noble gases and nitrogen released from lunar soils by acid etching. *Geochimica et Cosmochimica Acta* 59, 4983-4996.
- RISON, W., CRAIG, H. (1983) Helium isotopes and mantle volatiles in Loihi Seamount and Hawaiian Island basalts and xenoliths. *Earth and Planetary Science Letters* 66, 407-426.



- RIZO, H., BOYET, M., Blichert-Toft, J., O'NEIL, J., ROSING, M.T., PAQUETTE, J.-L. (2012) The elusive Hadean enriched reservoir revealed by  $^{142}\text{Nd}$  deficits in Isua Archean rocks. *Nature* 491, 96–100.
- ROTH, A., BOURDON, B., MOJZSIS, S.J., TOUBOUL, M., SPRUNG, P., GUITREAU, M., Blichert-Toft, J. (2013) Inherited  $^{142}\text{Nd}$  anomalies in Eoarchean protoliths. *Earth and Planetary Science Letters* 361, 50–57.
- SAMUEL, H., FARNETANI, C. (2003) Thermochemical convection and helium concentrations in mantle plumes. *Earth and Planetary Science Letters* 207, 39–56.
- SARDA, P. (1991) Aspect de la géochimie des gaz rares. Thèse Université Paris 7.
- SARDA, P. (2004) Surface noble gas recycling to the terrestrial mantle. *Earth and Planetary Science Letters* 228, 49–63.
- SARDA, P., GRAHAM, D.W. (1990) Mid-ocean ridge popping rocks: implications for degassing at ridge crests. *Earth and Planetary Science Letters* 97, 268–289.
- SARDA, P., STAUDACHER, T. (1991) Terrestrial primordial neon. *Nature* 352, 388.
- SARDA, P., STAUDACHER, T., ALLÈGRE, C.J. (1985)  $^{40}\text{Ar}/^{36}\text{Ar}$  in MORB glasses: constraints on atmosphere and mantle evolution. *Earth and Planetary Science Letters* 72, 357–375.
- SARDA, P., STAUDACHER, T., ALLÈGRE, C.J. (1988) Neon isotopes in submarine basalts. *Earth and Planetary Science Letters* 91, 73–88.
- SARDA, P., MOREIRA, M., STAUDACHER, T. (1998) Argon-lead isotopic correlation in Mid-Atlantic Ridge Basalts. *Science* 283, 666–668.
- SARDA, P., MOREIRA, M., STAUDACHER, T., SCHILLING, J.-G., ALLÈGRE, C.J. (2000) Rare gas systematics on the southernmost Mid-Atlantic Ridge: constraints on the lower mantle and the Dupal source. *Journal of Geophysical Research* 105, 5973–5996.
- SCHELHASS, N., OTT, U., BEGEMANN, F. (1990) Trapped noble gases in unquilted ordinary chondrites. *Geochimica et Cosmochimica Acta* 54, 2869–2882.
- SCHERSTÉN, A., ELLIOTT, T., HAWKESWORTH, C.J., NORMAN, M. (2004) Tungsten isotope evidence that mantle plumes contain no contribution from the Earth's core. *Nature* 427, 234–237.
- SCHIANO, P., PROVOST, A., CLOCCHIATTI, R., FAURE, F. (2007) Transcrystalline Melt Migration and Earth's Mantle. *Science* 314, 970–974.
- SCHILLING, J.G. (1975) Azores mantle blob: rare earth evidence. *Earth and Planetary Science Letters* 25, 103–115.
- SCHILLING, J.G. (1991) Fluxes and excess temperatures of mantle plumes inferred from their interaction with migrating mid-ocean ridges. *Nature* 352, 397–402.
- SCHULTZ, L., FRANKE, L. (2004) Helium, neon and argon in meteorites, a data collection. *Meteoritics and Planetary Science* 39, 1889–1890.
- SCHULTZ, L., WEBER, H., FRANKE, L. (2005) Rumuruti chondrites: Noble gases, exposure ages, pairing, and parent body history. *Meteoritics and Planetary Science* 40, 515–556.
- SCHWARTZMAN, D.W. (1973) Argon degassing models of the Earth. *Nature Physical Sciences* 245, 20–21.
- SHAW, A.M., HILTON, D.R., MACPHERSON, C.G., SINTON, J.M. (2001) Nucleogenic neon in high  $^3\text{He}/^4\text{He}$  lavas from the Manus back-arc basin: a new perspective on He–Ne decoupling. *Earth and Planetary Science Letters* 194, 53–66.
- SHAW, A.M., HILTON, D.R., FISHER, T.P., WALKER, J.A., DE LEEW, G.A.M. (2006) Helium isotope variations in mineral separates from Costa Rica and Nicaragua: Assessing crustal contributions, timescale variations and diffusion-related mechanisms. *Chemical Geology* 230, 124–139.
- SHILLIBEER, H.A., RUSSELL, R.D. (1955) The argon-40 content of the atmosphere and the age of the earth. *Geochimica et Cosmochimica Acta* 8, 16–21.
- SIEBERT, J., BADRO, J., ANTONANGELI, D., RYERSON, F.J. (2012) Metal–silicate partitioning of Ni and Co in a deep magma ocean. *Earth and Planetary Science Letters* 321–322, 189–197.



- STAUDACHER, T. (1987) Upper mantle origin for Harding County well gases. *Nature* 325, 605-607.
- STAUDACHER, T., ALLÈGRE, C.J. (1982) Terrestrial xenology. *Earth and Planetary Science Letters* 60, 389-406.
- STAUDACHER, T., ALLÈGRE, C.J. (1988) Recycling of oceanic crust and sediments: the noble gas subduction barrier. *Earth and Planetary Science Letters* 89, 173-183.
- STAUDACHER, T., KURZ, M.D., ALLÈGRE, C.J. (1986) New noble-gas data on glass samples from Loihi seamount and Hualalai and on dunite samples from Loihi and Reunion island. *Chemical Geology* 56, 193-205.
- STAUDACHER, T., SARDA, P., RICHARDSON, S.H., ALLÈGRE, C.J., SAGNA, I., DMITRIEV, L.V. (1989) Noble gases in basalt glasses from a Mid-Atlantic ridge topographic high at 14 °N: geodynamic consequences. *Earth and Planetary Science Letters* 96, 119-133.
- STUART, F.M., LASS-EVANS, S., FITTON, J.G., ELLAM R.M. (2003) High  $^3\text{He}/^4\text{He}$  ratios in picritic basalts from Baffin Island and the role of a mixed reservoir in mantle plumes. *Nature* 424, 57-59.
- SWINDLE, T.D. (2002) Martian Noble Gases. In: Porcelli, D., Ballentine, C.J., Wieler, R. (Eds.) *Noble Gases in Geochemistry and Cosmochemistry*, Reviews in Mineralogy and Geochemistry, Vol. 47. Mineralogical Society of America, Washington, D.C., pp. 171-190.
- TAKAOKA, N. (1972) An interpretation of general anomalies of xenon and the isotopic composition of primitive xenon. *Mass Spectroscopy* 20, 287-302.
- TERRIBILINI, D., EUGSTER, O., BURGER, M., JAKOB, A., KRAHENBUHL, U. (1998) Noble gases and chemical composition of Shergotty mineral fractions, Chassigny, and Yamato 793605: The trapped argon-40/argon-36 ratio and ejection times of Martian meteorites. *Meteoritics and Planetary Science* 33, 677-684.
- TOLSTIKHIN, I.N. (1975) Helium isotopes in the Earth's interior and in the atmosphere: a degassing model of the Earth. *Earth and Planetary Science Letters* 26, 88-96.
- TOLSTIKHIN, I., MARTY, B. (1998) The evolution of terrestrial volatiles: a view from helium, neon, argon and nitrogen isotope modelling. *Chemical Geology* 147, 27-52.
- TOLSTIKHIN, I., HOFMANN, A.W. (2005) Early crust on top of the Earth's core. *Physics of the Earth and Planetary Interiors* 148, 109-130.
- TRIELOFF, M., KUNZ, J. (2005) Isotope systematics of noble gases in the Earth's mantle: possible sources of primordial isotopes and implications for mantle structure. *Physics of the Earth and Planetary Interiors* 148, 13-38.
- TOLSTIKHIN, I., MAMYRIN, B.A., KHABARIN, L.B., ERLIKH, E.N. (1974) Isotope composition of helium in ultrabasic xenoliths from volcanic rocks of Kamchatka. *Earth and Planetary Science Letters* 22, 75-84.
- TRIELOFF, M., J. KUNZ, D. A. CLAGUE, D. HARRISON, ALLÈGRE, C.J. (2000) The Nature of pristine noble gases in mantle plumes. *Science* 288, 1036-1038.
- TRIELOFF, M., KUNZ, J., ALLÈGRE, C.J. (2002) Noble gas systematics of the Reunion mantle plume source and the origin of primordial noble gases in Earth's mantle. *Earth and Planetary Science Letters* 200, 297-313.
- TRIELOFF, M., FALTER, M., JESSBERGER, E.K. (2003) The distribution of mantle and atmospheric argon in oceanic basalt glasses. *Geochimica et Cosmochimica Acta* 67, 1229-1245.
- TUCKER, J.M., MUKHOPADHYAY, S., SCHILLING, J.-G. (2012) The heavy noble gas composition of the depleted MORB mantle (DMM) and its implications for the preservation of heterogeneities in the mantle. *Earth and Planetary Science Letters* 355-356, 244-254.
- TUREKIAN, K.K. (1959) The terrestrial economy of helium and argon. *Geochimica et Cosmochimica Acta* 17, 37-43.
- TURNER, G. (1989) The outgassing history of the Earth's atmosphere. *Journal of the Geological Society* 146, 147-154.



- TURNER, G., HARRISON, T.M., HOLLAND, G., MOJZSIS, S.J., GILMOUR, J.D. (2004) Xenon from extinct  $^{244}\text{Pu}$  in ancient terrestrial zircons. *Science* 89-91.
- TURNER, G., BUSFIELD, A., CROWTHER, S.A., HARRISON, M., MOKZSIS, S.J., GILMOUR, J.D. (2007) Pu-Xe, U-Xe, U-Pb chronology and isotope systematics of ancient zircons from Western Australia. *Earth and Planetary Science Letters* 261, 491-499.
- VALBRACHT, P.J., HONDA, M., MATSUMOTO, T., MATIELLI, N., MCDUGALL, I., RAGETTLI, R., WEIS, D. (1996) Helium, Neon and argon isotope systematics in Kerguelen ultramafic xenoliths Implications for mantle source signature. *Earth and Planetary Science Letters* 138, 29-38.
- VALBRACHT, P.J., STAUDACHER, T., MALAHOFF, A., ALLÈGRE, C.J. (1997) Noble gas systematics of deep riftzone glasses from Loihi seamount, Hawaii. *Earth Planetary Science Letters* 150, 399-411.
- VAN DER HILST, R.D., WIDIYANTORO, S., ENGDAHL, E.R. (1997) Evidence for deep mantle circulation from global tomography. *Nature* 386, 578-584.
- VAN Keken, P., BALLENTINE, C.J., PORCELLI, D. (2001) A dynamical investigation of the heat and helium imbalance. *Earth and Planetary Science Letters* 188, 421-434.
- VILLENEUVE, J., CHAUSSIDON, M., LIBOUREL, G. (2009) Homogeneous distribution of  $^{26}\text{Al}$  in the Solar System from the Mg isotopic composition of chondrules. *Science* 325, 985-988.
- VIS, R.D., HEYMANN, D. (1999) On the Q-phase of carbonaceous chondrites. *Nuclear Instruments and Methods in Physics Research B* 158, 538-543.
- WALSH, K.J., MORBIDELLI, A., RAYMOND, S.N., O'BRIEN, D.P., MANDELL, A.M. (2011) A low mass for Mars from Jupiter's early gas-driven migration. *Nature* 475, 206-209.
- WASSON, J.T., KALLEYMAN, G.W. (1988) Composition of chondrites. *Philosophical Transactions of the Royal Society A* 325, 535-544.
- WEIS, D., BASSIAS, Y., GAUTIER, I., MENNESSIER, J.-P. (1989) Dupal anomaly in existence 115 Ma ago: Evidence from isotopic study of the Kerguelen Palteau (South Indian Ocean), *Geochimica et Cosmochimica Acta* 53, 2125-2131.
- WHITE, W.M., HOFMANN, A.W. (1982) Sr and Nd isotope geochemistry of oceanic basalts and mantle evolution. *Nature* 296, 821-825.
- WHITE, W.M., SCHILLING, J.G., HART, S.R. (1976) Evidence for the Azores mantle plume from strontium isotopes geochemistry of the Central North Atlantic. *Nature* 263, 659-663.
- WIELER, R. (2002) Noble gases in the Solar System. In: Porcelli, D., Ballentine, C.J., Wieler, R. (Eds.) *Noble Gases in Geochemistry and Cosmochemistry, Reviews in Mineralogy and Geochemistry*, Vol. 47. Mineralogical Society of America, Washington, D.C., pp. 21-70.
- WIELER, R., BAUR, H. (1994) Krypton and xenon from the solar wind and solar energetic particles in two lunar ilmenites of different antiquity. *Meteoritics* 29, 570-580.
- WIELER, R., BAUR, H., PEDRONI, A., SIGNER, P., PELLAS, P. (1989) Exposure history of the regolithic chondrite Fayetteville: I. Solar-gas-rich matrix. *Geochimica et Cosmochimica Acta* 53, 1441-1448.
- WIELER, R., GRIMBERG, A., HEBER, V.S. (2007) Consequences of the non-existence of the "SEP" component for noble gas geo- and cosmochemistry. *Chemical Geology* 244, 382-390.
- WOODHEAD, J.D., DEVEY, C.W. (1993) Geochemistry of the Pitcairn seamounts, I: source character and temporal trends. *Earth and Planetary Science Letters* 116, 81-99.
- XIE, S., TACKLEY, P.J. (2004) Evolution of helium and argon isotopes in a convecting mantle. *Physics of the Earth and Planetary Interiors* 146, 417-439.
- YAMAMOTO, J., BURNARD, P. (2005) Solubility controlled noble gas fractionation during magmatic degassing: Implications for noble gas compositions of primary melts of OIB and MORB. *Geochimica et Cosmochimica Acta* 69, 727-734.
- YATSEVICH, I., HONDA, M. (1997) Production of nucleogenic neon in the Earth from natural radioactive decay. *Journal of Geophysical Research* 102, 10291-10298.
- YOKOCHI, R., MARTY, B. (2004) A determination of the neon isotopic composition of the deep mantle. *Earth and Planetary Science Letters* 225, 77-88.



- ZADNIK, M.G., JEFFERY, P.M. (1985) Radiogenic neon in Archean anorthosite. *Chemical Geology* 52, 119-125.
- ZARTMAN, R.E., DOE, B.R. (1981) Plumbotectonics- The Model. *Tectonophysics* 75, 135-162.
- ZINDLER, A., HART, S.R. (1986a) Chemical Geodynamics. *Annual Review of Earth and Planetary Sciences*, 4, 493-571.
- ZINDLER, A., HART, S. (1986b) Helium: problematic primordial signals. *Earth and Planetary Science Letters* 79, 1-8.



# GLOSSARY

- 2 $\pi$ D43:** Name of a gas-rich sample collected at 14 °N on the Mid Atlantic Ridge. This sample is a “popping rock” because it is so rich that on the bridge of the ship, the sample popped due to decompression.
- AMU:** Atomic Mass Unit.
- Angra dos Reis:** An angrite meteorite, derived from the crystallised igneous crust of a differentiated asteroid. Similar to eucrite meteorites but derived from a different parent asteroid. Angra dos Reis is widely used to inter-calibrate different meteorite chronometers.
- AVCC:** AVCC is a bulk chondrite composition, hence representing a mixture of phase Q and other components such as pre-solar grains.
- BMO:** Basal Magma Ocean. Labrosse *et al.* (2007) have suggested that the deep mantle of the Earth was molten during a long part of the Earth’s History. Its crystallisation may have produced peculiar chemical and isotopic signatures in the deep mantle.
- BSE:** Bulk Silicate Earth. This reservoir corresponds to the Bulk Earth minus the core. BSE contains all the non-siderophile elements.
- CAI:** Calcium-Aluminium Inclusions. These inclusions rich in Ca, Al, Ti are found in chondrites. They are the first solids to condense from a hot gas in the Solar System. Their age is estimated at 4.567 Ga.



**Cm<sup>3</sup> STP g<sup>-1</sup>:** Concentration of gas in a sample expressed in cubic centimetres (at standard pressure and temperature) per gram of sample.

**Chass-S:** Name of the xenon isotopic composition in Mars' Interior following Matthew and Marti (2001).

**Chondrites:** Chondrites are the most primitive meteorites. They are undifferentiated objects (*i.e.* unmelted), having the chemical compositions close to the Sun, except for the very volatile elements. Chondrites are cosmic sediments. They are comprised of chondrules, metal and refractory inclusions in a fine-grain matrix. There are different types of chondrites: carbonaceous, enstatite, ordinary and rumuruti.

**CI:** Carbonaceous chondrites of the Ivuna group. CI are the most primitive chondrite group. They have the chemical compositions that are the closest to that of the Sun.

**Cosmogenic:** Nuclides produced by interaction of cosmic rays (high energy extra-solar system particles) with samples. For example <sup>3</sup>He is produced as a product of the spallation of original sample atoms by cosmic rays.

**CV:** Carbonaceous chondrites of the Vigarano group.

**DICE:** Name of a sample collected in Iceland (under-glacier pillow) (Harrison *et al.*, 1999). This sample is gas-rich allowing the precise measurement of noble gases in the OIB source. This is the equivalent to the MORB sample 2πD43 for OIB.

**DUPAL:** The DUPAL anomaly (from DUPré and ALLègre) is the name of geochemical province, located mostly in the Indian Ocean. MORB and OIB from the Indian Ocean present peculiar isotopic ratios of lithophile elements compared to that of the other mantle domains.

**EPR:** East Pacific Rise.

**Eucrites:** Meteorites from the crystallised, igneous crust of a differentiated asteroid, believed to be Vesta 4.

**Fissiogenic:** Nuclides produced by the fission of heavy nuclides. For example, the heavy Xe isotopes <sup>131</sup>Xe–<sup>136</sup>Xe are products of the spontaneous fission of extant <sup>238</sup>U and now extinct <sup>244</sup>Pu.

**Genesis:** Space mission to collect solar wind on different collectors and return to Earth for analysis.

**HIMU:** In the isotopic systematics developed by Hart (1988), HIMU is the name of a mantle component having extreme, radiogenic lead isotopic signatures. The acronym derives from "High μ" where μ is the <sup>238</sup>U/<sup>204</sup>Pb ratio. Most of the scientists agree to say HIMU represents recycled oceanic crust into the mantle, old enough to have produced radiogenic lead isotopic ratios.

**HL:** A type of pre-solar grain, carrier of the signature.



**Late Veneer:** An addition of meteoritic material to the Earth after the main phase of accretion and notably post core formation. This flux (~0.5% by mass of the Earth) dominates the budgets of elements sequestered into the core (the highly siderophile elements) and potentially volatile elements lost during accretion.

**MORB:** Mid Ocean Ridge Basalts. Samples from the oceanic crust.

**Neon A and E:** Name of components observed in meteorites having peculiar neon isotopic signatures. These components reflect the presence of pre-solar diamonds in chondrites. They also have the name P3 or HL.

**Neon B:** Name of a component in meteorites and on the Lunar soil having a neon composition distinct to that of the Sun and the Earth's atmosphere. It certainly represents solar wind implantation that is accompanied with isotopic fractionation.

**Nucleogenic:** Nuclides formed by the reaction of naturally occurring neutrons (from the spontaneous nuclear fission of actinides, such as U) with host atoms in a sample. For example the addition of a neutron to  $^{24}\text{Mg}$  resulting in the ejection of an alpha particle and production of  $^{21}\text{Ne}$ .

**Popping Rock:** A gas-rich MORB sample (see **2πD43**).

**Pre-Solar Grains:** Micron-sized (and smaller) grains (diamonds, graphite, SiC) that formed outside our solar system. These grains survive in primitive (chondritic) meteorites and are identified by their exotic isotopic signatures, *e.g.*, the Neon A and E signatures. Pre-solar grains are often derived by aggressive dissolution of the meteorite host to leave these resistant grains in various acid-treated residues.

**OIB:** Oceanic Island Basalts. Intra-plate lavas that form the 'hotspot' islands in oceanic basins, which many workers link with deep-seated mantle plumes.

**P3:** A type of pre-solar grain, carrier of Neon A.

**Primitive:** A portion of mantle little-affected by magmatic processes since formation. Thus primitive mantle is thought to have un radiogenic He isotope ratios (low  $^4\text{He}/^3\text{He}$  or high  $\text{R}/\text{R}_a$ ).

**Primordial:** A portion of mantle un-affected by magmatic processes since formation. Often used synonymously with 'primitive', see above and to describe unradiogenic He isotope ratios.

**Q (Phase Q):** Name of the main carrier of heavy noble gases in chondrites. The Q stands for "quintessence". It can be isolated after HF-HCl acid digestion of chondrites. Phase Q is carbonaceous.

**R/R<sub>a</sub>:** Sample  $^3\text{He}/^4\text{He}$  relative to atmospheric  $^3\text{He}/^4\text{He}$ . This traditional nomenclature reports He isotope ratios in a manner inverse to the standard approach of radiogenic isotope of non-radiogenic isotope. Thus He isotopes are also reported as  $^4\text{He}/^3\text{He}$ .



- Radiogenic:** Daughter nuclides formed by the decay of radioactive parents. For example  $^{40}\text{Ar}$  produced by electron capture of  $^{40}\text{K}$ .
- SEP:** SEP refers to Solar Energetic Particles. They correspond to solar flares. Until Genesis probe return, it was proposed that the neon B component reflects a mixture of normal solar wind and SEP implantation.
- SNC:** Name of a group of meteorites supposed to come from Mars (S for Shergotty, N for Nakhla, C for Chassigny).
- U-Xe:** U-Xe is named after “Ur-xenon” for primitive in German (*e.g.*, *ursprünglichen* = initial). This is a mathematical construct to address particularly the issue of the xenon pattern in Earth’s atmosphere. U-Xe defined by Pepin and Phinney (1976) is similar to the “primitive” xenon of Takaoka (1972).
- Well-gases:** Natural,  $\text{CO}_2$ -rich gases with high noble gas contents with a mantle affinity.



# INDEX

## A

- accretion 229, 230, 239-242, 247, 258, 265,  
302, 314, 321, 326, 337, 339, 355, 357,  
358, 364, 371, 373, 377, 378, 386, 389,  
390, 399
- Allègre, C. IV, 235-238, 241, 244, 273-276,  
278, 284, 285, 289-294, 297, 309, 310,  
311, 318, 319, 324, 325, 340-342, 347,  
348, 351, 359, 362, 377, 378, 381,  
386-389, 392-394, 398
- Anderson, D. 273, 331, 334, 378, 388
- Apollo 246, 247, 353, 378, 381
- Archean 302, 366-369, 390, 391, 395
- ARESIBO 275, 292, 294, 302, 308, 321
- Argon 230, 232, 234, 240, 247, 250, 251,  
261, 263, 283-285, 287, 289-291, 307,  
308, 311, 318, 319, 321-324, 339, 340,  
342, 345, 352, 353, 362, 364-366, 368,  
371, 373, 378-380, 382-384, 386-388,  
390-394
- atmosphere 229, 230, 232, 234, 236, 239,  
240, 242, 244-247, 256, 263-267, 270,  
283-285, 289-292, 294-296, 299-302,  
304-312, 314, 315, 319, 322, 323, 326,  
341, 342, 344-347, 349, 350, 352-375,  
378-380, 382-384, 387-393, 399, 400
- atmospheric contamination 245-286, 288,  
295, 298, 304, 311, 314-319, 322, 324,  
339, 342, 353, 358, 381, 390
- AVCC 343, 344, 397

## B

- Baffin Island 275, 282, 393
- Ballentine, C. IV, 242, 265, 296, 297, 313,  
314, 316, 323, 339, 341-344, 347, 350,  
355, 358, 359, 366, 371-373, 378, 381,  
382, 384, 389, 393, 394
- BMO (Basal magma ocean) 326, 380, 397
- BSE (Bulk silicate Earth) 242, 289, 336,  
337, 397
- Burnard, P. IV, 286, 288, 331, 342, 379,  
380, 383, 388, 394
- Busemann, H. 245, 249, 251, 252, 254-266,  
283, 344, 354, 370, 379, 381

## C

- Cafee, M. 265, 342, 366, 380
- chondrite 248, 250, 254, 289, 355, 356,  
364, 366, 394, 397, 398
- Clarke, W. 233, 235, 240, 267, 268, 380
- comet 355

core 236, 238, 240, 241, 289, 325, 327-330, 338, 352, 367, 385, 386, 391-393, 397, 399

crust 236, 240, 241, 267, 274, 281, 282, 289-291, 296, 297, 316, 326, 334, 340, 341, 347, 360, 361, 380, 384, 386, 387, 389, 391, 393, 397-399

## D

degassing 229, 230, 236, 239, 240, 263, 267, 268, 274, 276-279, 283, 284, 286, 291, 294, 298, 299, 301, 302, 306, 308, 311, 321, 324, 326, 331, 333, 334, 338-340, 346-351, 354, 356, 357, 359-364, 370, 371, 378, 380, 382-385, 388, 390, 392-394

diffusion 229, 231, 234, 239, 281, 329, 330, 383, 392

DUPAL 273, 274, 318, 381, 388, 390, 392, 394, 398

## E

EUV 366

## F

Fisher, D. 268, 284, 285, 382, 387, 392

## G

Galapagos 273, 275, 286, 298, 313, 314, 322, 323, 333, 335, 336, 350, 352, 387

Genesis 234, 246, 247, 257, 333, 380, 383-385, 391, 398, 400

Girard, M. 236, 294

## H

Hawaii 273, 275, 284-286, 292, 313, 314, 333, 350, 380, 384, 386, 390, 394

Heber, V. 246, 247, 249, 259, 261, 322, 335, 358, 364, 383, 384, 394

helium 231-233, 243, 246, 247, 267-282, 291, 310-312, 314, 318-321, 324, 327-329, 331-336, 340, 352, 354, 359, 361, 362, 377-395

Helium 278

Hilton, D. 275, 277-279, 331, 333, 381, 384, 392

HL 248-250, 265, 364, 365, 398, 399

Holland, G. 240, 242, 265, 296, 297, 323, 342-345, 347, 350, 353, 357, 366, 369-373, 378, 384, 394

hydrodynamic escape 366, 385

## I

Iceland 273, 275, 286, 298, 305, 306, 313, 314, 322, 323, 333, 336, 350, 352, 358, 379, 382-384, 391, 398

isotope 232, 235, 236, 238, 239, 240, 250, 253, 254, 256-259, 270, 272, 283, 291, 292, 299, 304, 310, 311, 313, 326, 328, 331, 334, 335, 341-343, 345-347, 352, 354, 359, 362, 366, 367, 377-384, 387-394, 399

I-Xe 235, 301, 378

## J

Jupiter 246, 247, 354, 387, 394

## K

K-Ar 235, 284, 289

krypton 232, 234, 307, 339, 343, 351, 353, 354, 357, 364, 367, 369-373, 381, 384, 390, 394

Kunz, J. 285, 286, 296, 297, 302, 303, 322, 339, 342, 343, 359, 370, 371, 386, 393

Kurz, M. IV, 235, 241, 270, 274-277, 280, 312, 313, 318, 321, 325, 331, 335, 336, 352, 378-380, 382, 383, 385-387, 389, 390, 393

## L

Lecomte, A. 236, 294, 302

Lewis, R. 245, 248, 249, 251, 377, 385, 387  
lower mantle 241, 286, 289-291, 307, 325, 336, 338, 346, 352, 374, 381, 389, 392

## M

Mamyrin, B. 233, 268, 269, 387, 393

mantle 229-231, 233, 236, 239-243, 247, 254, 262, 263, 265, 267-286, 288-355, 357-366, 369-374, 377-394, 397-400

Mars 230, 239, 240, 242, 246, 263-266, 283, 346, 353, 354, 368, 370-372, 374, 381, 382, 390, 394, 398, 400

Marty, B. 262, 279, 319, 335, 352, 355, 358-360, 364-366, 371, 373, 378, 380, 381, 384, 387, 388, 390, 391, 393, 394

mass fractionation 239, 252, 253, 299, 310, 344, 360, 366, 373, 385

Mazor, E. 245, 249, 256, 357, 388

melt inclusion 264, 271, 284



meteorites 229, 231, 235, 239, 240, 242,  
244, 246-248, 250, 254-258, 263, 265,  
267, 269, 283, 289, 302, 312, 328, 345,  
352, 353, 364, 372, 375, 379, 381, 382,  
387-390, 392, 393, 397-400  
Moon 240, 326  
MORB 241, 268, 270, 272-277, 279, 282,  
284, 285-299, 302-306, 309-314,  
318-325, 327, 328, 331-334, 336, 337,  
338, 340, 343, 345, 350-353, 358-364,  
378, 380, 388, 389, 392-394, 398, 399  
Moureu, C. 233, 234, 389  
Mukhopadhyay, S. 262, 286, 298, 305, 313,  
314, 322, 331, 350, 358, 371, 382, 389,  
390, 393

## N

Neon 232, 247, 254-262, 265, 287, 291,  
296, 298, 307-315, 317-324, 331, 336,  
340, 345, 352, 353, 355, 357-359,  
364-366, 371, 373, 374, 378-381,  
383-395, 398-400  
Neon A 255, 256, 265, 365, 373, 399  
Neon B 254-262, 265, 309, 311, 312,  
314, 317-319, 321, 323, 353, 357-359,  
364-366, 371, 373, 399, 400  
Neon E 398  
nucleogenic 309-312, 314, 319-321, 324,  
352, 389, 392, 394, 399

## O

OIB 270, 272, 273, 275, 276, 278, 279, 282,  
284, 285, 286, 298, 299, 305, 306, 310,  
311, 313, 318, 320, 323, 324, 325, 327,  
329-337, 339, 345, 346, 350, 352, 353,  
358, 359, 361, 374, 378, 394, 398, 399  
olivine 264, 271, 272, 275, 279, 281, 284,  
331, 332, 335, 383, 384, 386  
Ozima, M. 270, 284, 294, 308, 309, 335,  
359, 378, 383, 384, 390

## P

P3 248, 364, 365, 399  
Parai, R. 274, 277, 296, 297, 302, 313, 314,  
318, 390  
partition coefficient 327, 328  
Pepin, R. 246, 247, 259-262, 266, 300, 322,  
323, 339, 343, 344, 352, 353, 358, 366,  
368, 371, 385, 388, 390, 391

phase Q (quintessence phase) 245-247,  
249-255, 265, 266, 299, 343-345,  
353-355, 357, 359, 364, 365, 370, 375,  
379, 397, 399  
popping rock 286, 289, 314, 315, 318, 334,  
342, 379, 389, 397, 399  
Porcelli, D. 270, 327-330, 332, 333, 335,  
341, 346, 352, 381, 382, 384, 389-391,  
393, 394  
pre-solar 249, 250, 254-256, 265, 364, 365,  
397, 398, 399  
primitive mantle 265, 268, 276, 289, 306,  
320, 329, 337, 342, 344, 346, 353, 358,  
370, 371, 387, 399  
primordial 229, 230, 232, 233, 239, 241,  
243, 247, 256, 258, 263, 267, 268, 275,  
276, 278, 282, 289, 291, 299-301, 307,  
309, 310, 312, 314, 320, 327-330, 335,  
337, 339, 345, 348, 349-353, 355,  
358, 361, 363-366, 368, 370-372, 374,  
378-380, 382, 384, 387, 392, 393, 395,  
399  
Pujol, M. 242, 366-369, 371, 372, 390, 391  
Pu-Xe 394

## R

Ramsay, W. 232, 391  
Raquin, A. 247, 257, 259, 261, 262, 274,  
286, 288, 298, 313, 315, 316, 322, 335,  
336, 339, 348, 358, 371, 388, 389, 391  
Réunion 275, 285, 298, 311, 322, 350, 385  
Reynolds, J. 275, 292, 294, 299-301, 377,  
379, 386, 391

## S

Samoa 298, 313, 314  
Sarda, P. 236, 254, 284-286, 291, 294,  
308-313, 316-319, 331, 339, 341, 359,  
362, 378, 388, 389, 392, 393  
SNC 263-265, 283, 352, 400  
solar 230, 234, 239, 240, 242, 244-266, 275,  
276, 283, 286, 292, 299-302, 308-312,  
314, 317, 318, 321-323, 339, 343-345,  
349, 350, 353-359, 364-374, 378-386,  
388-391, 394, 397-400  
solar wind 246, 247, 252, 254-262,  
264-266, 300, 314, 322, 323, 344, 345,  
353, 355, 358, 368, 371, 374, 375,  
380-384, 390, 391, 394, 398-400



spontaneous fission 231, 291, 292,  
294-297, 300-302, 304, 305, 306, 367,  
398

Staudacher, T. 235, 236, 284-286, 288,  
291-294, 297, 302, 310, 311, 340-342,  
347, 348, 351, 359, 378, 386, 389,  
392-394

step-crushing 314, 358

subduction barrier 296, 339, 341, 342, 347,  
348, 351, 366, 388, 393

## T

Tolstikhin, I. 241, 268, 269, 302, 325, 359,  
360, 378, 387, 393

Trieloff, M. 265, 286, 298, 313, 314, 316,  
319, 322, 331, 336, 350, 370, 383, 385,  
393

T-Tauri 239

Tucker, J. 296, 297, 302, 303, 314, 318, 319,  
321, 393

Turner, G. 302, 362, 379, 383, 393, 394

## V

Valbracht, P. 286, 298, 310, 311, 313, 314,  
319, 321, 322, 389, 394

Venus 230, 246, 283, 374, 390, 391

## W

well gases 233, 265, 267, 269, 292-294,  
296, 297, 313, 323, 342-347, 351, 358,  
366, 370, 372, 373, 378, 393

## X

xenon 231, 232, 239, 245, 246, 248-255,  
263, 264, 283, 291-307, 318, 319, 324,  
339, 341-344, 346-353, 357, 361, 363,  
364, 366-374, 378-381, 384-386,  
388-391, 393, 394, 398, 400





# SUBSCRIBE TO

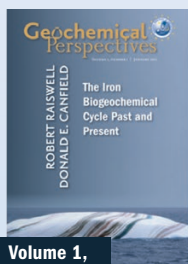
## Geochemical Perspectives



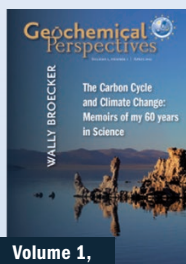
*Geochemical Perspectives* is provided to all members of the European Association of Geochemistry.

To join the European Association of Geochemistry visit:

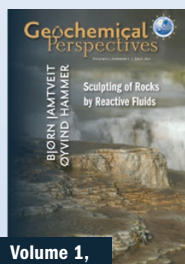
[www.eag.eu.com/membership](http://www.eag.eu.com/membership)



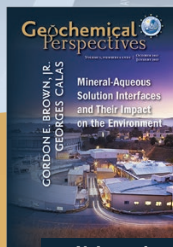
**Volume 1,  
Number 1**



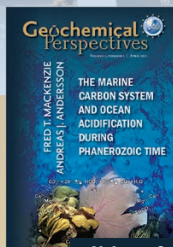
**Volume 1,  
Number 2**



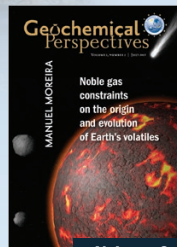
**Volume 1,  
Number 3**



**Volume 1,  
Number 4 and 5**



**Volume 2,  
Number 1**



**Volume 2,  
Number 2**

**Future issues  
will be written by:**

Nick Arndt, Al Hoffman,  
Bruce Yardley & Robert  
Bodnar, Henry Dick, Charlie  
Langmuir and many others.

For information, contact us at:  
[office@geochemicalperspectives.org](mailto:office@geochemicalperspectives.org)

[www.geochemicalperspectives.org](http://www.geochemicalperspectives.org)



***Geochemical Perspectives*** is an official journal  
of the European Association of Geochemistry



The European Association of Geochemistry, EAG, was established in 1985 to promote geochemistry, and in particular, to provide a platform within Europe for the presentation of geochemistry, exchange of ideas, publications and recognition of scientific excellence.

### Officers of the EAG Council

President	Chris Ballentine, University of Manchester, UK
Vice-President	Liane G. Benning, University of Leeds, UK
Past-President	Bernard Bourdon, ENS Lyon, France
Treasurer	Christa Göpel, IPG Paris, France
Secretary	Andreas Kappler, University of Tübingen, Germany
Goldschmidt Officer	Bernard Marty, CNRS Nancy, France
Goldschmidt Officer	Bernie Wood, University of Oxford, UK



**MANUEL MOREIRA** is Professor of Geochemistry at University Paris-Diderot and at the Institut de Physique du Globe de Paris. Manuel's research focuses on the Earth's origin and how the Earth has evolved during geological times. He principally uses the isotope geochemistry of oceanic basalts to constrain mantle structure and the origin of the atmosphere. After completion of his PhD in 1997 in Paris, under the supervision of Claude Allègre, he went to Woods Hole Oceanographic Institution to work with Mark Kurz for two years before coming back to France as an assistant professor in geochemistry at University Paris Diderot. He became a tenured professor in 2006 and member of the Institut Universitaire de France in 2007.

Outside his scientific life, Manuel dreams of playing tennis like Federer and acting like Jean-Paul Belmondo (in *Pierrot le Fou*) whilst learning to bake bread in the stone-oven of his country retreat in Normandy.